Final Project Report

OSSR Program Develop An Innovative Dispersant Spray Drift Model

Bureau of Safety and Environmental Enforcement (BSEE)

Engineering solutions

October 14th 2016

AMOG
770 South Post Oak Lane
Suite 310
Houston Texas 77056
United States
T   +1 713 255 0020

Final Project Report

OSSR Program Develop An Innovative Dispersant Spray Drift Model

Bureau of Safety and Environmental Enforcement (BSEE)

amogconsulting.com

This final report has been reviewed by the Bureau of Safety and Environmental Enforcement (BSEE) and approved for publication. Approval does not signify that the contents necessarily reflect the views and policies of the BSEE, nor does mention of the trade names or commercial products constitute endorsement or recommendation for use.

Document Number - r2015.j520.001, Issued as Revision 1   Reference # r2015.j520.001rev1

AI-E253-10v20130508

DOCUMENT ISSUE AND DISTRIBUTION

Document Number	Document Title
r2015.j520.001	Final Project Report

Job Number	Job Title
2015.j520	OSSR Program Develop an Innovative Dispersant Spray Drift Model

Client	Recipient
Bureau of Safety and Environmental Enforcement (BSEE)	Alex Ruttenberg

Client Address	Position
Oil Spill Preparedness Division 45600 Woodland Road, Mail Stop VAE-OSPD Sterling, VA 20166	Research Specialist

Issue	Date Issued	Author	Checked	Authorised
Revision 1	October 14th 2016	N Boustead P Kurts	P Sincock	D Washington
Revision 0	September 30th 2016	C Galtry N Boustead P Kurts	P Kriznic	D Washington

DISTRIBUTION OF COPIES

Copy Number	Location
1	AMOG Consulting
2	Bureau of Safety and Environmental Enforcement (BSEE)

REVISION REGISTER

Page	Revision	Date	Comment
20, 42	1	October 14th 2016	Revised to clarify DC-3 parameter set.

Document Number - r2015.j520.001
Issued as Revision 1, October 14th 2016
Doc Ref: Atlas:\...\r2015.j520.001.1.odt
amogconsulting.com
EIN 20-490647
TX PE Firm F-11821

AMOG®

AI-E253-10v20130508

EXECUTIVE SUMMARY

Aerial application of dispersants is an important tool used to respond to oil spills both in coastal waters and in the deeper waters of the Outer Continental Shelf. A number of tools currently exist for aerial dispersant planning such as the pesticide spray tools AGDISP and AgDRIFT. These tools have previously been used in oil spill response operations, however they were not developed for use in such scenarios. There is a need to improve upon the existing tools (such as AGDISP and AgDRIFT) to enable application to the equipment and missions typical of oil spill dispersant spraying missions rather than agricultural equipment and missions. The key differences between these two applications include aircraft altitude, the scale of the spraying operations and the specific aircraft used.

AMOG was contracted by the Bureau of Safety and Environmental Enforcement (BSEE) under Contract Number E15PC00015 to develop a Decision Support Tool (DST) to assist planners in identifying operational windows and safety setback distances based on forecast meteorological conditions, spray drift pattern, aircraft types and release rates. This report details the results of the studies undertaken under contract E15PC00015 and the development of the DST software.

Parameters that the tool sought to incorporate include:

- An inventory of aircraft likely to be used in the response.

- The dispersion characteristics of the dispersants used (i.e. droplet size distribution).

- The characteristics of spray equipment employed.

- The forecast weather conditions to occur within the target area.

To facilitate the development of the DST, AMOG:

1. **Executed a data gathering campaign** which involved engagement with a number of Oil Spill Removal Organizations (OSROs) and industry stakeholders. While this work was hampered by ongoing legal action, a Requirements Specification (included as Appendix C to this document) was developed which describes the functional requirements of the DST.

2. **Conducted a high level capability review** of existing aerial dispersion modeling tools to determine which tools have the functionality to model the aerial release of spray dispersant in an offshore oil spill response operational context. AGDISP was identified as the most appropriate existing regulatory model for predicting the extent of aerial spray drift.

3. **Assessed the performance of AGDISP for predicting extent of drift in offshore operations** by developing Computational Fluid Dynamic (CFD) models of representative oil spill response aircraft. The CFD models facilitated the examination of the effects of the combination of environmental conditions likely to be experienced by the aircraft coupled with the specific configuration of the aircraft/dispersal system geometry (such as nozzle configurations). The results from the CFD models were compared with AGDISP in order to identify conditions in which the existing modeling tools do not provide accurate results.

   The high fidelity CFD study found that for some aircraft, AGDISP does not capture important flow features and therefore under predicted the extent of spray drift. Specifically for each airframe the following was found:

AMOG®

3.i.   AGDISP is a suitably conservative tool for modeling the lateral drift extent of dispersant sprayed from an Air Tractor AT-802A. The DST uses AGDISP results to estimate the extent of spray drift for this aircraft.

3.ii. The simplifications inherent in AGDISP (in particular the omission of fuselage wake effects) result in an inability to accurately characterize the near field behavior of dispersant sprayed from a Lockheed C-130A. This inaccuracy can be corrected for by applying a correction factor derived from the difference between the CFD and AGDISP results. The DST uses the factored AGDISP results to estimate the extent of spray drift for this aircraft.

3.iii. AGDISP is unable to accurately represent the spray release from the DC-3, owing to the presence of main wing flap vortices which are not modeled in AGDISP and close proximity of spray nozzles. The DST uses the results from the CFD models (as extended by a Lagrangian particle calculation) to estimate the extent of spray drift for this aircraft.

3.iv. AGDISP is unable to accurately represent the spray release from the over wing arrangement used on the DC-4. The DST uses the results from the CFD models (as extended by a Lagrangian particle calculation) to estimate the extent of spray drift for this aircraft.

4.   Developed a Decision Support Tool based on the outcomes of the CFD study and using the methodology identified for each airframe to estimate the extent of dispersant spray drift.

The decision support tool was developed with a modular architecture based on a simple database structure combined with a surface fitting algorithm. This structure allows rapid computation time while facilitating the future expansion of the inventory of aircraft and spray systems.

The following conclusions are made as a result of the work undertaken during the project:

1.   A Decision Support Tool has been developed which meets the requirements identified during the stakeholder engagement phase of the project.

2.   Of the existing regulatory models used to predict the aerial extent of spray drift, AGDISP was identified as the most appropriate for use in offshore applications

3.   High fidelity CFD models were developed and used to predict the dispersant spray drift. The following major findings were made as a result of the CFD modeling activities:

3.i.   Qualitative validation of the results showed that the CFD models captured the significant flow structures affecting the dispersant trajectories.

3.ii. Flap vortices and fuselage wake were found to have a significant effect on the dispersant spray drift for the C-130A, DC-3 and DC-4. These effects are widely acknowledged features of the wake generated by aircraft, but have not previously been studied with regard to their effect on dispersant spray drift.

3.iii. For AT-802A and C-130A the wind angle did not significantly affect the total distance travelled by spray drift. As such, for wind directions outside the allowable input range of AGDISP, spray drift can be predicted on the basis of post-processed AGDISP extents.

3.iv. A set of AGDISP input parameters was developed which provided appropriately conservative estimates of spray drift for the C-130A and the AT-802A.

Document Number - r2015.j520.001
Issued as Revision 1, October 14th 2016
Doc Ref: Atlas:\...\r2015.j520.001.1.odt
amogconsulting.com
EIN 20-490647

TX PE Firm F-11821

AI-E253-10v20130508

4. The high fidelity CFD study found that for some aircraft, AGDISP was not capturing important flow features and was under predicting the extent of spray drift. Specifically for each airframe the following was found:

  4.i. AGDISP is a suitably conservative tool for modeling the drift extent of dispersant sprayed from an Air Tractor AT-802A. The DST uses AGDISP results to estimate the extent of spray drift for this aircraft.

  4.ii. The simplifications inherent in AGDISP (in particular the omission of fuselage wake effects) result in an inability to accurately characterize the near field behavior of dispersant sprayed from a Lockheed C-130A. This inaccuracy can be corrected for by applying a correction factor derived from the difference between the CFD and AGDISP results. The DST uses the factored AGDISP results to estimate the extent of spray drift for this aircraft.

  4.iii. AGDISP is unable to accurately represent the spray release from the DC-3, owing to the presence of main wing flap vortices, which are not modeled in AGDISP and their relative proximity to spray nozzles. The DST uses the results from the CFD models (as extended by a Lagrangian particle calculation) to estimate the extent of spray drift for this aircraft.

  4.iv. AGDISP is unable to accurately represent the spray release from the over wing arrangement used on the DC-4, and the resulting inaccuracy cannot be corrected. The DST uses the results from the CFD models (as extended by a Lagrangian particle calculation) to estimate the extent of spray drift for this aircraft.

5. The DST predicts drift extents for each of the four aircraft modeled which, particularly in headwind conditions, are significantly less than the setback distances which have been used in previous oil spill response campaigns. The maximum (i.e. crosswind) setback distances were found to be:

  5.i. DC-3 – 10,550 feet;

  5.ii. DC-4 – 8,250 feet;

  5.iii. C-130A – 7,400 feet; and

  5.iv. AT-802A – 2,650 feet.

6. The DST accounts for the effects of wind strength and direction such that, in favorable conditions (i.e. lower wind strength), setback distances may be defined which are significantly lower than those which have been previously used.

7. Significant differences exist between the predicted drift extents for the four airframes considered. While the low drift extents for the AT-802A are largely driven by the lower altitude used in modeling that aircraft (50 feet vs 100 feet for the other three aircraft), the differences between the DC-3, DC-4 and C-130A are influenced by a number of factors, including aircraft weight, flap configurations and spray boom length. The use of long spray booms on the DC-3, which inject dispersant into the airflow in the vicinity of the wingtip vortices, is likely to influence the large drift extents predicted for the DC-3.

TABLE OF CONTENTS

AMOG®

Document Number - r2015.j520.001
Issued as Revision 1, October 14th 2016
Doc Ref: Atlas:\...\r2015.j520.001.1.odt
amogconsulting.com
EIN 20-490647
TX PE Firm F-11821

AI-E253-10v20130508

LIST OF TABLES

LIST OF FIGURES

ABBREVIATIONS

ABL	Atmospheric Boundary Layer
AMOG	AMOG Consulting Inc.
ASAE	American Society of Agricultural Engineers
BSEE	Bureau of Safety and Environmental Enforcement
CAD	Computer Aided Design
CFD	Computational Fluid Dynamics
DMP2	Dispersant Mission Planner 2
DST	Decision Support Tool
EDAC	Effective Daily Application Capacities
GIS	Geographic Information System
IGE	In Ground Effect
ISC3	Industrial Source Complex 3
JIP	Joint Industry Project
KML	Keyhole Markup Language
NACA	National Advisory Committee for Aeronautics
NIMS	National Incident Management System
NOAA	National Oceanic and Atmospheric Administration
NWS	National Weather Service
OCD	Offshore and Coast Dispersion Model
OGE	Out of Ground Effect
OSC	On-Scene Coordinator
OSRO	Oil Spill Response Organization
PSD	Particle Size Distribution
RANS	Reynolds-Averaged Navier Stokes
RIDSS	Rapid Installation and Deployment Spray System
RPM	Revolutions Per Minute
SST	Shear Stress Transport
US EPA	United States Environmental Protection Agency
UTC	Coordinated Universal Time

Document Number - r2015.j520.001
Issued as Revision 1, October 14th 2016
Doc Ref: Atlas:\...\r2015.j520.001.1.odt
amogconsulting.com
EIN 20-4906471
TX PE Firm F-11821

AI-E253-10v20130508

1 INTRODUCTION

Aerial application of dispersants is an important tool used to respond to oil spills both in coastal waters and in the deeper waters of the Outer Continental Shelf. A number of tools currently exist for aerial dispersant planning such as the pesticide spray tools AGDISP and AgDRIFT. These tools have previously been used in oil spill response operations, however they were not developed for use in such scenarios. There is a need to improve upon the existing tools (such as AGDISP and AgDRIFT) to enable application to the equipment and missions typical of oil spill dispersant spraying missions rather than agricultural equipment and missions. The key differences between these two applications include aircraft altitude, the scale of the spraying operations and the specific aircraft used.

AMOG has been contracted by the Bureau of Safety and Environmental Enforcement (BSEE) under Contract Number E15PC00015 to develop a Decision Support Tool (DST) to assist planners in identifying operational windows and safety setback distances based on forecast meteorological conditions, spray drift pattern, aircraft types and release rates.

To facilitate the development of the DST, AMOG has developed Computational Fluid Dynamic (CFD) models of representative oil spill response aircraft. The CFD models facilitated examination of the effects of the combination of environmental conditions likely to be experienced by the aircraft coupled with the specific configuration of the aircraft/dispersal system geometry (such as nozzle configurations). The results from the CFD models were then compared with the existing inventory of dispersion models in order to identify conditions in which these existing models do not provide accurate results. This determined the suitability, or otherwise, of the existing models for incorporation into the DST.

1.1 BACKGROUND

During the response to an oil spill, spray dispersants are employed to break up the oil into smaller droplets to allow it to better mix with water. During the initial response to the Deepwater Horizon spill, aircraft from the 910th Airlift Wing conducted a 5-week deployment spraying 30,000 acres with 149,000 gallons of dispersant in 92 sorties (Davis, 2010). The aircraft operated by 910th Airlift Wing (C-130H with the Modular Aerial Spray System) were amongst the inventory of aircraft likely to be involved in the spill response, however other aircraft exist in the inventories of private Oil Spill Removal Organizations (OSROs).

1.1.1 Regulatory Environment

Multiple federal regulations have been promulgated requiring facilities to prepare oil spill response plans (*33 CFR 154*, 2016; *33 CFR 154*, 2016) as part of the broader National Contingency Plan (*40 CFR 300*, 2016). In particular, BSEE receives those response plans prepared for facilities located seaward of the coastline (*33 CFR 154*, 2016), however these plans must be consistent/integrated with the applicable Area Contingency Plan. With response plans prepared for compliance with the regulations, there exists an expectation of rapid deployment of dispersants via fixed-wing platforms in areas where pre-authorization of dispersant use is implemented (*33 CFR 154*, 2016). Figure 1 shows the various relationships between these plans.
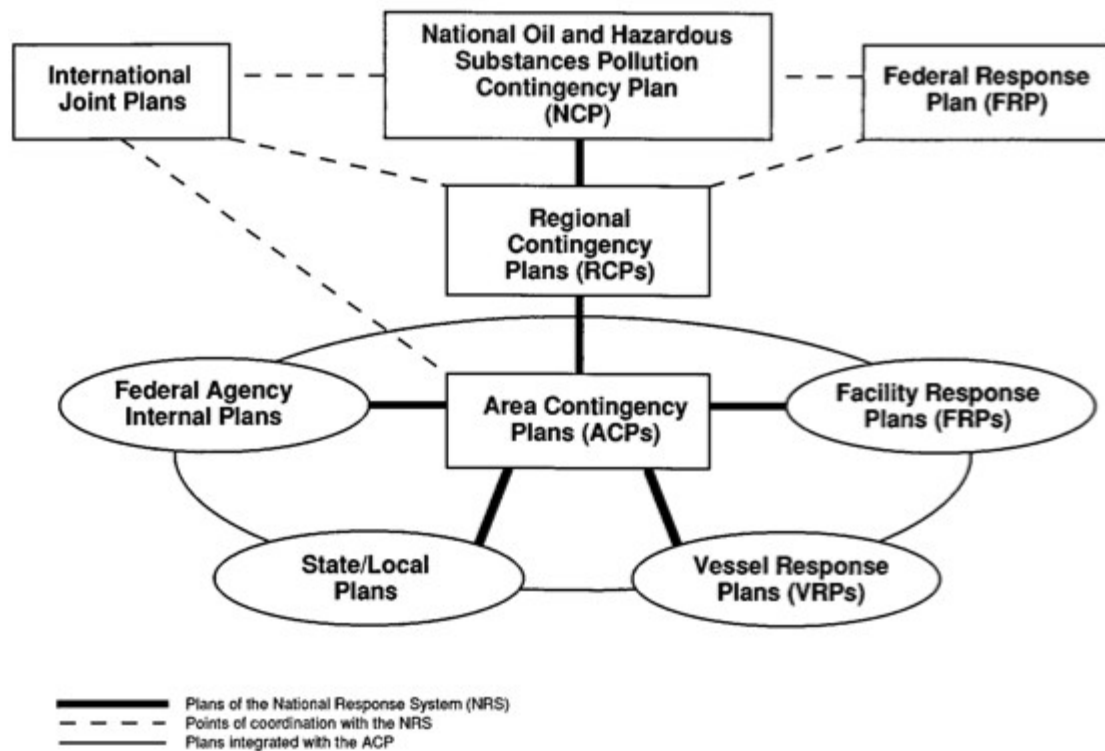
Figure 1 : Relationships between oil spill response plans as required by regulations (*40 CFR 300*, 2016)

As offshore oil and gas developments are often sited in challenging environments in terms of environmental conditions, the meteorological environment in the response area may be problematic for conducting aerial spray campaigns in terms of adverse wind speed, sea state, visibility, ceiling height, etc. In particular, as response times typically require delivery of minimum quantities of dispersant within a 7 to 12 hour window (*33 CFR 154*, 2016; US Coast Guard, 2013a), understanding the practicality of these responses is important in ensuring the safety of personnel during the initial phases of the oil spill response.

1.1.2 Planned Future Role For Aerial Dispersant

Significant interest in developing aerial platforms for oil spill response developed following the Macondo/Deepwater Horizon spill. An international Joint Industry Project (JIP) on Oil Spill Response sought to identify future platforms capable of acting as global first response assets in the event of future spills (IPIECA-OGP, 2012). As a result, it has been identified that higher speed, more efficient aircraft will be required in the future to allow for oil spill response to be met using fewer aircraft. In response to the findings of the JIP, a Boeing 727 modified to allow aerial spraying is currently under development by Oil Spill Response Limited, based in the UK (see Figure 2 [8]).

Document Number - r2015.j520.001
Issued as Revision 1, October 14th 2016
Doc Ref: Atlas:\...\r2015.j520.001.1.odt
amogconsulting.com
EIN 20-4906471
TX PE Firm F-11821

AI-E253-10v20130508

Figure 2 : Oil Spill Response Limited's Boeing 727 Dispersant Platform Under Development (Oil Spill Response Limited, 2013)

1.1.3 Current State Of Knowledge

1.1.3.1 Existing Aerial Spray Dispersion Models

The majority of existing spray dispersant models are focused on agricultural or forestry management applications where the chemical sprays are herbicides and pesticides. The most relevant examples of an existing tool within the US model inventory are AGDISP and AgDRIFT, originally developed by the Forestry Service to assist with assessing the drift of pesticides associated with aerial spray campaigns.

Literature surveys indicate that AGDISP and similar tools have some limitations with respect to non-linear fluid dynamics caused by the interaction of the aircraft's wake and crosswinds that may be present in the dispersal area (Ryan, Gerber, & Holloway, 2013). This interaction results in a significant alteration of the wake structures such as wingtip vortices and propeller wash. The crosswind can cause the droplets to be entrained in the wingtip vortices, influencing the resultant dispersal pattern as shown in Figure 3.

Document Number - r2015.j520.001
Issued as Revision 1, October 14th 2016
Doc Ref: Atlas:\...\r2015.j520.001.1.odt
amogconsulting.com
EIN 20-4906471
TX PE Firm F-11821

AI-E253-10v20130508
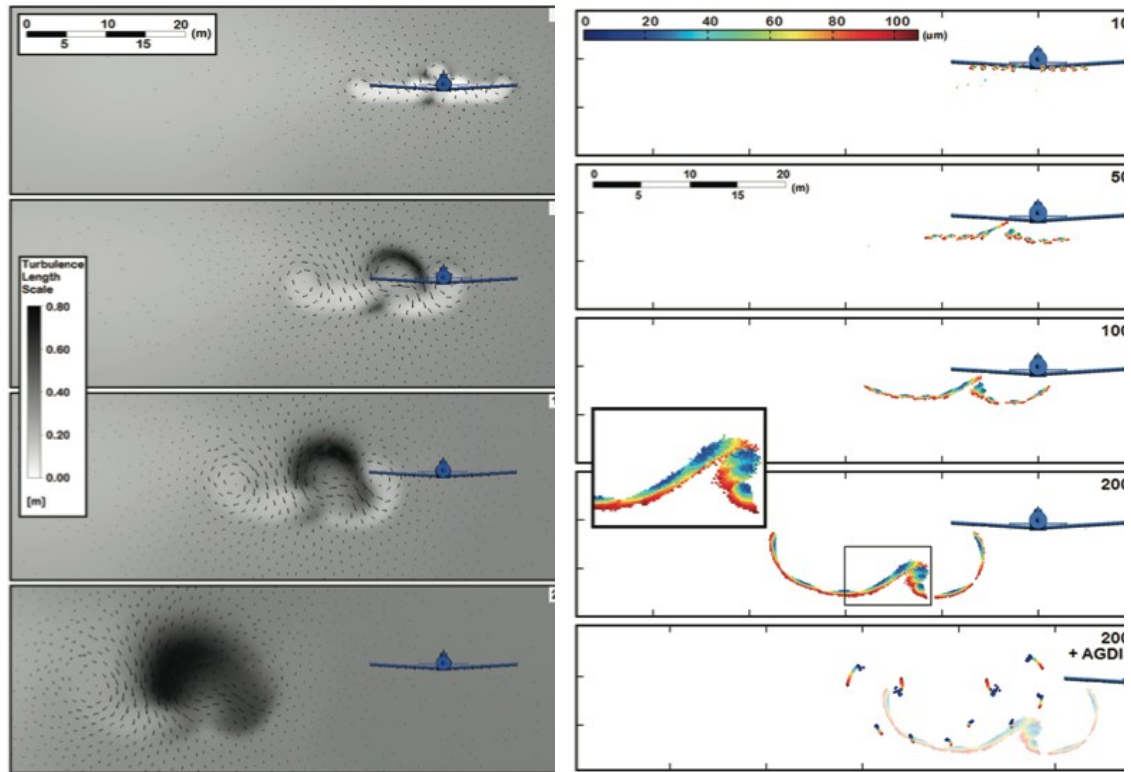
Figure 3 :The influence of crosswinds on the aircraft wake
The plots indicate the influence of crosswinds on (left) the wake structure behind an aircraft, indicated by velocity vectors and contours of turbulence length scale, and (right) the predicted droplet position behind the aircraft, entrained into the tip vortices (Ryan et al., 2013)

A recent study (Ryan et al., 2013) demonstrated that CFD may be used for the investigation of this effect, and provides a basis in the literature in support of this approach.

Although current tools, such as AGDISP and AgDRIFT (US EPA, n.d.), Offshore and Coast Dispersion Model (OCD), Calpuff and Aermod (US EPA, 2016a) are capable of predicting the extents of aerial spray dispersion, their use for rapid deployment is limited by the expert knowledge required in their operation. These tools rely on the user having sufficient knowledge and/or prior understanding in order to be used effectively. For instance, some tools require understanding of the behavior of the dispersant being released from the aircraft to allow the use of generic source types (i.e. point, line, area and/or volume sources) to replicate the spray dispersion pattern.

Whilst field trials have been undertaken to provide this underlying knowledge, it has been identified that this limited field trial data is insufficient in characterizing the drift associated with the aerial release of sprays, particularly in cross-wind conditions (Ryan et al., 2013).

AMOG®

AI-E253-10v20130508

1.1.3.2   *Dispersant Mission Planner 2*

The existing National Oceanic and Atmospheric Administration (NOAA) developed response planning tool Dispersant Mission Planner 2 (DMP2) allows for the rapid estimation of the Effective Daily Application Capacities (EDAC) as well as general performance estimates for the application of dispersants. However, the performance estimates rely on efficiency estimates based on data of varying degrees of applicability. Level 1 data is based on field trial data or fixed design values. Levels 2 and 3 are estimates based on operator experience, reasonable engineering calculation or performance of similar systems, as shown in Figure 4.

Currently the capabilities of DMP2 are useful at estimating EDAC and response time based on these general aircraft capabilities to demonstrate first response capability by OSROs. It is also currently used by the Coast Guard in the classification of OSROs (US Coast Guard, 2013a; Benggio, 2009).

PLATFORM

DOUGLAS DC-3

Operator: Airborne Support Incorporated
OSRO: Clean Gulf Associates

Photo compliments of
Airborne Support, Inc. (ASI)

DATA SOURCE LEGEND

1. (Black):   Indicates the data are based on documented field trials or is a fixed design value

2. (Blue):   Indicates the data are based on limited field observations or operator's stated practice or stated value (little or no documentation)

3. (Red):   Indicates the data are based on reasonable calculations or performance of comparable systems

		Unit	U.S. Regulatory Calculation Values	Data Source 1-2-3	Range	Reference(s)
	AIRCRAFT PARAMETERS					
1	Swath Width	feet	120	3	70-120	Airborne Support Inc. estimated value
	a. Application (gallons per acre)	gpa	5	3	1-10	Airborne Support Inc. estimated value
	b. Altitude	feet	50	2	50-100	Airborne Support Inc.
	c. Application Speed	knots	130	2	120-160	Airborne Support Inc.
	d. Pump Rate (gallons per minute)	gpm	-----	3	40-600	Estimate for typical

Figure 4 : Aircraft capability form incorporated into DMP2 (Benggio, 2009)

Document Number - r2015.j520.001
Issued as Revision 1, October 14th 2016
Doc Ref: Atlas:\...\r2015.j520.001.1.odt
amogconsulting.com
EIN 20-4906471
TX PE Firm F-11821

AI-E253-10v20130508

1.2   OBJECTIVES

The objective of this package of work was the production of a software tool which is capable of achieving two key functions:

1.   Determining operability windows for aircraft spray missions based upon the rapid evaluation of forecast and/or measured meteorological conditions over the response area.

2.   Determining the maximum extent of dispersant drift based on environmental conditions at the site. As a minimum, to protect the safety of workers on response vessels in the field, the tool needs to be capable of providing input into the decision for establishing the minimum safe setback distance from the aerial dispersant operations.

1.3   ACKNOWLEDGEMENTS

AMOG would like to acknowledge the following contributors to the work described in this report. Their assistance in the provision of design data, expertise and operational knowledge has assisted in the completion of the current project:

- The Bureau of Safety and Environmental Enforcement (BSEE)

- Air Tractor Inc.

- UTC Aerospace Systems

- Hartzell Propeller Inc.

- Envenio Inc.

- Mr Charles A Huber of CAH, Inc.

- The National Oceanic and Atmospheric Administration (NOAA)

- Oil Spill Response Limited

1.4   DOCUMENT LAYOUT

This document is structured as follows:

- Section 2 presents a description of the methodology used to execute the project;

- Section 3 presents a description of the Decision Support Tool;

- Section 4 presents a high level capability review and selection of an existing regulatory dispersion model;

- Section 5 presents details of the DST software development;

- Section 6 presents the conclusions of this work;

- Section 7 presents the recommendations arising from this project;

Document Number - r2015.j520.001
Issued as Revision 1, October 14th 2016
Doc Ref: Atlas:\...\r2015.j520.001.1.odt
amogconsulting.com
EIN 20-4906471
TX PE Firm F-11821

AI-E253-10v20130508

- Section 8 presents the references used in this document;

- Appendix A contains the DST User Manual;

- Appendix B contains a comprehensive summary of the CFD analysis conducted in this study; and

- Appendix C contains the DST Software Requirements Specification.

Document Number - r2015.j520.001
Issued as Revision 1, October 14th 2016
Doc Ref: Atlas:\...\r2015.j520.001.1.odt
amogconsulting.com
EIN 20-4906471
TX PE Firm F-11821

AI-E253-10v20130508

2 EXECUTION METHODOLOGY

In order to deliver a DST capable of determining the extent of dispersant drift, the project was broken into three distinct phases, as shown in Figure 5. In Phase 1, a Requirements Specification (AMOG Consulting Inc., 2016a) was developed which details the DST requirements and operability limits as identified through a stakeholder engagement process.

Phase 2 was the intermediate phase of the support tool development process, whereby CFD modeling was used to determine the suitability of existing airborne dispersion models for incorporation into the tool. This involved a source characterization of the dispersant spray suitable for input into traditional dispersion models (Work Pack 2) and the evaluation of the CFD model results as compared to real world imagery and data (Work Pack 3).

Phase 3 constituted the development of the DST itself. In order to meet the requirements identified in Phase 1 the DST was developed using results from the evaluation of the existing Airborne Dispersion Models (AgDRIFT and AGDISP) against the validated CFD results obtained in Phase 2.

Phase I: Requirements Development
- WP1: Development of Operability Criteria

Phase II: Source Characterization of Aerial Dispersant Platforms
- WP2: Source Characterization of Dispersant Spray Through CFD Modeling
- WP3: CFD Model Evaluation

Phase III: Development of Dispersant Response Planning Tool
- WP4: Evaluation of Airborne Dispersion Model for Predicting Spray Drifts
- WP5: Development of Aerial Spray Dispersion Operation Support Tool

Figure 5 : Overall Project Execution Methodology

2.1 PHASE 1

2.1.1 Work Package 1: Development Of Operability Criteria

This work package was focused on developing a thorough operational understanding of aerial dispersant spray campaigns.

2.1.1.1 Task 1: Consideration Of Operational Aspects

This task involved the engagement, in the form of a stakeholder survey, of organizations both private and public likely to be involved in the execution of aerial spray campaigns during future spill responses. The outcome from this activity was the consolidation of the stakeholders' inputs and the development of a list of operability requirements, including parameters affecting the safe conduct of flight operations.

The requirements extracted fall broadly into two categories:

- Aircraft spray dispersant operability limits. These define limiting conditions based on either:

  - safe to conduct spraying missions; or

Document Number - r2015.j520.001
Issued as Revision 1, October 14th 2016
Doc Ref: Atlas:\...\r2015.j520.001.1.odt
amogconsulting.com
EIN 20-4906471
TX PE Firm F-11821

AI-E253-10v20130508

- effective to conduct spraying missions.

- The response management team's requirements for a decision support tool: these were used to define the requirements needed by the personnel managing the response to a spill in the response planning tool, with particular regard to:

  - defining requirements such as expected solution time and required input data formats; and

  - prioritizing requirements and/or features.

The approach to achieving these goals consisted of the following broad tasks:

1. Identification of stakeholders relevant to the management of aerial spray dispersant responses. These included:

   1.i.   Private Oil Spill Removal Organizations (OSROs) which provide aerial dispersant response capability;

   1.ii. US Agencies which may provide aerial dispersant response capability;

   1.iii. US Agencies which will provide management/coordination of the oil spill response operation in the event of a spill; and

   1.iv. US Agencies which may rely on the outputs of this tool for the purposes of Facility Response Plan verification.

2. Development of surveys depending on stakeholder role in oil spill response, namely:

   2.i.   A specific survey for those stakeholders providing an operational capability such as operation of a spray platform; and

   2.ii. A specific survey for those stakeholders coordinating and/or managing the response of multiple operational agencies.

3. Initial telephone discussions with stakeholders stating the nature of the project and its purpose followed by a request to participate in the survey.

4. Compilation of all survey results into the categories identified above.

2.1.1.2   Task 2: Collation Of Operability Requirements As A Requirement Specification

Following Task 1, the identified requirements were ranked and appropriately prioritized, and inter-relationships between the requirements identified. Prioritization of the operability requirements was articulated in terms of large-scale and local-scale requirements to assist in their use as screening tools.

To ensure prioritization of these requirements met the needs of the stakeholders, a workshop was held at the BSEE offices in Virginia to allow the requirements list to be discussed and prioritized such that a single, consolidated list could be developed, inter-dependencies identified and stakeholders given the opportunity to reach agreement prior to finalization.

Document Number - r2015.j520.001
Issued as Revision 1, October 14th 2016
Doc Ref: Atlas:\...\r2015.j520.001.1.odt
amogconsulting.com
EIN 20-4906471
TX PE Firm F-11821

AMOG®

AI-E253-10v20130508

The workshop provided an opportunity for participants to provide input and/or comment on the program of works being conducted, rather than seeking to gather the participants to answer a set of formatted questions.

2.1.2   Outcomes Of Phase 1

The final outcome of Phase 1 were a consolidated list of:

- Operability requirements for the conduct of spray missions such as:

  ○ Permissible wind conditions;

  ○ Permissible sea states.

- Aircraft operational parameters such as:

  ○ Aircraft fleet composition, including manufacturer, type, spray system, ownership type (i.e. private vs public asset);

  ○ Application parameters such as application speed, application height, etc.

- Decision Support Tool requirements, such as:

  ○ Environmental input data requirements such as real-time meteorological measurement data, meteorological and oil spill dispersion forecasts data;

  ○ Aircraft input data requirements such as available aircraft, aircraft type, spray system installed, storage capacity;

  ○ Output data requirements such as extent of spray drift, buffer zone recommendations for response vessels;

  ○ Potential for integration with other tools such as DMP2.

The Requirements Specification (included as Appendix C to this document) details the identified requirements.

2.2   PHASE 2

In Phase 2, CFD modeling was used to determine the suitability of existing airborne dispersion models for incorporation into the DST. This consisted of two work packages:

1. Work Package 2: Develop numerical (CFD) models of representative oil spill response aircraft to facilitate examination of the particular effects of the combination of environmental conditions likely to be experienced by the aircraft coupled with the specific configuration of the aircraft/spray system geometry.

2. Work Package 3: Evaluate the modeled behavior of the spray release based on the best available data. The level of model evaluation (i.e. qualitative vs quantitative) was determined by the availability of any field trial data.

Document Number - r2015.j520.001
Issued as Revision 1, October 14th 2016
Doc Ref: Atlas:\...\r2015.j520.001.1.odt
amogconsulting.com
EIN 20-4906471
TX PE Firm F-11821

AI-E253-10v20130508

Details of the methodology used in the CFD models are included in Appendix B. A high level overview is presented below.

Four aircraft types were modeled in order to provide a cross-section of the aircraft types currently employed by oil spill response contractors and federal agencies. The aircraft modeled cover a wide range in terms of size, engine and spray system configurations, in order to increase the likelihood of the aircraft used in any individual oil spill response being similar to one of the aircraft modeled. This also allowed for a broad comparison of these types of aircraft against existing tools such as AGDISP and AgDRIFT to evaluate whether the performance of various aircraft types are well represented by the models proposed. The aircraft modeled were as follows:

- Lockheed Martin C-130A;

- Air Tractor AT-802A;

- Douglas DC-3; and

- Douglas DC-4.

The purpose of the tool is to provide decision makers with an understanding of the areas likely to be impacted by spray drift associated with a planned spray campaign in order to assist with the establishment of safety setback distances. Accordingly, the CFD models were designed to allow an estimate of the likely drift caused by a range of operational parameters that may be used in the course of spraying. The results were then used to identify scenarios where the existing modeling tools provide poor performance, as identified in an earlier study (Ryan et al., 2013). Where poor performance of the existing tools was identified, the CFD results were considered in order to provide an improved better estimate of the area impacted by spray drift.

Although it was originally anticipated that quantitative validation data would enable validation of the CFD spray drift predictions no such quantitative data was able to be obtained during the project. As such, the validation performed in Work Package 3 was largely qualitative in nature.

The execution methodology for Phase 2 is shown diagrammatically in Figure 6.

Document Number - r2015.j520.001
Issued as Revision 1, October 14th 2016
Doc Ref: Atlas:\...\r2015.j520.001.1.odt
amogconsulting.com
EIN 20-4906471
TX PE Firm F-11821

AI-E253-10v20130508
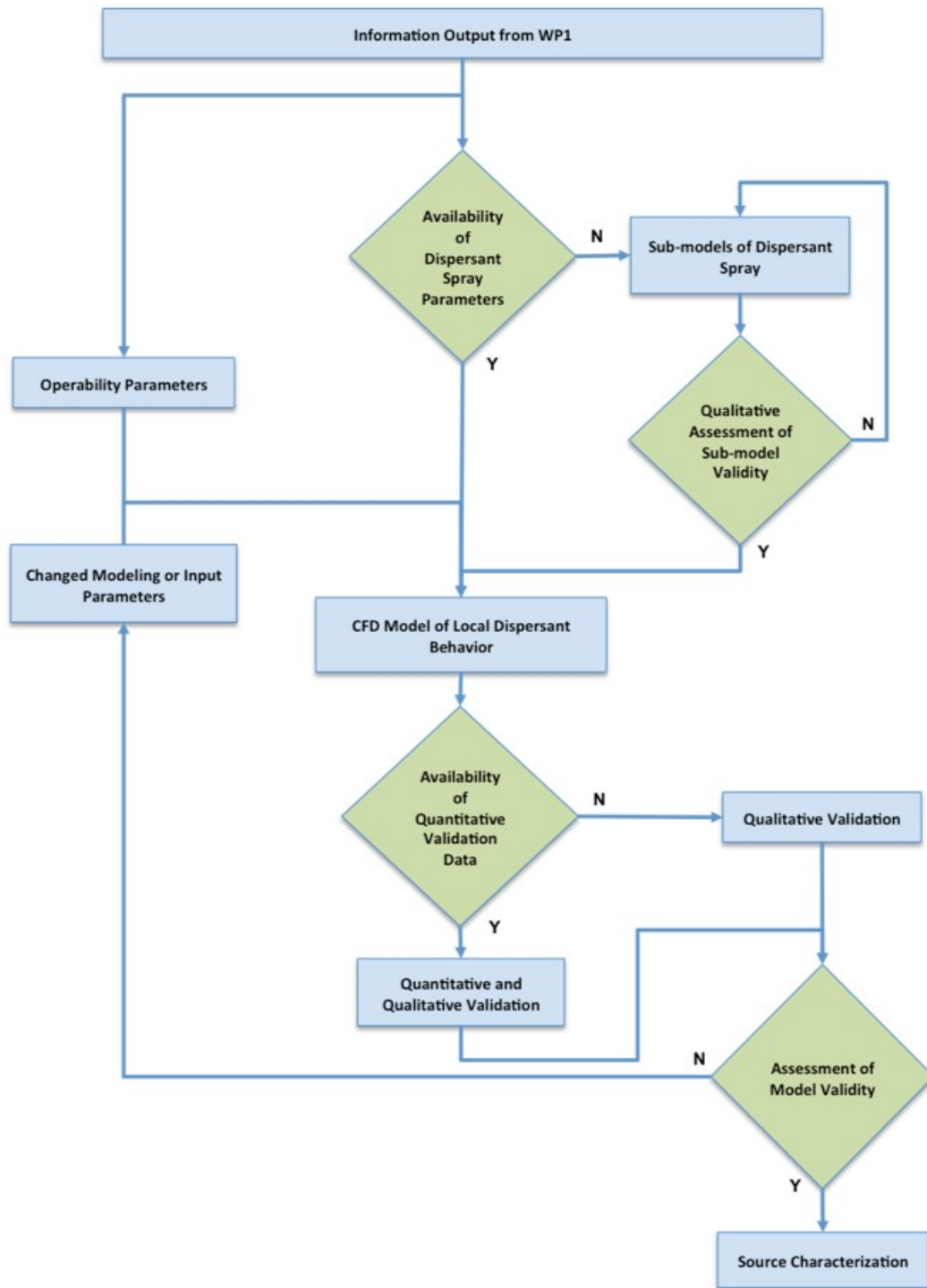
Figure 6 : Execution methodology for Phase 2

2.3   PHASE 3

In Phase 3 of the project, the range of existing airborne dispersion models were evaluated against the results of the CFD modeling conducted in Phase 2, and the most appropriate means of predicting the spray drift extent was identified for each aircraft. The identified methodologies were then implemented to produce the data which underpins the spray drift extent prediction functionality of the DST. An overview of the methodology used for Phase 3 is shown in Figure 7.

In order to determine whether preexisting dispersion models could be used in the development of the DST, the following activities were undertaken:

1.   A high level capability review of existing aerial dispersion modeling tools was conducted to determine which tools have the functionality to model the aerial release of spray dispersant.

2.   The outputs from appropriate modeling tools were evaluated against the outcomes of the CFD modeling activities. For each aircraft, the ability of the existing tools to accurately model the extent of the spray drift was determined. In cases where the accuracy of existing tools was insufficient, adjustment of the outputs was investigated against CFD predictions to determine whether modified results could be used in the DST.

3.   For those aircraft which could not be accurately modeled by any existing tool, a methodology was developed by which the CFD results could be used to predict the extent of spray drift.

For each aircraft, consideration was given to the means by which the selected modeling approach would be incorporated into the DST, by either:

●   Incorporating the selected model directly into the DST; or

●   Including the range of possible outputs for a given operational envelope as an embedded data set or response surface, based on the runtime inputs, to be stored within the DST.
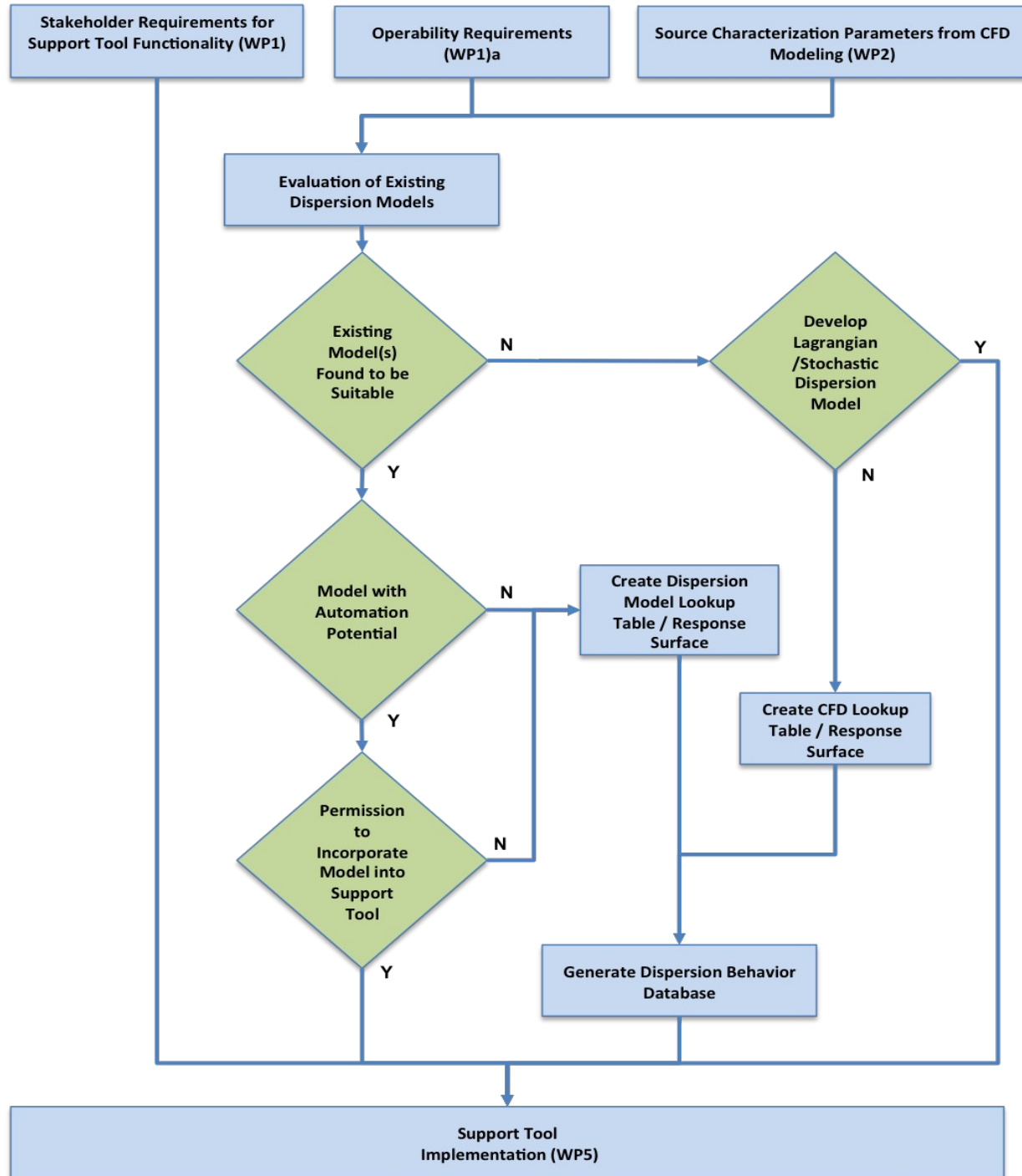
Figure 7 : Flow Chart Outlining The Process For Evaluating Dispersion Models

Document Number - r2015.j520.001
Issued as Revision 1, October 14th 2016
Doc Ref: Atlas:\...\r2015.j520.001.1.odt
amogconsulting.com
EIN 20-4906471
TX PE Firm F-11821

AI-E253-10v20130508

3 DST DESCRIPTION

3.1 INTENDED USAGE

The DST is envisaged to be employed by a set of users who will participate in the response to oil spill emergencies under the National Incident Management System (NIMS). In particular, two specific types of use have been identified for the DST during an oil spill response. Additionally, there is the potential for OSROs to use the tool to plan their initial response. The anticipated users and their requirements are:

- The Aerial Dispersant Group, in conjunction with the Environmental Unit and NOAA, for determining when and where spraying can effectively be conducted based on standard operational limits.

- The Aerial Dispersant Group, in conjunction with Planning Section Personnel to evaluate how forecast conditions will affect the ability to conduct spraying operations in the response area. This is expected to assist in the preparation of the Daily Aerial Dispersant Application Plans provided to the Federal On-Scene Coordinator (OSC); and

- Oil Spill Removal Organizations to assist with evaluating their initial response to a spill, prior to the response being escalated to a larger scale incident. In these incidents, the OSRO may require both operational and planning support capabilities.

To facilitate the requirements of each of these users, the DST has been developed to be used in either an operational mode or a planning mode. Details about the functionality of each of these modes are provided in Sections 3.2 and 3.3. A description of the algorithms used in the DST is provided in Section 3.4.

3.2 DST OPERATIONAL MODE

The operational mode of the DST facilitates the decisions required to be made by the Aerial Dispersant Group in conducting oil spill responses. The purpose of this mode is to allow the input of a single wind speed and direction likely to occur over the course the dispersant spray operations in order to provide input into establishing setback distances.

3.2.1 Runtime Inputs

In the operational mode, the following data is acquired from the user at runtime:

- Flight operational data likely determined from DMP2 mission planner. This data includes:

  ○ Airframe (selected from a drop down list);

  ○ Aircraft heading during spray operations, as bearing from True North;

  ○ Aircraft ground speed during spray operations, in kn; and

  ○ Aircraft altitude during spray operations, in ft.

Document Number - r2015.j520.001
Issued as Revision 1, October 14th 2016
Doc Ref: Atlas:\...\r2015.j520.001.1.odt
amogconsulting.com
EIN 20-4906471
TX PE Firm F-11821

AI-E253-10v20130508

- Meteorological data including:

    ○   A single time invariant wind speed defined at 10 m above the surface, in kn; and

    ○   A single time invariant wind direction as bearing from True North.

- A safety factor to be applied to the operational mode outputs.

It should be noted that the appropriate meteorological conditions are defined at the discretion of the user, however, as a guide the following conditions typically represent the worst case conditions:

- Maximum altitude;

- Highest wind speed; and

- Wind direction from directly upwind of potential receptors.

3.2.2   Outputs

In the operational mode the following information is output to the user:

- The maximum extent of drift (see Appendix B) behind the aircraft (trackwise) rounded up to the 50 ft;

- The maximum extent of drift perpendicular to the track of the aircraft (spanwise) rounded up to the nearest 50 ft;

- The total maximum drift extent in any direction; and

- The direction as bearing from True North in which the total maximum drift extent acts.

This information may be used to define a set back distance from the edge of a spray application area. If the input conditions are not operable for spraying operations, a message is displayed informing the user that the conditions have been assessed as inoperable, and no drift extent calculation is performed.

3.3   DST PLANNING MODE

The planning mode of the DST facilitates the identification of suitable spraying windows for the purpose of assisting with planning decisions on the basis of forecast data. The purpose of this mode is to allow the input of forecast time-varying forecast data to facilitate the identification of windows conducive to spraying operations (i.e. operability windows).

In addition, this mode also provides the ability to graphically integrate set back distances predicted using the DST with other oil spill response tools by producing a map layer illustrating the area affected by drift.

3.3.1   Runtime Inputs

In the planning mode, the following data is acquired from the user at runtime:

Document Number - r2015.j520.001
Issued as Revision 1, October 14th 2016
Doc Ref: Atlas:\...\r2015.j520.001.1.odt
amogconsulting.com
EIN 20-4906471
TX PE Firm F-11821

AI-E253-10v20130508

- Flight operational data likely determined from DMP2 Mission planner. This data will include:

  ○ Airframe (selected from a drop down list);

  ○ Aircraft heading during spray operations, as a bearing from True North;

  ○ Aircraft ground speed during spray operations, in kn;

  ○ Aircraft altitude during spray operations, in ft.

- Time varying meteorological forecast data formatted in a .csv file which the user imports into the DST. The following data will be included in the forecast data file:

  ○ Date and time information including the year, month, day, hour-minute (in 24 hour local time), and the Coordinated Universal Time (UTC) time zone for the area in which spraying will occur;

  ○ Wind speed at 10 m elevation, in kn;

  ○ Wind direction as bearing from True North;

  ○ Significant wave height, in ft; and

  ○ Visibility, in statute miles.

- Spill response data in the form of map layers as output from GIS packages used in the oil spill response planning. This data includes:

  ○ The predicted area of the oil spill (defined as a polygon in a .kml file); and

  ○ The area in which spraying operations are planned (defined as a polygon in a .kml file).

- A safety factor to be applied to the calculated spray drift extent.

The Keyhole Markup Language (KML) file format has been selected for compatibility with most Geographic Information System (GIS) software packages. The required files can also be generated by Google Earth. Full details of the requirements for input file formats and instructions for generating the required files are included in the DST User Manual (Appendix A).

3.3.2   Outputs

In the planning mode the following information is output to the user:

- An operability table, which includes the forecast data input by the user with an additional column indicating whether each forecast time is suitable for conducting spray operations.

  ○ For cases that are deemed to be not suitable the operability criteria that have been exceeded for each case are displayed in the output window of the DST.

- A map layer containing the area affected by drift. This area is the union of all areas affected by drift as predicted by the DST for each forecast time.

Document Number - r2015.j520.001
Issued as Revision 1, October 14th 2016
Doc Ref: Atlas:\...\r2015.j520.001.1.odt
amogconsulting.com
EIN 20-4906471
TX PE Firm F-11821

AI-E253-10v20130508

3.4 ALGORITHM

A high level overview of the DST is provided in Figure 8. There are three main modules in which the inputs are processed to generate the final outputs. Specifically these are:

- The operability algorithm,

- The drift extent algorithm, and

- The graphical output algorithm.

A short description of each of these algorithms is provided in Sections 3.4.1 to 3.4.3
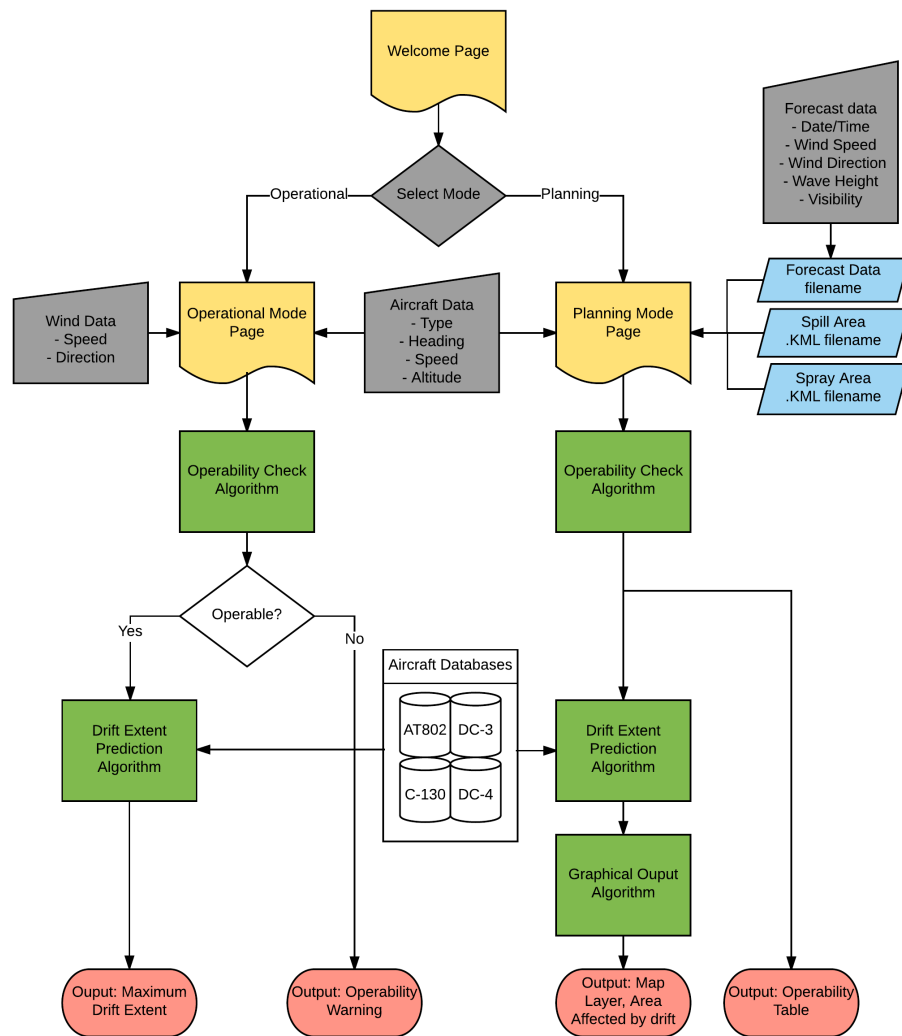
Figure 8 : High level overview of DST structure

3.4.1 Operability Algorithm

The operability algorithm is called in both the operational mode and the planning mode. It performs two functions:

1. It confirms that the input data is provided in the correct format, and if the format is correct it determines whether the input conditions are operable.

2. Within the second function a set of operability checks determine whether the specified flight conditions are within the regulatory guidelines for each aircraft, as specified in DMP2 and summarized in Table 1.

Table 1: Aircraft Specific Operability Criteria

Aircraft	Altitude (ft)		Ground Speed (kn)	
	Min	Max	Min	Max
AT-802A	15	50	110	180
C-130A	50	100	150	200
DC-3	50	100	120	160
DC-4	50	100	120	160

Finally efficacy of the planned spray operation is considered in the context of the forecast meteorological conditions. Operability of the aircraft in the forecast conditions is simply determined by comparing the forecast conditions to the operability criteria determined during Phase 1 of the project. The operability criteria incorporated into the tool are as documented in the Requirements Specification (Appendix C):

- Maximum wind speed – 35 knots;

- Maximum crosswind – 20 knots;

- No operations in tail wind conditions; and

- Maximum significant wave height – 10 feet;

- Minimum visibility – 3 statute miles;

- Operations only during day light hours.

To perform these operability checks calculations are made to determine the headwind and crosswind speeds at the reference height of 10 m.

In addition to wind component calculations, the operability algorithm also estimates the sunrise and sunset time based on the position of the centre of the oil spill. This prediction uses a simple sunrise and sunset calculation based on the local latitude, the sun's declination and the solar time correction. The model accounts for the eccentricity of the earths orbit but not the eccentricity of the earth itself, and assumes that the sunrise is defined as when the sun rises above the horizon, defined as greater than 90° declination.

Document Number - r2015.j520.001
Issued as Revision 1, October 14th 2016
Doc Ref: Atlas:\...\r2015.j520.001.1.odt
amogconsulting.com
EIN 20-4906471
TX PE Firm F-11821

AI-E253-10v20130508

The output of this algorithm is a boolean variable indicating weather the input conditions are operable or not, and when required an error message describing why the case is not operable.

It should be noted that the DST provides an assessment of operability based on the input weather conditions only. Additional factors such as precipitation or thunder storms may impact on operability in conditions that are otherwise suitable for conducting spraying operations. Final decisions as to whether or not operations are conducted should be made by the pilots in charge considering all available information as to the safety of conducting spraying operations.

3.4.2   Drift Extent Algorithm

The DST seeks to quantify the limits of spray drift. There are a number of parameters upon which the spray drift is dependent. One of the outcomes of Phase 2 of this project was an understanding of which parameters affect the extent of spray drift. These parameters are required inputs to the DST prediction.

Based on the outcomes of the CFD modeling conducted in Phase 2, the key parameters affecting spray drift are wind speed, wind direction, aircraft speed and spray release height. At the conclusion of Phase 2 a database was created for each aircraft considered which contained the predicted extent behind the aircraft (trackwise) and perpendicular to the aircraft track (spanwise) for the full range of dependent parameters in the operational envelope. The drift extent algorithm is described in Figure 9 and summarized here:

- The drift extent algorithm takes the input operational conditions which are provided in a global coordinate system and converts them to an aircraft centered local coordinate system.

- The drift extent algorithm then loads the results database for the specified aircraft and finds a subset of the data nearest the input parameters.

- The drift extent algorithm fits a localized linear shape function to the existing results in the data base.

- The drift extent algorithm then interpolates the drift extent behind and perpendicular to the aircraft.

- Finally the results are post processed by applying the user specified safety factor and rounding the result up to the nearest 50 ft before being presented to the user. At this stage data is output in both local and global coordinates.

The parameter space for the DC-3 is smaller than the other airframes because at the higher airspeed ranges considered for the other three aircraft, it is known that the DC-3 would typically be flown without flaps deployed. As all CFD assessments were undertaken with a single typical flap setting for each aircraft, this limits the range of validity for the DST.

Document Number - r2015.j520.001
Issued as Revision 1, October 14th 2016
Doc Ref: Atlas:\...\r2015.j520.001.1.odt
amogconsulting.com
EIN 20-4906471
TX PE Firm F-11821

AI-E253-10v20130508
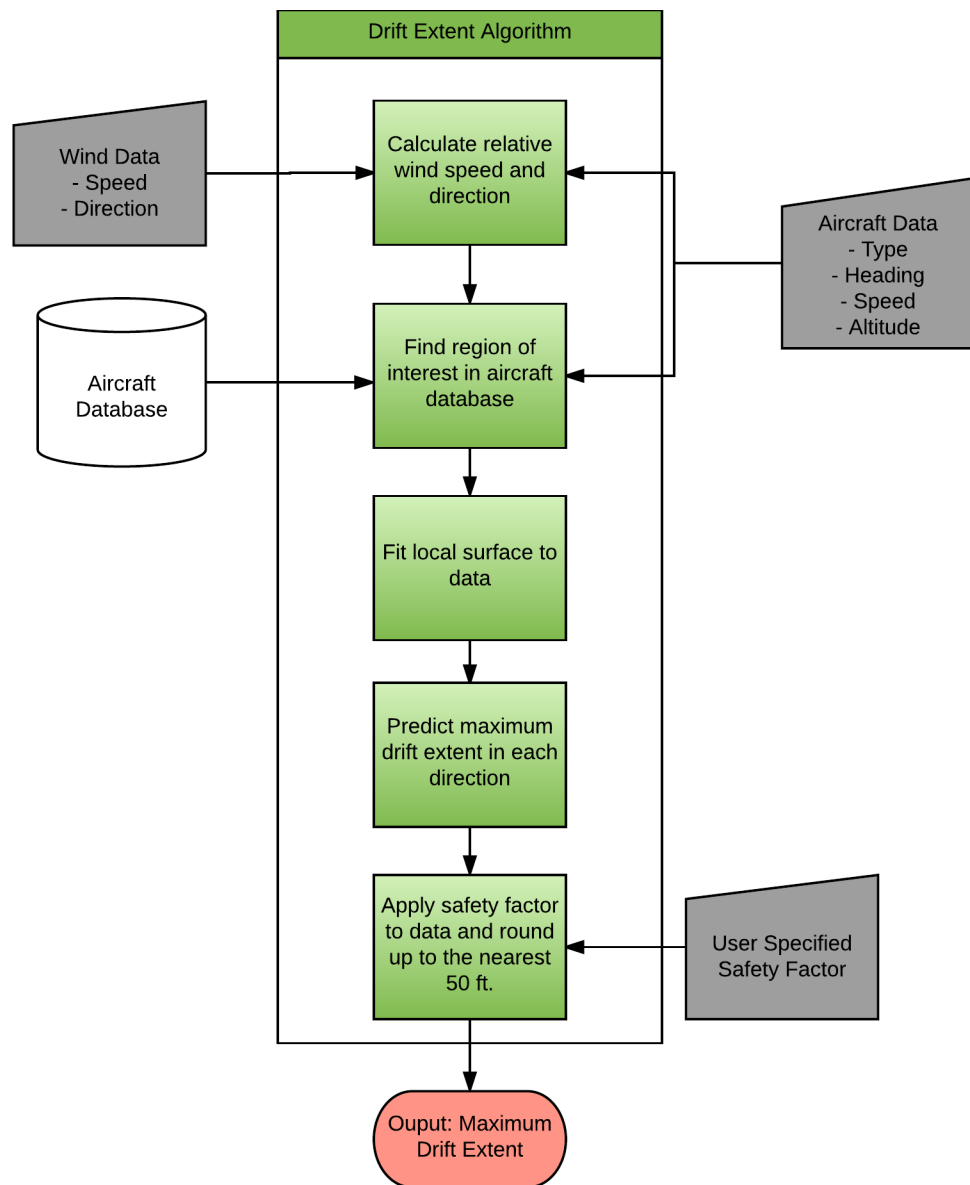
Figure 9 : High level algorithm for drift extent function

3.4.3 Graphical Output Algorithm

The graphical output algorithm is used in the planning mode to convert the predicted maximum extent into a map layer showing the area affected by spray drift. A high level overview of the algorithm is provided in Figure 10 and summarized as follows:

- The graphical output algorithm reads in the oil spill area and the area intended for spraying as polygons directly from the .kml file.

- The intersection of the oil spill area and the area intended for spraying is found. This "intersecting polygon" represents the area to which the dispersant will be applied.

- For each operable wind condition in the forecast data the drift extent is predicted using the drift extent algorithm. This extent is applied to each point of the intersecting polygon to create a new shifted polygon describing the area affected by drift. It is assumed that spraying will be released up to, but not beyond, the edges of the intersecting polygon.

- Find the union of all spray drift polygons for all operable times in the forecast data and the intersecting polygon in which spray operations are expected to occur. This will produce a polygon which encompasses the entire spray area and all areas affected by drift over the entire forecast period.

- Write this final polygon to a .kml file.

For each of the steps in the graphical output algorithm a number of boolean operations are applied to a set of polygons, specifically union and intersection operations are conducted. For these operations the POLYPACK fortran library was used.

It should be noted that factors such as changes to conditions during operations may affect the accuracy of the drift extent predictions made by the DST. Operators should continue to use spotter aircraft to ascertain whether drift extent is exceeding the predictions made.

Document Number - r2015.j520.001
Issued as Revision 1, October 14th 2016
Doc Ref: Atlas:\...\r2015.j520.001.1.odt
amogconsulting.com
EIN 20-4906471
TX PE Firm F-11821

AI-E253-10v20130508
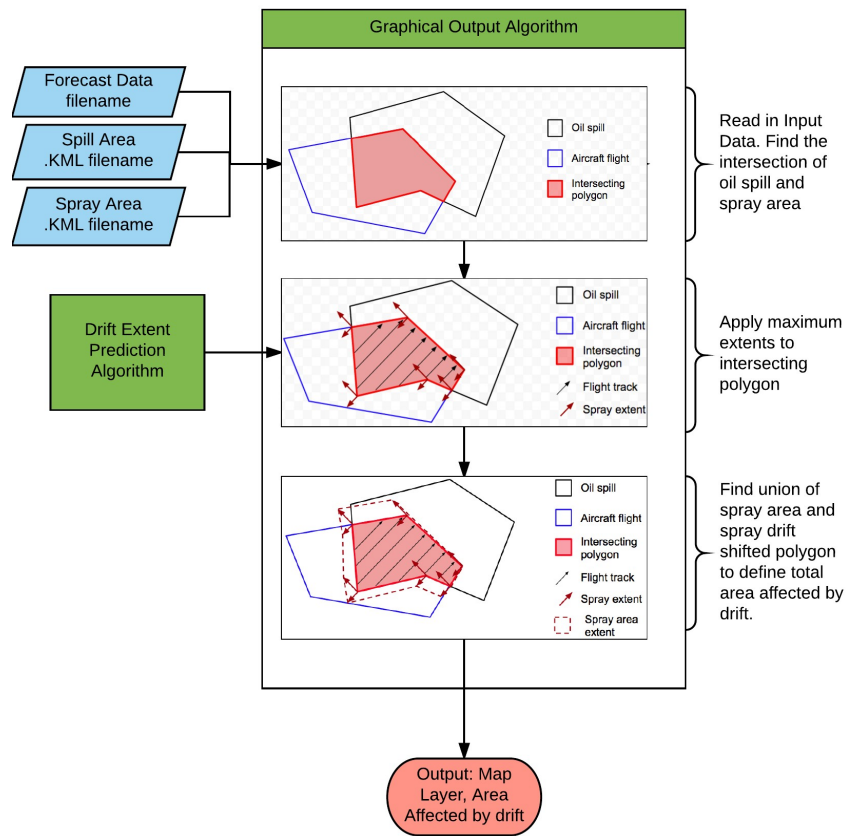
Figure 10 : High level algorithm for graphical output algorithm

3.5 ARCHITECTURE

The architecture of the DST was designed such that it facilitates:

- Fast run times; and

- Expansion for future model improvements, additional airframes and spray systems, and additional required outputs.

With these design requirements in mind a database approach combined with a surface fitting algorithm was selected as the basis for the DST drift extent calculations.

Using a database to store the necessary airframe specific drift data ensures rapid access, which does not require significant runtime to generate. The use of a database also facilitates the inclusion of data generated from a variety of sources, including CFD model results, which could not feasibly be obtained at runtime. The database approach also has advantages in that the existing data itself may be upgraded over time (i.e. if refined estimates of the drift extent are available) and new datasets added (e.g. drift estimates for additional airframes, configurations and spray products). The interface between the databases and the DST algorithms is illustrated in Figure 8.

4 EXISTING TOOLS FOR THE PREDICTION OF SPRAY DRIFT

In order to determine whether pre-existing dispersion models could be used in the development of the DST, a high level capability review of existing aerial dispersion modeling tools was conducted to determine which tools have the functionality to model the aerial release of spray dispersant. Once an appropriate dispersion modeling tool was identified, it was evaluated against the CFD model results to determine its ability to accurately predict spray drift extents for each of the four aircraft under consideration.

4.1 CATEGORIES OF EXISTING TOOLS

Currently, there are only three methods that are widely employed as the basis for atmospheric dispersion[1] modeling, namely Lagrangian particle, Lagrangian/Gaussian puff and Gaussian plume models. Within the models currently listed by the United States Environmental Protection Agency (US EPA) for use in atmospheric dispersion modeling, all three types of models are represented. The principal tools which have regulatory recognition for the dispersion of spray behind aircraft in the US are models based on empirical/first-principle methods, rather than the detailed and complex physics which underpins CFD. While CFD is increasingly recognized as a potentially useful tool for use in exploring complex dispersion scenarios, it is currently limited to applicability on a case-by-case basis due to lengthy simulation times and requisite high degree of expert knowledge. As such, the CFD models used in this study have been used either to evaluate the predictions from existing models, or as an input to far-field dispersion using another modeling approach.

4.2 REQUIRED CAPABILITIES

If a model is to be used to predict the extent of aerial spray drift in an offshore oil spill context, it should be capable of meeting the following requirements. As not all models are capable of representing the process directly, an order of precedence has been established for the requirements such that the selection process may be as broad as possible. The model should:

(i) **Have recognition as a tool for use in establishing the impact caused by dispersion of chemicals:** Any dispersion model should have recognition from a US-based regulator in the use of evaluating the atmospheric dispersion of chemicals. The process of gaining a recommendation from a regulator such as the US EPA is strenuous, and as such will ensure that the model has undergone sufficient peer review to gain acceptance.

(ii) **Be capable of directly computing the influences on drift from aircraft:** Any model selected must be capable of computing the impact of fluid dynamic effects caused by the wake of the aviation platform being used for dispersant spraying.

(iii) **Be capable of modeling the dispersion of particles:** As a minimum, the modeling tool must be capable of representing the dispersion of droplets of dispersant as they drift from the release zone to the point where they settle out of the air.

---

1. Note that atmospheric dispersion refers to the dispersal, or drift, of chemicals in air. This phenomenon, as relevant to the current study, is usually referred to as spray drift.

AMOG®

4.3   DESCRIPTION OF EXISTING MODELS

4.3.1   Lagrangian Particle Models

Within the current inventory of US EPA recommended models for conducting pesticide risk assessments from aircraft there are two suitable Lagrangian particle models (US EPA, 2016b):

(i)   **AGDISP (AGricultural DISPersal):** AGDISP is a first-principles model used to predict spray drift from application sites for the purposes of optimizing agricultural spraying operations. The model is capable of estimating downwind deposition from aerial applications and has a library of aircraft to employ for modeling purposes (Alan J. Bilanin, Milton E. Teske, John W. Barry, & Robert B. Ekblad, 1989). AGDISP also incorporates a "Gaussian extension" model to allow drift to be evaluated beyond the limit of its Lagrangian particle model (US EPA, 2010).

(ii)   **AgDRIFT:** AgDRIFT is a modified version of AGDISP, and retains much of the same functionality (Teske, M.E. et al., 2002). The additional algorithms added to AgDRIFT are primarily to allow the estimate of drift from ground and orchard airblast applications, and the tool largely retains AGDISP as the computational engine for aerial applications (Bird, Perry, Ray, & Teske, 2002). As AgDRIFT is functionally equivalent to AGDISP for aerial applications, it has not been evaluated further.

4.3.2   Gaussian Dispersion Models

Within the current inventory of US EPA recommended models for conducting atmospheric dispersion there are four suitable Gaussian dispersion models (US EPA, 2016):

(i)   **Aermod:** Aermod is the default regulatory dispersion model for near-field modeling and incorporates a Gaussian plume model. Aermod also incorporates dry-deposition of particles, allowing particle removal mechanisms to be incorporated into model predictions. This technique assumes that a plume will act in a steady manner, extending to the edge of the model domain, and assumes that the wind field does not change between the point of release and the horizon (i.e. steady-state wind conditions are modeled).

(ii)   **Industrial Source Complex 3 (ISC3):** ISC3 was the default regulatory dispersion model for near-field modeling for permitting purposes prior to the adoption of Aermod. The meteorological data required as an input to Aermod may prevent its use in this particular application, and as such ISC3 may be more appropriate.

(iii)   **CALPUFF:** The CALMET/CALPUFF modeling system is a Gaussian puff model which tracks individual "puffs" of a pollutant as Lagrangian particles, however each particle is itself able to disperse using a Gaussian approach. It is the default regulatory dispersion model for far-field (> 50 km) modeling The Lagrangian approach allows the individual puffs to be tracked with time, and as such provides a much more representative prediction of concentrations downwind as they change with time. The modeling package similarly allows for dry-deposition removal mechanisms to be incorporated into the solution.

(iv)   **AGDISP Gaussian Extension model:** AGDISP incorporates a Gaussian extension model based on the algorithms contained in ISC3. The extension model uses ISC3's Gaussian plume

Document Number - r2015.j520.001
Issued as Revision 1, October 14th 2016
Doc Ref: Atlas:\...\r2015.j520.001.1.odt
amogconsulting.com
EIN 20-4906471
TX PE Firm F-11821

AI-E253-10v20130508

algorithm, however it does not incorporate any removal algorithms. The intent of this approach is to ensure that the predictions are conservative, as over the ground there are numerous particle sinks such as vegetation that have not been considered (US EPA, 2010).

It should be noted that there are a number of removal mechanisms that may cause mass to drop out of the plume. Examples of removal mechanisms include evaporation, deposition on vegetation or over water, waves (Zufall, Dai, Davidson, & Etyemezian, 1999). A number of the plume models discussed, including AGDISP's Gaussian plume extension model, do not account for any removal mechanisms. Gaussian plume models not employing any particle removal mechanism may be considered conservative as particles will only disperse and no mass is removed from the computational domain.

4.4   MODELING SYSTEM FOR FURTHER EVALUATION

An evaluation for the particular application as the computation core of the DST, the ideal candidate was AGDISP due to:

1.   Its recognition by the EPA for evaluating the drift of aerial application of pesticides in agricultural and forestry applications;

2.   Its ability to estimate the aerodynamic forcing caused by the presence of the aircraft using a combination of first-principles and empirical relationships;

3.   Its ability to model the dispersion of particles using a Lagrangian approach, while incorporating the ability to extend this solution through the use of a Gaussian extension model when the spray drift extends beyond the influence of the aircraft wake; and

4.   AGDISP has the benefit of being able to incorporate the influence of atmospheric stability into the modeling results, addressing a key limitation of the CFD models for extending the results of the simulation to all potential environmental conditions at distances beyond the immediate wake region.

4.5   SHORTCOMINGS OF EXISTING TOOLS FOR USE IN OIL SPILL RESPONSE

In recent years, there has been at least one paper which has identified potential issues in AGDISP's representation of the wake under certain crosswind conditions (Ryan et al., 2013). While AGDISP has undergone extensive validation against field trials for its intended purpose in modeling pesticide application, its has not been validated as a tool for modeling the different operational parameters which apply in oil spill response operations. As a result of this, AGDISP drift extent predictions for the aircraft included in the DST were evaluated by comparison with CFD models configured to represent spray systems employed by actual Oil Spill Removal Organizations.

4.5.1   Simplifications Present In AGDISP

To decrease computational time, AGDISP limits which aircraft wake mechanisms are computed, and how these in turn influence the dispersant particles. The factors affecting the wake modeled by AGDISP are as follows (Bird et al., 2002):

Document Number - r2015.j520.001
Issued as Revision 1, October 14th 2016
Doc Ref: Atlas:\...\r2015.j520.001.1.odt
amogconsulting.com
EIN 20-4906471
TX PE Firm F-11821

AI-E253-10v20130508

(i) **Downwash from the wing:** The downwash caused by the lift generated by the wing is estimated using lifting line theory. The downwash is assumed to be uniformly distributed and pointed downward at the trailing edge of the wing.

(ii) **Wingtip vortices:** Similarly estimated assuming an elliptical lift distribution across the wing in conjunction with lifting line theory. The vortex decay rate has been estimated for all airframes to be based on a value established from aircraft flyovers.

(iii) **Propellers:** The influence of propellers is computed using actuator disc theory. In order to establish the required thrust, all aircraft have a default assumed drag coefficient of 0.1, which is typically a conservative value.

(iv) **Crosswind:** The influence of crosswind is computed on the basis of the vertical velocity gradient predicted by an atmospheric boundary layer approach.

The simplified approach adopted by AGDISP neglects the following additional sources of aerodynamic influences on the dispersant behavior:

(i) **Fuselage wake: T**he influence of the fuselage in contributing to the aircraft wake is neglected.

(ii) **Flap and tail vortices:** AGDISP models only the wingtip vortices, and the generation of vortices by the tail of the aircraft or as a result of the use of flaps is neglected.

Notwithstanding the noted simplifications in AGDISP's modeling of the aircraft wake, results from field trials (Duan, Yendol, Mierzejewski, & Reardon, 1992) indicated that the mechanisms modeled appear sufficient for the agricultural aircraft AGDISP was designed to model.

4.5.2   Different Operational Context

The AGDISP modeling package was designed for use in optimizing pesticide spraying operations employing agricultural aircraft. A significant body of validation data has been built surrounding the use of AGDISP, though this has been largely driven by the Spray Drift Task Force using agricultural aircraft. Many of the studies referenced in the development (Teske, M.E. et al., 2002) and the validation (Duan et al., 1992) of AGDISP cite the use of small agricultural aircraft such as Air Tractors, or variants of the Cessna 188 (e.g. Ag Truck, Ag Husky, etc.).

The majority of the aircraft employed in the offshore oil spill response context are larger, multi-engined aircraft with significantly larger tank capacities, though some cross-over occurs (i.e. Air Tractor AT-802A). Furthermore, the offshore context requires a large quantity of dispersant to be released as rapidly as possible (US Coast Guard, 2013b). This difference in operational context and aircraft types was evaluated for its potential impact on the prediction of spray drift.

4.6   CFD STUDY

As described in Section 4.5, AGDISP was identified as the most suitable of the existing tools for determining the extent of dispersant spray drift. CFD modeling of each of the aircraft to be incorporated into the DST was conducted in order identify any flow features around the aircraft which significantly affect the spray drift that are not accounted for by AGDISP. In order to achieve this aim, the CFD models were critical to perform the following functions:

AMOG®

AI-E253-10v20130508

- Resolve the aerodynamic flow features around the aircraft likely to impact on the spray release trajectory. In particular, resolution of the overall lift generation, strength and location of vortical structures and large-scale wake/blockage effects should be resolved.

- Represent the aircraft geometry to a level of detail commensurate with the first objective, removing any geometric detail which will not have a significant effect on the aerodynamics affecting the spray release.

- Implement a representative model of the propellers in order to resolve the effect of the propeller wash on the spray release.

- Model the trajectory of the spray droplets, accounting for aerodynamic forces on the particles and, in particular, turbulent dispersion.

It should be noted that many of the organizations identified in Phase 1 of the project were unable to provide the required aircraft geometry and operational parameters. Direct contact was made with aircraft and propeller manufacturers, and data was obtained where possible from publicly available sources. While the lack of data inconvenienced both the model construction and validation activities, efforts were made to ensure that the CFD study was conducted in accordance with best practice, and that any assumptions made have been documented for traceability. The full details of the methodology employed and the results obtained are included in Appendix B - CFD Methodology and Full Results.

4.7   EXISTING TOOLSET EVALUATION

Based on an assessment of the capabilities of the existing modeling tools, AGDISP was selected as the tool most suitable for modeling the aerial dispersant spray release. In order to determine whether the identified simplifications in AGDISP have a significant effect on the predicted drift extent, the predicted fraction aloft with distance from AGDISP was compared to the results from CFD simulations for similar spraying conditions. The results of this comparison are presented below. The comparison was conducted based on answering the following questions shown in Table 2.

Table 2: Questions Tested In AGDISP-CFD Comparison

No.	Question	Answer
1	In general, is there good correlation between the CFD and AGDISP results in the near field region?	Yes /No
2	For crosswind cases which model is more conservative?	AGDISP/CFD
3	For intermediate wind direction cases which model is more conservative?	AGDISP/CFD
4	For headwind cases which model is more conservative?	AGDISP/CFD
5	Does altitude change which model is more conservative?	Yes/No
6	Does aircraft speed change which model is more conservative?	Yes/No
7	Does dispersant particle size distribution change which model is more conservative?	Yes/No

Document Number - r2015.j520.001
Issued as Revision 1, October 14th 2016
Doc Ref: Atlas:\...\r2015.j520.001.1.odt
amogconsulting.com
EIN 20-4906471
TX PE Firm F-11821

AI-E253-10v20130508

This comparison was made for each airframe by extracting the following variables from the CFD models and entering them into AGDISP:

- Wind speed and direction;

- Release height;

- Aircraft drag;

- Aircraft mass (based on the lift generation predicted by the CFD model for each case);

- Propeller rotation rate; and

- Spray nozzle positions, particle size distribution and flow rate.

All other variables were set to the default settings in AGDISP.

Full details of the comparative study conducted are contained in Appendix B. The key outcomes of the CFD evaluation of the AGDISP modeling system for use in offshore spill response are summarized as follows:

- Air Tractor AT-802A: For the purposes of offshore spill response, the AT-802A is well represented by AGDISP in that no significant modifications to the results are required. Interpretation and extrapolation of AGDISP results were required for wind angles outside of AGDISP's allowable input range.

- Lockheed C-130A: It has been identified that, due to the wake effect caused by the shape of the fuselage in the vicinity of the rear cargo door, the results from AGDISP are not representative in the near field, in that the fuselage wake delays the deposition of the spray. However, in the far field, AGDISP predicts a lower deposition rate than the CFD model, and as such AGDISP results may be modified to provide a conservative estimate of the extent of spray drift. Interpretation and extrapolation of AGDISP results were required for wind angles outside of AGDISP's allowable input range.

- Douglas DC-3: Due to the presence of vortices generated at the outboard end of the main wing flaps, and the spray boom extending sufficiently along the wing semi-span to inject particles into the combined flap and wing tip vortices, the DC-3 is poorly represented by AGDISP, and an alternative approach is required to determine the drift impacted area.

- Douglas DC-4: The DC-4 has a unique spray boom which lies above the trailing edge of the wing. AGDISP will not allow spray nozzle positions above the trailing edge of the wing, as such, the DC-4 cannot be modeled using AGDISP. While the presence of flap vortices also appears to influence the DC-4 spray, the closer proximity of the flaps to the wing tips causes the two vortices to merge earlier than those generated by the DC-3, reducing the influence of the flap vortices.

AI-E253-10v20130508

5   DST DEVELOPMENT

This section describes the development of the DST, subsequent to the identification of the adequacy, or otherwise, of AGDISP for predicting the dispersant spray drift extent from each of the aircraft under consideration. The development activities included the implementation of detailed methodologies for the prediction of drift extent for each aircraft, as well as the actual development of the DST software.

5.1   DRIFT EXTENTS ESTIMATES INCORPORATED INTO THE DST

Based on the outcomes of the comparative evaluation of the CFD models and AGDISP, tailored methodologies were developed to obtain estimates of the drift extent of dispersant spray released from each of the aircraft under consideration.

5.1.1   Methodology For Air Tractor AT-802A

AGDISP has been demonstrated to accurately represent the aerodynamic phenomena influencing the behavior of the dispersant spray released by the AT-802A, and is therefore considered suitable for incorporation within the DST. The algorithm detailed in Figure 11 was used to provide conservative drift extent estimates for the AT-802A.

The algorithm approach was based on a combination of the following factors:

1.   Where conditions were outside of those AGDISP is capable of computing natively, application of a computation of intermediate angles using sine and cosine components of the maximum crosswind extent (defined as the predicted extent with the same wind speed but a wind angle at 90 degrees). The change in spray drift extent for intermediate wind angles has been investigated, as reported in Appendix B. In effect, it was identified that these could be predicted by computing the lateral and track wise components using the wind angle.

2.   An uplift of the AGDISP predicted spray extents based on comparisons between the CFD model and AGDISP as well as comparisons between the crosswind extent and the headwind axial extent, it was identified that AGDISP predicted a slightly lower extent by approximately 10% to 15%. As such, a scaling factor of 15 % to address this uncertainty has been applied prior to computing the crosswind components where lateral and track wise resolution of the drift extents was required.

3.   A minimum drift prediction is based upon a published investigation of lateral spread of vortices in still conditions in ground effect at a speed of 4 kn (Hallock, 1991). This was considered to be a reasonable conservative minimum for all cases where the wind speed in the lateral direction was less than 4 kn.

AMOG®

AI-E253-10v20130508

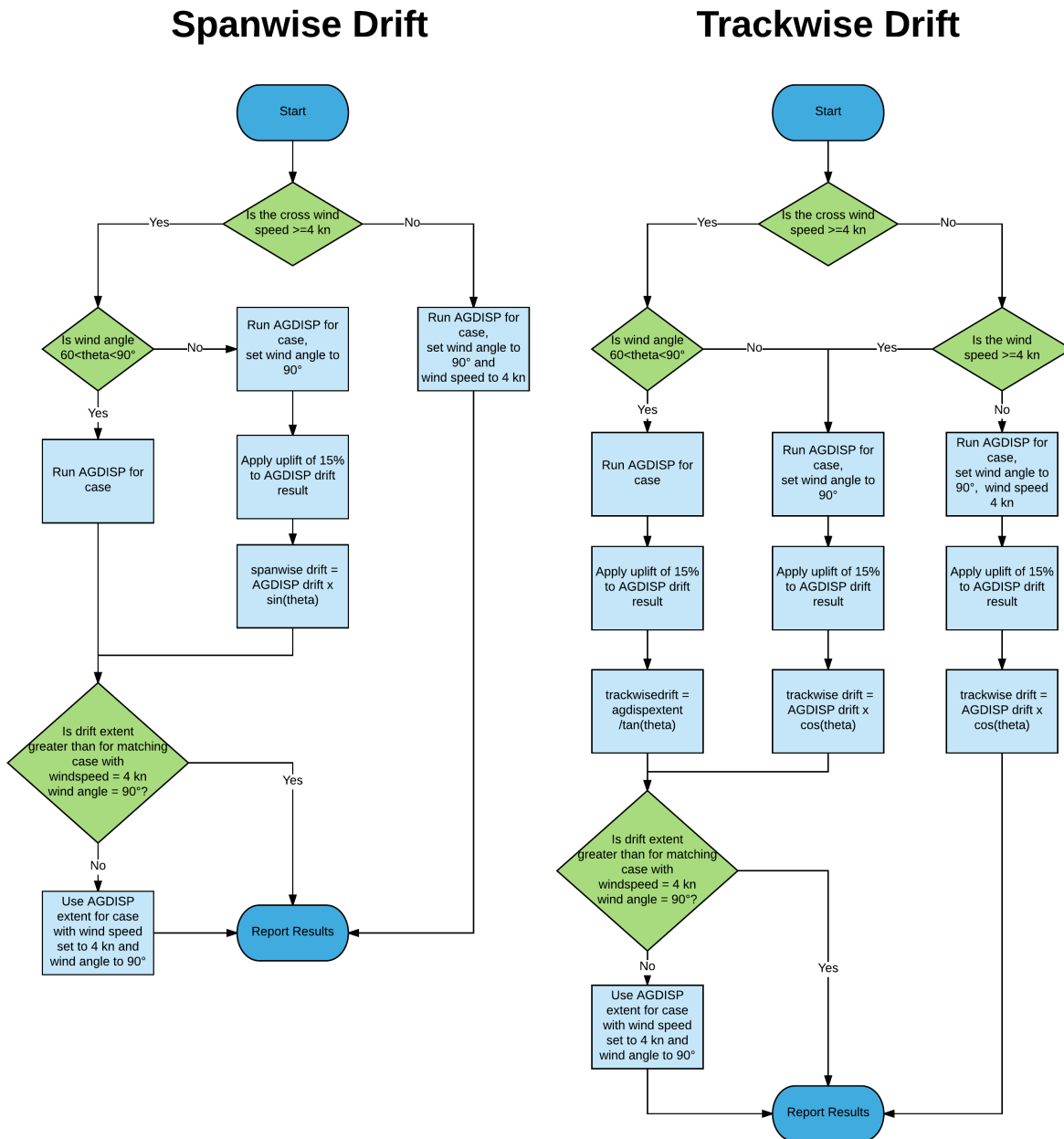# Spanwise Drift

Trackwise Drift

Figure 11 : Drift Extent estimate algorithm for AT-802A and C-130

5.1.2   Methodology For Lockheed C-130A

While a deficiency was identified in AGDISP's representation of the C-130A, this was determined to only affect the near-field results. The effect of this is that the amount of mass remaining aloft is under-represented by AGDISP close to the aircraft, but at larger distances the behavior of the dispersant is conservatively modeled, albeit from the incorrect starting point of an under-prediction of the amount of mass aloft. Accordingly, a scaling factor was applied to the spray drift extents predicted by AGDISP in order to produce a conservative estimate of the spray drift extent from the C-130. This scaling factor is in addition to the 15 % scaling factor for resolution of lateral and track wise drift components as discussed in Section 5.1.1 above. The algorithm used to generate the drift estimates for different wind directions is otherwise identical to that applied in Figure 11.

5.1.2.1   Development Of Scaling Factor For The C-130A

To develop the required scaling factor for the estimation of drift extent from the C-130A, three scenarios were identified as suitable for direct comparison between AGDISP and the extended CFD results (with the conditions described below). These cases all considered a crosswind of 20 kn at a variety of flight speeds and altitudes, with the results of the comparison presented in Table 3.

The fuselage scaling factor was calculated by:

- Identifying the fraction aloft for which the difference between the CFD and AGDISP predictions is greatest.

- Determining the percentage difference in predicted distance at this fraction aloft.

- Applying this to all AGDISP results for the C-130A.

The maximum difference between the CFD results and the AGDISP simulations occurs at a similar fraction aloft and distance behind the aircraft in all the cases investigated. The maximum difference in extent for a given fraction aloft was found to be 150 ft (a maximum difference of 38 %). In order to be conservative a 40 % scaling factor was applied to all AGDISP results for the C-130. This is considered appropriately conservative in light of the simplifications and assumptions made in generating the C-130A CFD model.

Table 3: Assessment Of CFD And AGDISP For Scaling Factor

Wind Speed (kn)	Altitude (ft)	Ground Speed (kn)	Fraction of spray aloft at maximum difference	CFD Distance at Threshold (ft)	AGDISP Distance at Threshold (ft)	Difference (ft)	Difference
20	75	150	0.42	490.1	354.6	135.5	38 %
20	100	150	0.43	634.5	477.7	156.8	33 %
20	100	200	0.58	523.6	394.3	129.3	33 %

Document Number - r2015.j520.001
Issued as Revision 1, October 14th 2016
Doc Ref: Atlas:\...\r2015.j520.001.1.odt
amogconsulting.com
EIN 20-4906471
TX PE Firm F-11821

AI-E253-10v20130508

5.1.3 Methodology For Douglas DC-3 And DC-4

The comparison between the CFD and AGDISP results indicated that the DC-3 and DC-4 could not be accurately modeled within AGDISP. As such, the following algorithm was used to model these aircraft:

1. Identify a distance behind the aircraft where the vortical structures have largely stabilized and formed clear, distinct vortices.

2. At this distance, extract the following data on a cut plane, perpendicular to the aircraft's direction of travel, through the aircraft wake:

    2.i. The position, strength and size of the wake vortices; and

    2.ii. The droplet sizes and positions of the dispersant spray remaining aloft at the cut plane.

3. Use inviscid vortex transport and a Lagrangian particle model to calculate the distance at which 99 % of the particle mass has touched down.

This methodology relies on having CFD simulations to initialize the inviscid vortex transport calculation. To minimize the number of CFD cases required a limited case list was generated to determine the effect of wind speed and direction on spray drift. To develop a database with sufficient resolution for inclusion in the DST, the vortex and particle properties at cases not simulated were interpolated based on the limited case list.

Aside from sea surface deposition, no removal mechanisms were modeled in the Lagrangian particle calculations. Particles were modeled until the point of impact on the sea surface and the sea surface was assumed to be flat. In reality wave action and evaporation may contribute to mass loss from the dispersant spray plume. Given that the Lagrangian Particle calculations do not include these removal mechanisms the predicted extent of spray drift is considered conservative.

5.1.4 Impact Of Dispersant Outside The 99 % Mass Fraction Boundary

The DST calculates spray drift extents based on the predicted distance to 99 % of the released mass touching down on the sea surface. This is considered to be a conservative measure of drift extent. While a detailed assessment of the variation in concentration of dispersant with distance away from the aircraft has not been conducted, preliminary calculations indicate that remaining 1 % of mass represents approximately 0.03 ounces of dispersant for every foot traveled by the aircraft. If the entirety of the mass falling outside the 99 % boundary was assumed to fall within a 1 foot wide corridor, this would result in a surface concentration of dispersant of 0.03 ounces/square foot. In reality the surface concentration will be significantly lower, as the dispersant will spread out as it drifts away from the point of release, and the area impacted by the final 1 % of mass will cover a distance from the 99 % boundary significantly greater than 1 foot.

AMOG®

5.1.5   Response Surface Of Extent Data

Based on the algorithms presented in Sections 5.1.1 to 5.1.3 databases were created for each aircraft containing data for the maximum extent behind and perpendicular to the aircraft.

Each unique point in the data base is defined by four variables: aircraft velocity, aircraft altitude, wind direction and wind speed. For each of these data points there is a maximum extent behind the aircraft and perpendicular to the aircraft which was derived using the algorithms described in Sections 5.1.1 to 5.1.3.

To ensure that a smooth response surface was created that captured any local minima and maxima in the solution a large number of cases were considered, for example the C-130A database has over 12,000 data points within the operational envelope.

Figures 12 and 13 show 3D representations of the response surfaces generated for the C-130A for a number of altitudes. The red points indicate the actual data while the surface contour shows the surface fit to the data points.

The extent behind the aircraft shown in Figure 12 shows a trend of increasing extent with increasing wind speed at small angles (i.e. headwinds). Similarly the extent perpendicular to the aircraft (Figure 13) shows a trend of increasing extent with increasing wind speed at large wind angles (i.e. crosswinds). In both cases the extent increases with higher altitudes.

In addition to the expected trends in the results there are two important features of the surfaces that are a result of the algorithms used to generate them:

●   In cases where the relevant component of the wind is less than 4 kn the extent predicted is constant. This is a result of the 4 kn minimum wind speed applied to low wind cases, this provides a conservative estimate of the extent at low wind speeds.

●   At a wind angle of 60° there is a discontinuity in the surface. This is the boundary between results that can be directly simulated in AGDISP and those which have been calculated using AGDISP with an additional scaling factor to account for the altered direction. The scaling factor causes a discontinuity at the interface with a more conservative prediction used for the non-standard AGDISP cases. It should be noted that as AGDISP was not used to generate data for the DC-3 and DC-4 airframes, this feature is not present in the response surfaces for those aircraft.

Similar response surfaces were generated for the AT-802A, DC-3 and DC-4, and are incorporated into the DST.

Document Number - r2015.j520.001
Issued as Revision 1, October 14th 2016
Doc Ref: Atlas:\...\r2015.j520.001.1.odt
amogconsulting.com
EIN 20-4906471

TX PE Firm F-11821

AI-E253-10v20130508

Response Surface Maximum Extent X (Altitude)
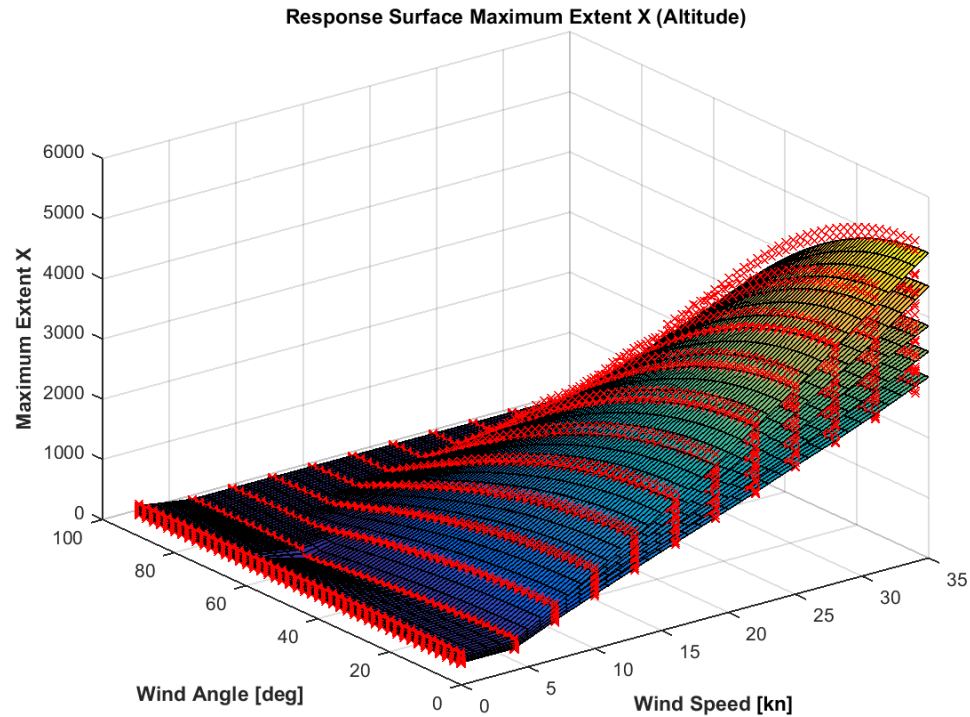
Figure 12 : Response surface for the C-130A spray drift behind the aircraft.

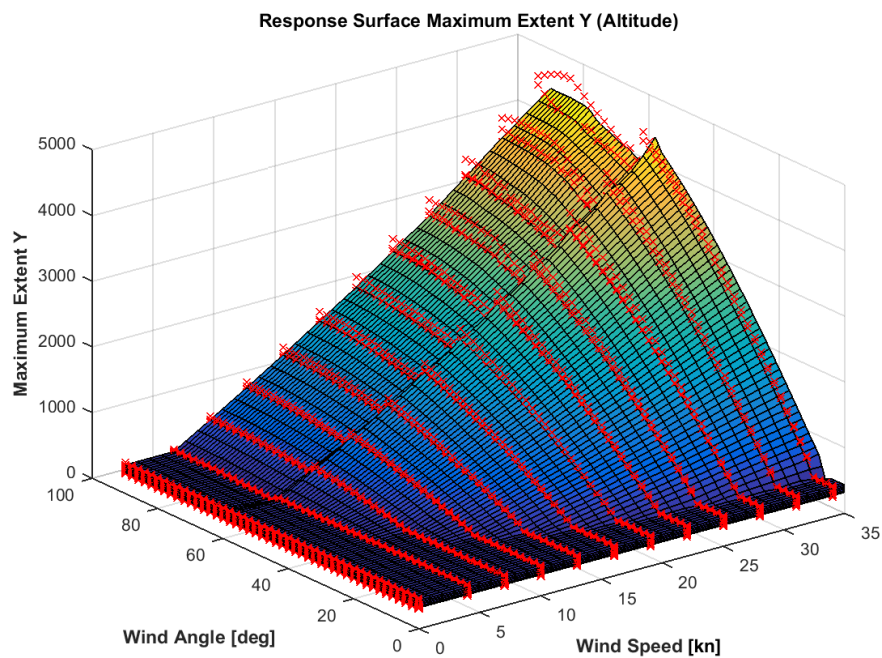**Response Surface Maximum Extent Y (Altitude)**

Figure 13 : Response surface for the C-130A spray drift perpendicular to the aircraft.

5.1.6 Analysis Of Data Set

Inspection of the data set incorporated into the DST provides the maximum (i.e. crosswind) spray drift extents shown in Table 4 when using each of the four aircraft. The drift extents listed are predicted when flying at 90 degrees to a 20 knot crosswind and at the maximum altitude for the respective airframes. This corresponds to an altitude of 100 feet for the C-130A, DC-3 and DC-4, and 50 feet for the AT-802A.

Table 4: Maximum Crosswind Drift Extents

Aircraft	Perpendicular Drift Extent (ft)
DC-3	10,550
DC-4	8,250
C-130A	7,400
AT-802A	2,650

Additionally, the maximum spray drift extents predicted when spraying in headwind conditions are as shown in Table 5. The drift extents listed are when flying at 10 degrees to a 35 knot headwind and at the maximum altitude for the respective airframes. These conditions were selected as a realistic bound on operations conducted in the maximum strength headwind.

Table 5: Maximum Headwind Drift Extents

Aircraft	Perpendicular Drift Extent (ft)
DC-3	2,350
DC-4	1,500
C-130A	2,750
AT-802A	900

Noting that spray operations are generally conducted with the aircraft flying into the wind, the results shown in Table 5 are considered representative of the drift extents which could be used as input into determining setback distances during operations in the highest operable wind strength. These distances compare favorably with the setback distances of over 2 nautical miles (approximately 12,000 feet) which were used in the response to the Deepwater Horizon spill.

Significant differences exist between the predicted drift extents for the four airframes considered. While the low drift extents for the AT-802A are largely driven by the lower altitude used in modeling that aircraft (50 feet vs 100 feet for the other three aircraft), the differences between the DC-3, DC-4 and C-130A are influenced by a number of factors, including aircraft weight, flap configurations and spray boom length. The use of long spray booms on the DC-3, which inject dispersant into the airflow in the vicinity of the wingtip vortices, is likely to influence the large drift extents predicted for the DC-3.

Document Number - r2015.j520.001
Issued as Revision 1, October 14th 2016
Doc Ref: Atlas:\...\r2015.j520.001.1.odt
amogconsulting.com
EIN 20-4906471
TX PE Firm F-11821

AI-E253-10v20130508

5.2   SOFTWARE DEVELOPMENT

The development of the DST was undertaken using a structured approach. This approach was designed to maximize the usability and expandability of the end product. The following activities were conducted:

- User Engagement – In Phase 1 on the project a number of potential end users were identified as potential stakeholders. Workshops were conducted to determine what functionality was desired in the DST.

- Requirements Specification - At the conclusion of the user engagement process a requirements specification was developed which summarized the functionality requirements for both a planning and operational mode. This defined the requirements of the DST.

- Technical specification – using the requirements specification a methodology was developed for delivering the functionality required. Throughout this process of developing a methodology a number of additional inputs and outputs were identified and high level design of the algorithms was documented.

- Flow charting of DST algorithms – Based on the technical specification flow charts were developed to identify the information flow throughout the algorithm. This process helped to determine the best data structures for the DST and develop a modular architecture that facilitates expansion of the DST.

- Modular code development and testing – Based on the flow charts modules were created for each of the main processing algorithms (as shown in Figure 8). Each module was created independently and verification tests for each module were conducted before the modules were combined into the main DST program.

- GUI interface design – Based on the requirements specification a number of GUI windows were mapped out. Coding of these GUI pages was done using the ABSOFT Fortran libraries interfacing with the Qt graphics package.

- DST Verification and testing – Once the DST was completed a comprehensive validation test suite was developed to test the inputs and outputs of the code for a set of known values. In addition to this an alpha version of the code was distributed to project staff for testing of the GUI interface.

5.3   SOFTWARE VERIFICATION

In order to demonstrate that the DST was developed in accordance with the requirements identified in Phase 1 of the project (as reported in the Requirements Specification included as Appendix C to this report), a verification activity was conducted whereby the performance of the software against each of the identified requirements has been documented. The documented verification of the DST is included as Appendix D to this report. It should be noted that repeated statements of a requirement in the Requirements Specification have been omitted for clarity.

Document Number - r2015.j520.001
Issued as Revision 1, October 14th 2016
Doc Ref: Atlas:\...\r2015.j520.001.1.odt
amogconsulting.com
EIN 20-4906471
TX PE Firm F-11821

AI-E253-10v20130508

The DST has full or partial compliance against all of the requirements outlined in the specification in Appendix C. The only requirement for which partial compliance was achieved was in relation to an optional output in terms of concentration contours. It was noted in the specification that:

This is a preference that was raised at the Working Group Meeting; whether it is included in the final program will depend on its feasibility with the CFD technique implemented.

Concentration gradient was not developed in this scope of work. However, the architecture of the DST has been developed such that only minor alterations to the database structure would be required to provide a concentration gradient output.

Document Number - r2015.j520.001
Issued as Revision 1, October 14th 2016
Doc Ref: Atlas:\...\r2015.j520.001.1.odt
amogconsulting.com
EIN 20-4906471
TX PE Firm F-11821

AI-E253-10v20130508

6 CONCLUSIONS

The following conclusions are made as a result of the work undertaken during the project:

1. A Decision Support Tool has been developed which meets the requirements identified during the stakeholder engagement phase of the project.

2. Of the existing regulatory models used to predict the aerial extent of spray drift, AGDISP was identified as the most appropriate for use in offshore applications

3. High fidelity CFD models were used to predict the dispersant spray drift. The following major findings were made as a result of the CFD modeling activities:

    3.i. Qualitative validation of the results showed that the CFD models captured the significant flow structures affecting the dispersant trajectories.

    3.ii. The flap vortices and fuselage wake were found to have a significant effect on the dispersant spray drift for the C-130A, DC-3 and DC-4. These effects are widely acknowledged features of the wake generated by aircraft, but have not previously been studied with regard to their effect on dispersant spray drift.

    3.iii. For AT-802A and C-130A the wind angle did not significantly affect the total distance travelled by spray drift. As such, for wind directions outside the allowable input range of AGDISP, spray drift can be predicted on the basis of post-processed AGDISP extents.

    3.iv. A set of AGDISP input parameters was developed which provided appropriately conservative estimates of spray drift for the C-130A and the AT-802A.

4. The high fidelity CFD study found that for some aircraft, AGDISP was not capturing important flow features and was under predicting the extent of spray drift. Specifically for each airframe the following was found:

    4.i. AGDISP is a suitably conservative tool for modeling the drift extent of dispersant sprayed from an Air Tractor AT-802A. The DST uses AGDISP results to estimate the extent of spray drift for this aircraft.

    4.ii. The simplifications inherent in AGDISP (in particular the omission of fuselage wake effects) result in an inability to accurately characterize the near field behavior of dispersant sprayed from a Lockheed C-130A. This inaccuracy can be corrected for by applying a correction factor derived from the difference between the CFD and AGDISP results. The DST uses the factored AGDISP results to estimate the extent of spray drift for this aircraft.

    4.iii. AGDISP is unable to accurately represent the spray release from the DC-3, owing to the presence of main wing flap vortices, which are not modeled in AGDISP and their relative proximity to spray nozzles. The DST uses the results from the CFD models (as extended by a Lagrangian particle calculation) to estimate the extent of spray drift for this aircraft.

    4.iv. AGDISP is unable to accurately represent the spray release from the over wing arrangement used on the DC-4, and the resulting inaccuracy cannot be corrected. The DST uses the results from the CFD models (as extended by a Lagrangian particle calculation) to estimate the extent of spray drift for this aircraft.

Document Number - r2015.j520.001
Issued as Revision 1, October 14th 2016
Doc Ref: Atlas:\...\r2015.j520.001.1.odt
amogconsulting.com
EIN 20-4906471
TX PE Firm F-11821

AI-E253-10v20130508

5. The DST predicts drift extents for each of the four aircraft modeled which, particularly in headwind conditions, are significantly less than the setback distances which have been used in previous oil spill response campaigns. The maximum (i.e. crosswind) setback distances were found to be:

    5.i.   DC-3 – 10,550 feet;

    5.ii.   DC-4 – 8,250 feet;

    5.iii.   C-130A – 7,400 feet; and

    5.iv.   AT-802A – 2,650 feet.

6. The DST accounts for the effects of wind strength and directions such that in favorable conditions (i.e. lower wind strength), setback distances may be defined which are significantly lower than those which have been previously used.

7. Significant differences exist between the predicted drift extents for the four airframes considered. While the low drift extents for the AT-802A are largely driven by the lower altitude used in modeling that aircraft (50 feet vs 100 feet for the other three aircraft), the differences between the DC-3, DC-4 and C-130A are influenced by a number of factors, including aircraft weight, flap configurations and spray boom length. The use of long spray booms on the DC-3, which inject dispersant into the airflow in the vicinity of the wingtip vortices, is likely to influence the large drift extents predicted for the DC-3.

Document Number - r2015.j520.001
Issued as Revision 1, October 14th 2016
Doc Ref: Atlas:\...\r2015.j520.001.1.odt
amogconsulting.com
EIN 20-4906471
TX PE Firm F-11821

AI-E253-10v20130508

7   RECOMMENDATIONS

During the project a number of phenomenon and trends affecting spray drift were observed. The CFD investigations in particular identified a number of key flow features affecting spray drift behavior. Based on the work conducted and the results obtained during this project, a number of recommendations have been made, as follows.

7.1   AREAS FOR FURTHER INVESTIGATION

7.1.1   Extensions To Existing Model Inventory

A large number of airframes are used during oil spill response operations. Only a small subset of these have been included in the initial release of the DST. Furthermore there are a number of different spray configurations and parameters that have a significant impact on spray drift that should be assessed and could be included in the DST inputs. These include:

(i)   Additional Airframes.

(ii)   Multiple spray systems for each aircraft (different boom layouts or nozzle dimensions).

(iii)   Different particle size distributions. In the current scope of work the American Society of Agricultural Engineers (ASAE) Medium to coarse distribution was applied to all airframes. This was selected on the basis of a limited amount of data. Coarser particle size distributions are likely to lead to smaller extents of drift.

(iv)   Multiple dispersant options, for example gel dispersants or other liquid dispersant varieties. This study only investigated the Corexit EC9500A dispersant.

(v)   The inclusion of multiple mass removal mechanisms from the spray cloud including, for example, evaporation.

(vi)   Modeling of the DC-3 without flaps deployed, which would allow realistic evaluation of higher ground speeds and wind speeds, thereby extending the DC-3 drift extent prediction parameter space.

7.1.2   Quantitative Validation Of CFD Results

No quantitative data from experimental spray trials was available during the CFD validation activities. While the CFD models were qualitatively validated against images of dispersant spray operations, and the modeling was conducted in accordance with best practice, quantitative validation of the predicted drift extents would increase confidence in the results of the CFD models. The resulting increased confidence in the CFD models is likely to provide the following:

(i)   AT-802A – Confirmation that AGDISP is a suitably conservative tool for modeling the extent of spray drift. If AGDISP is found to be overly conservative, a CFD model could be used to provide higher fidelity estimates of the spray drift in order to reduce setback distances.

(ii) C-130A – A reduction in the degree of conservatism applied in factoring the results from AGDISP. If CFD results compare well with the experimental data, the CFD models could be used directly to predict the drift extent. This would likely lead to a reduction in setback distances.

(iii) DC-3 and DC-4 – Increased confidence in the modeling results. This would then lead to a reduction in setback distances as lower safety factors could appropriately be used by the operators of the DST.

Accordingly, it is recommended that OSROs be asked to provide spray trial data to enable quantitative validation of the modeling results. Furthermore, consideration should be given to requiring spray trials to be conducted before granting approval for new airframes and/or spray systems to be used in oil spill response. Data acquired from such programs could be used to update the DST.

7.1.3 Determination Of Surface Concentration Of Dispersant

Consideration should be given to modifying the DST to provide concentration of dispersant as an output. Contours of dispersant deposition could be used to help oil spill responders confirm they are applying sufficient spray to the oil spill. If contours of a ground level concentration (in the air or in the water) are generated, this may be linked to acceptable concentrations in terms of human health impacts.

7.1.4 Human Health And Environmental Impact Assessment

Consideration should be given to studying the health effects of dispersants with a view to determining the allowable exposure threshold. This should include dermal and inhalation limits, including exposure to the eyes. Such health effect studies could further inform exposure limits for setback distances.

7.2 CONDUCT OF SPRAYING OPERATIONS

7.2.1 Use Of The DST

The DST should be used with appropriate safety factors applied to its drift extent outputs. When determining the appropriate factor for a given oil spill operation, consideration should be given to:

(i) The modeled aircraft, operational parameters and spray system properties used to generate the data in the DST, and any differences with actual values.

(ii) The inbuilt conservatism in the AT-802A and C-130A drift extent predictions (achieved through the use of AGDISP), which is greater than that for the DC-3 and DC-4.

(iii) Changes to conditions during operations which may affect the accuracy of the drift extent predictions made by the DST. Operators should continue to use spotter aircraft to ascertain whether drift extent is exceeding the predictions made.

Document Number - r2015.j520.001
Issued as Revision 1, October 14th 2016
Doc Ref: Atlas:\...\r2015.j520.001.1.odt
amogconsulting.com
EIN 20-4906471
TX PE Firm F-11821

AI-E253-10v20130508

It should be noted that the DST provides an assessment of operability based on the input weather conditions only. Additional factors such as precipitation or thunder storms may impact on operability in conditions that are otherwise suitable for conducting spraying operations. Final decisions as to whether or not operations are conducted should be made by the pilots in charge considering all available information as to the safety of conducting spraying operations.

7.2.2 Selection Of Aircraft And Spray Systems

The results obtained in developing the DST indicate that spray drift extents vary considerably for the various aircraft considered. This project has resulted in the development of models which may in future be used to determine the effects of spray system parameters on the drift extent. While the selection of specific aircraft is likely to be informed by considerations other than spray drift extent (such as availability and aircraft flight range), ongoing development of spray systems should, where practical, consider the selection of spray boom geometry in order to minimize the spray drift extent.

Document Number - r2015.j520.001
Issued as Revision 1, October 14th 2016
Doc Ref: Atlas:\...\r2015.j520.001.1.odt
amogconsulting.com
EIN 20-4906471
TX PE Firm F-11821

AI-E253-10v20130508

8   REFERENCES

Alan J. Bilanin, Milton E. Teske, John W. Barry, & Robert B. Ekblad. (1989). AGDISP: The Aircraft Spray Dispersion Model, Code Development and Experimental Validation. *Transactions of the ASAE*, *32*(1), 0327–0334. http://doi.org/10.13031/2013.31005

Benggio, B. (2009). *NOAA Dispersant Mission Planner 2*. Presented at the Caribbean Regional Response Team Fall Meeting, St Croix. Retrieved from http://www.crrt.nrt.org/production/NRT/RRTHome.nsf/AllPages/rrt_caribbean-meetingsummaries.htm?OpenDocument

Bird, S. L., Perry, S. G., Ray, S. L., & Teske, M. E. (2002). Evaluation of the AgDISP aerial spray algorithms in the AgDRIFT model. *Environmental Toxicology and Chemistry*, *21*(3), 672–681. http://doi.org/10.1002/etc.5620210328

Davis, B. J. (2010, June 24). Air Force Reserve's 910th Airlift Wing provides initial response to Deepwater Horizon spill. Retrieved from http://www.youngstown.afrc.af.mil/News/ArticleDisplay/tabid/822/Article/179269/air-force-reserves-910th-airlift-wing-provides-initial-response-to-deepwater-ho.aspx

Duan, B., Yendol, W. G., Mierzejewski, K., & Reardon, R. (1992). Validation of the AGDISP aerial spray deposition prediction model. *Pesticide Science*, *36*(1), 19–26.

Hallock, J. N. (1991). *Aircraft Wake Vortices: An Assessment of the Current Situation* (Final Report No. DOT-FAA-RD-90-29) (p. 68). Washington DC: US Department of Transport. Retrieved from http://www.dtic.mil/dtic/tr/fulltext/u2/a231658.pdf

IPIECA-OGP. (2012). *Current status and future industry needs for aerial dispersant application* (Final Report No. Finding 14) (pp. 1–16). London: IPIECA-OGP JIP.

Oil Spill Response Limited. (2013). Subsea Well Intervention Service EGM June 2013 - Petronas_Aviation_14th_Aug_14.pdf. Retrieved April 21, 2015, from http://www.oilspillresponse.com/files/Papers%20& %20Presentations/2014/Petronas_Aviation_14th_Aug_14.pdf

Ryan, S. D., Gerber, A. G., & Holloway, A. G. L. (2013). A Computational Study on Spray Dispersal in the Wake of an Aircraft. *Transactions of the ASABE*, *56*(3), 847–868.

Teske, M.E., Sandra L. Bird, David M. Esterly, Thomas B. Curbishley, Scott L. Ray, & Steven G. Perry. (2002). AgDRIFT: A Model for Estimating Near-Field Spray Drift From Aerial Applications. *Environmental Toxicology and Chemistry*, *21*(3), 659–671.

Title 33—Navigation and Navigable Waters, 33 CFR 154 - Facility Transferring Oil or Hazarous Materials in Bulk Electronic Code of Federal Regulations § Part 154—Facilities Transferring Oil or Hazardous Material in Bulk (2016). Retrieved from http://www.ecfr.gov/cgi-bin/text-idx? tpl=/ecfrbrowse/Title33/33cfr154_main_02.tpl

Title 40 - Protection of Environment, 40 CFR 300 - National Oil and Hazardous Substances Pollution Contingency Plan Code of Federal Regulations § Part 300—National Oil and Hazardous Substances

Document Number - r2015.j520.001
Issued as Revision 1, October 14th 2016
Doc Ref: Atlas:\...\r2015.j520.001.1.odt
amogconsulting.com
EIN 20-4906471
TX PE Firm F-11821

AI-E253-10v20130508

Pollution Contingency Plan (2016). Retrieved from http://www.ecfr.gov/cgi-bin/text-idx?tpl=/ecfrbrowse/Title40/40cfr300_main_02.tpl

US Coast Guard. (2013a, April). Guidelines for the U.S. Coast Guard Oil Spill Removal Organization Classification Program. US Department of Homeland Security.

US Coast Guard. (2013b, April 24). Oil Spill Removal Organization (OSRO) Classification Program. MER Poicy Letter 03-13.

US EPA. (2016a, February 23). Preferred/Recommended Models | TTN - Support Center for Regulatory Atmospheric Modeling. Retrieved June 27, 2016, from https://www3.epa.gov/ttn/scram/dispersion_prefrec.htm

US EPA, O. (2016b, June 1). Models for Pesticide Risk Assessment [Data and Tools]. Retrieved June 27, 2016, from https://www.epa.gov/pesticide-science-and-assessing-pesticide-risks/models-pesticide-risk-assessment

Zufall, M. J., Dai, W., Davidson, C. I., & Etyemezian, V. (1999). Dry deposition of particles to wave surfaces: I. Mathematical modeling. *Atmospheric Environment*, *33*(26), 4273–4281. http://doi.org/10.1016/S1352-2310(99)00177-6

Document Number - r2015.j520.001
Issued as Revision 1, October 14th 2016
Doc Ref: Atlas:\...\r2015.j520.001.1.odt
amogconsulting.com
EIN 20-4906471
TX PE Firm F-11821

APPENDIX A   DST USER MANUAL

Appendix Contents List

Document Name/Number	No Of Pages
t2015.j520.008.1	44
Notes: 1. All documents in this appendix maintain their original numbering.	

AMOG®

Decision Support Tool User Manual

OSSR Program Develop An Innovative Dispersant Spray Drift Model

Bureau of Safety and Environmental Enforcement (BSEE)

Engineering solutions

October 14th 2016

Decision Support Tool User Manual

OSSR Program Develop An Innovative Dispersant Spray Drift Model

Bureau of Safety and Environmental Enforcement (BSEE)

Document Number - t2015.j520.008, Issued as Revision 1   Reference # t2015.j520.008rev1

AC-E253-09v20130508

DOCUMENT ISSUE AND DISTRIBUTION

Document Number	Document Title
t2015.j520.008	Decision Support Tool User Manual

Job Number	Job Title
2015.j520	OSSR Program Develop an Innovative Dispersant Spray Drift Model

Client	Recipient(s)
Bureau of Safety and Environmental Enforcement (BSEE)	Alex Ruttenberg

Client Address	Position(s)
Oil Spill Preparedness Division 4 5600 Woodland Road, Mail Stop VAE-OSPD Sterling VA 20166	Research Specialist

Issue	Date Issued	Author	Checked	Authorised
Revision 1	October 14th 2016	N Boustead P Kurts	P Sincock	D Washington
Revision 0	September 30th 2016	L Ryan P Kurts	P Kriznic	D Washington

DISTRIBUTION OF COPIES

Copy Number	Location
1	AMOG Consulting
2	Bureau of Safety and Environmental Enforcement (BSEE)

REVISION REGISTER

Page	Revision	Date	Comment
26	Revision 1	October 14th 2016	Included warnings and errors for DC-3 spray drift prediction outside of the parameter set.

Document Number - t2015.j520.008
Issued as Revision 1, October 14th 2016
Doc Ref: Atlas:\...\t2015.j520.008.1.odt
amogconsulting.com
EIN 20-4906471
TX PE Firm F-11821

AC-E253-09v20130508

TABLE OF CONTENTS

Document Number - t2015.j520.008
Issued as Revision 1, October 14th 2016
Doc Ref: Atlas:\...\t2015.j520.008.1.odt
amogconsulting.com
EIN 20-4906471
TX PE Firm F-11821

AC-E253-09v20130508

LIST OF TABLES

LIST OF FIGURES

Document Number - t2015.j520.008
Issued as Revision 1, October 14th 2016
Doc Ref: Atlas:\...\t2015.j520.008.1.odt
amogconsulting.com
EIN 20-4906471

TX PE Firm F-11821

AC-E253-09v20130508

ACRONYMS AND ABBREVIATIONS

AMOG	AMOG Consulting Inc.
ASAE	American Society of Agricultural Engineers
BSEE	Bureau of Safety and Environmental Enforcement
CDF	Cumulative Density Function
CFD	Computational Fluid Dynamics
DST	Decision Support Tool
DMP2	Dispersant Mission Planner 2
GIS	Geographic Information System
GLC	Ground Level Concentration
GUI	Graphical User Interface
KML	Keyhole Markup Language
PDF	Probability Density Function
UTC	Coordinated Universal Time
UTM	Universal Transverse Mercator
XML	Extensible Markup Language

Document Number - t2015.j520.008
Issued as Revision 1, October 14th 2016
Doc Ref: Atlas:\...\t2015.j520.008.1.odt
amogconsulting.com
EIN 20-4906471
TX PE Firm F-11821

AC-E253-09v20130508

1 INTRODUCTION

1.1 DST SCOPE

The Decision Support Tool (DST) was developed by AMOG on behalf of the Bureau of Safety and Environmental Enforcement (BSEE) under contract number E15PC00015. The purpose of the DST is to assist planners to identify operational windows and estimate appropriate setback distances for aerial dispersant sorties based on forecast meteorological conditions, aircraft types and release rates.

It is envisioned that the DST will be used in conjunction with existing oil spill response planning tools such as Dispersant Mission Planner 2 (DMP2) [1] and Geographic Information System (GIS) mapping packages for fast and effective planning of oil spill response.

1.2 DST CONCEPT

The DST leverages the numerical accuracy and efficiency of a number of modeling techniques, including AGDISP, and Computational Fluid Dynamics (CFD) simulations. Care was taken when developing the DST to use the most robust models that accurately represent the complex flow structures present behind each aircraft. The results of these models were used to develop a database for each aircraft which is accessed by the DST at run time to predict the extent of spray drift.

1.3 DEFINITION OF MAXIMUM EXTENT

The outputs of the DST planning tool include the maximum extent of spray drift.

The prediction of extent of dispersant drift distance at the sea surface is the horizontal distance from the aircraft flight path at which 99 % of the released mass has touched down.

As this is a definition based on a percentage of mass released from the aircraft, the total mass released will have an influence on the concentration of dispersant at the point of maximum extent. The DST makes no assumptions about what Ground Level Concentration (GLC) of dispersant is acceptable to human health. Use of the maximum extent predicted by the DST should be informed by the toxicology of the dispersant used in the spraying operations.

While a detailed assessment of the variation in concentration of dispersant with distance away from the aircraft has not been conducted, preliminary calculations indicate that remaining 1 % of mass represents approximately 0.03 ounces of dispersant for every foot traveled by the aircraft (for a 5 gpa application rate). If the entirety of the mass falling outside the 99 % boundary was assumed to fall within a 1 foot wide corridor, this would result in a surface concentration of dispersant of 0.03 ounces/square foot. In reality the surface concentration will be significantly lower, as the dispersant will spread out as it drifts away from the point of release, and the area impacted by the final 1 % of mass will cover a distance from the 99 % boundary significantly greater than 1 foot.

Given that the prediction of extent is based on a mass fraction, the DST does not account for multiple spray passes being made. It is assumed that additional spray passes will be made at a full swath width inside the boundary of the area to be sprayed. As such, additional passes will not increase the maximum extent of spray drift. They will however have an impact on the GLC at the distance defined as the maximum extent of spray drift.

1.4   SYSTEM REQUIREMENTS

The DST supports both Windows and Mac OS X operating systems. See Section 5.1 for details of the specific operating system versions for which the software has been tested. The Planning mode of the DST requires the use of a GIS package capable of viewing .kml files, as described in Section 5.3.

Document Number - t2015.j520.008
Issued as Revision 1, October 14th 2016
Doc Ref: Atlas:\...\t2015.j520.008.1.odt
amogconsulting.com
EIN 20-4906471

TX PE Firm F-11821

AC-E253-09v20130508

2 DISCLAIMER

This software has been developed to provide input guidance to the setting of setback distances for aerial dispersant spraying operations for the application of dispersants to maritime oil spills. Its use in other applications should be undertaken with care and no warranty, implied or otherwise is made for its use in such applications.

Whilst every effort has been made to ensure the predictions produced by the software are accurate, the production of the software has required certain assumptions and simplifications to be made. Full details of the technical basis for the software and its development process are contained in the suite of technical reports that accompanied its development.

The predictions produced by this software are intended as a guide only. Environmental conditions over the target area may vary from those used to generate predictions and localized effects may influence the degree of dispersant spread. Accordingly, final responsibility for the setting of setback distances and the application of dispersants lies with flight operations personnel.

Under no circumstances should this software be used to set safe setback distances for the application of material known to be hazardous to human health.

Document Number - t2015.j520.008
Issued as Revision 1, October 14th 2016
Doc Ref: Atlas:\...\t2015.j520.008.1.odt
amogconsulting.com
EIN 20-4906471

TX PE Firm F-11821

AC-E253-09v20130508

3   GETTING STARTED

This section provides instructions for running the test cases distributed with the DST. Additional detail on the functionality of the DST is presented in the remaining sections of the user guide. The following input files are included with the DST:

- *GoM_Oil_Spill.kml* – an example oil spill in the Gulf of Mexico.

- *GoM_Spray_Area.kml* – an example area in which spraying is allowed. This area intersects with *GoM_Oil_Spill.kml*

- *Forecast1.csv* – an example forecast in which weather conditions gradually increase beyond the operability limits.

- *Forecast2.csv* – a more complex example forecast in which weather conditions change dramatically.

The following steps will demonstrate the key features of the DST:

(i)   Ensure that the system requirements have been met, as described in Section 5. In particular, you will need:

- Software capable of viewing *.kml files. Google Earth is suggested, or a free online tool is available at http://ivanrublev.me/kml/

- For Windows operating systems, the required Visual Studio libraries (see Section 5.2) must be installed.

(ii)   Copy the folder corresponding to your operating system (either DST_Windows or DST_Mac) to your desired instal location.

(iii)   Double click on DST.exe (Windows) or DST.app (Mac) to start the DST.

(iv)   Read the welcome message and click OK if you agree.

Operational mode:

(i)   Select the Operational mode and click OK.

(ii)   Enter all required inputs and click OK.

(iii)   The DST will generate output indicating the predicted drift extents in the input conditions.

The output from the instructions above is shown in Figure 1. The depicted output was generated using the following inputs:

- Aircraft – AT-802A

- Aircraft Heading – 10 degrees (relative to True North)

- Altitude – 45 feet

- Aircraft Ground Speed – 120 knots

Document Number - t2015.j520.008
Issued as Revision 1, October 14th 2016
Doc Ref: Atlas:\...\t2015.j520.008.1.odt
amogconsulting.com
EIN 20-4906471

TX PE Firm F-11821

AC-E253-09v20130508

- Safety Factor – 1

- Wind Speed – 15 knots

- Wind Direction – 10 degrees (relative to True North)

```
Results
-------
Maximum Spray Extent Behind Aircraft:                        2100 ft
Maximum Spray Extent Perpendicular to Aircraft (Port):        550 ft
Maximum Spray Extent Perpendicular to Aircraft (Starboard):   550 ft
Maximum Spray Extent:                                        2150 ft
Maximum Spray Extent Direction:                              176 °N
```

Figure 1 : Example Output from DST Operational Mode

Planning mode:

(i) Change modes by either selecting **Re-run→Select New Mode** from the top menu bar, or pressing control-M (Windows) or command-M (Mac).

(ii) Select the Planning mode and click OK.

(iii) Select an aircraft, and input the Aircraft Heading and Safety Factor (Altitude and Aircraft Velocity can be defined, but are optional).

(iv) Select the Wind Forecast file, choosing *Forecast1.csv*

(v) Select the Oil Spill Area file, choosing *GoM_Oil_Spill.kml*

(vi) Select the Planned Spray Release Area file, choosing *GoM_Spray_Area.kml* and click OK.

(vii) The DST generates the following outputs:

- An Operability Table, indicating whether each forecast point is suitable for conducting spray operations using the aircraft and heading selected.

- Output results in the main window, which summarise the inputs and outputs, and list any operability messages.

- The file *Spray_Extent.kml*, which includes the oil spill region (black), the planned spray release area (red) and the total area predicted to be impacted by spray drift during the forecast period (yellow).

(viii) Open *Spray_Extent.kml* in software capable of viewing .kml files.

(ix) Restart the DST by either selecting **Re-run→Restart** from the top menu bar, or pressing control-R (Windows) or command-R (Mac).

(x) The test case for *Forecast2.csv* can be run in the same way.

The output from the instructions above is shown in Figure 2. The depicted output was generated using the following inputs:

- Aircraft – C-130A.

- Aircraft Heading – 45

- Altitude – 85

- Aircraft Velocity – 175

- Safety Factor – 1.2

- Wind Forecast – Forecast1.csv
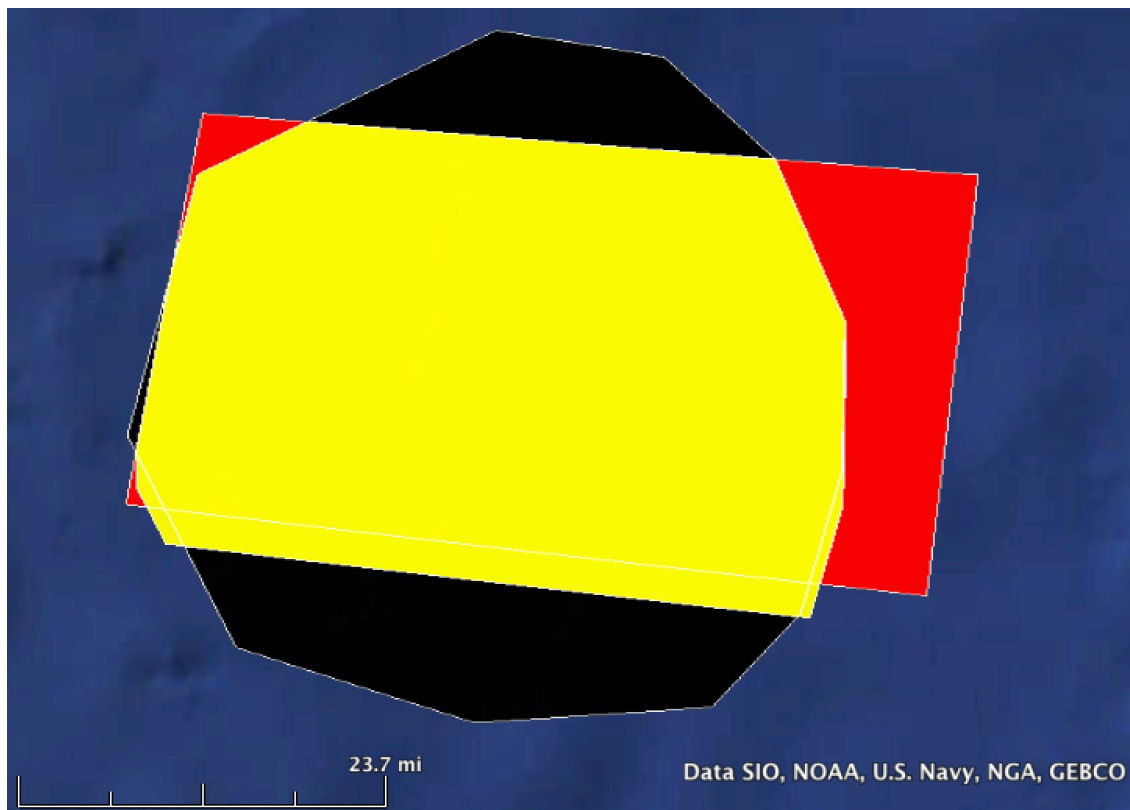
Figure 2 : Example Output from DST Planning Mode

Document Number - t2015.j520.008
Issued as Revision 1, October 14th 2016
Doc Ref: Atlas:\...\t2015.j520.008.1.odt
amogconsulting.com
EIN 20-4906471
TX PE Firm F-11821

AC-E253-09v20130508

4   VERSION INFORMATION

Table 1 displays the version information for the DST:

Table 1: Version Information

Version No.	Change Log
1.0.0	First Release

Document Number - t2015.j520.008
Issued as Revision 1, October 14th 2016
Doc Ref: Atlas:\...\t2015.j520.008.1.odt
amogconsulting.com
EIN 20-4906471
TX PE Firm F-11821

AC-E253-09v20130508

5 SYSTEM REQUIREMENTS

5.1 SUPPORTED OPERATING SYSTEMS

The DST supports the following operating systems:

- Windows 7 (32 and 64-bit)

- Windows 8 (32 and 64-bit)

- Windows 10 (32 and 64-bit)

- Mac OS X 10.11 El Capitan

- Mac OS X 10.10 Yosemite

- Mac OS X 10.9 Mavericks

5.2 RUNTIME REQUIREMENTS ON WINDOWS

In order to run the DST on a Windows operating system, the DST must be maintained within the directory in which it was distributed. Runtime libraries required by the DST are included within this directory.

5.3 GIS PACKAGE

The DST outputs the extent of dispersant spray in the form of a polygon defined by a set of latitude-longitude coordinates. The output polygon is provided in the form of a .kml file. Users will require the use of third party software to visualize the polygonal output of the DST. Software capable of opening .kml files is freely available. The .kml files output by the DST have been tested with:

- Google Earth

- The online mapping tool accessible at http://ivanrublev.me/kml/

Document Number - t2015.j520.008
Issued as Revision 1, October 14th 2016
Doc Ref: Atlas:\...\t2015.j520.008.1.odt
amogconsulting.com
EIN 20-4906471
TX PE Firm F-11821

AC-E253-09v20130508

6   USER INTERFACE

The user operates the DST via a Graphical User Interface (GUI). The DST user interface consists of a main text window that displays summary results and a series of dialog windows that allow for user input, as shown in Figure 3:
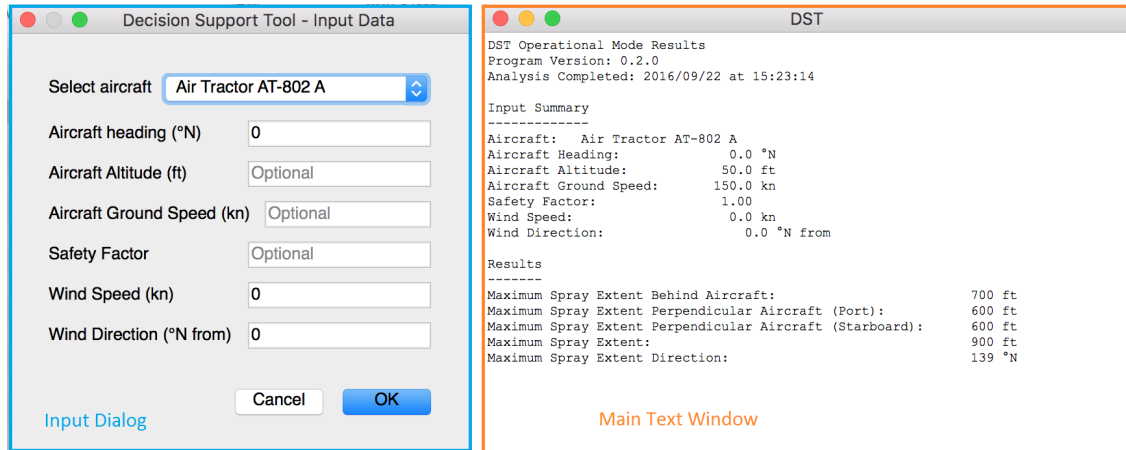
Figure 3 : DST User Interface

The information displayed in the main text window can be directly saved to a text file or printed.

6.1   DISCLAIMER ACCEPTANCE

Upon startup of the program, the user is presented with the *Disclaimer Acknowledgement Dialog* shown in Figure 4. By clicking **OK**, the user acknowledges that they are aware of the underlying assumptions and intended use of the DST.

Document Number - t2015.j520.008
Issued as Revision 1, October 14th 2016
Doc Ref: Atlas:\...\t2015.j520.008.1.odt
amogconsulting.com
EIN 20-4906471
TX PE Firm F-11821

AC-E253-09v20130508
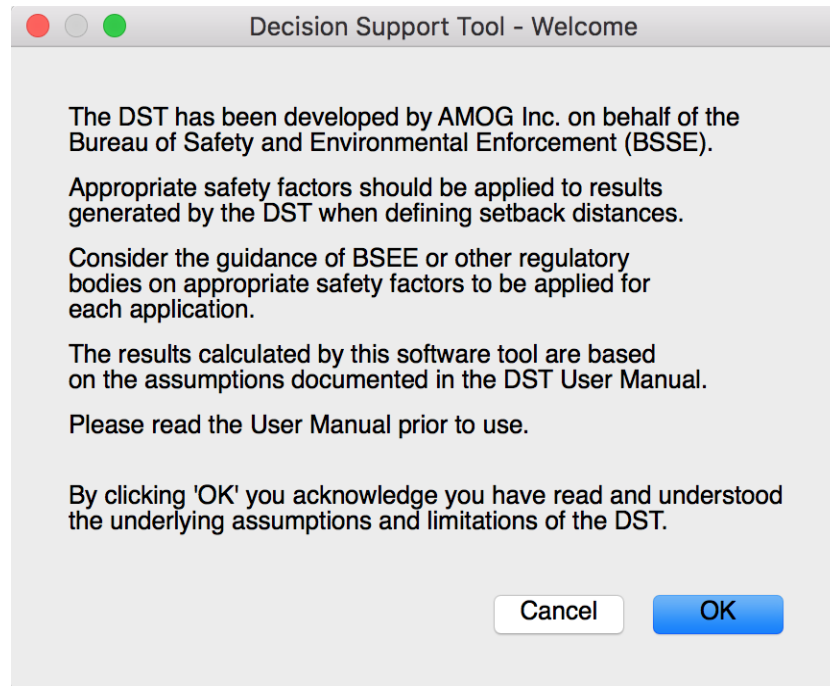
Figure 4 : Disclaimer Acknowledgement Dialog

If this disclaimer is discarded by clicking **Cancel**, the program will not continue to the next dialog window and no analyses can be run. The program must be closed and re-opened to return functionality. The program can be closed by clicking **DST→Quit DST** (Mac OS X) or **File→Quit DST** (Windows) from the top menu bar.

6.2   MODES OF OPERATION

After acknowledging the disclaimer the user is presented with the *Mode Selection Dialog* (shown in Figure 5).

The DST has two operating modes:

(i)   **Operational Mode:** takes as input a single wind speed and direction and provides information to aid in establishment of setback distances.

(ii)   **Planning Mode:** takes time varying meteorological data to assist with the identification of operability windows in which conditions are conducive to spraying operations.

The user selects the required mode with either the **Operational** or **Planning** radio button and then clicks **OK** to move to the appropriate input dialog.

Document Number - t2015.j520.008
Issued as Revision 1, October 14th 2016
Doc Ref: Atlas:\...\t2015.j520.008.1.odt
amogconsulting.com
EIN 20-4906471
TX PE Firm F-11821

AC-E253-09v20130508
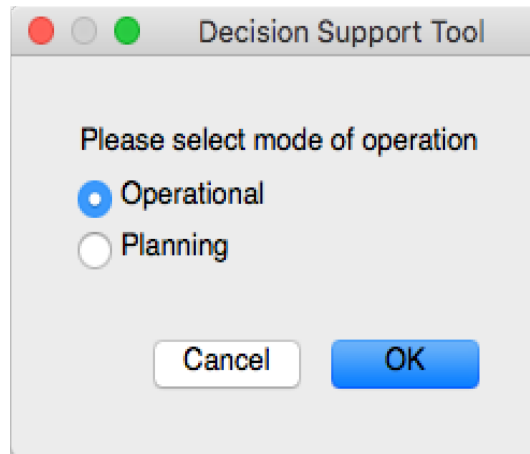
Figure 5 : Mode Selection Dialog

If the user selects **Cancel** the program will return to a neutral state where it can either be reset or closed.

If the user wishes to re-start after cancelling the *Mode Selection Dialog* or at anytime during use, the analysis can be restarted by selecting **Re-run→Restart** from the top menu bar (shown in Figure 6). Once restarted, the program will remain in the previously selected mode. To change modes, select **Re-run→Select New Mode** from the top menu bar. This will relaunch the *Mode Selection Dialog*.
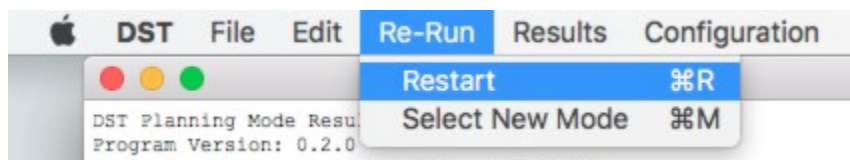
Figure 6 : Program Restart

7 OPERATIONAL MODE

The operational mode of the DST will facilitate the decisions required to be made by Operational personnel in conducting oil spill response. The purpose of this mode will be to allow the input of a single wind speed and direction likely to occur over the course of a day in order to provide input into establishing setback distances.

7.1 INPUTS

On selection of Operational Mode at the *Mode Selection Dialog*, the *Operational Mode Input Dialog* will display (Figure 7). A description of the user input fields are as follows:

I.   **Select aircraft:** The aircraft types can be selected from the drop down list.

II. **Aircraft heading (N°):** Angle for aircraft heading, this should be provided as an angle in degrees as measured from True North. This value must be between 0° and 360°, inclusive.

III. **Altitude (ft):** Altitude of aircraft in feet. This value must be greater than or equal to zero. If this field is left blank by the user the default aircraft altitude is assumed, depending on the airframe selected.

IV. **Aircraft Ground Speed (kn):** Ground speed of the aircraft in knots. This value must be greater than or equal to zero. If this field is left blank by the user the default aircraft velocity is assumed, depending on the airframe selected.

V.   **Safety Factor:** User-supplied Safety Factor for spray drift extent calculations, must be provided as a value greater than or equal to one. If this field is left blank by the user a Safety Factor of 1 is assumed. The Safety Factor is applied as a multiplicative factor to the predicted spray extent distance. For example, a Safety Factor of 2 will cause the DST to report double the predicted drift extent distances.

VI. **Wind Speed (kn):** Wind speed in knots. This value must be greater than or equal to zero.

VII. **Wind Direction (N° from):** A single, time invariant wind direction specified in clockwise degrees from True North. This value must be between 0° and 360°, inclusive.

Document Number - t2015.j520.008
Issued as Revision 1, October 14th 2016
Doc Ref: Atlas:\...\t2015.j520.008.1.odt
amogconsulting.com
EIN 20-4906471
TX PE Firm F-11821

AC-E253-09v20130508
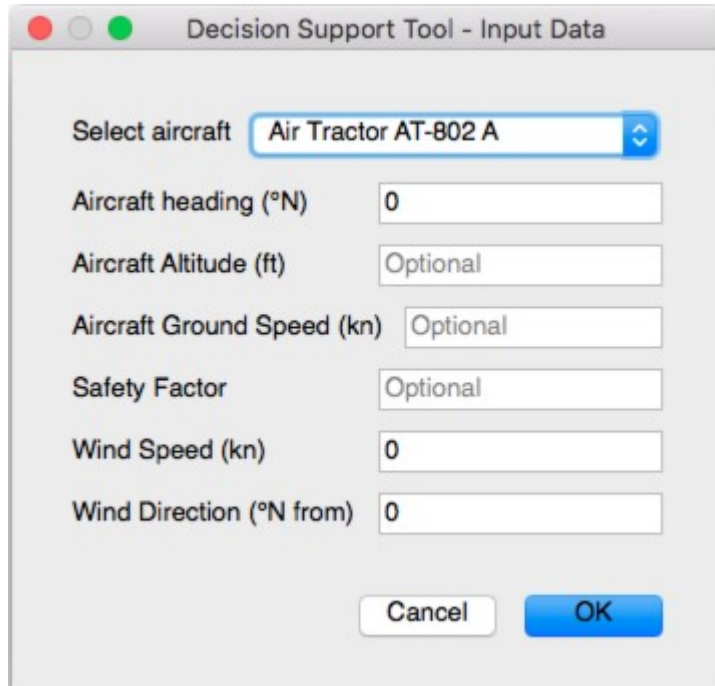
Figure 7 : Operational Mode Input Dialog

After clicking **OK** on the *Operational Mode Input Dialog*, the program will perform the operability analysis and spray extent prediction. If **Cancel** is clicked the program will remain idle. The analysis can be restarted by selecting **Re-run→Restart** from the top menu bar. The user may return to the *Mode Selection Dialog* by selecting **Re-run→Select New Mode** from the top menu bar (as shown in Figure 6). This will relaunch the *Mode Selection Dialog*.

7.2   RESULTS

On completion of the analysis the program will automatically display the results in the main window. The results from the Operational Mode analysis are as follows (example shown in Figure 8):

● The program version;

● The date and time the analysis was run;

● A summary of all the input fields;

● Results:

  ○ Maximum extent behind aircraft rounded up to the nearest 50 feet;

  ○ Maximum extent perpendicular to the aircraft rounded up to the nearest 50 feet; and

  ○ Absolute maximum extent rounded up to the nearest 50 feet, and the direction (bearing in degrees from True North) of the maximum extent.

Document Number - t2015.j520.008
Issued as Revision 1, October 14th 2016
Doc Ref: Atlas:\...\t2015.j520.008.1.odt
amogconsulting.com
EIN 20-4906471
TX PE Firm F-11821

AC-E253-09v20130508

- Any operability messages that occurred during run time, including any messages specifying the inoperability cause(s).

- Any errors or warnings resulting from an inability to predict the drift extent under the input conditions. This occurs for limited cases for the DC-3 only.


```
DST Operational Mode Results
Program Version: 1.0.0
Analysis Completed: 2016/09/23 at 09:53:07

Input Summary
-------------
Aircraft:   Air Tractor AT-802 A
Aircraft Heading:              0.0 °N
Aircraft Altitude:            50.0 ft
Aircraft Ground Speed:       150.0 kn
Safety Factor:                1.00
Wind Speed:                    0.0 kn
Wind Direction (from):         0.0 °N


Results
-------
Maximum Spray Extent Behind Aircraft:                        700 ft
Maximum Spray Extent Perpendicular to Aircraft (Port):       600 ft
Maximum Spray Extent Perpendicular to Aircraft (Starboard):  600 ft
Maximum Spray Extent:                                        900 ft
Maximum Spray Extent Direction:                              139 °N
```

Figure 8 : Operational Mode Output Summary

7.3   SAVING OUTPUT

The user can save the results of the analysis as plain text to a file. This can be done in one of two ways (as shown in Figure 9):

- Select **File→Save**: This will save the file with a default name, *DST output,* in the same directory as the DST GUI.

- Select **File→Save As**: The user can save the file with a custom name (and extension), in a custom directory.
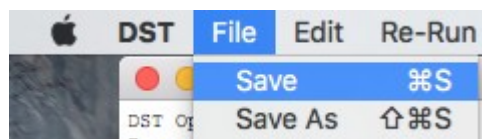
Figure 9 : Saving Operational Results

Document Number - t2015.j520.008
Issued as Revision 1, October 14th 2016
Doc Ref: Atlas:\...\t2015.j520.008.1.odt
amogconsulting.com
EIN 20-4906471
TX PE Firm F-11821

AC-E253-09v20130508

7.4 PRINTING OUTPUT

The user can print the results if required. Select **File→Print** and choose the desired printing settings. Additionally, select **File→Print Setup** before printing to adjust the print setup.

The print functionality described above is shown in Figure 10.

Figure 10 : Printing Operational Results

Document Number - t2015.j520.008
Issued as Revision 1, October 14th 2016
Doc Ref: Atlas:\...\t2015.j520.008.1.odt
amogconsulting.com
EIN 20-4906471
TX PE Firm F-11821

AC-E253-09v20130508

8   PLANNING MODE

The planning mode of the DST facilitates the identification of potential spraying windows for the purpose of assisting with planning decisions on the basis of forecast data. The purpose of this mode is to allow the input of forecast time-varying forecast data to facilitate the identification of windows conducive to spraying operations (i.e. operability windows).

In addition, this mode also provides the ability to graphically integrate set back distances predicted using the DST with other oil spill response tools by producing a map layer illustrating the area affected by drift.

8.1   INPUTS

On selection of Planning Mode at the *Mode Selection Dialog*, the *Planning Mode Input Dialog* will display (Figure 11). The required user input fields are as follows:

I.   **Select aircraft:** The aircraft types can be selected from the drop down list.

II.   **Aircraft Heading (N°):** Angle for aircraft heading, this should be provided as an angle in degrees as measured from True North. This value must be between 0° and 360°, inclusive.

III.   **Altitude (ft):** Altitude of aircraft in feet. This value must be greater than or equal to zero. If this field is left blank by the user the default aircraft altitude is assumed, depending on the airframe selected.

IV.   **Aircraft Ground Speed (kn):** Ground speed of the aircraft in knots. This value must be greater than or equal to zero. If this field is left blank by the user the default aircraft velocity is assumed, depending on the airframe selected.

V.   **Safety Factor:** User-supplied Safety Factor for spray drift extent calculations, must be provided as a value greater than or equal to one. The Safety Factor is applied as a multiplicative factor to the predicted spray extent distance.

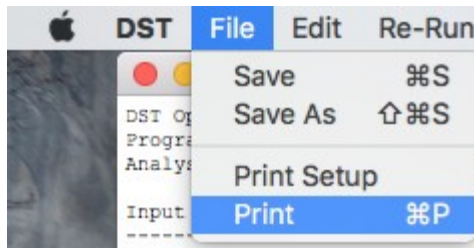VI.   **Wind Forecast:** Wind forecast data. The user must provide time-varying meteorological forecast data formatted as a .csv file. Users can search for and select the desired .csv file with the browse button to the right of the input field (Figure 11). Refer to Section 8.1.1 – Wind Forecast Data File, for more details.

VII.   **Oil Spill Layer:** Polygonal area for oil spill. The user must provide a .kml file containing the coordinates of the polygon. Users can search for and select the desired .kml file with the browse button to the right of the input field (Figure 11). See 8.1.2 – Oil Spill Region, for more details.

VIII.   **Planned Spray Release Area:** Polygonal area for allowable flight coverage for spray. The user must provide a .kml file containing the coordinates of the polygon. Users can search for and select the desired .kml file with the browse button to the right of the input field (Figure 11). See 8.1.3 – Planned Spray Release Area, for more details.

Document Number - t2015.j520.008
Issued as Revision 1, October 14th 2016
Doc Ref: Atlas:\...\t2015.j520.008.1.odt
amogconsulting.com
EIN 20-4906471
TX PE Firm F-11821

AC-E253-09v20130508

IX. **Output .kml filename:** Filename given to the map layer output. This filename can included a path relative to the directory containing the forecast file. If this field is left blank by the user the default filename *Spray_Extent.kml* is given to the file.

X. **Operability Table filename:** Filename given to the Operability Table output. This filename can included a path relative to the directory containing the forecast file. If this field is left blank by the user the default filename *Operability_Table.csv* is given to the file.

Figure 11 : Planning Mode Input Dialog

8.1.1   Wind Forecast Data File

In the Planning Mode, the user must supply wind forecast data table in the form of a .csv file (an example is shown in Figure 12). The data table should contain column headers as follows:

I. **Year:** The year of the weather forecast [yyyy];

II. **Month:** The month of the weather forecast [mm];

III. **Day:** The day of the weather forecast [dd];

IV. **HourMin:** The hour of the weather forecast in 24-hour time format [hhmm];

Document Number - t2015.j520.008
Issued as Revision 1, October 14th 2016
Doc Ref: Atlas:\...\t2015.j520.008.1.odt
amogconsulting.com
EIN 20-4906471
TX PE Firm F-11821

AC-E253-09v20130508

V.   **UTCOffset:** The Coordinated Universal Time (UTC) offset in the format [hh]. Negative offsets may be used;

VI.   **Wind Speed:** The forecast wind speed in knots, at 10 metres above sea level;

VII.   **Wind Heading:** The forecast wind direction in degrees from True North;

VIII.   **Wave Height:** The forecast significant wave height in feet; and

IX.   **Visibility:** The forecast visibility in statute miles.

Year	Month	Day	HourMin	UTCOffset	Wind Speed	Wind Heading	Wave Height	Visibility
2016	12	25	1220	10	10	50	0	5
2016	4	10	1430	10	10	50	6.2	5

Figure 12 : Wind Forecast Data File Example

The corresponding data for each variable should be populated in the file.

8.1.2   Oil Spill Region

For the Planning Mode, the user must supply an oil spill region in the form of a defined polygon contained in a .kml file. Requirements concerning the input .kml files are:

● The polygon must not contain more than 1000 points;

● The polygon must not be degenerate, i.e. the polygon must form a single closed area.

8.1.3   Planned Spray Release Area
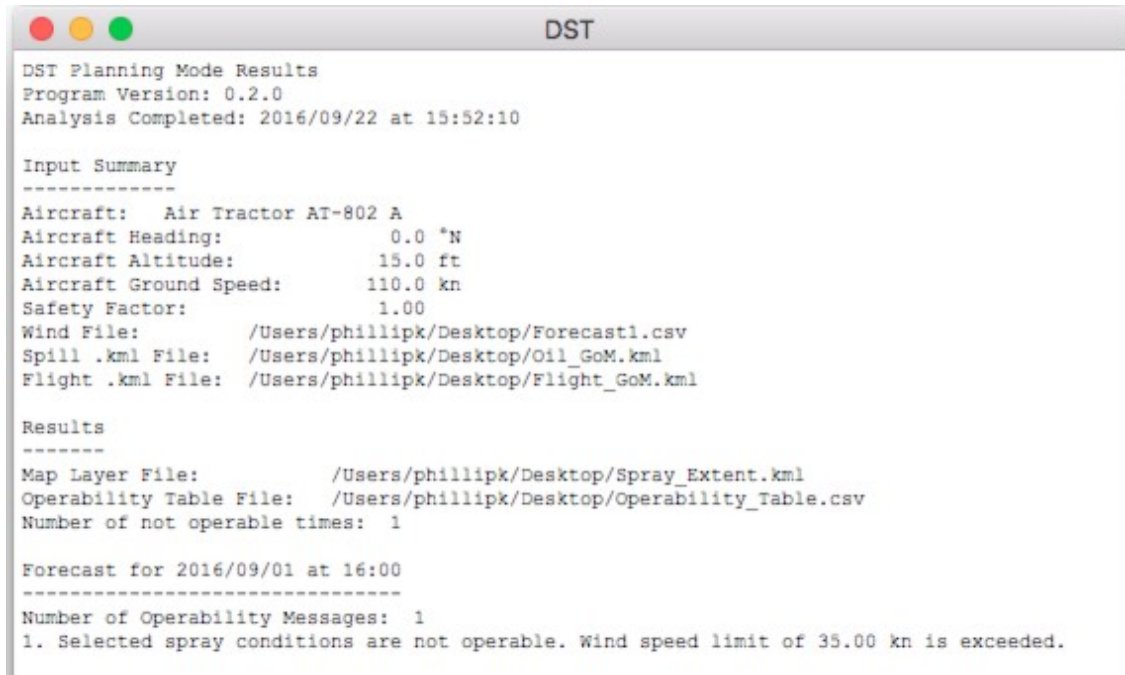
For the Planning Mode, the user must supply a planned spray release area in the form of a defined polygon contained in a .kml file.

8.2   RESULTS

On completion of the analysis the program will automatically display the results in the main window. The results from the Planning Mode analysis are as follows (also shown in Figure 13):

● The program version;

● The date and time the analysis was run;

● A summary of all the input fields;

● Results:

○ The name of the map layer file generated with the spray region (Refer to Section 8.2.1 – Map Layer Output for detail);

Document Number - t2015.j520.008
Issued as Revision 1, October 14th 2016
Doc Ref: Atlas:\...\t2015.j520.008.1.odt
amogconsulting.com
EIN 20-4906471
TX PE Firm F-11821

AC-E253-09v20130508

○ The name of the operability table CSV file (Refer to Section 8.2.2 – Operability Table for detail); and

○ The number of times from the forecast file that were not operable.

● Any operability messages that occurred during run time, including any messages specifying the inoperability cause(s).

● Any errors or warnings resulting from an inability to predict the drift extent under the input conditions. This occurs for limited cases for the DC-3 only.


```
● ● ●                          DST

DST Planning Mode Results
Program Version: 0.2.0
Analysis Completed: 2016/09/22 at 15:52:10

Input Summary
--------------
Aircraft:   Air Tractor AT-802 A
Aircraft Heading:              0.0 °N
Aircraft Altitude:            15.0 ft
Aircraft Ground Speed:       110.0 kn
Safety Factor:                 1.00
Wind File:          /Users/phillipk/Desktop/Forecast1.csv
Spill .kml File:    /Users/phillipk/Desktop/Oil_GoM.kml
Flight .kml File:   /Users/phillipk/Desktop/Flight_GoM.kml

Results
-------
Map Layer File:            /Users/phillipk/Desktop/Spray_Extent.kml
Operability Table File:    /Users/phillipk/Desktop/Operability_Table.csv
Number of not operable times:  1

Forecast for 2016/09/01 at 16:00
---------------------------------
Number of Operability Messages:  1
1. Selected spray conditions are not operable. Wind speed limit of 35.00 kn is exceeded.
```

Figure 13 : Example Planning Mode Output Summary

8.2.1   Map Layer Output

By default, the DST outputs a .kml file to the directory containing the forecast file, with the filename *Spray_Extent.kml.* This file contains the coordinate sets for the following polygon objects:

● The oil spill region;

● The planned spray release area; and

● The union between the area that forms the intersection between the oil spill region and planned spray release areas, as well as the area predicted to be impacted by spray drift.

The user may open the resulting *Spray_Extent.kml* in suitable 3rd party software to view the polygons. The following conventions are used to identify each region:

Document Number - t2015.j520.008
Issued as Revision 1, October 14th 2016
Doc Ref: Atlas:\...\t2015.j520.008.1.odt
amogconsulting.com
EIN 20-4906471
TX PE Firm F-11821

AC-E253-09v20130508

- The spill region is colored black and is labeled "OilRegion".

- The flight region is colored red and is labelled "FlightRegion".

- The spray extent region is colored yellow and is labelled "SprayRegion".

Figure 14 shows an example output *Spray_Extent.kml* file as displayed in Google Earth.
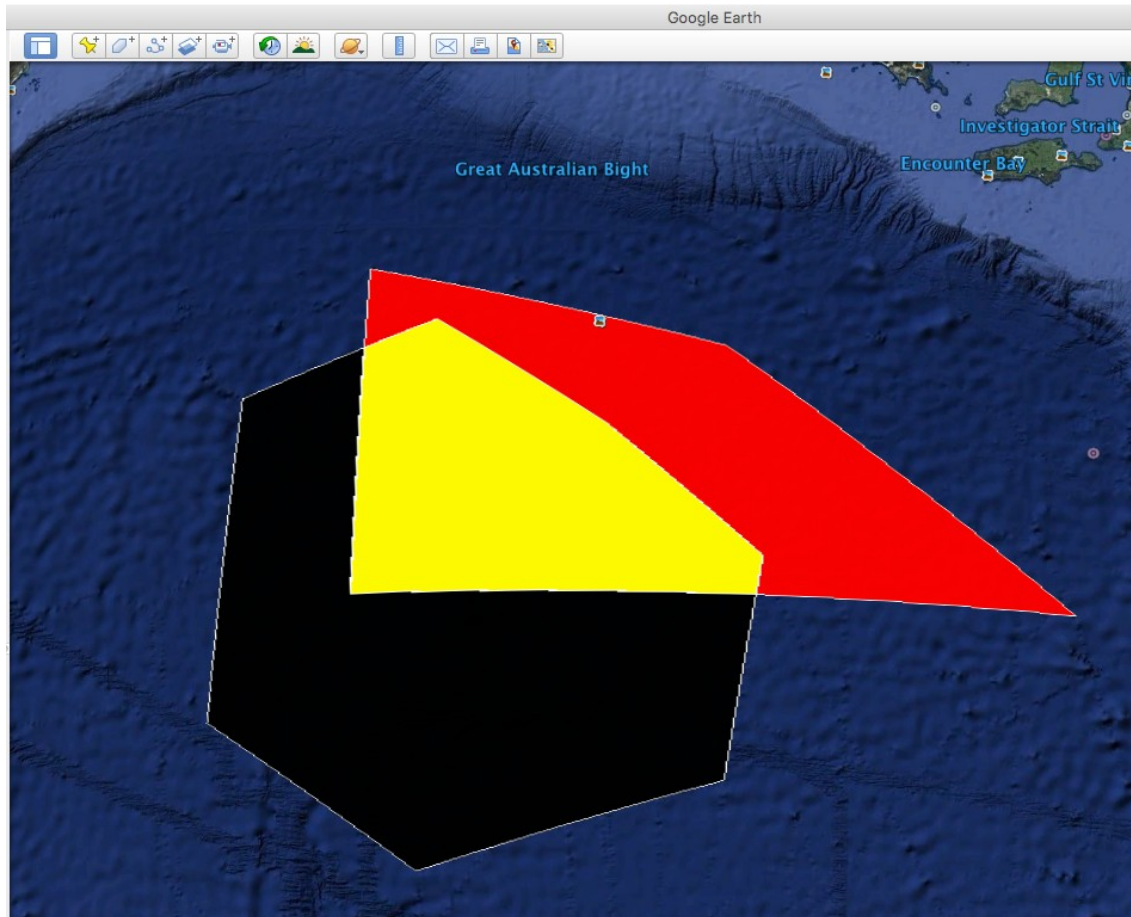
Figure 14 : Example Resultant Spray Region

Note: A single map layer is generated as the output of the planning mode. The area output is the envelope of the 99 % drift extents for all conditions during the input forecast period.

In generating the final map layer the longitude and latitude coordinates input in the oil spill .kml file are converted to Universal Transverse Mercator (UTM) coordinates. If a spill is located on the boundary of multiple UTM zones, a small error in the mapping of the spray extent may occur. This error will be more severe at high latitudes. It is assumed that the polygons are at sea level; altitude information is discarded.

Document Number - t2015.j520.008
Issued as Revision 1, October 14th 2016
Doc Ref: Atlas:\...\t2015.j520.008.1.odt
amogconsulting.com
EIN 20-4906471
TX PE Firm F-11821

AC-E253-09v20130508

8.2.2   Operability Table

By default, the DST outputs a .csv file to the directory containing the forecast file, with the filename *Operability_Table.csv.* An example table is shown in Figure 15. The table is essentially an appended form of the forecast input table, but shows for each set of environmental conditions whether or not they are operable. The *Operability_Table.csv* has the following column headers:

I.   **Year:** The year of the weather forecast [yyyy];

II.   **Month:** The month of the weather forecast [mm];

III.   **Day:** The day of the weather forecast [dd];

IV.   **HourMin:** The hour of the weather forecast in 24-hour time format [hhmm];

V.   **UTCOffset:** The Coordinated Universal Time (UTC) offset in the format [hh]. Negative offsets may be used;

VI.   **Wind Speed:** The forecast wind speed in knots, at 10 metres above sea level;

VII.   **Wind Heading:** The forecast wind direction in degrees from True North;

VIII.   **Wave Height:** The forecast significant wave height in feet; and

I.   **Visibility:** The forecast visibility in statute miles.

II.   **Operable?:** Yes/No output indicating whether or not the each set of conditions is within the operability limits for the aircraft to be used.

	Date	Time	GMT Offset	Wind Speed (kn)	Wind Direction (°N from)	Head Wind (kn)	Cross Wind (kn)	Significant Wave Height (ft)	Visibility (nm)	Operable?
1	2016/09/01	12:00	-6.00	0.00	0.00	0.00	0.00	4.00	5.00	Yes
2	2016/09/01	12:30	-6.00	5.00	0.00	5.00	0.00	4.00	5.00	Yes
3	2016/09/01	13:00	-6.00	10.00	0.00	10.00	0.00	4.00	5.00	Yes
4	2016/09/01	13:30	-6.00	15.00	0.00	15.00	0.00	4.00	5.00	Yes
5	2016/09/01	14:00	-6.00	20.00	0.00	20.00	0.00	4.00	5.00	Yes
6	2016/09/01	14:30	-6.00	25.00	0.00	25.00	0.00	4.00	5.00	Yes
7	2016/09/01	15:00	-6.00	30.00	0.00	30.00	0.00	4.00	5.00	Yes
8	2016/09/01	15:30	-6.00	35.00	0.00	35.00	0.00	4.00	5.00	Yes
9	2016/09/01	16:00	-6.00	40.00	0.00	40.00	0.00	4.00	5.00	No

Figure 15 : Example Operability Table Output

Document Number - t2015.j520.008
Issued as Revision 1, October 14th 2016
Doc Ref: Atlas:\...\t2015.j520.008.1.odt
amogconsulting.com
EIN 20-4906471

TX PE Firm F-11821

AC-E253-09v20130508

8.3 SAVING OUTPUT

8.3.1 Planning Mode Summary

The user can save the results of the operability summary to a desired file. This can be done in one of two ways:

- Select **File→Save**: This will save the file with a default name, *DST output,* in the same directory as the DST GUI.

- Select **File→Save As**: The user can save the file with a custom name (and extension), in a custom directory.

8.3.2 Planning Mode Operability Table

The user can save the resulting table to a desired file. This can be done in one of two ways:

- Select **File→Save**: This will save the file with a default name, *Operability_Table.csv,* in the same directory as the DST GUI.

- Select **File→Save As**: The user can save the file with a custom name (with .csv extension), in a custom directory.

8.4 PRINTING OUTPUT

The user can print the summary results if required. The instructions for printing outlined in Section 7.4 – Printing Output are applicable to the Planning Mode summary.

8.5 NOTES ON USAGE

Users may wish to use the DST without defining separate areas for the oil spill and the planned spray release area. Use of the Planning mode with a single input area can be achieved by inputing the same file as both the Oil Spill Area and the Planned Spray Release Area.

Changes to the wind direction during the forecast period may result in inoperable times which would be operable if spraying was conducted on a different aircraft heading. All inoperable times will be ignored when predicting the drift extent. Splitting the forecast input file into two separate files (both with the required column headings) allows for running the DST for two time periods with different aircraft headings. This will allow prediction of operational drift extents during periods in which the wind direction changes significantly.

Document Number - t2015.j520.008
Issued as Revision 1, October 14th 2016
Doc Ref: Atlas:\...\t2015.j520.008.1.odt
amogconsulting.com
EIN 20-4906471

TX PE Firm F-11821

AC-E253-09v20130508

9   MISCELLANEOUS

9.1   PREFERENCES

Users can edit font preferences for the printout of the output summary. Select **Edit→Font** as shown in Figure 16, and the font editor interface will appear. The use of monospaced, i.e., fixed-pitch or fixed-width, fonts will retain the alignment of the results output.
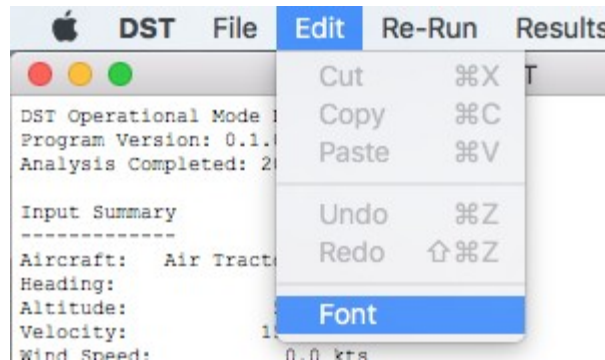
Figure 16 : Edit Font Access

9.2   CONFIGURATION

Users can access data sheets for each of the available airframes. Select Configuration→[Airframe of Choice] as shown in Figure 17, to view the configuration data for each airframe. Refer to Section 12 – Assumed Aircraft and Spray Configurations for full detail on the individual airframe configurations.

Figure 17 : Configuration Data Access

Document Number - t2015.j520.008
Issued as Revision 1, October 14th 2016
Doc Ref: Atlas:\...\t2015.j520.008.1.odt
amogconsulting.com
EIN 20-4906471
TX PE Firm F-11821

AC-E253-09v20130508

10   TROUBLESHOOTING

The following sections describe the means of troubleshooting possible issues users may face when using the DST.

In general, the DST may return errors or warnings in one of two interfaces, as follows:

- A GUI pop-up dialog box; or

- Printed to output stream during an analysis.
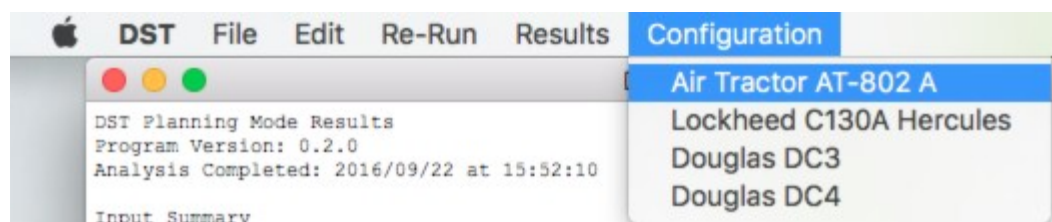
10.1   ERROR DIALOGS

The pop-dialog errors prevent the user from using the program in an unstable fashion with inadvertent or missing data. This type of error will stop the execution of the program, and may be caused by:

- Undefined input fields;

- Attempting to access non-existent files; or

- Attempting to access incorrectly configured files.

Table 2 describes specific instances of error dialogs and how to troubleshoot them.

Table 2: Error Dialogs

Message Provided To User	Execution Halted (Yes/No)	Description
Example: Aircraft Heading must be provided.	Yes	**Cause:** If the user fails to enter values in input fields whilst in either Operational or Planning Mode, an error dialog will be shown. **Resolution:** Ensure that all required fields are filled with inputs.
Safety Factor must be greater than or equal to 1.	Yes	**Cause:** If the user fails to enter a value for the Safety Factor greater or equal to 1 whilst in either Operational or Planning Mode, an error dialog will be shown. **Resolution:** Ensure that the Safety Factor is equal to or greater than 1.
Example: Wind forecast file can not be found.	Yes	**Cause:** Whilst in Planning mode, if the user attempts to load a file that does not exist or cannot be found, an error dialog will be shown. **Resolution:** Ensure that the desired file exists and has appropriate read/write permissions.

Document Number - t2015.j520.008
Issued as Revision 1, October 14th 2016
Doc Ref: Atlas:\...\t2015.j520.008.1.odt
amogconsulting.com
EIN 20-4906471
TX PE Firm F-11821

AC-E253-09v20130508

Table 2: Error Dialogs

Message Provided To User	Execution Halted (Yes/No)	Description
Example: Oil Spill .kml cannot be read.	Yes	**Cause:** Whilst in Planning mode, if the user attempts to load a file that does not exist or cannot be read, an error dialog will be shown. **Resolution:** Ensure that the desired file exists and has appropriate read/write permissions.
KML file configuration error	Yes	**Cause:** Whilst in Planning mode, if the user attempts to load a .kml file that is incorrectly configured or lacks coordinate data, an error dialog will be shown. **Resolution:** Ensure that the desired .kml file is correctly configured.
KML File Coordinate Point Limit Exceeded	Yes	**Cause:** Whilst in Planning mode, if the user attempts to load a .kml file that contains 1000 or more coordinate data points as part of the polygon, an error dialog will be shown. **Resolution:** Ensure that the desired .kml file has less than 1000 coordinate points.
The Spill polygon provided in the .kml file is degenerate.	Yes	**Cause:** Whilst in Planning mode, if the user attempts to load a .kml file that contains coordinates that produce a degenerate polygon, an error dialog will be shown. **Resolution:** Ensure that the desired .kml file contains coordinates that do not produce a degenerate polygon.
No intersection points between the provided .kml files.	Yes	**Cause:** Whilst in Planning mode, if the user supplies polygonal coordinates for the oil spill and planned spray release area that do not intersect, an error dialog will be shown. **Resolution:** Ensure that the latitude and longitude coordinates defining the polygon boundaries in input .kml files intersect.
Wind Forecast File is missing data.	Yes	**Cause:** Whilst in Planning mode, if the user attempts to load a wind forecast .csv file that is missing data, an error dialog will be shown. **Resolution:** Ensure that the wind forecast data .csv file is fully populated.

Document Number - t2015.j520.008
Issued as Revision 1, October 14th 2016
Doc Ref: Atlas:\...\t2015.j520.008.1.odt
amogconsulting.com
EIN 20-4906471
TX PE Firm F-11821

AC-E253-09v20130508

Table 2: Error Dialogs

Message Provided To User	Execution Halted (Yes/No)	Description
Error during read of Wind Forecast File. This is likely due to the incorrect line endings.	Yes	**Cause:** Whilst in Planning mode, if the user attempts to load a wind forecast .csv file that is incorrectly configured, an error dialog will be shown. The format of the .csv file must be as outlined in 8.1.1 – Wind Forecast Data File. Additionally, it is theoretically possible to generate a .csv file with line endings which are not recognised by the DST. **Resolution:** Ensure the .csv file has the same structure as outlined in 8.1.1 – Wind Forecast Data File. If incorrect line endings are the suspected cause, generate the .csv file with Microsoft Excel.
Wind speed exceeds 10 knots. The DST is unable to predict the spray drift extent for the DC-3 when the wind speed exceeds 10 knots.	Yes	**Cause:** At the present time, spray drift extents cannot be predicted for the DC-3 in wind speeds greater than 10 knots, because the DC-3 is known to operate without flaps under these conditions, which is not within the present data set.

10.2   WARNING DIALOGS

A warning will be issued by the DST if the inputs exceed the maximum calculable groundspeed for the DC-3 of 130 knots.

Table 3: Warning Dialogs

Message Provided To User	Execution Halted (Yes/No)	Description
Groundspeed exceeds 130 knots. The DST is unable to predict the spray drift extent for the DC-3 when the groundspeed exceeds 130 knots.	No	**Cause:** Groundspeeds greater than 130 knots results in unrealistic flight conditions when using the assumed flap deployment angle. **Effect:** The DST will provide a spray drift extent prediction which corresponds to a groundspeed of 130 knots.

Document Number - t2015.j520.008
Issued as Revision 1, October 14th 2016
Doc Ref: Atlas:\...\t2015.j520.008.1.odt
amogconsulting.com
EIN 20-4906471
TX PE Firm F-11821

AC-E253-09v20130508

11 INBUILT OPERABILITY LIMITS

When using the DST, the following airframes can be selected:

- Air Tractor AT-802A

- Lockheed C-130A

- Douglas DC-3

- Douglas DC-4

The airframes are subject to different operability limits for aircraft speed found in the Dispersant Mission Planner [1] data. In additional, environmental operability limits were established during the development of the DST [2]. The DST assesses the suitability of the selected aircraft in the specified environmental conditions for conducting spraying operations against the operability limits as follows. It should be noted that the operability limits incorporated in the DST were selected during the DST development project as the limits of the numerical modeling which underpins the DST. As such, while the DST cannot predict the extent of spray drift outside of the inbuilt operability limits, it is possible that dispersant spraying operations could be safely conducted in such conditions. Similarly, conditions which meet the operability criteria are not a guarantee of safe operations, and final assessments as to the safety of any given operation should be made by the pilots in charge.

11.1 ALTITUDE

Table 4 shows the operability limits on altitude for each airframe:

Table 4: Altitude Operability Limits

Airframe	Minimum Altitude (ft)	Maximum Altitude (ft)
Air Tractor AT-802A	15	50
Lockheed C-130A	50	100
Douglas DC-3	50	100
Douglas DC-4	50	100

Document Number - t2015.j520.008
Issued as Revision 1, October 14th 2016
Doc Ref: Atlas:\...\t2015.j520.008.1.odt
amogconsulting.com
EIN 20-4906471
TX PE Firm F-11821

AC-E253-09v20130508

11.2   AIRCRAFT APPLICATION GROUND SPEED

Table 5 shows the operability limits on application ground speed for each airframe:

Table 5: Application Ground Speed Operability Limits

Airframe	Minimum Application Ground Speed (kn)	Maximum Application Ground Speed (kn)
Air Tractor AT-802A	110	180
Lockheed C-130A	150	200
Douglas DC-3	120	130 for prediction of spray drift extents, but operation is possible up to 160 knots
Douglas DC-4	120	160

11.3   WIND SPEED AND DIRECTION

The operability limits on wind speed and direction are as follows:

- The crosswind component of the wind must be less than 20 knots.

- The wind speed must be less than 35 knots.

- Spraying is not performed in a tailwind (defined as a wind angle of greater than 90 degrees relative to the aircraft heading). While aircraft are capable of spraying in a tailwind, the current version of the DST cannot predict the spray drift extent in tailwind conditions.

11.4   SIGNIFICANT WAVE HEIGHT

Operable significant wave height is less than 10 feet.

11.5   VISIBILITY

Operable visibility distance is greater than 3 statute miles.

Document Number - t2015.j520.008
Issued as Revision 1, October 14th 2016
Doc Ref: Atlas:\...\t2015.j520.008.1.odt
amogconsulting.com
EIN 20-4906471
TX PE Firm F-11821

AC-E253-09v20130508

11.6   DAYLIGHT

Conditions are only considered suitable for conducting spray operations during daylight hours.

Daylight hours are determined based on sunrise and sunset, which are estimated based on the average latitude and longitude position of the spill region, the input date and the input UTC offset.

In addition to wind component calculations, the operability algorithm also estimates the sunrise and sunset time based on the position of the centre of the oil spill. This prediction uses a simple sunrise and sunset calculation based on the local latitude, the sun's declination and the solar time correction. The model accounts for the eccentricity of the earths orbit but not the eccentricity of the earth itself, and assumes that the sunrise is defined as when the sun rises above the horizon, defined as greater than 90 degrees declination.

Document Number - t2015.j520.008
Issued as Revision 1, October 14th 2016
Doc Ref: Atlas:\...\t2015.j520.008.1.odt
amogconsulting.com
EIN 20-4906471
TX PE Firm F-11821

AC-E253-09v20130508

12   ASSUMED AIRCRAFT AND SPRAY CONFIGURATIONS

The following tables show the assumed configuration data used for each airframe within the DST.

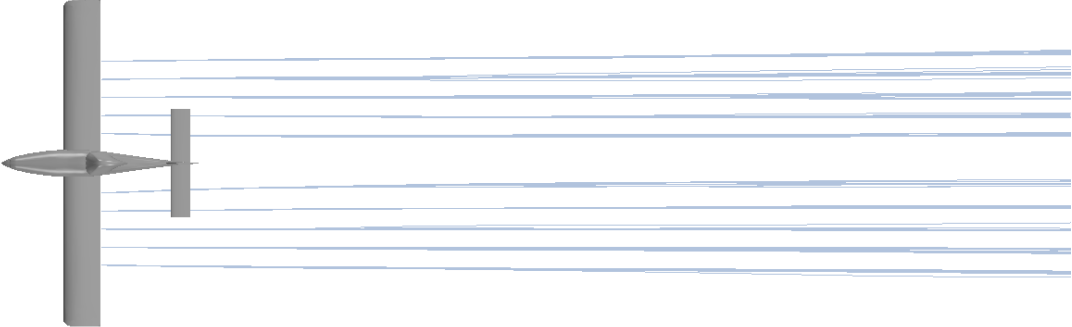Table 6: Air Tractor AT-802A Configuration Data Sheet

Parameter	Information
Spray Altitude Minimum	15.0 ft
Spray Altitude Maximum	50.0 ft
Application Speed Minimum (Ground Speed)	110.0 kn
Application Speed Maximum (Ground Speed)	180.0 kn
Assume Flap Angle	0.0°
Assumed Airframe Mass	16,000 lbs
Spray System	10 nozzles are evenly spread approximately 3 ft apart, starting at 11ft from the wingtip, below the wing.
Nozzle Type	BETE NF70

Document Number - t2015.j520.008
Issued as Revision 1, October 14th 2016
Doc Ref: Atlas:\...\t2015.j520.008.1.odt
amogconsulting.com
EIN 20-4906471
TX PE Firm F-11821

AC-E253-09v20130508

Table 7: Lockheed C-130A Configuration Data Sheet
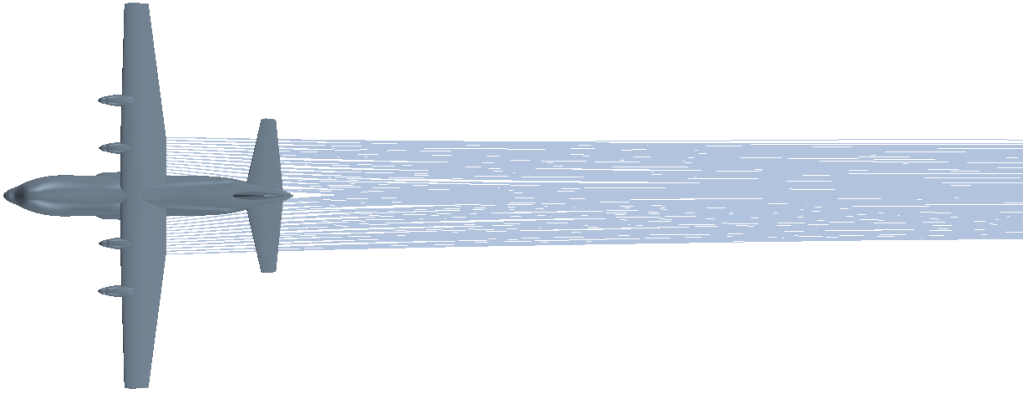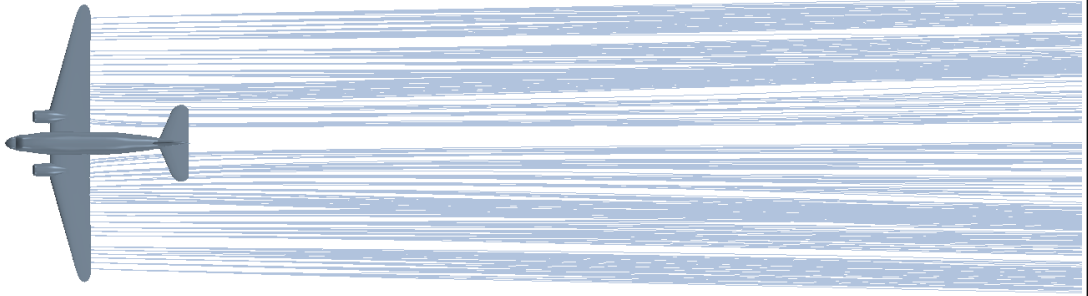
Parameter	Information
Spray Altitude Minimum	50.0 ft
Spray Altitude Maximum	100.0 ft
Application Speed Minimum (Ground Speed)	150.0 kn
Application Speed Maximum (Ground Speed)	200.0 kn
Assume Flap Angle	18.0°
Assumed Airframe Mass	108,000 lbs
Spray System	The spray boom in the model was located vertically in line with the bottom of the main cargo door, and longitudinally immediately behind the side door. A total of 28 nozzles were included, spray nozzles were equally spaced 1 ft apart on the booms.
Nozzle Type	BETE NF70

Document Number - t2015.j520.008
Issued as Revision 1, October 14th 2016
Doc Ref: Atlas:\...\t2015.j520.008.1.odt
amogconsulting.com
EIN 20-4906471
TX PE Firm F-11821

AC-E253-09v20130508

Table 8: Douglas DC-3 Configuration Data Sheet
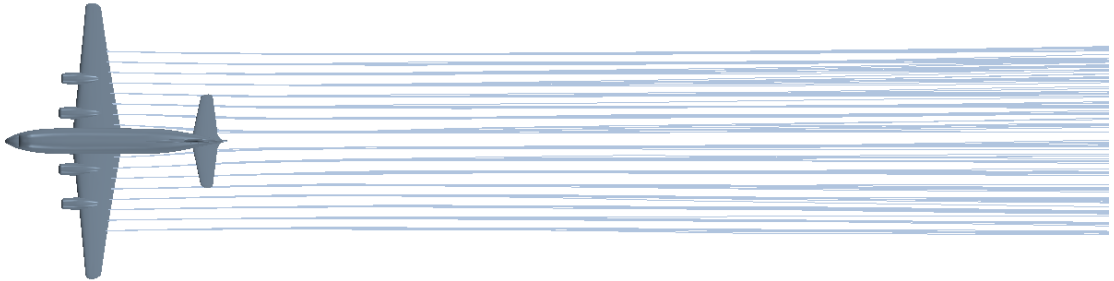
Parameter	Information
Spray Altitude Minimum	50.0 ft
Spray Altitude Maximum	100.0 ft
Application Speed Minimum (Ground Speed)	120.0 kn
Application Speed Maximum (Ground Speed)	130 kn for prediction of spray drift extents, but operation is possible up to 160 kn
Assume Flap Angle	11.3°
Assumed Airframe Mass	25,200 lbs
Spray System	Injectors are located immediately aft of the trailing edge of the wing, 23 nozzles per wing, distributed across the wingspan from the root of the wing to a maximum of 86% of the span.
Nozzle Type	BETE NF70

Document Number - t2015.j520.008
Issued as Revision 1, October 14th 2016
Doc Ref: Atlas:\...\t2015.j520.008.1.odt
amogconsulting.com
EIN 20-4906471
TX PE Firm F-11821

AC-E253-09v20130508

Table 9: Douglas DC-4 Configuration Data Sheet

Parameter	Information
Spray Altitude Maximum	50.0 ft
Spray Altitude Minimum	100.0 ft
Application Speed Minimum (Ground Speed)	120.0 kn
Application Speed Maximum (Ground Speed)	160.0 kn
Assume Flap Angle	10.0°
Assumed Airframe Mass	70,000 lbs
Spray System	The system has been modeled with nine nozzles per wing, located approximately 1 foot above the top surface of the wing and approximately located following the trailing edge to a maximum of 60% of wingspan.
Nozzle Type	BETE NF70

12.1 PARTICLE SIZE DISTRIBUTION

The DST has been developed utilising spray droplets that are modeled with an ASAE Medium to Coarse particle size distribution. Table 10 shows the Cumulative Density Function (CDF) for the Medium to Coarse particle sizes:

Table 10: ASAE Medium To Coarse CDF

Number	Particle Size (um)	Cumulative Density Function
1	35.01	0.0003
2	40.57	0.0006
3	47.03	0.0016
4	54.50	0.0043
5	63.16	0.0093
6	73.23	0.0156
7	84.85	0.0213
8	98.12	0.0283
9	113.71	0.0406
10	131.73	0.0623
11	152.79	0.0950
12	177.84	0.1330
13	205.84	0.1760
14	238.45	0.2393
15	276.48	0.3263
16	320.60	0.4500
17	372.18	0.5897
18	430.74	0.7244
19	498.91	0.8394
20	578.54	0.9211
21	670.72	0.9564
22	777.39	0.9691
23	900.61	0.9791
24	1044.42	0.9874
25	1210.66	0.9941
26	1403.04	1.0000

Document Number - t2015.j520.008
Issued as Revision 1, October 14th 2016
Doc Ref: Atlas:\...\t2015.j520.008.1.odt
amogconsulting.com
EIN 20-4906471
TX PE Firm F-11821

AC-E253-09v20130508

Figure 18 below shows a plot of the ASAE Medium to Coarse particle size Probability Density Function (PDF).

Figure 18 : ASAE Medium to Coarse PDF
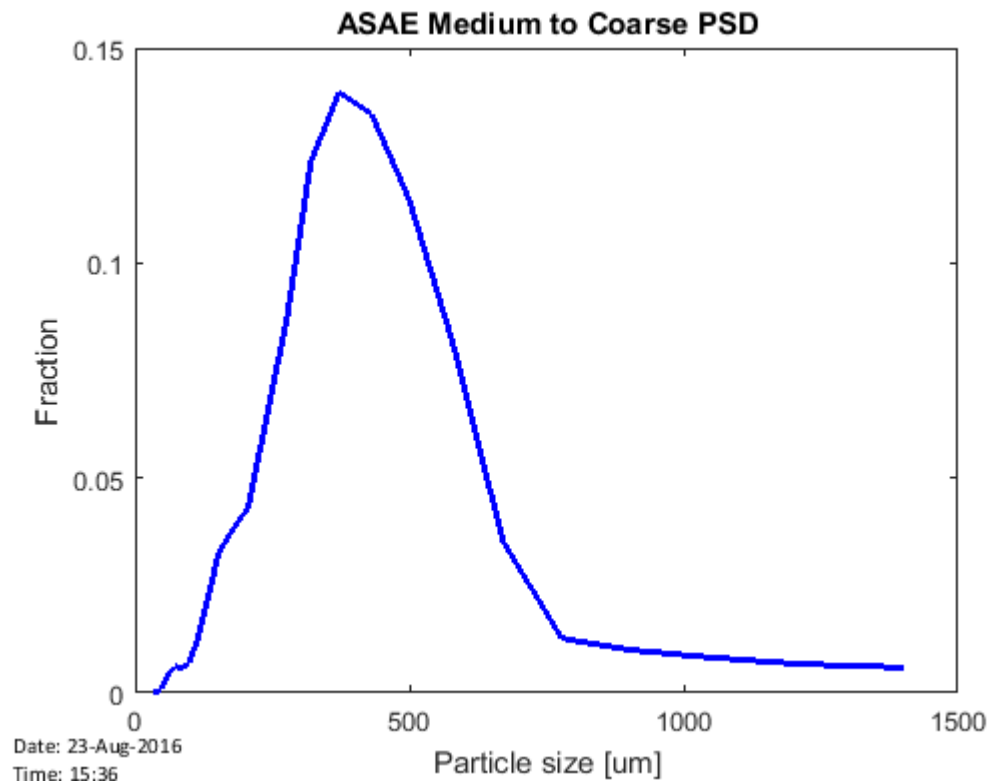
Document Number - t2015.j520.008
Issued as Revision 1, October 14th 2016
Doc Ref: Atlas:\...\t2015.j520.008.1.odt
amogconsulting.com
EIN 20-4906471
TX PE Firm F-11821

AC-E253-09v20130508

13   REFERENCES

[1] Genwest Systems. (2008). Dispersant Mission Planner (Version 2). National Atmospheric and Oceanographic Administration. Retrieved from http://response.restoration.noaa.gov/oil-and-chemical-spills/oil-spills/response-tools/dispersant-mission-planner-dmp2.html

[2] AMOG Consulting Inc. (2016). Development of Spray Mechanics CFD Model. Doc. No. r2015.j087.001.A.

[3] URL, https://developers.google.com/kml/documentation/. Retrieved 16th August, 2016.

[4] URL, https://developers.google.com/kml/documentation/kmlreference. Retrieved 16th August 2016.

Document Number - t2015.j520.008
Issued as Revision 1, October 14th 2016
Doc Ref: Atlas:\...\t2015.j520.008.1.odt
amogconsulting.com
EIN 20-4906471
TX PE Firm F-11821

AC-E253-09v20130508

APPENDIX B   CFD METHODOLOGY AND FULL RESULTS

Appendix Contents List

Document Name/Number	No Of Pages
t2015.j520.009.0	96
Notes: 1. All documents in this appendix maintain their original numbering.	

Document Number - r2015.j520.001
Issued as Revision 1, October 14th 2016
Doc Ref: Atlas:\…\r2015.j520.001.1.odt
amogconsulting.com
EIN 20-4906471
TX PE Firm F-11821

AI-E253-10v20130508

CFD Methodology and Full CFD Results

OSSR Program Develop An Innovative Dispersant Spray Drift Model

Bureau of Safety and Environmental Enforcement (BSEE)

Engineering solutions

September 30th 2016

CFD Methodology and Full CFD Results

OSSR Program Develop An Innovative Dispersant Spray Drift Model

Bureau of Safety and Environmental Enforcement (BSEE)

Document Number - t2015.j520.009, Issued as Revision 0   Reference # t2015.j520.009rev0

DOCUMENT ISSUE AND DISTRIBUTION

Document Number	Document Title
t2015.j520.009	CFD Methodology and Full CFD Results

Job Number	Job Title
2015.j520	OSSR Program Develop an Innovative Dispersant Spray Drift Model

Client	Recipient
Bureau of Safety and Environmental Enforcement (BSEE)	Alex Ruttenberg

Client Address	Position
Oil Spill Preparedness Division 45600 Woodland Road, Mail Stop VAE-OSPD Sterling, VA 20166	Research Specialist

Issue	Date Issued	Author	Checked	Authorised
Revision 0	September 30th 2016	C Galtry N Boustead P Kurts	P Kriznic	D. G. Washington

DISTRIBUTION OF COPIES

Copy Number	Location
1	AMOG Consulting
2	Bureau of Safety and Environmental Enforcement (BSEE)

REVISION REGISTER

Page	Revision	Date	Comment

Document Number - t2015.j520.009
Issued as Revision 0, September 30th 2016
Doc Ref: Atlas:\...\t2015.j520.009.0.odt
amogconsulting.com
EIN 20-4906471
TX PE Firm F-11821

AI-E253-09v20130508

TABLE OF CONTENTS

Document Number - t2015.j520.009
Issued as Revision 0, September 30th 2016
Doc Ref: Atlas:\...\t2015.j520.009.0.odt
amogconsulting.com
EIN 20-4906471
TX PE Firm F-11821

AI-E253-09v20130508

LIST OF TABLES

LIST OF FIGURES

AI-E253-09v20130508

ABBREVIATIONS

ABL	Atmospheric Boundary Layer
AMOG	AMOG Consulting Inc.
ASAE	American Society of Agricultural Engineers
BSEE	Bureau of Safety and Environmental Enforcement
CAD	Computer Aided Design
CFD	Computational Fluid Dynamics
DMP2	Dispersant Mission Planner 2
DST	Decision Support Tool
IGE	In Ground Effect
NACA	National Advisory Committee for Aeronautics
OGE	Out of Ground Effect
OSRO	Oil Spill Response Organization
PSD	Particle Size Distribution
RANS	Reynolds-Averaged Navier Stokes
RIDSS	Rapid Installation and Deployment Spray System
RPM	Revolutions Per Minute
SST	Shear Stress Transport
UTC	Coordinated Universal Time

Document Number - t2015.j520.009
Issued as Revision 0, September 30th 2016
Doc Ref: Atlas:\...\t2015.j520.009.0.odt
amogconsulting.com
EIN 20-4906471
TX PE Firm F-11821

AI-E253-09v20130508

NOMENCLATURE

C_D	Drag coefficient
C_μ	Empirical constant in k-ω SST turbulence model
d	Nozzle effective diameter
F_D	Drag force
F_p	Pressure gradient force on a fluid droplet
k	Turbulent kinetic energy
p_{static}	Static pressure
Q	Dispersant flow rate (per minute)
Q_A	Dispersant flow rate (per acre)
q	Dynamic pressure
Re	Reynolds Number
Re_p	Fluid droplet Reynolds Number
u_*	ABL friction velocity
U_w	Wind velocity
U_x	Streamwise velocity
U_y	Lateral velocity
$V_{airspeed}$	Airspeed
$V_{groundspeed}$	Groundspeed
V_p	Droplet velocity
$V_{p,inlet}$	Droplet velocity at the nozzle
w_s	Swath width
x	Streamwise axis
y	Lateral axis
z	Height axis
z_0	Sea surface roughness height
z_a	Aircraft height above sea surface
β'	Empirical constant in k-ω SST turbulence model
θ	Angle between aircraft track and wind direction
κ	Von Karman Constant
ω	Specific dissipation rate

AI-E253-09v20130508

1 INTRODUCTION

AMOG was contracted by the Bureau of Safety and Environmental Enforcement (BSEE) under Contract Number E15PC00015 to develop a Decision Support Tool (DST), to assist planners to identify operational windows and safety setback distances based on forecast meteorological conditions, spray drift pattern, aircraft types and release rates.

A number of tools currently exist for aerial dispersant planning such as the pesticide spray tools AGDISP and AgDRIFT. These tools have previously been used in oil spill response operations, however they were not developed for use in such scenarios.

In Phase 2 of the project high fidelity Computational Fluid Dynamics (CFD) models were developed to assess the suitability (or otherwise) of the existing airborne dispersion models for incorporation into the DST. In Phase 3 of the project the CFD models were used to assess the results from existing aerial dispersant modeling tools, and where necessary to aid in the development of the DST. This document provides a comprehensive summary of the CFD modeling conducted in Phases 2 and 3 of the project.

1.1 DOCUMENT SCOPE

This Appendix presents the full methodology and results of the CFD modeling conducted in order to develop the DST. It accompanies AMOG document r2015.j520.001.A, the draft final report for the DST development project. This document is limited to a discussion of the CFD results. The implications thereof on the development of the DST are described in full in the final report.

1.2 DOCUMENT LAYOUT

This document is structured as follows:

- Section 2 outlines the configuration of each of the aircraft and spray systems upon which the CFD models were created;

- Section 3 presents the implementation of the CFD modeling activities including a description of the meshing strategies employed, the physical phenomena modeled and the boundary conditions that were applied;

- Section 4 contains a summary of verification and validation activities conducted on the CFD models;

- Sections 5 and 6 present a full summary of the results extracted from the CFD models; and

- Section 7 contains the references list.

Document Number - t2015.j520.009
Issued as Revision 0, September 30th 2016
Doc Ref: Atlas:\...\t2015.j520.009.0.odt
amogconsulting.com
EIN 20-4906471
TX PE Firm F-11821

AI-E253-09v20130508

2 AIRCRAFT GEOMETRY

This section describes the Computer Aided Design (CAD) geometries constructed for each of the aircraft platforms under consideration, as defined in the Requirements Specification (AMOG Consulting Inc., 2016). For each aircraft, the geometry created is detailed, and discussion is included of any decisions made as to the level of detail required for the CFD models. The geometries were created using the Autodesk Inventor CAD package.

For all aircraft the level of detail was selected based on the objectives of the CFD modeling activities (presented in detail in Section 3). Specifically, this included accurate representation of the wings and tail, overall size and shape of the fuselage and the omission of small details such as landing gear, flap hinges, surface roughness and ancillary equipment (e.g. lights and antennae).

Significant difficulties were encountered in securing engineering drawings of the airframes, and as such model geometry has been generated on the basis of the most accurate sources of geometric data available. Where simplifications or assumptions have been made which differ from the sources of geometric information, these are noted in the relevant airframe descriptions outlined in following sections. The modeling methodology has been developed in a modular fashion such that should more accurate CAD models, drawings or operational parameters become available, these may be incorporated into the existing models to further improve the fidelity of the CFD.

2.1 LOCKHEED MARTIN C-130A

Geometric data for the C-130A was primarily sourced from a manufacturer report on Aerodynamic Data for Structural Loads (Lockheed Aircraft Corporation, 1953). This reference provided the airfoil sections, angles of incidence, wing taper and twist profiles. The fuselage geometry was drafted based on publicly available images and models (TurboSquid, 2012) of the C-130A. The model geometry is displayed in Figure 1. Leading particulars for the CAD geometry are compared with published figures for the C-130A in Table 1. This comparison was made in the absence of legible overall dimensions in the Lockheed report. All major dimensions are accurate to within 5%, with the exception of the overall height, for which the reference value is uncertain due to the possible inclusion of the landing gear. In particular, the span of each aerodynamic surface is within 1.5% of the reference value.

Figure 1 : C-130A model geometry

Table 1: C-130A Airframe Particulars

Dimension	Actual C-130A	CAD Geometry	% Difference
Wing Span (ft)	132.5	131.9	-0.5
Horizontal Tail Span (ft)	52.8	52.2	-1.2
Vertical Tail Span (ft)	23.3	23.0	-1.4
Overall Length (ft)	96.1[2]	99.7	3.8
Height (ft)	39.0[2, 3]	35.4[4]	-9.2

Notes:
1. All data sourced from Lockheed unless noted otherwise.
2. Ref: (US Air Force, 2003).
3. The quoted height is assumed to include landing gear.
4. Height measured from lowest point on fuselage to top of tail (does not include landing gear).

While engineering drawings of the C-130A (including main wing flap details) were identified as being available from the Smithsonian Institution and a request for this data submitted, delivery of the data was delayed beyond the timeline required to incorporate it into the models and simulations for the C-130A based on available data was complete. As such, in the absence of detailed main wing flap geometry, the wing flaps were represented in a simplified form.

Document Number - t2015.j520.009
Issued as Revision 0, September 30th 2016
Doc Ref: Atlas:\...\t2015.j520.009.0.odt
amogconsulting.com
EIN 20-4906471
TX PE Firm F-11821

AI-E253-09v20130508

Inclusion of the main wing flaps was considered necessary to represent the typical C-130A configuration during spray operations. As limited geometry detail was available, a sub-model of a C-130A wing was constructed including an estimated flap geometry based on publicly available data (Paulson 1976) to investigate the effect on the local wake and tip vortex formation. Preliminary investigations based on this sub-model indicated that including the slot between the fowler flap and the main wing is likely to reduce the strength of the flap tip vortex and affect the downwash over the span of the flap.

The interaction between the flap tip vortex and downwash is complex and in order to quantify the effect on spray drift extent further accurate modeling of the flap detail would be required. Owing to the need to resolve the flow in the gap between the main wing and the flap, detailed modeling is expected to lead to a significant increase in CFD mesh cell count and a corresponding increase in the size and complexity of the CFD model.
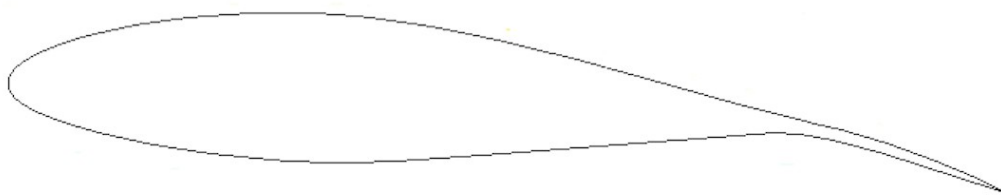
Figure 2 : Cross section of main wing inboard showing simplified flap geometry
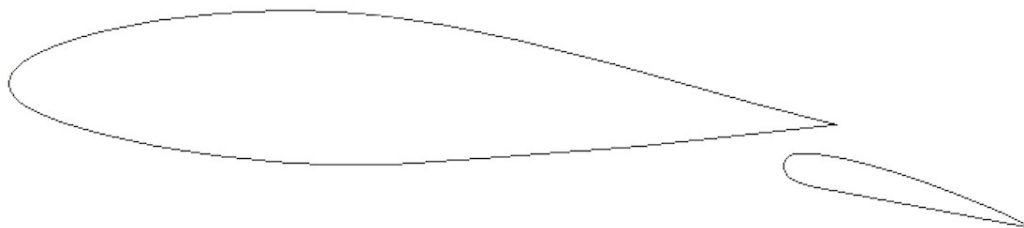
Figure 3 : Cross section of main wing inboard showing estimated fowler flap geometry

Photographs of the C-130A, such as that shown in Figure 4, were used to confirm that no fences, vortex generators or other flow management devices are present on the wings of the aircraft used for dispersant spraying. The additional pylon mounted fuel tanks as seen in Figure 4 were not modeled, as no drawings of these components were available. It was assumed that the pylons and tanks are designed to present minimum drag, and therefore that they have minimal influence on the flow closer to the fuselage where the dispersant is released.

In the absence of detailed drawings the fairing of the vertical stabilizer into the fuselage has been simplified, as shown in Figure 5. Given that this fairing is located on the upper surface of the aircraft

Document Number - t2015.j520.009
Issued as Revision 0, September 30th 2016
Doc Ref: Atlas:\...\t2015.j520.009.0.odt
amogconsulting.com
EIN 20-4906471
TX PE Firm F-11821

AI-E253-09v20130508

and away from any interaction with the dispersant spray, this simplification is considered appropriate and unlikely to result in any discrepancy between the modeled and actual spray behaviors.

Figure 4 : Image of C-130A ((Lawrence, n.d.)

Document Number - t2015.j520.009
Issued as Revision 0, September 30th 2016
Doc Ref: Atlas:\...\t2015.j520.009.0.odt
amogconsulting.com
EIN 20-4906471
TX PE Firm F-11821

AI-E253-09v20130508

Figure 5 : Comparison of modeled and actual C-130A vertical stabilizers

2.1.1   Operational Configuration

Based on images of the C-130A platform during spraying operations (as shown in Figure 6) it is clear that the main wing flaps are deployed, and that significant flap angle is used. In the absence of operational information from spray dispersant operators as to the flap angle during spraying, an angle of 18 $^\circ$ (half of the maximum flap angle on the C-130A (Lockheed Aircraft Corporation, 1953) has been used. This is considered to be comparable to the angle shown in Figure 6 and is sufficient to generate the required lift to maintain level flight.

Further detail on the methodology for determining the required angle of attack to sustain level flight during the cases modeled is presented in Section 3.3.4. The validation of this methodology is presented in Section 4.3.

Document Number - t2015.j520.009
Issued as Revision 0, September 30th 2016
Doc Ref: Atlas:\...\t2015.j520.009.0.odt
amogconsulting.com
EIN 20-4906471

TX PE Firm F-11821

AI-E253-09v20130508

Figure 6 : Image of C-130A during dispersant spraying operations (International Air Response, 2015a)

2.1.2   Propeller Representation

The C-130A has been modeled with a Hamilton Standard 4-bladed propeller, type 54H60 as typically used on the C-130A (Hamilton Sundstrand, 2011). The 54H60 propeller is a fully feathering propeller modeled with a diameter of 13.5 ft which is configured to rotate at a constant rate of 1020 RPM.

AMOG secured a non-disclosure agreement with Coordinated Universal Time (UTC) Aerospace Systems, who hold performance data for this propeller, and utilized the provided performance curves to perform representative modeling of the 54H60 within the CFD model in accordance with methodology presented in Section 3.3.5.

2.1.3   Spray System Geometry

The spray system geometry has been estimated based on imagery of the C-130A during dispersant spray operations, examples of which are shown in Figure 5. Dimensions were scaled from the available images based on known dimensions of the aircraft. In the CFD model, 28 spray nozzles were equally spaced 1 ft apart, as shown in Figure 6. The spray boom in the model was located vertically in line with the bottom of the main cargo door, and longitudinally immediately behind the side door.

Document Number - t2015.j520.009
Issued as Revision 0, September 30th 2016
Doc Ref: Atlas:\...\t2015.j520.009.0.odt
amogconsulting.com
EIN 20-4906471
TX PE Firm F-11821

AI-E253-09v20130508
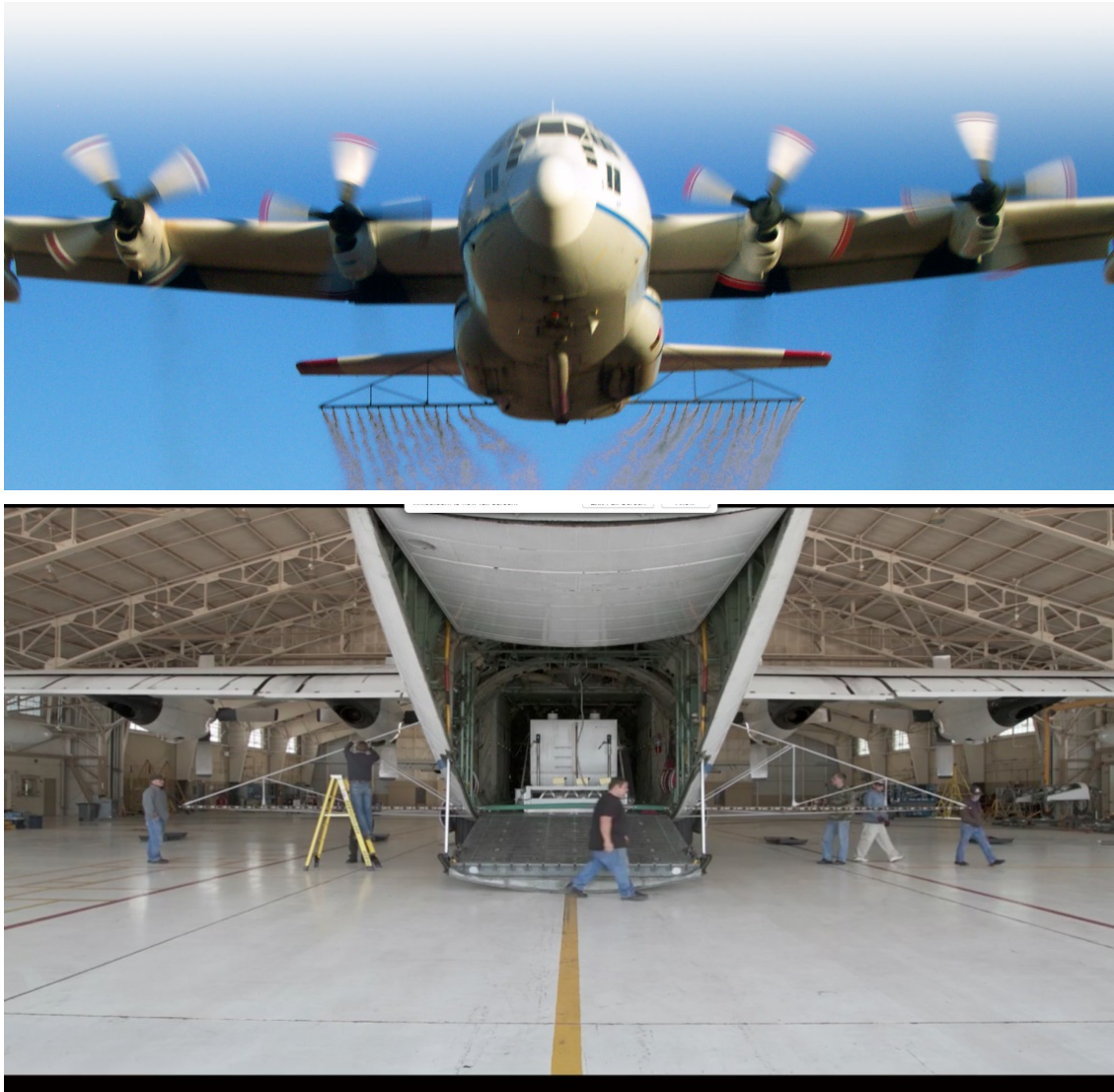
Figure 7 : C-130A spray boom arrangement (MSRC, 2016)

Document Number - t2015.j520.009
Issued as Revision 0, September 30th 2016
Doc Ref: Atlas:\...\t2015.j520.009.0.odt
amogconsulting.com
EIN 20-4906471
TX PE Firm F-11821

AI-E253-09v20130508
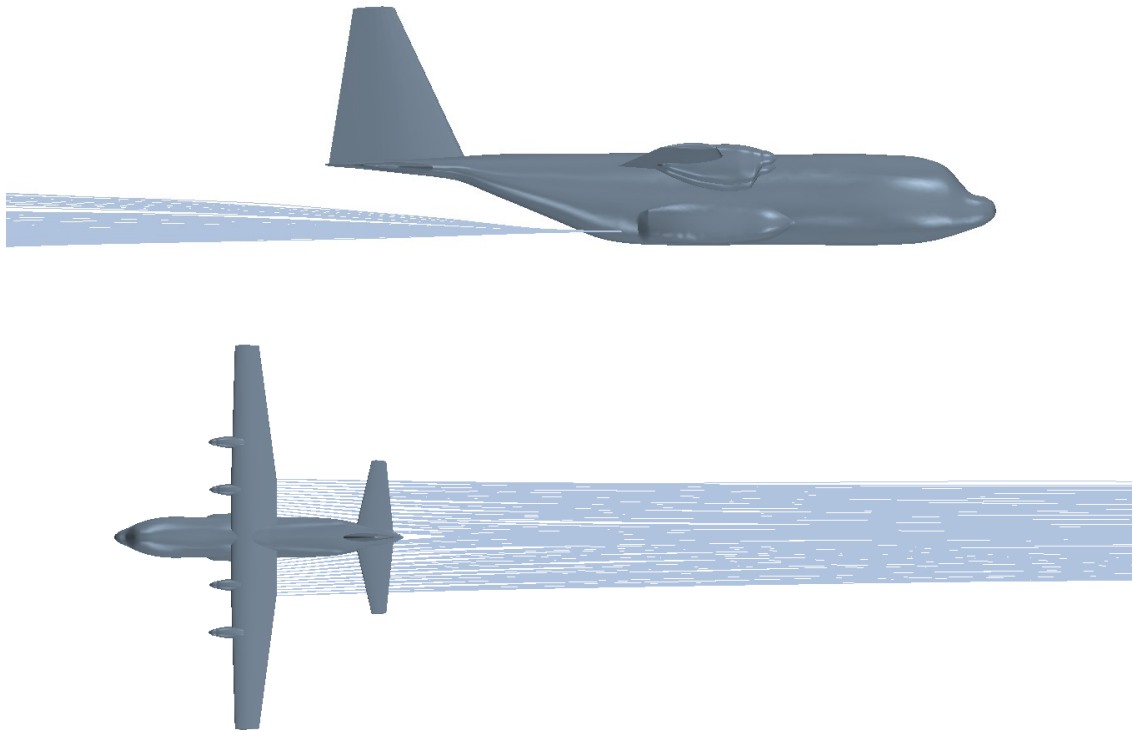
Figure 8 : Modeled C-130A spray boom arrangement

Document Number - t2015.j520.009
Issued as Revision 0, September 30th 2016
Doc Ref: Atlas:\...\t2015.j520.009.0.odt
amogconsulting.com
EIN 20-4906471

TX PE Firm F-11821

AI-E253-09v20130508

2.2   DOUGLAS DC-3

Technical data for the DC-3 was primarily sourced from Maircraft (2016). The obtained information has been supplemented, and validated, by the description provided in a general arrangement document (Quebecair Inc. Regulations, 1957a). Together these two references provided the airfoil sections, angles of incidence, wing taper and twist profiles, as well as the fuselage stations. The split trailing edge flap was modeled as shown by Maircraft. The DC-3 model geometry is shown in Figure 9.

Leading particulars for the CAD geometry are compared with published figures for the DC-3 in Table 2. All major dimensions are accurate to within 3%.

Figure 9 : Douglas DC-3 model geometry

Table 2: DC-3 Airframe Particulars

Dimension	Actual DC-3	CAD Geometry	% Difference
Wing Span (ft)	95	96.4	1.4
Overall Length (ft)	64.5	64.5	-0.1
Height (ft)	16.9	17.4	2.6
Notes: 1. All actual DC-3 dimensions sourced from Airborne Support Inc. (2016) 2. Dimension percentage difference considers length differences less than the resolution of significant figures of dimensions presented above.			

Document Number - t2015.j520.009
Issued as Revision 0, September 30th 2016
Doc Ref: Atlas:\...\t2015.j520.009.0.odt
amogconsulting.com
EIN 20-4906471
TX PE Firm F-11821

AI-E253-09v20130508

2.2.1   Operational Configuration

As described above, the DC-3 main wing flaps are of a split trailing edge type and the full flap deployment angle is 45° (Quebecair Inc. Regulations, 1957b, p. 61). A training reference for DC-3 pilots (DC3Training.com, 2012) indicates flap extension settings of ¼, ½, ¾ and full are available. A flap setting of ¼ has been selected for modeling as this setting corresponds to the only 'do-not-exceed' speed (135 kn) that is greater than the application speed of 130 kn. It is recognized that the true airspeed for some of the cases modeled is beyond the allowable flap deployment speeds as indicated in the flight manual, however these models conservatively maintain the ¼ flap deflection as this configuration exhibited the greatest impact on spray drift extents.

The aircraft angle of attack was established on the basis of balancing the weight of the aircraft with the lift produced in order to simulate steady level flight conditions.

Further detail on the methodology for determining the required angle of attack to sustain level flight during the cases modeled is presented in Section 3.3.4. The validation of this methodology is presented in Section 4.3.

2.2.2   Propeller Representation

The DC-3 has been modeled with 3 bladed variable pitch Hamilton Standard propellers, model 23E50 hub with blade model 6477 having a diameter of 11.6 ft, configured to rotate at a constant rate of 1200 RPM (Delta Flight Museum, 2016).

In the absence of detailed performance curves, the DC-3 model includes propeller momentum based on representative propeller performance data. This was implemented in the CFD model over the propeller diameter by means of a virtual disk model. Further detail on the methodology for modeling the effect of added propeller momentum to the aircraft wake is discussed in Section 3.3.5.

2.2.3   Spray System Geometry

The spray boom of the DC-3 has been modeled from available images released by Airborne Support, an organization known to provide support to oil dispersant operations.

Document Number - t2015.j520.009
Issued as Revision 0, September 30th 2016
Doc Ref: Atlas:\...\t2015.j520.009.0.odt
amogconsulting.com
EIN 20-4906471
TX PE Firm F-11821

AI-E253-09v20130508

Figure 10 : DC-3 spray boom arrangement (Airborne Support Inc., 2016)

From Figure 8 it can be seen that on this aircraft the nozzles are not equally distributed along the wing. Additionally, it appears that the nozzles are located immediately aft of the trailing edge of the wing, ejecting dispersant inline with the free-stream flow direction.

Due to the limited availability of DC-3 spray system geometry, the span-wise distribution of the injectors for the DC-3 has been estimated from a Basler BT-67 in operation as shown in Figure 11. The BT-67 is a modified DC-3 with a lengthened fuselage and altered wingtips. Given that the section of the wings to which the spray system connects are identical for the DC-3 and BT-67, it was assumed that the spray systems used are the same.

The spray system arrangement modeled in the CFD consisted of 23 nozzles per wing, distributed across the wingspan to a maximum span-wise extent as estimated from Figure 11. The modeled injector locations for the DC-3 can be seen in Figure 12.
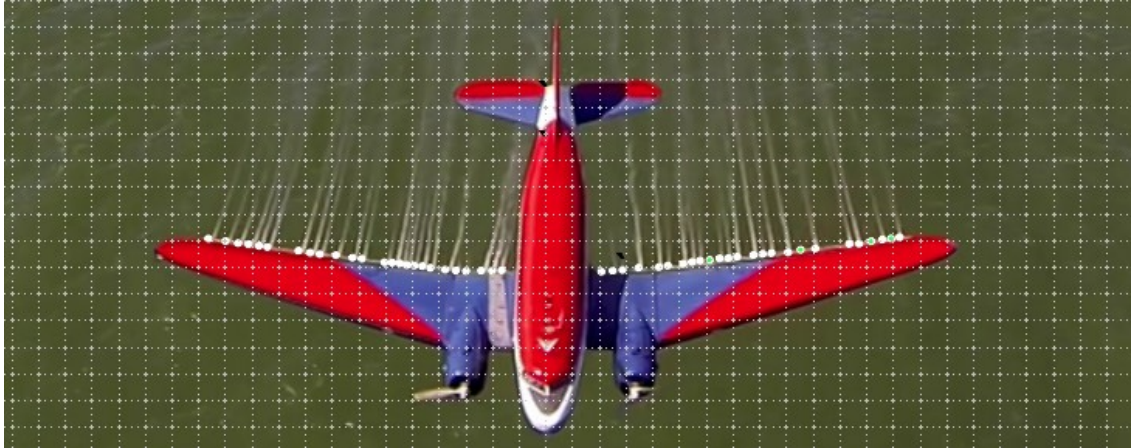
Figure 11 : BT-67 spray boom arrangement with gridlines and injector markers included (Airborne Support Inc., 2016)
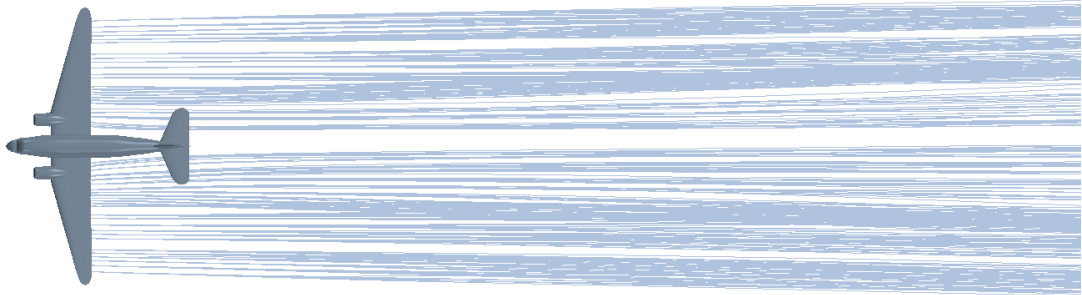
Figure 12 : Modeled DC-3 spray boom arrangement

Document Number - t2015.j520.009
Issued as Revision 0, September 30th 2016
Doc Ref: Atlas:\...\t2015.j520.009.0.odt
amogconsulting.com
EIN 20-4906471
TX PE Firm F-11821

AI-E253-09v20130508

2.3   DOUGLAS DC-4

In the absence of detailed aircraft technical drawings of the DC-4 in the public domain, a set of scale plans were obtained for the DC-4 (C Smith Plans, 2016), based on the original aircraft technical drawings. These scale plans are sold primarily for the purpose of building replica scale models. The modeled geometry of the DC-4 fuselage and tail section was drafted on the basis of these scale plan drawings.

The wing geometry was constructed from NACA sections as specified in publicly available data sources ("Airfoils, Webpage," 2016) at dihedral and washout angles as indicated in the model drawings (C Smith Plans, 2016). The model geometry is displayed in Figure 13. Leading particulars for the CAD geometry are compared with published figures for the DC-4 in Table 3.

The length and span of the modeled DC-4 are accurate to within 1 %. The apparent discrepancy in overall height is assumed to be due to the inclusion of the landing gear in the reference measurement.
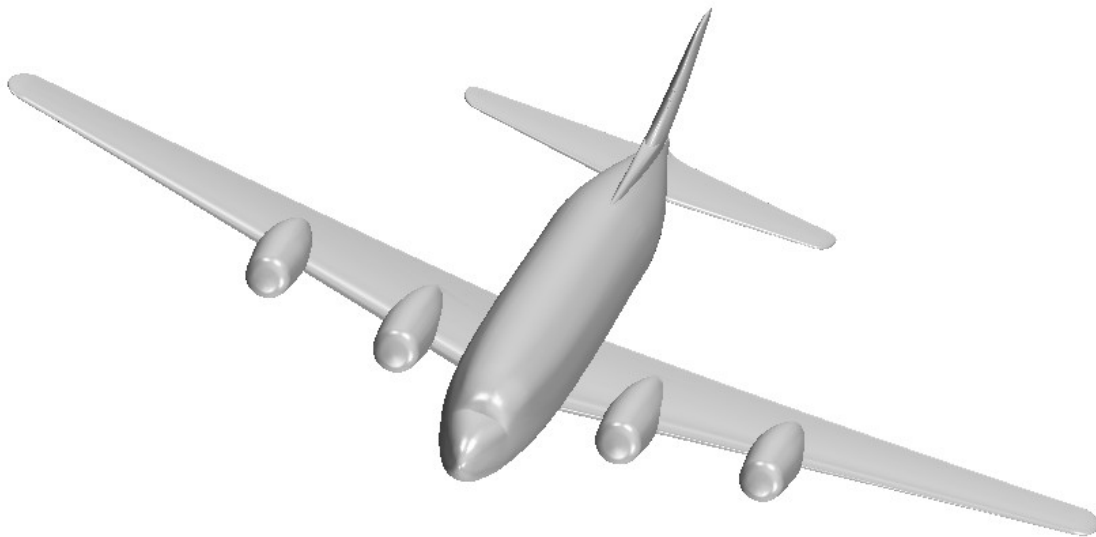
Figure 13 : Douglas DC-4 model geometry

Document Number - t2015.j520.009
Issued as Revision 0, September 30th 2016
Doc Ref: Atlas:\...\t2015.j520.009.0.odt
amogconsulting.com
EIN 20-4906471
TX PE Firm F-11821

AI-E253-09v20130508

Table 3: DC-4 Airframe Particulars

Dimension	Actual DC-4	CAD Geometry	% Difference
Wing Span (ft)	117.5[1]	116.5	-0.8
Overall Length (ft)	93.8[2]	93.7	-0.1
Height (ft)	27.5[3,4]	23.5[5]	-14.5

Notes:
1. Dimension from various sources ("Take Flight Video Productions - The Makers of the Real Life Aviator Video Series!," 2016), ("Douglas DC-4 | Airliners.net," 2016), ("The Douglas DC-4, DC-6, & DC-7," 2016)
2. ("Douglas DC-4 | Airliners.net," 2016)
3. ("Douglas DC-4 commercial aircraft. Pictures, specifications, reviews.," 2016), ("Douglas DC-4 (C-54) - Specifications - Technical Data / Description," 2016)
4. The quoted height is assumed to include landing gear
5. Height measured from lowest point on fuselage to top of tail (does not include landing gear)

2.3.1   Operational Configuration

Given the cruise speed of the DC-4 is approximately 197 kn ("Douglas DC-4 | Airliners.net," 2016) and the application speed is 150 kn (Genwest Systems, 2008), the DC-4 was assumed to require some flap deflection to achieve steady level flight whilst maintaining a reasonable angle of attack for cases at the lower end of the application speed envelope. This assumption is reinforced by the operational spray photo sourced from the Dispersant Mission Planner 2 (DMP2) program (Genwest Systems, 2008), shown in Figure 14.

As operator data on typical flap deflection settings during spray operations was unavailable at the time of modeling, the trailing edge flap deployment was estimated on the basis on information from a DC-4 Flight manual ("The Vietnam Center and Archive: Virtual Vietnam Archive," n.d.). The flight manual states the maximum flap extension of approximately 40° in the full down position (pg. 1-47) and indicates for a base leg of a landing approach with a speed of 120 kn that flap deployment of 10° is recommended (pp. 2-19).

The required aircraft angle of attack was established on the basis of balancing the weight of the aircraft with the lift produced in order to simulate steady level flight conditions. Further detail on the methodology for determining the required angle of attack to sustain level flight during the cases modeled is presented in Section 3.3.4. The validation of this methodology is presented in Section 4.3.

Document Number - t2015.j520.009
Issued as Revision 0, September 30th 2016
Doc Ref: Atlas:\...\t2015.j520.009.0.odt
amogconsulting.com
EIN 20-4906471
TX PE Firm F-11821

AI-E253-09v20130508

Figure 14 : DC-4 spray, operational configuration

2.3.2   Propeller Representation

In the absence of verifiable data the DC-4 has been modeled with 3 bladed variable pitch Hamilton Standard propellers, hub model 23E50, with an assumed blade diameter of 11.6 ft, configured to rotate at a constant rate of 1450 RPM.

In the absence of detailed performance curves, the DC-4 model includes propeller thrust based on representative propeller performance data. This was implemented in the CFD model over the propeller diameter by means of a virtual disk model. Further detail on the methodology for modeling the effect of added propeller momentum to the aircraft wake is discussed in Section 3.3.5.

2.3.3   Spray System Geometry

The spray system for the DC-4 geometry has been estimated based on imagery of a Florida Air Transport aircraft, known to have been utilized for spray dispersant operations. The system has been modeled with nine injectors per wing, with positions of the injector in the CFD approximated from available images such as those shown in Figures 14 and 15 using known dimensions (such as wingspan) for scale. The injectors appear to be located above the top surface of the wing and approximately located following the trailing edge. The modeled injector locations for the DC-4 can be seen in Figure 17.

Document Number - t2015.j520.009
Issued as Revision 0, September 30th 2016
Doc Ref: Atlas:\...\t2015.j520.009.0.odt
amogconsulting.com
EIN 20-4906471
TX PE Firm F-11821

AI-E253-09v20130508

Figure 15 : DC-4 spray boom arrangement (Florida Air Transport, 2016)

Figure 16 : DC-4 spray boom arrangement (Florida Air Transport, 2016)
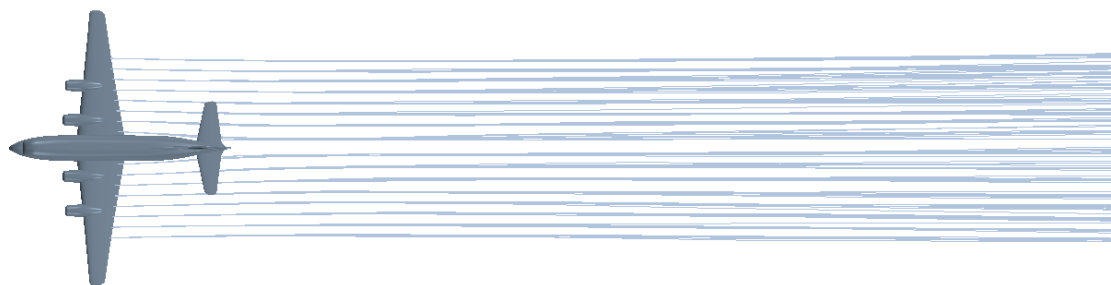
Figure 17 : Modeled DC-4 spray boom arrangement

Document Number - t2015.j520.009
Issued as Revision 0, September 30th 2016
Doc Ref: Atlas:\...\t2015.j520.009.0.odt
amogconsulting.com
EIN 20-4906471
TX PE Firm F-11821

AI-E253-09v20130508

2.4 AIR TRACTOR AT-802A

Technical drawings and additional information on the AT-802A geometry were obtained directly from Air Tractor. A CAD model of the AT-802A provided by Envenio Inc. was compared with the data provided from Air-Tractor. The Envenio Inc. CAD model has previously been used to construct a CFD model of the AT-802A during spraying operations, as described by Ryan et al. (2013) . However it was found to include a number of simplifications and was considered to be of a lower fidelity than required for the purposes of this project. The representation of the wingtips in particular was expected to affect the aircraft wake, and the Envenio model wingtips were constructed as a blunt edge. Publicly available information indicates that the AT-802A includes Hoerner wingtips (Air Tractor Inc., n.d.), and this was confirmed by communications with Air Tractor. As the CFD model was intended to identify the presence of phenomena related to the tip vortices and their interaction with the aircraft wake, the blunt edge simplification of the wingtips was considered a potential source of inaccuracy. Such wingtip features have been demonstrated to have an effect on the total lift produced, and in particular affect the spanwise location of the wingtip vortices (Hoerner, 1952).

The data provided by Air Tractor enabled a higher fidelity CAD representation of the AT-802A to be produced. The Hoerner wingtips and fuselage have been modeled based on the provided drawings. Leading particulars for the CAD geometry are compared with published figures for the AT-802A in Table 4. All major dimensions are accurate to within 2%.

The produced CAD geometry is shown in Figure 18. For comparison, a photograph of the AT-802A is provided in Figure 19.

Table 4: AT-802A Airframe Particulars

Dimension	Actual AT-802A	CAD Geometry	% Difference
Wing Span (ft)	59.2[1]	59.3	0.2
Overall Length (ft)	36.5[1]	36.4	-0.3
Height (ft)	10.6[1]	10.4	-1.9
Notes: 1. (Air Tractor Inc., 2016)			

Document Number - t2015.j520.009
Issued as Revision 0, September 30th 2016
Doc Ref: Atlas:\...\t2015.j520.009.0.odt
amogconsulting.com
EIN 20-4906471
TX PE Firm F-11821

AI-E253-09v20130508
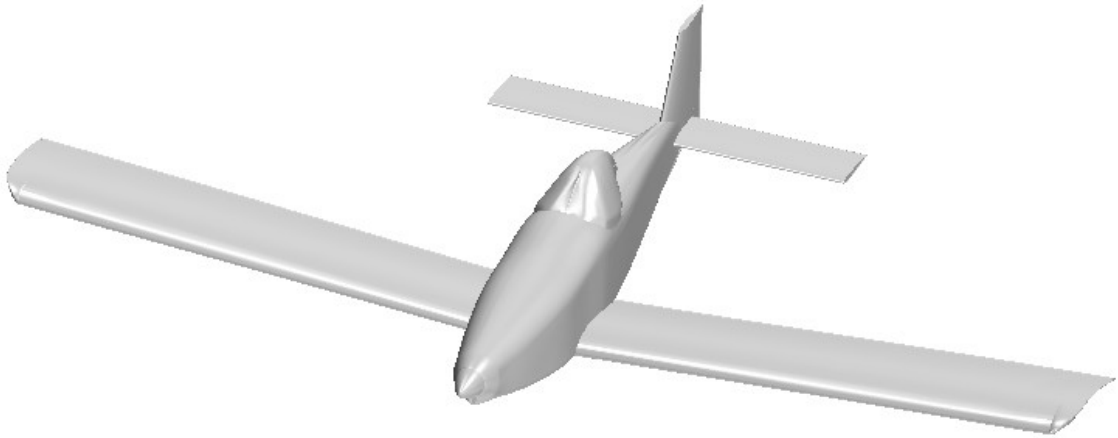
Figure 18 : AT-802A model geometry

Figure 19 : Image of AT-802A (Air Tractor Inc., n.d.)

2.4.1   Operational Configuration

Air Tractor have indicated that at typical spray speeds for the AT-802A, flap deflection is not required. The aircraft angle of attack was established on the basis of balancing the weight of the aircraft with the lift produced in order to simulate steady level flight conditions. Further detail on the methodology for determining the required angle of attack to sustain level flight during the cases modeled is presented in Section 3.3.4. The validation of this methodology is presented in Section 4.3.

2.4.2   Propeller Representation

The AT-802A was modeled with a Hartzell 5-bladed propeller (model HC-B5MA-5H/M11691 as advised by Air Tractor) with a diameter of 9.9 feet (Hartzell Propeller Inc., 2014a) powered by a 1650HP Honeywell engine (model TPE331-14GR), configured for a constant shaft output of 1552

Document Number - t2015.j520.009
Issued as Revision 0, September 30th 2016
Doc Ref: Atlas:\...\t2015.j520.009.0.odt
amogconsulting.com
EIN 20-4906471
TX PE Firm F-11821

AI-E253-09v20130508

RPM (Hartzell Propeller Inc., 2014b). Propeller geometry and characteristic curves detailing thrust, torque and power coefficients were provided by Hartzell Propeller Inc. under a non-disclosure agreement and are implemented into the CFD model. Further detail on the methodology for modeling the effect of added propeller momentum to the aircraft wake is discussed in Section 3.3.5.

2.4.3 Spray System Geometry

The spray system geometry of the AT-802A was based on the operational configuration for oil spill operations in publicly available images (as shown in Figure 20).

Figure 20 : AT-802A during coastal dispersing operation
(Australian Maritime Safety Authority, 2000)

The 10 injectors were modeled as evenly spread approximately 3 feet apart, starting at 11 feet from the wingtip (as shown in Figure 21).
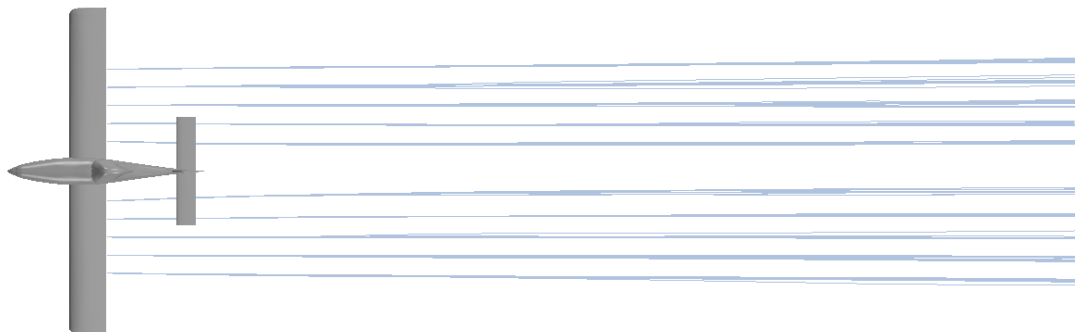
Figure 21 : Modeled AT-802A spray boom arrangement

Document Number - t2015.j520.009
Issued as Revision 0, September 30th 2016
Doc Ref: Atlas:\...\t2015.j520.009.0.odt
amogconsulting.com
EIN 20-4906471
TX PE Firm F-11821

AI-E253-09v20130508

3 CFD IMPLEMENTATION

The purpose of the CFD modeling activities was to investigate the near-field behavior of the spray dispersant, and to determine whether any phenomena exist which significantly affect the eventual drift of the dispersant, which are not accounted for in the currently available models (i.e. AgDRIFT and AGDISP). Such phenomena include the previously identified interaction between the wake of the fuselage (which is not modeled by AGDISP or AgDRIFT) and the tip vortices, and the resulting effect on the entrainment of the dispersant within the tip vortex (Ryan et al., 2013).

The CFD models were intended to provide an understanding of the effect of the typical range of operational parameters that may be used in the course of spraying on any relevant phenomena affecting the dispersant. The focus was on modeling the near-field flow that may impact the trajectory of the dispersant as it is sprayed from the aircraft, and subsequently travels to the sea surface. The following objectives were identified for the CFD models:

- Resolve the aerodynamic flow features around the aircraft likely to impact on the spray release trajectory. In particular, the overall lift generation, strength and location of vortical structures and large-scale wake/blockage effects should be resolved.

- Represent the aircraft geometry to a level of detail commensurate with the first objective, removing any geometric detail which will not have a significant effect on the aerodynamics affecting the spray release.

- Implement a representative model of the propellers in order to resolve the effect of the propeller wash on the spray release.

- Model the trajectory of the spray droplets, accounting for aerodynamic forces on the particles and, in particular, turbulent dispersion.

- Demonstrate that the results obtained are grid independent and unaffected by blockage of the fluid domain.

3.1 OVERVIEW OF THE MODELING APPROACH

The CFD model of each aircraft was developed within a structured framework which allows aircraft and aircraft operating conditions to be changed in an automated fashion. Constructing the CFD models in this way is beneficial as it creates models of a consistent quality in a time effective manner. The modeling approach consisted of the following stages:

Stage 1 – Data gathering: Geometric and operational particulars for each aircraft were gathered and processed into inputs for the CFD models.

Stage 2 – Sub-model development: The effects of various model details were explored using sub-models in order to determine which details were critical to modeling the spray release from the aircraft. The sub-model development also allowed small scale testing of the accuracy and stability of different physics models such as those used for the spray dispersant and propellers.

Document Number - t2015.j520.009
Issued as Revision 0, September 30th 2016
Doc Ref: Atlas:\...\t2015.j520.009.0.odt
amogconsulting.com
EIN 20-4906471
TX PE Firm F-11821

AI-E253-09v20130508

Stage 3 – Mesh generation and refinement: A mesh refinement scheme was developed to capture wingtip vortex formation, spray dispersion and wake interactions. The mesh refinement was created in a parameterized form so as to be consistently transferable to the different airframes.

Stage 4 – Base model development: Once the CFD implementation of each sub model had been tested a single base model was created which contained all of the required physics and meshing parameters.

Stage 5 – Automation: The mesh generation and case-list implementation was automated so that the selection of different aircraft, environmental conditions and aircraft operating conditions can be made parametrically.

As a result of this structured development methodology the mesh structure and physics models are consistent across all the modeled cases. The following sections describe the details of the CFD implementation using the C-130A model for illustration.

3.2   MESH GEOMETRY

In order to capture an appropriate level of detail in the flow, a suitable mesh was developed with key refinement areas common to each aircraft including inner domain (the area immediately surrounding the aircraft), wake, wing and propeller refinements. The mesh definition was parametrized such that the aircraft geometry could be made a modular input to the model whilst keeping the defined refinement ratios and mesh discretization consistent and valid across each of the airframe models. The refinement zones used for the C-130A model are shown in Figure 22.
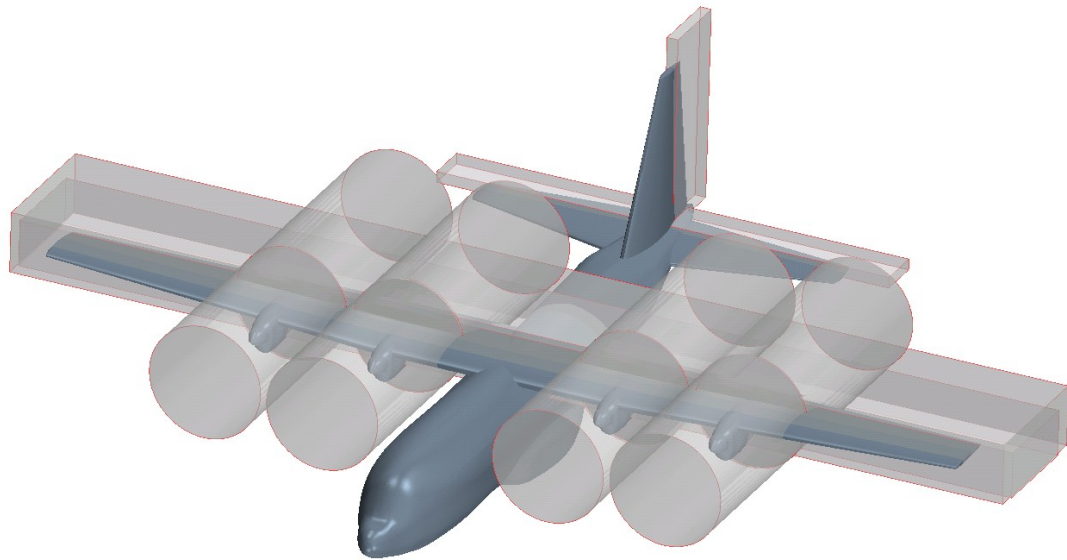
Figure 22 : Parametrically defined mesh refinements zones

Document Number - t2015.j520.009
Issued as Revision 0, September 30th 2016
Doc Ref: Atlas:\...\t2015.j520.009.0.odt
amogconsulting.com
EIN 20-4906471
TX PE Firm F-11821

AI-E253-09v20130508

3.2.1   Domain Size/Resolution

The size of the computational domain was designed to be a function of the aircraft geometry. In this way, multiplicative factors were used to determine the overall dimensions (Table 5). The inner domain length listed in Table 5 is the length of the section of the domain aligned with the heading of the aircraft containing regular polyhedral cells; the extrusion length is the length made up of extruded prism cells extending much farther downstream to capture the sprayed particle trajectories.

The domain height and width were set to ensure any blockage effects were avoided and that enforcement of the boundary conditions did not affect the flow in the vicinity of the aircraft. The extrusion length was held constant for all airframes at a distance sufficient to fully capture the near field wake while minimizing the effect of the pressure outlet boundary condition on the trajectory of the particles for all cases.

Post-processing of CFD results confirmed that significant wake features were not being affected by insufficient domain size and that the enforced boundary conditions were not constraining the flow unreasonably.

Table 5: Outer Domain Size Characterization

Dimension	Factor	Variable
Domain Height	4	Aircraft Length
Domain Width	8	Main Wing Span
Inner Domain Length	2	Aircraft Length
Extrusion Length	Constant	Constant 8200 ft for Particle Settlement on Sea Surface for each aircraft

3.2.2   Inflation Layer/Y+ Study

The non-dimensional wall distance (y+) on the aircraft surfaces is shown in Figure 23. Modeling to ensure a y+ value of less than 150 is in accordance with best practice when modeling the boundary layer by means of a wall function. Direct resolution of the boundary layer was considered impractical for the high Reynolds Number flow around the aircraft. However, it should be noted that the "all Y+" implementation of the k-ω SST model within Star CCM+ has been used, and that any cells with sufficiently low y+ values will resolve the boundary layer flow directly.

Document Number - t2015.j520.009
Issued as Revision 0, September 30th 2016
Doc Ref: Atlas:\...\t2015.j520.009.0.odt
amogconsulting.com
EIN 20-4906471
TX PE Firm F-11821

AI-E253-09v20130508
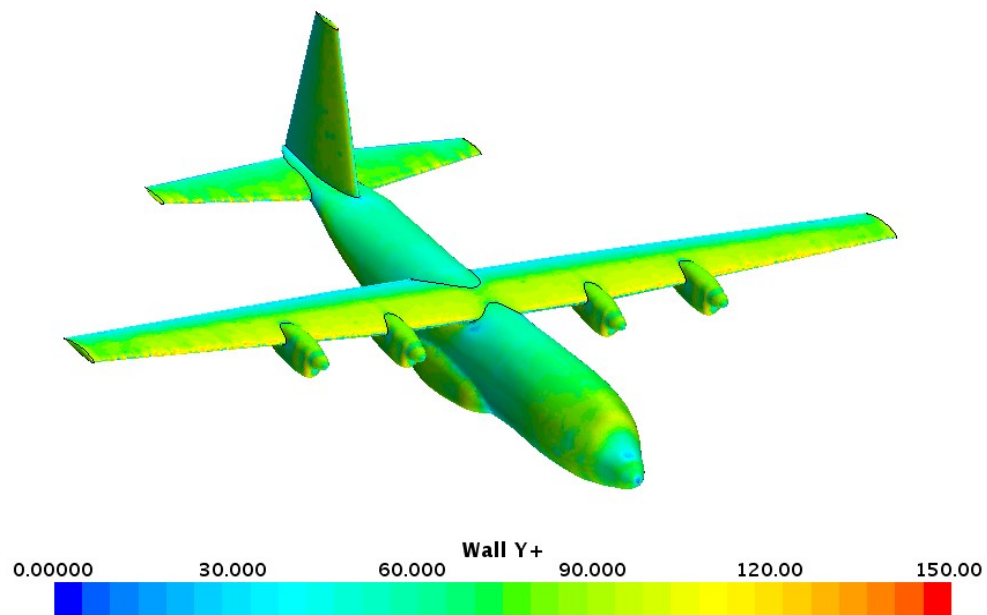
Figure 23 : Contour of non-dimensional wall distance (y+)

3.2.3   Propeller Refinement

To determine the mesh resolution required to adequately capture the propeller wash effects, a mesh resolution study was conducted on a sub-model of the propeller. The sub-model contained a propeller modeled using the virtual disk methodology as applied in the global CFD model. The required refinement settings were then applied to the global model. The resulting propeller refinement areas can be seen in Figure 24.

Document Number - t2015.j520.009
Issued as Revision 0, September 30th 2016
Doc Ref: Atlas:\...\t2015.j520.009.0.odt
amogconsulting.com
EIN 20-4906471
TX PE Firm F-11821

AI-E253-09v20130508
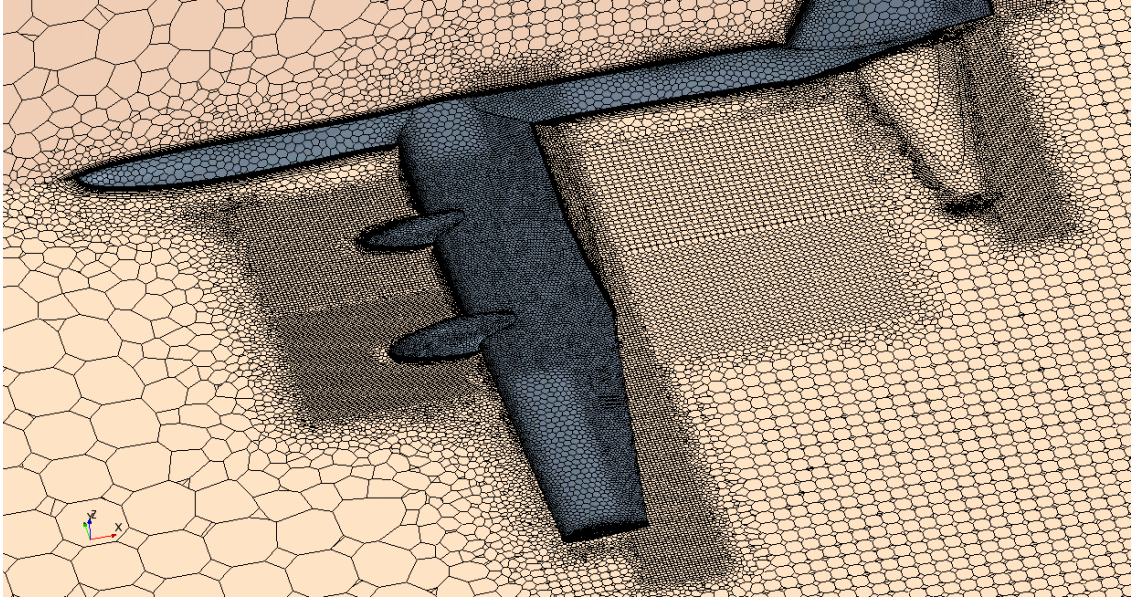
Figure 24 : Propeller wake refinement region (port wing visible)

3.2.4   Wing Refinement

Each wing refinement region was modeled as a box encompassing the outer dimensions of the wing. Wing refinement boxes were created for the main wing, horizontal tail and vertical tail. Again, factors were used against known aircraft dimensions to determine the refinement size. These factors are listed in Table 6.

Table 6: Wing Refinement Size Characterization

Dimension	Refinement	Factor	Variable
Height	Main Wing	1.1	Vertical height from lower surface of wing at the root to upper surface at the tip
	Tail - Horizontal	1.2	Horizontal tail thickness
	Tail - Vertical	1.2	Vertical tail thickness
Length	Main Wing	1.25	Wing chord
	Tail - Horizontal	0.5	Horizontal tail chord
	Tail - Vertical	0.5	Vertical tail chord
Width	Main Wing	1.1	Wing span
	Tail - Horizontal	1.2	Horizontal tail span
	Tail - Vertical	1.2	Vertical tail thickness

Document Number - t2015.j520.009
Issued as Revision 0, September 30th 2016
Doc Ref: Atlas:\...\t2015.j520.009.0.odt
amogconsulting.com
EIN 20-4906471
TX PE Firm F-11821

AI-E253-09v20130508

3.2.5   Wake Refinement

The wake refinement region was defined as an oval with an angled extrusion. The dimensions assume the wake of the aircraft to be dependent on the aircraft length and wing span, and this was confirmed by verifying that the wake was captured within the refined region.

Table 7: Wake Refinement Size Characterization

Dimension	Factor	Variable
Minor Axis	0.8	Aircraft Length
Major Axis	1.1	Main Wing Span

The wake refinement region began at the main wing root chord centre, ensuring the wingtip vortices were captured. Additionally, this refinement ensured that turbulence could be resolved at the location of the injectors. The wake region refinement zones (inner and outer) can be seen in Figure 25.
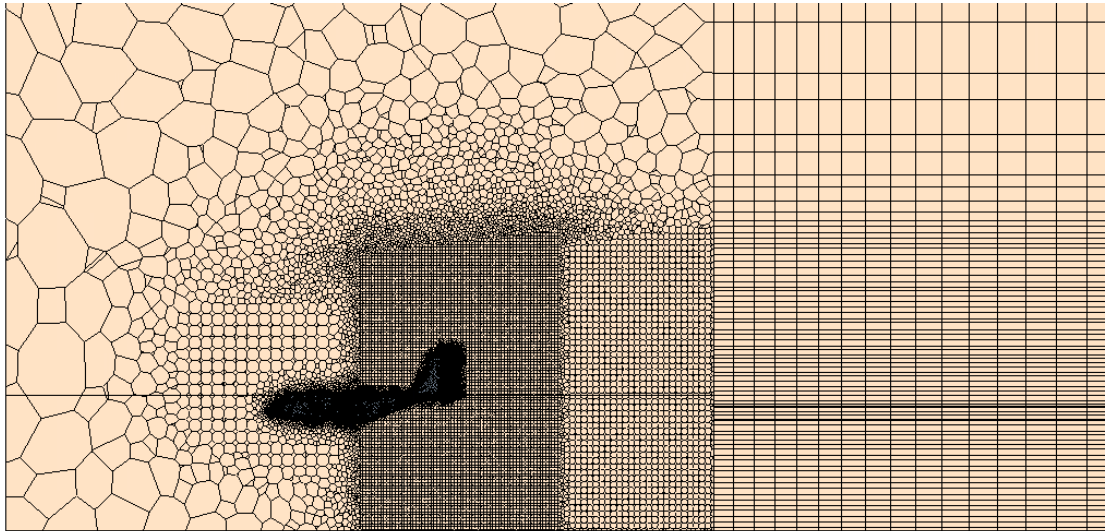
Figure 25 : Side View of the Three-Dimensional Mesh
Showing wake zones and extruded downstream region

3.2.6   Mesh Quality Metrics

Mesh quality metrics were checked for each aircraft in order to ensure that no mesh quality issues were affecting the results, as shown in Table 8. It should be noted that the criteria listed were used to determine the relative quality of the meshes for each aircraft; all of the meshes used were considered to be of sufficient quality to produce accurate results.

Table 8: Mesh Quality Metrics

Cell Metric	Criteria	Percentage Of Non-Compliant Cells [%]			
		C-130A	DC-3	DC-4	AT-802A
Quality	> 0.001	0	0	0	0
Volume Change	> 0.01	0.002	0.002	0.001	0.003
Aspect Ratio	> 0.02	0.1	0.1	0.13	0.02
Skewness Angle	< 85 degrees	0.01	0.01	0.02	0.03

3.3   PHYSICS METHOD

Star CCM+ v10.06.009 was used to solve the discretized Reynolds-Averaged Navier-Stokes (RANS) equations. Reynolds Averaging decomposes the flow into its time-averaged and fluctuating quantities, and requires an additional turbulence model for closure of the governing equations. The k-ω SST (Shear Stress Transport) turbulence model was used for all CFD models and a segregated flow solver was used with a second order upwind convection scheme to solve the resulting system of equations. The k-ω SST model has previously been used to accurately predict the aerodynamic performance of complete aircraft of comparable size to those modeled in this project (Menter, Kuntz, & Langtry, 2003), and has been shown to out-perform the Spalart-Allmaras turbulence model (also commonly used for aerospace applications) in cases involving flow separation (Brodersen et al., 2005). The k-ω SST model combines two existing turbulence models, namely the k-ω and k-ε models. The k-ω model represents the time-varying turbulence in the flow via two turbulence transport variables; k, the turbulent kinetic energy and ω, the specific dissipation rate. The k-ε model instead makes use of k and ε, the turbulent dissipation rate. The combination of these two models via the SST model retains the advantages of the k-ω model in modeling adverse pressure gradients and separated flow, while rectifying the excessive sensitivity of that model to the specified free-stream turbulence conditions. The use of the k-ω SST model (and two-equation turbulence models in general) introduces a simplification to the model in the form of the Boussinesq approximation, the primary effect of which is the treatment of turbulence within the flow as isotropic. While higher order turbulence models are available for modeling anisotropic turbulence, the extra computational expense incurred when using such a model is viewed as unjustified in light of the number of cases to be run and the well validated nature of the k-ω SST model for flows of this type, as referred to above.

The air was modeled as incompressible, in accordance with commonly accepted assumptions when modeling aerodynamic flows below Mach 0.3 (Anderson, 2001, pp. 435–463). This is considered appropriate for modeling the operational speeds of the various aircraft under consideration, defined within the Requirements Specification (AMOG Consulting Inc., 2016) as between 100 and 200 kn (i.e. Mach 0.15 – 0.3).

Document Number - t2015.j520.009
Issued as Revision 0, September 30th 2016
Doc Ref: Atlas:\...\t2015.j520.009.0.odt
amogconsulting.com
EIN 20-4906471
TX PE Firm F-11821

AI-E253-09v20130508

3.3.1 Fluid Properties

The air around the aircraft was modeled as the US Standard Atmosphere (National Aeronautics and Space Administration, 1976), and accordingly values of 2.37×10^{-3} slug/ft^3 and 3.78×10^{-7} lb s/ft^2 have been used for the density and dynamic viscosity respectively. It is expected that high humidity conditions will prevail over the sea surface, and that spraying will therefore not be conducted in dry air. Sverdrup (1946) presented measurements of relative humidity values at varying heights above the sea surface. The measurements reported by Sverdrup indicate that the relative humidity at the sea surface may be as high as 80 %. The humidity varies significantly with height, and can be as low as 55% at around 100 ft above the sea surface. According to published data for air properties at 80 % humidity (Melling, Noppenberger, Still, & Venzke, 1997), differences of approximately 1 % in the viscosity and density values compared to dry air are expected. The differences are less for lower humidity values. As such, neglecting the change in the air fluid properties with humidity is considered appropriate and unlikely to result in any significant inaccuracy.

3.3.2 Boundary Conditions

The upstream, top and side faces of the fluid domain were modeled as inlets with flow velocity specified. The aft face of the domain has been modeled as a pressure outlet, with a fixed pressure of 0 psi gauge. Owing to the model being constructed in a reference frame fixed relative to the aircraft, the stationary sea surface was treated as a wall moving with velocity determined by the ground speed and track of the aircraft.

The surfaces of the aircraft were modeled as non-slip walls. Roughness of the aircraft skin has not been considered, and these wall boundaries were modeled as hydraulically smooth.

When operating in a crosswind, the aircraft was considered to be piloted on a heading such that the resultant ground track was aligned with the intended course for dispersant spraying. Given the groundspeed, the windspeed, and the angle between the aircraft's track (dispersant spraying path) and the wind, the required airspeed and heading can be calculated, as shown in Figure 26.

Document Number - t2015.j520.009
Issued as Revision 0, September 30th 2016
Doc Ref: Atlas:\...\t2015.j520.009.0.odt
amogconsulting.com
EIN 20-4906471
TX PE Firm F-11821

AI-E253-09v20130508
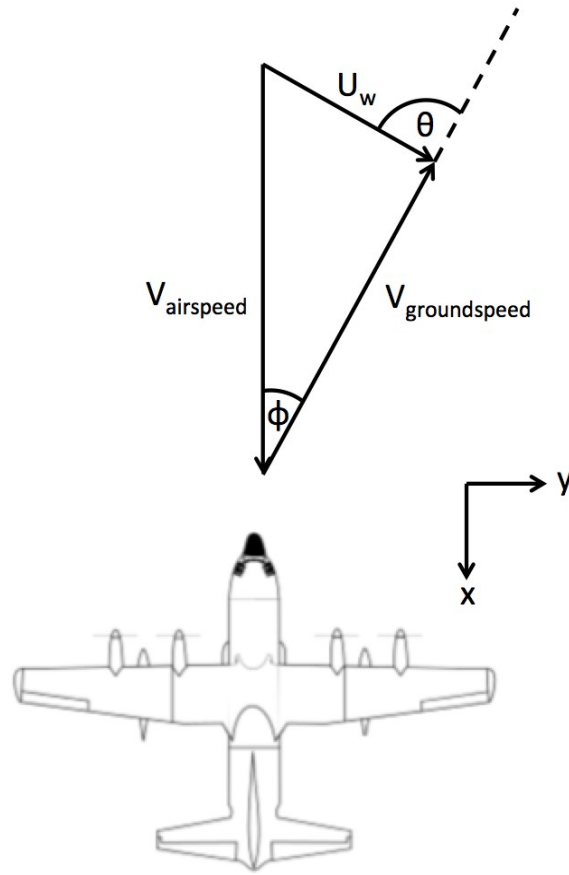
Figure 26 : Diagram of aircraft velocity vectors (not to scale, angles exaggerated)

The component of the inlet velocity which corresponds to the wind was modeled with an Atmospheric Boundary Layer (ABL) profile, using the equations described by Norris & Richards (2010). The flow velocity was calculated as shown in Equation 1, with the von Karman constant, κ, set in accordance with the description provided by Norris & Richards (2010). Similarly, the turbulent kinetic energy and specific dissipation rate are given by Equations 2 and 3 respectively, with C_μ and β' being additional constants within the turbulence model.

$$U_w = \frac{u_* \ln\left(z/z_0\right)}{\kappa}$$

Equation 1

$$k = \frac{u_*^2}{\sqrt{C_\mu}}$$

Equation 2

Document Number - t2015.j520.009
Issued as Revision 0, September 30th 2016
Doc Ref: Atlas:\...\t2015.j520.009.0.odt
amogconsulting.com
EIN 20-4906471
TX PE Firm F-11821

$$\omega = \frac{u_*}{\sqrt{\beta'}\,\kappa\,z}$$

Equation 3

The roughness height on the sea surface, z_0, was taken as 0.0002 m as reported by Wieringa (1992).

As the wind speed varies with height above the sea surface, the resultant inlet velocity also varies with height. The inlet velocity components in the streamwise (x) and lateral (y) directions were therefore calculated as per Equations 4 and 5, where θ is the angle between the wind direction and the aircraft's track (defined as 0° for a headwind), z_a is the height of the aircraft above the ground and ϕ is the angle by which the aircraft's track is deviated from its heading by the effect of the wind.

$$U_x(z) = \sqrt{U_w(z)^2 + V_{groundspeed}^2 + 2U_w(z)V_{groundspeed}\cos(\theta)}\cos(\phi(z) - \phi(z_a))$$
$$\text{where } \phi(z) = \sin^{-1}\left(\frac{U_W(z)\sin(\theta)}{\sqrt{U_w(z)^2 + V_{groundspeed}^2 + 2U_w(z)V_{groundspeed}\cos(\theta)}}\right)$$

Equation 4

$$U_y(z) = \sqrt{U_w(z)^2 + V_{groundspeed}^2 + 2U_w(z)V_{groundspeed}\cos(\theta)}\sin(\phi(z) - \phi(z_a))$$

Equation 5

Turbulence properties from the ABL calculations (Equations 2 and 3) were implemented directly at the boundaries, as the airspeed of the aircraft was considered to have no fluctuating (i.e. turbulent) components.

3.3.3 Dispersant Spray Nozzles

Motion of the dispersant spray droplets has been modeled as the result of three fluid forces (drag force, pressure gradient and shear lift force), combined with the effects of turbulent dispersion and gravity. The drag coefficient is formulated as shown in Equation 6, where Re_p is defined as the particle Reynolds Number based on the particle diameter. The pressure gradient force accounts for the force exerted on a droplet which exists within a varying pressure field, and is formulated as per Equation 7. The shear lift force represents the force acting on a droplet within a velocity gradient orthogonal to the droplet motion, and the lift coefficient developed by Sommerfeld (2000) was implemented.

$$C_d = \begin{cases} \dfrac{24}{Re_p}(1 + 0.15Re_p^{0.687}) & \text{for } Re_p \leq 10^3 \\[2ex] 0.44 & \text{for } Re_p > 10^3 \end{cases}$$

Equation 6

$$F_p = -V_p \nabla p_{static}$$

Equation 7

Turbulent dispersion, the phenomenon by which the turbulent fluctuations in the flow produce time varying deflections in the path of each individual droplet, was accounted for by the use of a random

Document Number - t2015.j520.009
Issued as Revision 0, September 30th 2016
Doc Ref: Atlas:\...\t2015.j520.009.0.odt
amogconsulting.com
EIN 20-4906471
TX PE Firm F-11821

AI-E253-09v20130508

walk procedure and the turbulent transport variables generated by the turbulence model. The spray was modeled in a number of 'parcels', whereby the spectrum of droplet sizes was modeled by a discrete number of individual droplets. Increasing the number of parcels increases the accuracy of the turbulent dispersion model at the cost of additional computation time. The sensitivity of the dispersion pattern to the number of parcels was determined iteratively, and final results were converged with respect to increasing parcel count as described in Section 4.1.2. Two way coupling of the Eulerian and Lagrangian phases has been included in the model. This accounts for the effect of the droplets on the surrounding fluid velocity.

In order to achieve the desired application rate for each of the dispersant spray nozzles, the volume flow rate was calculated for each case as per Equation 8, where Q is the volume flow rate in gal/min, Q_A is the volume flow rate in gal/acre and w_s is the swath width in ft.

$$Q = 2.3248\text{E-}3\, Q_A\, w_s\, V_{groundspeed}$$

Equation 8

The behavior of the spray exiting the nozzle was estimated on the basis of the BETE NF70 nozzle for all four aircraft. The velocity of the spray exiting the nozzle was established on the basis of equations included in the Spray Engineering Handbook. (PNR Nozzles, n.d.), as shown in Equation 9, where d_{nozzle} is the effective diameter of the nozzle in inches (0.203" for the NF70 nozzle (BETE, n.d.)) and $V_{p,inlet}$ is the inlet velocity of the spray droplets in ft/s.

$$V_{p,inlet} = 1.2833\, \frac{Q}{\pi\, d^2_{nozzle}}$$

Equation 9

The effect of evaporation of the dispersant spray has not been included in the model. Experimental studies have demonstrated that the percentage of mass lost by Corexit 9500 under a range of spraying conditions is less than 10% over a period of 20 minutes (Ebert, Downer, Clark, & Huber, 2008). The dispersant is expected to take significantly less than 20 minutes to reach the sea surface once released, and as such the amount of evaporation is expected to be correspondingly less. Given that an evaporation model would require calibration against high fidelity experimental work, the omission of evaporation of the dispersant is considered appropriate and unlikely to be the source of significant inaccuracy.

The shape of the spray release from the nozzles was established based on spray trials conducted with Corexit 9500 sprayed from a King Air E90 (Hoffmann, 2010). The spray system on the E90 made use of 28 BETE NF70 nozzles. Published information for these nozzles (BETE, n.d.) was compared with publicly available images of the spray exiting the nozzles (of which an example is shown in Figure 27) and a spray angle of 15° was estimated. Each nozzle was modeled as an injection point. The velocity distribution of the particles leaving the point injector was uniformly distributed in the spanwise direction so that particles fanned out from the point injector. The velocity distribution was specified such that the spanwise velocity components resulted in a spray angle matching that estimated for the NF70 nozzle.
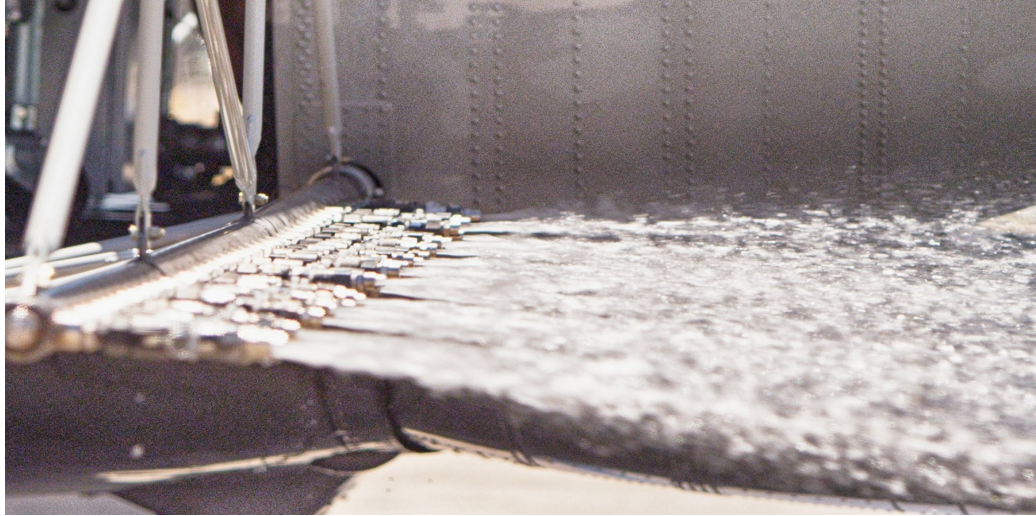
Figure 27 : Close-up image of dispersant spray (International Air Response, 2015b)

The spray dispersant has been modeled using a Lagrangian particle formulation with a density of 1.84 slug/ft^3. The American Society of Agricultural Engineers (ASAE) 'Medium to Coarse' size distribution (sourced from AGDISP) has been used. The probability density function for this distribution is shown in Figure 28, and a summary of the relevant parameters is shown in Table 9. 58% of the of the droplets fall within the 300 – 700 μm size referred to in the Requirements Specification (AMOG Consulting Inc., 2016).

Document Number - t2015.j520.009
Issued as Revision 0, September 30th 2016
Doc Ref: Atlas:\...\t2015.j520.009.0.odt
amogconsulting.com
EIN 20-4906471
TX PE Firm F-11821

AI-E253-09v20130508
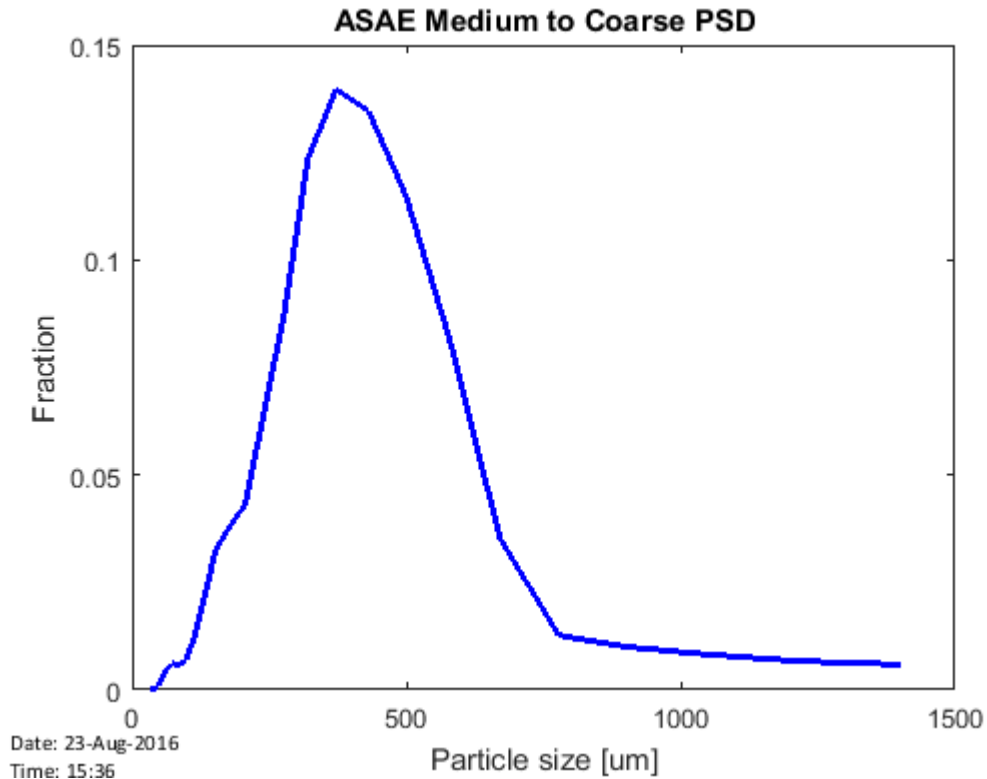
Figure 28 : Particle size distribution for the spray droplets (based on the ASAE Medium to Coarse distribution)

Table 9: Droplet Size Distribution Parameters

Parameter	Value (µm)
Median Droplet Diameter	340
5th Percentile Droplet Diameter	130
95th Percentile Droplet Diameter	660
Peak (Mode) Droplet Diameter	380

3.3.4   Estimation Of Required Angle Of Attack To Maintain Level Flight

The magnitude of lift generated by an aircraft is a key determinant of the size and strength of the vortical flow structures generated by its lifting surfaces. As the vortices were expected to affect the spray particle trajectories, the angle of attack at which each aircraft would generate the required lift to maintain level flight was calculated as an input to the CFD model for each different airframe and flight condition modeled.

Document Number - t2015.j520.009
Issued as Revision 0, September 30th 2016
Doc Ref: Atlas:\...\t2015.j520.009.0.odt
amogconsulting.com
EIN 20-4906471
TX PE Firm F-11821

AI-E253-09v20130508

For the C-130A, lift vs. angle of attack curves were available (Lockheed Aircraft Corporation, 1953) and using this data the required angle of attack could be estimated for each flight condition modeled.

For the AT-802A, DC-3 and DC-4 no such data was found to be publicly available. In order to estimate the required angle of attack for each case being modeled, CFD models of each of the airframes were run for a simple flight condition (no crosswind and 'regulatory' altitudes and application speeds as per DMP2) at several angles of attack. From these models the lift generated was extracted and used to generate lift vs. angle of attack curves for each of the AT-802A, DC-3 and DC-4. The resulting curves were then used to estimate the required angle of attack. The validation of this angle of attack estimation methodology is presented in Section 4.3.

3.3.5   Propeller Modeling

As the spray dispersant behavior was modeled as a steady state phenomenon, some simplification was required in order to model the propeller wash. The degree of interaction between the propeller wash and the dispersant behavior was not expected to warrant the additional complexity required to fully represent the transient behavior of the propellers by explicitly modeling the rotating blades.

Since full geometric details of the propeller could not be obtained for each aircraft, the propeller was represented by a virtual disk, a section of the fluid domain within which a momentum source was introduced to approximate the thrust and swirl effects of the propeller. Under steady level flight conditions the thrust generated by the propellers is equal to the total aircraft drag.

CFD modeling of aircraft to accurately predict total aircraft drag under varying flight conditions is a complex task far beyond the scope of this project. In particular, the parasitic drag of small geometric details not included in the CFD models (landing gear, lights, antennae, etc.) can be a significant contributor. As such, to estimate the magnitude of thrust required for each aircraft and flight condition being modeled simple drag estimation techniques typically employed during preliminary aircraft design were utilized (Raymer, 2003; Torenbeek, 1982) in conjunction with aerodynamic performance data where available, such as for the C-130A (Lockheed Aircraft Corporation, 1953).

For the C-130A, since a total lift vs. drag curve was available (Lockheed Aircraft Corporation, 1953) the drag coefficient corresponding to the lift coefficient required to maintain steady level flight could be interpreted from the curve. The resulting drag coefficient could then be input to Equation 10 in conjunction with the dynamic pressure (calculated based on the true airspeed which accounts for wind speed and direction at the height of the aircraft, and the air density at altitude) for each of the cases being modeled.

$$F_D = C_D q$$

<div align="right">Equation 10</div>

Where F_D is the drag force, C_D is the total drag coefficient and q is the dynamic pressure.

For the AT-802A, DC-3 and DC-4, conservative zero lift drag coefficients were assumed, assuming that increased thrust (corresponding to increased drag) would result in additional spray drift and therefore be conservative. Further details of the effect of the propeller wash on spray drift are included in Section 3.3.5.1. Total drag was calculated by assuming the lift generated was equal to the

Document Number - t2015.j520.009
Issued as Revision 0, September 30th 2016
Doc Ref: Atlas:\...\t2015.j520.009.0.odt
amogconsulting.com
EIN 20-4906471
TX PE Firm F-11821

weight of the aircraft and applying calculated dynamic pressure values for each of the cases being modeled as shown in Equation 11.

$$D = q\, S_{ref}\, C_{D0} + \frac{W^2}{(\pi\, A\, e\, q\, S_{ref})} \qquad\qquad \text{Equation 11}$$

Where q is the dynamic pressure, S_{ref} is the airframe planform main wing reference area, C_{D0} is the zero lift drag coefficient, W is the aircraft weight, A is the main wing aspect ratio, and e is the Oswald efficiency number (conservatively assumed as 0.75 (Raymer, 2006)).

The drag estimates calculated as described above were used to set the total amount of thrust required per airframe which was divided evenly between the number of engines for the multi-engined airframes. The model was simplified by assuming that all thrust is generated by the propellers themselves without contribution from exhaust thrust of the turbopropeller engines. This assumption was considered conservative as particle drift extents were assumed to be influenced by the added momentum perpendicular to the direction of travel (due to the swirl components) forcing the dispersant particles spanwise into more complex vortex structures where they may be entrained and remain aloft for longer.

The propeller rotation rate in conjunction with the aircraft true airspeed was used to determine the advance ratio of the propeller. Using the advance ratio and required thrust, values for torque coefficient and propeller efficiency matching each operating condition were then determined for the AT-802A and the C-130A using the proprietary data and software supplied by Hartzell Propeller Inc. and UTC Aerospace Systems respectively. In the absence of information from the propeller manufacturer (for the DC-3 and DC-4) values of torque coefficient and propeller efficiency were assumed at 0.02 and 0.80 respectively as representative values for variable pitch large turbopropeller aircraft similar to that of the C-130A propellers.

As all of the airframes considered utilize variable pitch propellers designed to operate at a constant rotation rate, the virtual disk model was implemented in the CFD using the rotation rate to define the operating set point where the virtual disk model imparts axial and swirl momentum to the flow field using the derived propeller coefficients described above.

In reality, especially for airframes where the propeller wash interacts with lifting surfaces or the fuselage, as was the case for all airframes modeled in the project, the addition of propeller momentum will affect the aerodynamic performance of the aircraft.

The interconnected nature of the Lift, Weight, Drag and Thrust calculations generally require a number of iterations to converge and such methodology (as is usually reserved for design of aircraft) was considered unnecessarily intensive for general wake characterization of the airframes given the level of detail of available inputs. Future work could consider higher fidelity modeling including trim effects, however compared to the current project this would increase the number of parameters in the solution space considerably and require significantly more detail for both aircraft geometry and operational information to ensure accurate results.

3.3.5.1   Thrust Sensitivity Study

As limited data was available with which to validate the aircraft drag and required thrust for the range of cases investigated, a sensitivity study was conducted to investigate the affect on spray particle drift of including momentum sources from the propellers in the CFD models.

In reality, in a steady level flight condition the amount of thrust is equal the drag generated, which is heavily dependent on the flight conditions of the aircraft and also to some extent on effect of the propeller wake on the flow around the aircraft. For modeling purposes, some estimation of the thrust was required as the CFD model necessarily omits minor exterior surface details such as landing gear, flap hinges, surface roughnesses and ancillary equipment (e.g. lights and antennae), all of which add parasitic drag. Accurate prediction of the total aircraft drag using CFD modeling is a highly complex task beyond the scope of the project.

Given that the required thrust could not be absolutely determined using the CFD models, a sensitivity analysis was conducted using the AT-802A CFD model to determine whether the amount of thrust produced by the propeller affected the distribution of particles in the aircraft wake. The details of the cases used to assess the sensitivity of the results to the thrust generated are presented in Table 10.

Table 10: Thrust Comparison Case Details

Parameter	Low Thrust	Higher Thrust
Height Above Ground (ft)	16	16
Wind Speed (kn)	20	20
Wind Direction, relative to aircraft heading (°)	90	90
Aircraft Velocity (kn)	150	150
Particle Size Distribution	Coarse to medium	Coarse to medium
Propeller Thrust (lbf)	1,030	1,620

The results of the propeller thrust comparison are shown in Figures 29 and 30. Figure 29 shows that the additional thrust pushes some of the lighter particles further behind the aircraft. However, Figures 29 and 30 illustrate that in terms of the maximum extent of particle drift (which is predominantly in the crosswind direction), the amount of thrust does not affect the solution within the 50 ft accuracy with which results will be reported.

Based on these results additional CFD iterations and further detailed modeling of thrust to obtain a more accurate estimated of the propeller wake and magnitude of thrust required of the aircraft are not recommended for crosswind cases.

Document Number - t2015.j520.009
Issued as Revision 0, September 30th 2016
Doc Ref: Atlas:\...\t2015.j520.009.0.odt
amogconsulting.com
EIN 20-4906471
TX PE Firm F-11821

AI-E253-09v20130508
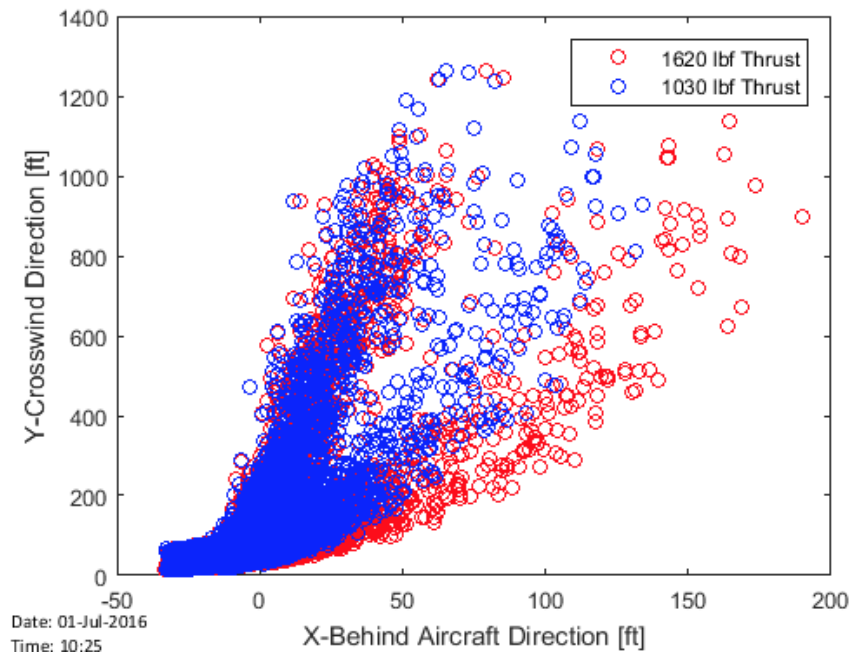
Figure 29 : Scatter of particles from CFD simulations with high and low thrust
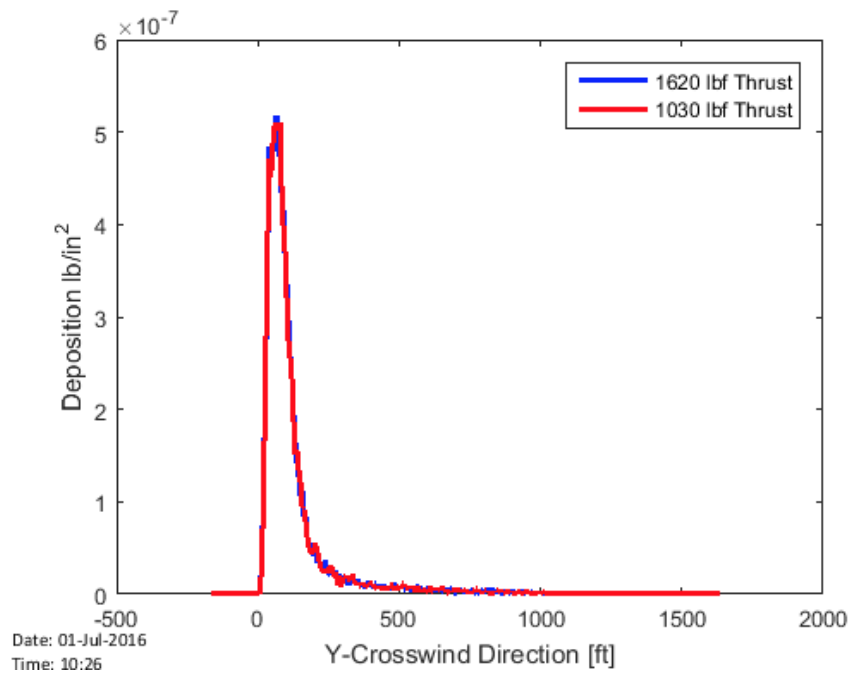
Figure 30 : Deposition of particles in the crosswind direction from CFD simulations with high and low thrust

4   VERIFICATION AND VALIDATION

Having developed the CFD models as described in Sections 2 and 3, a number of verification and validation activities were conducted to demonstrate their accuracy. Three types of activities were conducted, specifically:

1.   Verification Studies – these studies include mesh independence studies used to ensure that the numerical discretization is sufficiently fine so as to not affect the solution.

2.   Qualitative Validation Studies – in lieu of field spray trial data, a qualitative comparison of the motion of spray drift provides validation of the large scale fluid motion

3.   Quantitive Validation Studies – where possible, the CFD models were validated against numerical data.

Validation activities were conducted on a single operational case for each airframe. Given the underlying physics, algorithms and mesh do not change for each operational case, as the CFD models passed each of the validation activities, the models were considered representative for all operational scenarios in the CFD case list.

4.1   NUMERICAL VERIFICATION STUDIES

The CFD models described in Section 3 model both the airflow in the wake of the aircraft and resulting motion of the dispersant particles. To model these two fluid phases, two different numerical models were used. A mesh independence study and a parcel count independence study were conducted to ensure both the airflow and dispersant motions were accurately represented in the numerical models.

4.1.1   Mesh Independence Study

The airflow was modeled using an Eulerian frame of reference in a finite volume approach based on discretizing space with a mesh. A mesh independence study was conducted to determine the level of mesh refinement required for each of the modeled aircraft. The mesh independence study involved two phases:

(i)   The level of mesh resolution required to resolve the near field flow around the aircraft was investigated, using the calculated lift and drag values as the determinant of whether mesh independence had been reached.

(ii)   The level of far-field mesh resolution required to model the decay of the wake and wingtip vortices was determined, using the extent of the spray dispersant drift as the criteria for mesh independence.

4.1.1.1   Near Field Mesh Resolution

This phase of the mesh resolution study was conducted using the no wind base case for each airframe. The results of the AT-802A have been included below. Similar results were found for the other three airframes.

Document Number - t2015.j520.009
Issued as Revision 0, September 30th 2016
Doc Ref: Atlas:\...\t2015.j520.009.0.odt
amogconsulting.com
EIN 20-4906471
TX PE Firm F-11821

The mesh independence study was based on the no wind base case for the AT-802A (i.e. no wind, 16 ft altitude, 150 kn airspeed). Based on these results a base size of 13 ft was used for meshing the AT-802A. At this mesh size the estimated error with respect to the theoretical mesh independent solution was 0.26 % for lift and 4.6 % for drag. The convergence behavior of the predicted lift and drag is shown in Figures 32 and 33 respectively.

During this phase of the mesh resolution study, the near field mesh resolution was demonstrated to have no significant effect on the mean position of the dispersant particles impacting the sea surface.

Table 11: Air Tractor - Gird Resolution Study Results

Case Number	Base Size (ft)	Number Of Cells	Lift		Drag	
			(lbf)	% Error	(lbf)	% Error
1	26	2,572,388	17,553	0.82	1,075	17.87
2	21	3,469,931	17,603	0.54	1,032	13.16
3	16	5,592,873	17,624	0.42	989	8.44
4	13	8,883,001	17,652	0.27	954	4.61
5	11.5	11,806,131	17,675	0.14	945	3.62
Extrapolated value	0	-	17699	0	912	0
Notes: 1. Extrapolated value is the theoretical mesh independent solution found by extrapolating the fit of the data to the 0 cell size.						

Document Number - t2015.j520.009
Issued as Revision 0, September 30th 2016
Doc Ref: Atlas:\...\t2015.j520.009.0.odt
amogconsulting.com
EIN 20-4906471
TX PE Firm F-11821

AMOG®

AI-E253-09v20130508
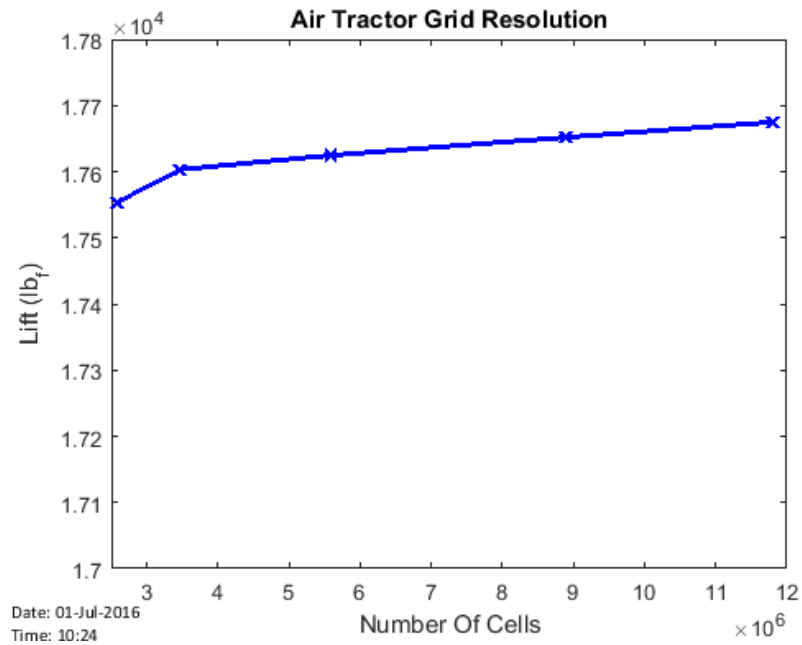
Figure 31 : AT-802A mesh resolution study lift
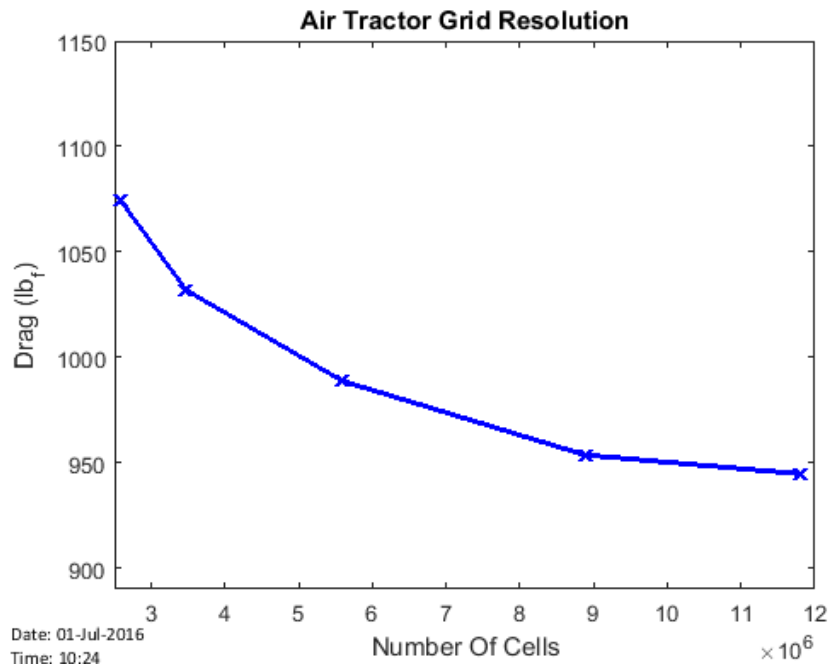
Figure 32 : AT-802A mesh resolution study drag

Identical mesh independence studies were conducted for each of the airframes, and a summary of the findings is presented in Table 12.

Document Number - t2015.j520.009
Issued as Revision 0, September 30th 2016
Doc Ref: Atlas:\...\t2015.j520.009.0.odt
amogconsulting.com
EIN 20-4906471
TX PE Firm F-11821

AI-E253-09v20130508

Table 12: Summary Near Field Mesh Independence Studies

Airframe	Number Of Cells	Lift Error (%)	Drag Error (%)
AT 802A	8,883,001	0.27	4.61
C-130A	10,115,546	1.15	8.80
DC-3	12,278,713	0.30	6.70
DC-4	12,434,626	0.23	9.17

Notes:
1. Error estimates are based on the theoretical mesh independent solution found by extrapolating the fit of the data to the 0 cell size.

Document Number - t2015.j520.009
Issued as Revision 0, September 30th 2016
Doc Ref: Atlas:\...\t2015.j520.009.0.odt
amogconsulting.com
EIN 20-4906471
TX PE Firm F-11821

AI-E253-09v20130508

4.1.1.2 Far Field Mesh Resolution

Although the purpose of the CFD was to assess the effect of near field wake structures on the dispersion of particles, an investigation was undertaken to determine if the far field region was providing a mesh independent solution.

To reduce the size of the mesh the downstream mesh was created using a mesh extrusion zone, as shown in Figure 33. This method takes the final cell count at a boundary (selected at 2 aircraft lengths behind the aircraft) and extrudes this mesh downstream. The domain was extended downstream using a slow growth factor such that the cells close to the aircraft maintain an aspect ratio close to 1.0. The relatively low number of layers and growth rate, used to limit the number of cells in the mesh, causes the cells at the end of the domain to have poor aspect ratios as they become stretched.
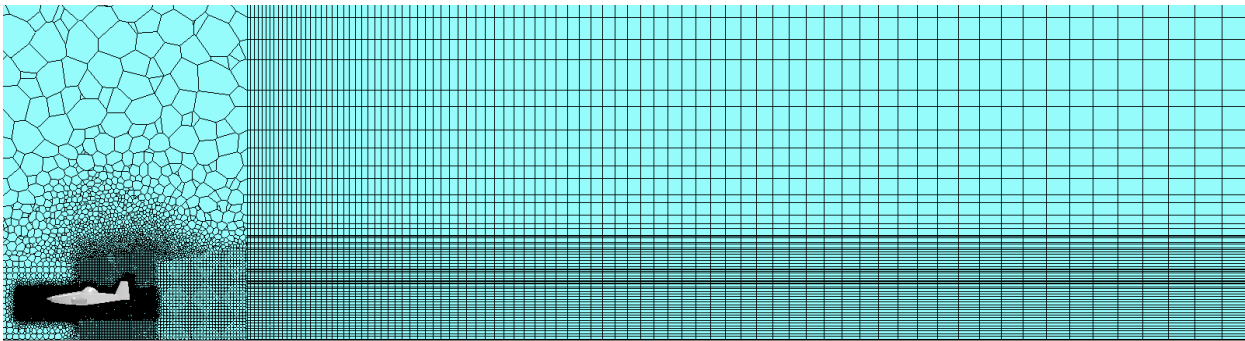
Figure 33 : Mesh expansion in the far field zone

Given the limitations of the available computing hardware, increasing the mesh density in this region whilst solving the near-field flow was not feasible. As such, the flow field and particle positions at a location 330 ft downstream of the aircraft were extracted and used as the input boundary conditions to a new downstream domain. This new downstream domain was meshed with simple hexahedral mesh elements and uniform cell spacing in the wake region. The particle touch down locations were then extracted and compared to the original mesh resolution.

Figure 34 shows the results of this study. It demonstrates that the mesh resolution in the far field has an effect on the vortex decay rate and subsequent location of particle deposition. The resolution in the original simulation increases the vortex decay rate and causes particles to impact the sea surface sooner. While there is a marked difference between the predicted fraction aloft, at large distances downstream the refined solution approaches the original results. These results indicate that further investigation of the far field mesh refinement would be required in order to develop a CFD model which maintained the desired level of accuracy at large distances downstream. The level of mesh resolution and corresponding computational expense required to do so was prohibitive within the bounds of the current project.

As such, to determine a cut off location at which the CFD results will be used the aspect ratio of the cells in the aircraft wake was considered. At a distance of 4000 ft behind the aircraft the aspect ratio is less than 0.1. CFD results were not used beyond this point (note that for a crosswind case of 20 kn

Document Number - t2015.j520.009
Issued as Revision 0, September 30th 2016
Doc Ref: Atlas:\...\t2015.j520.009.0.odt
amogconsulting.com
EIN 20-4906471
TX PE Firm F-11821

AMOG®

AI-E253-09v20130508

this equates to approximately 500 ft downstream). It should be noted that the original intent of the CFD models was to assess the near-field wake effects on the aerial dispersant. As the mesh resolution has been determined to be adequate in the near field region, the comparison of results between AGDISP and the CFD models should only be relied upon in the near field region.
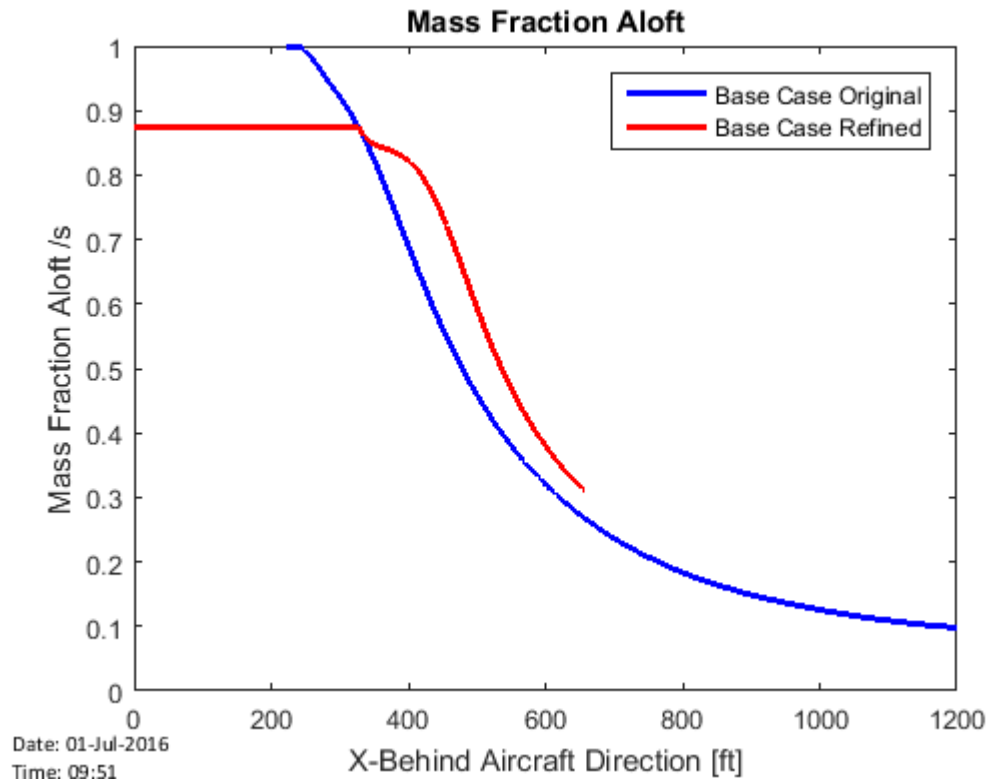
Figure 34 : Comparison of fraction of dispersant aloft for original and refined far field CFD simulations

4.1.2   Parcel Count Independence Study

The motion of the dispersant was modeled using a Lagrangian particle tracking algorithm. In the Lagrangian particle tracking algorithm the mass is represented by parcels. Each parcel represents a number of individual particles which have the same properties, i.e. diameter and density. Because each parcel represents a number of particles, and those particles are assumed to move together, the solution is dependent on the number of parcels used. To confirm that the number of parcels used was sufficient to describe the motion of the particles a parcel count independence study was conducted.

In conducting the study, the base crosswind case (20 kn at 90 ° to aircraft track) for the AT-802A was used and the total number of parcels was varied from 10 to 10,000 parcels per injector. Figure 35 shows the fraction aloft in the direction perpendicular to the aircraft for different parcel counts. These results show that beyond 1,000 parcels the mass fraction aloft does not change significantly. At low parcel counts the fraction aloft curve is visibly jagged, this is due to the low number of

Document Number - t2015.j520.009
Issued as Revision 0, September 30th 2016
Doc Ref: Atlas:\...\t2015.j520.009.0.odt
amogconsulting.com
EIN 20-4906471
TX PE Firm F-11821

AI-E253-09v20130508

parcels resulting in insufficient resolution of the particle size distribution. Based on this study a parcel count of at least 1,000 was used for all CFD comparison simulations with AGDISP.
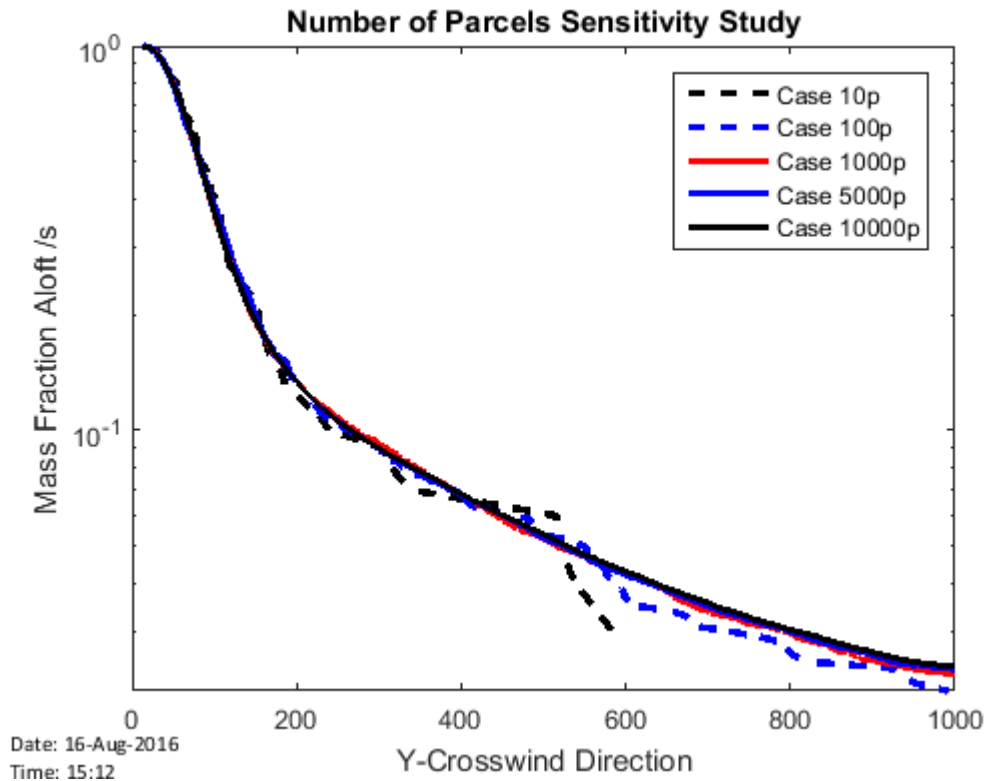
Figure 35 : Variation of predicted fraction aloft with the number of parcels used in the CFD model

4.2   QUALITATIVE MODEL VALIDATION STUDIES

During the project an exhaustive search was undertaken to identify quantitative data sources for verification of the CFD models. Unfortunately experimental spray trial data could not be sourced due to ongoing legal proceedings with a number of the potential data providers. In lieu of quantitative data a qualitative comparison of the dispersant trajectory behind the aircraft was conducted. The qualitative comparison was conducted by comparing the simulated particle trajectories to photographs of the aircraft conducting spraying operations.

4.2.1   Spray Drift Comparison AT-802A

A qualitative comparison was conducted between the modeled and photographed spray behavior behind the AT-802A. Figure 36 shows the mean particle volume fraction distribution at a number of downstream positions. As expected, the further downstream positions illustrate the gravitational forces dominating over the initial release momentum with the particles sinking down. The effect of the wingtip vortices is shown to entrain a portion of the outboard particles that prolongs their

Document Number - t2015.j520.009
Issued as Revision 0, September 30th 2016
Doc Ref: Atlas:\...\t2015.j520.009.0.odt
amogconsulting.com
EIN 20-4906471
TX PE Firm F-11821

AMOG®

AI-E253-09v20130508

downward drift. This phenomenon has been observed in actual low altitude spraying activities as depicted in Figure 37 and was also identified in the CFD modeling conducted by Ryan et al. (2013)

These results show that the CFD models are capturing the significant flow structures affecting the dispersant trajectories.
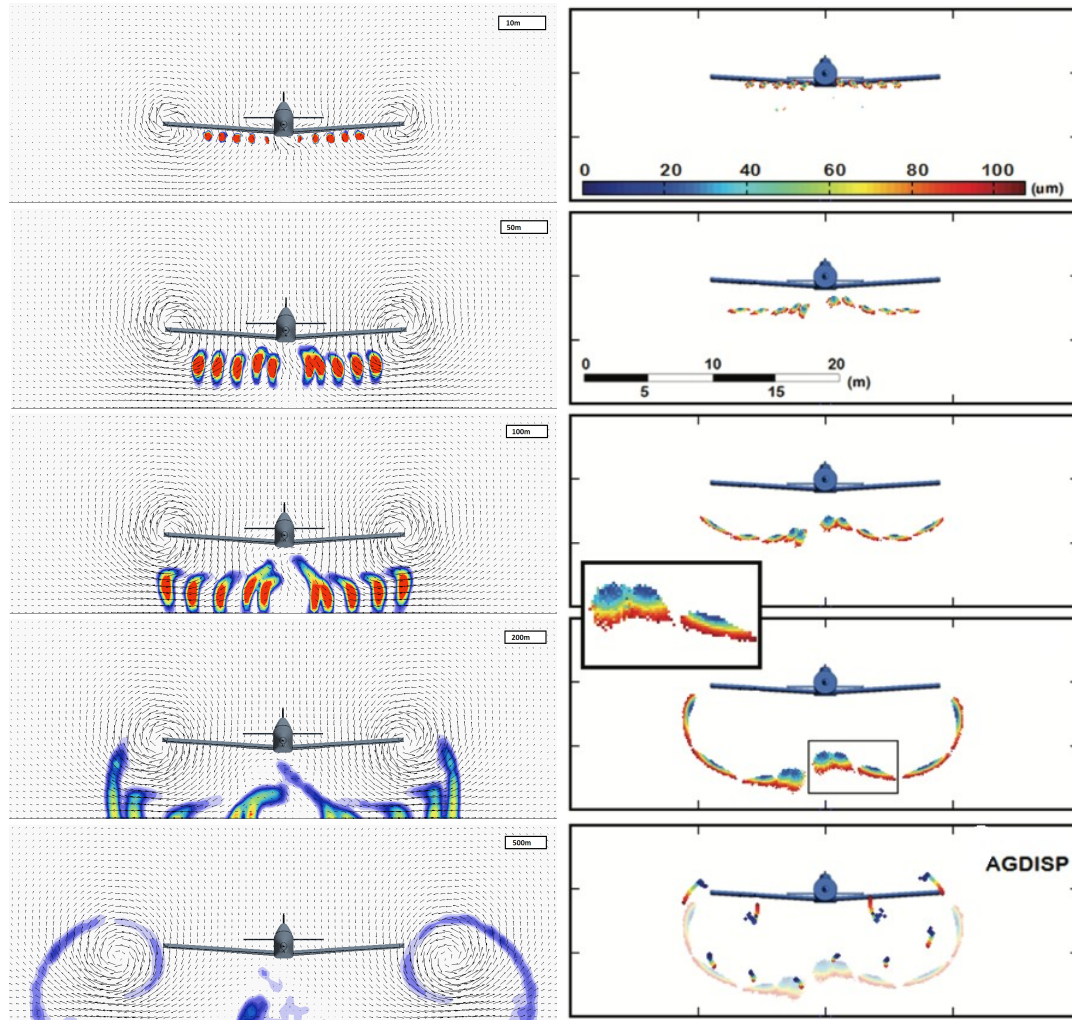
Figure 36 : Comparison of mean particle volume fraction downwind of the aircraft
The left pane shows results from AMOG's CFD study, the right pane shows AGDISP and CFD results from (Ryan et al., 2013)

Document Number - t2015.j520.009
Issued as Revision 0, September 30th 2016
Doc Ref: Atlas:\...\t2015.j520.009.0.odt
amogconsulting.com
EIN 20-4906471
TX PE Firm F-11821

AI-E253-09v20130508

Figure 37 : AT-802A low altitude aerial spray operations

4.2.2   Spray Drift Comparison C-130A

A qualitative comparison was conducted between the modeled and photographed behavior of the spray behind the C-130A. Figure 38 shows the near field spray trajectories behind the C-130A predicted by the CFD model. The fuselage causes a local change in the flow which causes the particles to be drawn upward and inward following the flow past the rear cargo door. This unique flow structure is also clearly visible behind an actual C-130A during spray operations (as shown in Figure 39).

These results show that the CFD models are capturing the significant flow structures affecting the dispersant trajectories.
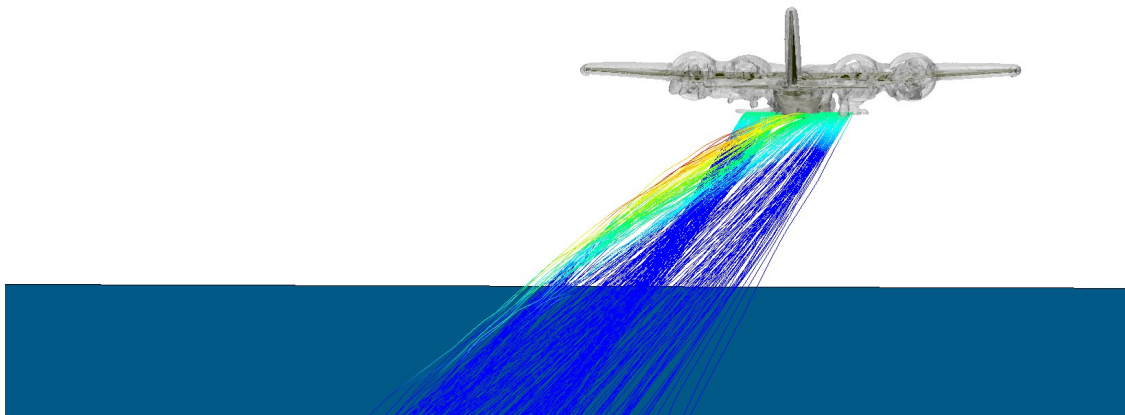
Figure 38 : Visualization of near field spray trajectories behind the C-130A

Document Number - t2015.j520.009
Issued as Revision 0, September 30th 2016
Doc Ref: Atlas:\...\t2015.j520.009.0.odt
amogconsulting.com
EIN 20-4906471
TX PE Firm F-11821

AMOG®

AI-E253-09v20130508

Figure 39 : C-130A conducting spray operations

4.3   QUANTITATIVE MODEL VALIDATION STUDIES

The angle of attack required to maintain steady flight was estimated in accordance with methodology described in Section 3.3.4. In order to validate the lift being generated by the CFD methodology, a study was performed comparing the lift coefficient vs. angle of attack data with lift coefficients derived from the CFD of the C-130A.

The C-130A CFD model was run for a number of cases with varying operational parameters at 0° angle of attack. For each of these cases the expected lift was calculated using aerodynamic data (Lockheed Aircraft Corporation, 1953), which was then compared with results extracted from the CFD model. A summary of the results is presented in Table 13.

Document Number - t2015.j520.009
Issued as Revision 0, September 30th 2016
Doc Ref: Atlas:\...\t2015.j520.009.0.odt
amogconsulting.com
EIN 20-4906471
TX PE Firm F-11821

AI-E253-09v20130508

Table 13: C-130A Calculated Lift Comparison Against CFD Generated Lift

Altitude (ft)	Application Speed (kn)	Wind Speed (kn)	Wind Angle (° Relative To Aircraft Track)	Calculated Lift Estimate (lb)	CFD Lift (lb)	% Error
75	150	0	0	96,507	81,029	-16.0%
75	150	0	0	96,507	70,214	-27.2%
75	150	20	0	126,214	99,965	-20.8%
75	150	20	90	98,494	71,892	-27.0%
75	150	35	0	151,074	121,695	-19.4%
75	150	20	30	122,494	96,627	-21.1%
100	150	20	90	98,595	70,032	-29.0%
100	200	20	90	173,643	137,830	-20.6%

The results demonstrate that the C-130A CFD model consistently produced less lift than expected from the theoretical calculations at zero degrees angle of attack with 18° flap extension. This could be due to inaccuracies introduced in the model geometry due to required assumptions in the absence of detailed data, such as the simplification of the main wing flaps.

Without performing additional validation of the DC-3 and DC-4 against reliable aerodynamic performance data it is difficult to determine whether the trend of CFD lift under-prediction would extend to the DC-3 and DC-4 CFD models. If the DC-3 and DC-4 CFD models also under-predict the lift generated this would serve to increase the angle of attack required beyond what is realistically required to maintain level flight for a given weight and potentially lead to greater fuselage wake effects.

Since for the DC-3 and DC-4 models the angle of attack required for each case was determined via CFD lift results (as described in Section 3.3.4), the angle of attack used could be calibrated to ensure that the amount of lift generated, and hence the size and strength of major wake features (i.e. wingtip vortices) was accurate against the chosen modeling weight, as shown in Table 15. The angles of attack required to generate the targeted weights were not considered unreasonably large, although further validation using operator feedback and additional aerodynamic data is suggested for future works.

As an example for validation of the angle of attack estimation methodology, Table 14 shows the range of lift generated for the DC-4 across a subset the set of cases run.

Document Number - t2015.j520.009
Issued as Revision 0, September 30th 2016
Doc Ref: Atlas:\...\t2015.j520.009.0.odt
amogconsulting.com
EIN 20-4906471
TX PE Firm F-11821

AI-E253-09v20130508

Table 14: DC-4 Calculated Lift Comparison Against CFD Predicted Lift

Altitude (ft)	Application Speed (kn)	Wind Speed (kn)	Wind Angle (° Relative To Aircraft Track)	Calculated Lift Estimate (lb)	CFD Lift (lb)	% Error[1]
50	150	0	-	3.16	72,965	4.2%
50	150	10	0	2.3	74,061	5.8%
50	150	10	30	2.4	74,062	5.8%
50	150	10	60	2.7	73,778	5.4%
50	150	10	90	3.1	73,195	4.5%
50	150	35	0	0.7	75,914	8.4%
50	150	40	30	0.7	75,817	8.3%
50	150	23	60	2.1	74,368	6.2%
50	150	20	90	3.03	73,231	4.6%

Notes:
1. The targeted DC-4 Lift was 70,000 lb, representative of the upper range of take-off weights for a DC-4.

For comparison, the lift generated for a simple no-wind case for all airframes is presented in Table 15. It is noted that the AT-802A and the C-130A models were not run with the angles of attack estimated as required to achieve a targeted lift, nevertheless the results demonstrate that the magnitude of lift generated is reasonable for all airframes for the configurations modeled.

Table 15: Airframe CFD Lift Generated At Angle Of Attack As Estimated To Be Required To Maintain Level Flight

Aircraft	Targeted Aircraft Weight (lb)	Angle Of Attack (°)	CFD Lift (lb)	% Error From Targeted Aircraft Weight
AT-802A	16,000	0[1]	17,646	10.3%
C-130A	108,000	0[1]	81,001	-25.0%
DC-3	25,200	0	24,987	-0.9%
DC-4	70,000	3.2	72,965	4.2%

Notes:
1. The angle of attack for these cases was not set in the CFD against an estimated angle required to produce lift equal to the target aircraft weight.

Document Number - t2015.j520.009
Issued as Revision 0, September 30th 2016
Doc Ref: Atlas:\...\t2015.j520.009.0.odt
amogconsulting.com
EIN 20-4906471
TX PE Firm F-11821

AI-E253-09v20130508

A search of publicly available sources shows a range of design masses and maximum take of weights depending on airframe configurations, modifications and cargo. In the absence of typical aircraft loads for spraying operations, airframe masses were assumed as either design weights or in the upper range of maximum take-off weights as shown in Table 15. Whilst it is recognized that spray operations may occur at aircraft masses lower than that assumed, modeling the higher masses was considered conservative as greater lift is required to maintain steady flight, leading to potentially greater impact from the generated vortices on spray particle trajectories. If actual operational aircraft loads are lower than those assumed, further modeling may reduce the predicted spray extents.

Validation of the flap deployment settings and angles of attack against operator advice and aerodynamic data is suggested as an area of future study to ensure the CFD model results are reflective of actual operating conditions.

Document Number - t2015.j520.009
Issued as Revision 0, September 30th 2016
Doc Ref: Atlas:\...\t2015.j520.009.0.odt
amogconsulting.com
EIN 20-4906471

TX PE Firm F-11821

AI-E253-09v20130508

5   CFD RESULTS – EXPLORATORY STUDY

At the conclusion of Phase 2 of the project, a set of CFD models were developed and validated for four airframes (as described in Sections 3 and 4). To determine the most robust method for predicting the extent of aerial spray drift in the DST, an exploratory CFD study was undertaken. In this exploratory CFD study the results from the validated CFD models were compared to existing aerial dispersant models to determine whether the existing aerial dispersant models were suitable for modeling the extent of spray drift in oil spill operations.

AGDISP was selected as the existing model most applicable to modeling aerial spray release. As such, the predicted fraction aloft from AGDISP was compared to the results from CFD simulations for similar spraying conditions. The following sections present the results of the comparison. The comparison was conducted based on answering the following questions shown in Table 16.

Table 16: Questions Tested In AGDISP-CFD Comparison

No.	Question	Answer
1	In general, is there good correlation between the CFD and AGDISP results in the near field region?	Yes /No
2	For crosswind cases which model is more conservative?	AGDISP/CFD
3	For intermediate wind direction cases which model is more conservative?	AGDISP/CFD
4	For headwind cases which model is more conservative?	AGDISP/CFD
5	Does altitude change which model is more conservative?	Yes/No
6	Does aircraft speed change which model is more conservative?	Yes/No
7	Does dispersant particle size distribution change which model is more conservative?	Yes/No

This comparison was made for each airframe by extracting the following variables from the CFD models and entering them into AGDISP:

● Wind speed and direction;

● Release height;

● Aircraft drag;

● Aircraft mass (based on the lift produced for a particular case);

● Propeller rotation rate; and

● Spray nozzle positions, particle size distribution and flow rate.

All other variables were set to the default settings in AGDISP.

Document Number - t2015.j520.009
Issued as Revision 0, September 30th 2016
Doc Ref: Atlas:\...\t2015.j520.009.0.odt
amogconsulting.com
EIN 20-4906471
TX PE Firm F-11821

AI-E253-09v20130508

5.1   AIR TRACTOR AT-802A

The extent of aerial spray from the Air Tractor AT-802A airframe was predicted using both the CFD and AGDISP models. Tables 6 and 7 show the distances in line with the aircraft track and perpendicular to the aircraft track for 50 %, 75 %, 90 % and 95 % of the mass to touch down. Figure 40 shows a comparison of the mass fraction aloft for the crosswind base case (20 kn at 90 ° to aircraft track). This demonstrates close correlation between the CFD and AGDISP predictions in the near field region, beyond which AGDISP provides a more conservative prediction of the mass aloft as a function of down wind distance. Beyond 500 ft the mesh resolution in the CFD has been reduced, in order to reduce computational time. The mesh was extended in order to allow qualitative examination of the wake in the far field region, however there is insufficient mesh resolution in this region for quantitative comparisons of deposition.
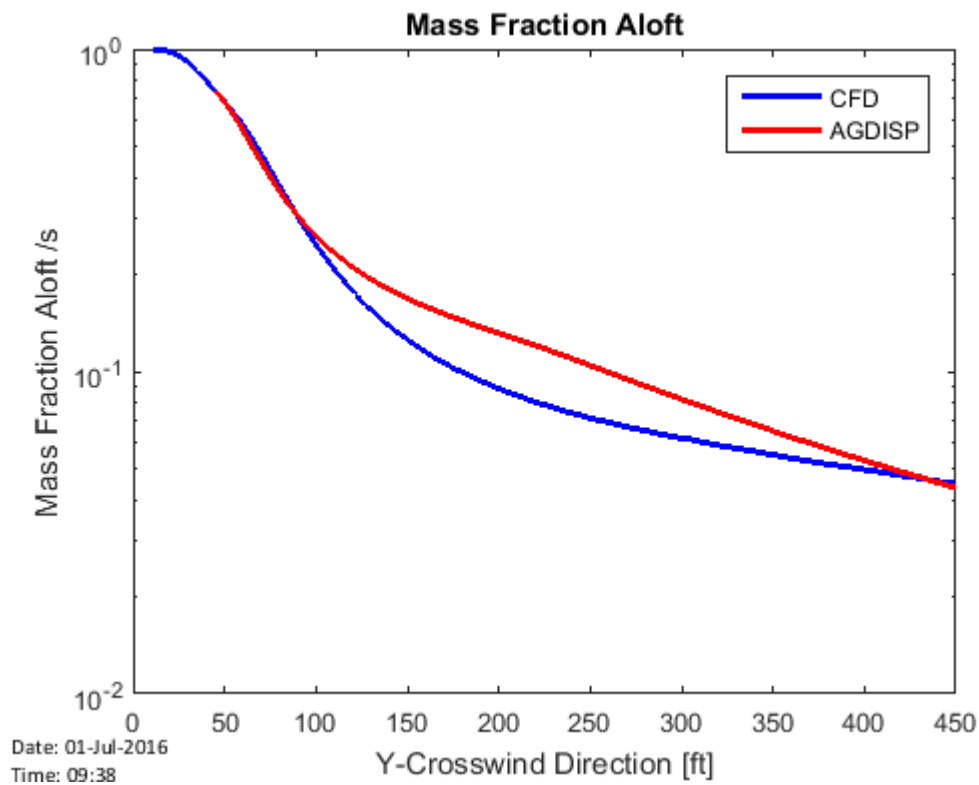
Figure 40 : AT-802A comparison of CFD and AGDISP results for crosswind base case

Document Number - t2015.j520.009
Issued as Revision 0, September 30th 2016
Doc Ref: Atlas:\...\t2015.j520.009.0.odt
amogconsulting.com
EIN 20-4906471
TX PE Firm F-11821

AI-E253-09v20130508

Table 17: AT-802A Comparison Of Position Of Deposited Mass In Line With The Aircraft Track

Case	Altitude (ft)	Ground Speed (kn)	Wind Speed (kn)	Wind Angle (°)	PSD[1]	CFD (ft)				AGDISP (ft)				Ratio CFD/AGDISP				Comment
						50%[3]	75%	90%	95%	50%	75%	90%	95%	50%	75%	90%	95%	
No Wind[2]	16	150	0	0	Standard	-4	1	13	-	-	-	-	-	-	-	-	-	AGDISP cannot assess
Base Case (Headwind)[2]	16	150	20	0	Standard	98	118	184	-	-	-	-	-	-	-	-	-	AGDISP cannot assess
Base Case (Crosswind)	16	150	20	90	Standard	0	9	23	48	3	5	8	10	0.12	1.60	2.84	5.06	CFD conservative
Intermediate Wind angle	16	150	21.9	60	Standard	29	49	99	245	35	60	154	246	0.85	0.81	0.64	1.00	Good correlation far field
Intermediate Wind angle[2]	16	150	24.8	30	Standard	54	84	181	-	-	-	-	-	-	-	-	-	AGDISP cannot assess
Minimum Altitude	15	150	20	90	Standard	0	8	23	46	1	4	6	7	0.15	2.10	3.75	6.25	CFD conservative
Maximum Altitude	50	150	20	90	Standard	27	51	146	0	4	6	8	10	6.75	8.24	17.8	-	CFD conservative
Minimum Speed	16	110	20	90	Standard	4	13	27	47	3	6	9	11	1.38	2.21	3.10	4.39	CFD conservative
Lighter Particles	16	150	20	90	Fine	12	26	67	154	3	5	6	8	4.11	5.65	10.5	19.2	CFD conservative
Heavier Particles	16	150	20	90	Coarse	0	8	21	39	-2	2	4	6	0.06	4.65	5.39	7.05	CFD conservative

Notes:
1. Particle Size Distribution: Fine, Standard and Coarse refer to ASAE Fine to Medium, Medium to Coarse and Coarse to Very Coarse respectively.
2. Headwind, no wind and intermediate wind cases with wind angles less than 60° could not be simulated in AGDISP.
3. Position at which 50% of the released mass has touched down.
4. AGDISP does not provide results for fraction aloft behind the aircraft, these results were back calculated from Lagrangian particle tracks.
5. Due to limitations in the mesh refinement in the far field results beyond 650 ft were not reported for the CFD cases.

Document Number - t2015.j520.009
Issued as Revision 0, September 30th 2016

Doc Ref: Atlas:\...\t2015.j520.009.0.odt
amogconsulting.com
EIN 20-4906471
TX PE Firm F-11821

AI-E253-09v20130508

Table 18: AT-802A Comparison Of Results Perpendicular To The Aircraft Track

Case	Altitude (ft)	Ground Speed (kn)	Wind Speed (kn)	Wind Angle (°)	PSD[1]	CFD (ft)				AGDISP (ft)				Ratio CFD/AGDISP				Comment
						50%[3]	75%	90%	95%	50%	75%	90%	95%	50%	75%	90%	95%	
No Wind[2]	16	150	0	0	Standard	7	24	48	-	-	-	-	-	-	-	-	-	AGDISP cannot assess
Base Case (Headwind)[2]	16	150	20	0	Standard	-1	17	35	55	-	-	-	-	-	-	-	-	AGDISP cannot assess
Base Case (Crosswind)	16	150	20	90	Standard	67	100	179	396	66	106	279	455	1.02	0.94	0.64	0.87	AGDISP conservative
Intermediate Wind angle	16	150	21.9	60	Standard	59	89	166	392	62	103	266	417	0.96	0.86	0.62	0.94	AGDISP conservative
Intermediate Wind angle[2]	16	150	24.8	30	Standard	38	62	118	287	-	-	-	-	-	-	-	-	AGDISP cannot assess
Minimum Altitude	15	150	20	90	Standard	63	93	165	359	62	97	264	429	1.02	0.96	0.62	0.84	AGDISP conservative
Maximum Altitude	50	150	20	90	Standard	259	412	-	-	275	489	901	1367	0.94	0.84	-	-	AGDISP conservative
Minimum Speed	16	110	20	90	Standard	62	92	150	268	71	110	293	486	0.89	0.84	0.51	0.55	AGDISP conservative
Lighter Particles	16	150	20	90	Fine	108	195	526	-	88	203	456	708	1.23	0.96	1.15	-	Inconclusive
Heavier Particles	16	150	20	90	Coarse	67	98	166	312	56	79	156	298	1.20	1.23	1.06	1.05	Good correlation far field

Notes:
1. Particle Size Distribution: Fine, Standard and Coarse refer to ASAE Fine to Medium, Medium to Coarse and Coarse to Very Coarse respectively.
2. Headwind, no wind and intermediate wind cases with wind angles less than 60° could not be simulated in AGDISP.
3. Position at which 50% of the released mass has touched down.
4. Due to limitations in the mesh refinement in the far field results beyond 650 ft were not reported for the CFD cases.

In general there is good agreement between the predicted fraction aloft using the AGDISP and CFD models for prediction of spray drift perpendicular to the aircraft track. AGDISP is shown to be more conservative in a majority of crosswind conditions, including the intermediate wind angle cases.

To facilitate the comparison of deposition behind the aircraft a non-standard output from AGDISP was used and the deposition pattern was calculated. It should be noted that using this approach is limited by the number of trajectory files that AGDISP will produce. The results shown in Table 18 show that there is good correlation in the predicted deposition pattern behind the aircraft for cases with a component of the wind acting in line with the track of the aircraft. This is confirmed by the scatter plot of particle touch down for the intermediate wind case shown in Figure 41.
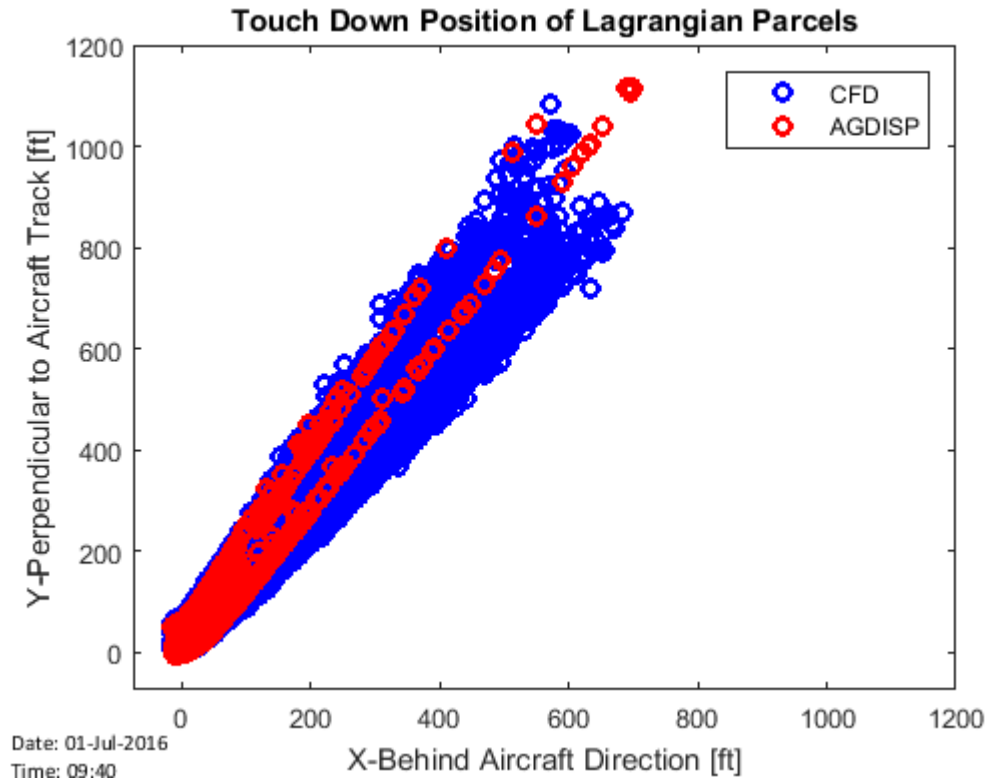
Figure 41 : AT-802A comparison of CFD and AGDISP results - intermediate wind angle case (60°)

AGDISP was designed such that it only provides a prediction of drift perpendicular to the track of the aircraft, this makes comparison of headwind cases difficult. To assess whether headwind cases would be governing in terms of defining maximum extent, the results from CFD simulations were compared directly. Specifically the drift behind the aircraft for the 20 kn headwind case (436 ft for 95% of particles to touch down) was compared to the drift perpendicular to the aircraft track in the 20 kn crosswind case (396 ft for 95 % of particles to touch down). This result indicates that headwind cases and crosswind cases create a similar amount of drift for the AT-802A, indicating that the effect of the wing tip vortices on the dispersant is not pronounced for this aircraft. AGDISP provides a more conservative prediction for the distance to 95 % of mass touching down for the crosswind case (453 ft) which is greater than the CFD prediction for both crosswind and headwind

Document Number - t2015.j520.009
Issued as Revision 0, September 30th 2016
Doc Ref: Atlas:\...\t2015.j520.009.0.odt
amogconsulting.com
EIN 20-4906471
TX PE Firm F-11821

AI-E253-09v20130508

cases. As such, for the DST the drift in headwind cases was predicted based on the maximum extent in the perpendicular direction for a crosswind case, with a 115 % safety factor applied to account for the extra drift in headwind cases. The safety factored was determined as described in Section 7.2.

When assessing the effect of altitude, the results in Table 18 show that the results from AGDISP and CFD are in agreement for the 50th percentile touch down and 75th percentile touchdown. For the high altitude case, the predicted distance to 90 % of mass touching down is beyond the refined region in the CFD for which quantitative comparison is reliable. As such it is unclear which numerical method is more conservative.

The sensitivity of the extent of spray drift to the particle size distribution is shown in Figure 42. The predicted fraction aloft is well correlated in the near field for all particle size distributions. Further downwind in the less refined region the correlation between AGDISP and CFD is not as strong.

Since the completion of this study, additional information has become available regarding the most representative Particle Size Distribution (PSD). This information indicates that in particular for the C-130A a coarser PSD would likely be more appropriate for the spray system used in offshore oil spill response. In light of this new information, it would be prudent to revisit this analysis as the extent of spray drift is likely to change significantly. However, in the current release of the DST it was identified that a finer PSD will produce a more conservative estimate of spray drift, thus limiting any risk of exposure to workers in the area.

Document Number - t2015.j520.009
Issued as Revision 0, September 30th 2016
Doc Ref: Atlas:\...\t2015.j520.009.0.odt
amogconsulting.com
EIN 20-4906471
TX PE Firm F-11821

AI-E253-09v20130508
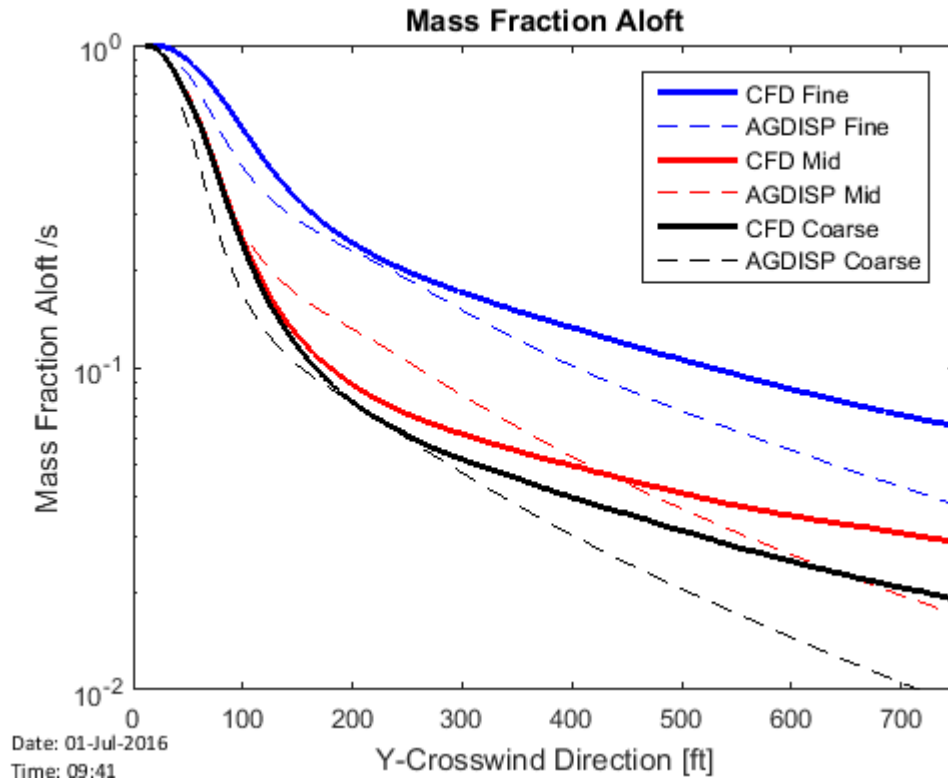
Figure 42 : AT-802A comparison of CFD and AGDISP results for different Particle Size Distributions Fine, Standard and Coarse refer to ASAE Fine to Medium, Medium to Coarse and Coarse to Very Coarse respectively.

Based on the results presented in Tables 17 and 18 and the subsequent discussion above the following conclusions are drawn about the prediction of spray drift from an Air-Tractor AT-802A using AGDISP:

Table 19: Conclusions For AT-802A AGDISP-CFD Comparison

No.	Question	Answer
1	In general, is there good correlation between the CFD and AGDISP results in the near field region?	Yes
2	For crosswind cases which model is more conservative?	AGDISP
3	For intermediate wind direction cases which model is more conservative?	AGDISP
4	For headwind cases which model is more conservative?	Inconclusive
5	Does altitude change which model is more conservative?	Inconclusive
6	Does aircraft speed change which model is more conservative?	No
7	Does dispersant particle size distribution change which model is more conservative?	Inconclusive

5.2   LOCKHEED C-130A HERCULES

The extent of aerial spray from the Lockheed C-130A Hercules airframe was predicted using both the CFD and AGDISP models. Tables 8 and 9 show the distances in line with and perpendicular to the aircraft track for 50 %, 75 %, 90 % and 95 % of the mass to touch down. Figure 43 shows a comparison of the mass fraction aloft for the crosswind base case. These results show that there is a significant difference between the predicted particle transport behavior using AGDISP and CFD. In the near field region the CFD simulations appear more conservative, conversely in the far field (beyond 650 ft for the case shown in Figure 43) AGDISP provides a conservative prediction of the extent of spray drift.

The flow field behind the C-130A was analyzed to determine the cause of the difference in predictions. Figure 44 shows the flow field behind the C-130A, wherein the gray iso-contour indicates the presence of vortices while the streamlines show the trajectory of the particles. This image clearly shows the particles released from the spray boom being drawn up behind the C-130A. The effect occurs in a region where vortices are not present, indicating that this is likely due to the tapered fuselage shape of the rear of the C-130A. As AGDISP does not account for the effect of the fuselage wake it is not suitable for predicting the extent of spray immediately behind the C-130A.
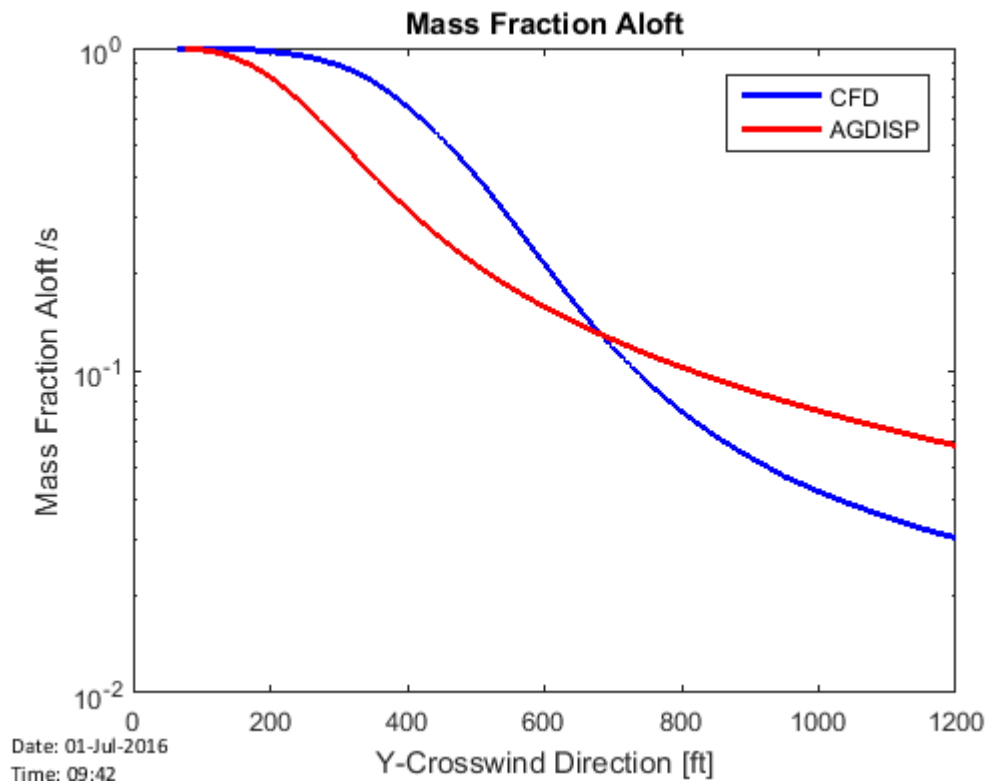

Figure 43 : C-130A comparison of CFD and AGDISP results for crosswind base case
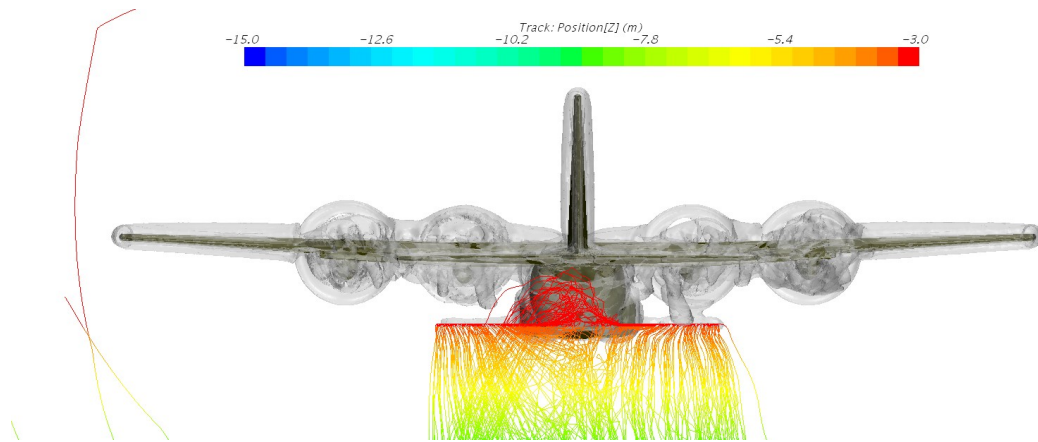
Figure 44 : C-130A visualization of particle tracks in near field fuselage wake effect

Document Number - t2015.j520.009
Issued as Revision 0, September 30th 2016
Doc Ref: Atlas:\…\t2015.j520.009.0.odt
amogconsulting.com
EIN 20-4906471
TX PE Firm F-11821

AI-E253-09v20130508

Table 20: C-130A Comparison Of Position Of Deposited Mass In Line With The Aircraft Track

Case	Altitude (ft)	Ground Speed (kn)	Wind Speed (kn)	Wind Angle (°)	PSD[1]	CFD (ft)				AGDISP (ft)				Ratio CFD/AGDISP				Comment
						50%[3]	75%	90%	95%	50%	75%	90%	95%	50%	75%	90%	95%	
No Wind No Propellers[2]	75	150	0	0	Standard	70	95	132	160	-	-	-	-	-	-	-	-	AGDISP cannot assess
No Wind[2]	75	150	0	0	Standard	75	132	199	228	-	-	-	-	-	-	-	-	AGDISP cannot assess
Headwind Regulatory Max[2]	75	150	35	0	Standard	758	943	1203	1500	-	-	-	-	-	-	-	-	AGDISP cannot assess
Base Case (Headwind)[2]	75	150	20	0	Standard	491	616	763	923	-	-	-	-	-	-	-	-	AGDISP cannot assess
Base Case (Crosswind)	75	150	20	90	Standard	142	203	245	280	239	278	339	389	0.59	0.73	0.72	0.72	AGDISP conservative
Intermediate Wind angle[2]	75	150	20	30	Standard	452	554	669	800	-	-	-	-	-	-	-	-	AGDISP cannot assess
Maximum Altitude	100	150	20	90	Standard	165	238	298	-	271	311	373	419	0.61	0.76	0.80	-	AGDISP conservative
Maximum Altitude and speed	100	200	20	90	Standard	171	217	-	-	183	209	250	290	0.93	1.04	-	-	AGDISP conservative

Notes:
1. Particle Size Distribution: Fine, Standard and Coarse refer to ASAE Fine to Medium, Medium to Coarse and Coarse to Very Coarse respectively.
2. Headwind, no wind and intermediate wind cases with wind angles less than 60° could not be simulated in AGDISP.
3. Position at which 50% of the released mass has touched down.
4. AGDISP does not provide results for fraction aloft behind the aircraft, these results were back calculated from Lagrangian particle tracks.

Document Number - t2015.j520.009
Issued as Revision 0, September 30th 2016

Doc Ref: Atlas:\...\t2015.j520.009.0.odt
amogconsulting.com
EIN 20-4906471
TX PE Firm F-11821

AI-E253-09v20130508

Table 21: C-130A Comparison Of Results Perpendicular To The Aircraft Track

Case	Altitude (ft)	Ground Speed (kn)	Wind Speed (kn)	Wind Angle (°)	PSD[1]	CFD (ft)				AGDISP (ft)				Ratio CFD/AGDISP				Comment
						50%[3]	75%	90%	95%	50%	75%	90%	95%	50%	75%	90%	95%	
No Wind No Propellers[2]	75	150	0	0	Standard	-7	3	17	49	-	-	-	-	-	-	-	-	AGDISP cannot assess
No Wind[2]	75	150	0	0	Standard	-7	10	24	31	-	-	-	-	-	-	-	-	AGDISP cannot assess
Headwind Regulatory Max[2]	75	150	35	0	Standard	-15	5	23	42	-	-	-	-	-	-	-	-	AGDISP cannot assess
Base Case (Headwind)[2]	75	150	20	0	Standard	-12	7	23	38	-	-	-	-	-	-	-	-	AGDISP cannot assess
Base Case (Crosswind)	75	150	20	90	Standard	460	576	732	927	393	569	1031	1749	1.17	1.01	0.71	0.53	AGDISP conservative (Far field)
Intermediate Wind angle[2]	75	150	20	30	Standard	186	232	299	388	-	-	-	-	-	-	-	-	AGDISP cannot assess
Maximum Altitude	100	150	20	90	Standard	650	806	1038	-	568	825	1471	2375	1.14	0.98	0.71	-	AGDISP conservative (Far field)
Maximum Altitude and speed	100	200	20	90	Standard	556	692	-	-	497	735	1392	2629	1.12	0.94	-	-	AGDISP conservative (Far field)

Notes:
1. Particle Size Distribution: Fine, Standard and Coarse refer to ASAE Fine to Medium, Medium to Coarse and Coarse to Very Coarse respectively.
2. Headwind, no wind and intermediate wind cases with wind angles less than 60° could not be simulated in AGDISP.
3. Position at which 50% of the released mass has touched down.

AMOG®

5.2.1 Fuselage Wake Effect

The CFD study of the C-130A identified a fuselage wake effect that altered the trajectory of the dispersant immediately behind the aircraft. This fuselage wake effect is not modeled in AGDISP. The results shown in Figure 43 indicate that in the CFD simulations the fraction of dispersant aloft is greater in the near field before settling out of the air faster further downstream. A study was undertaken to further understand the flow characteristics which lead to this counter intuitive result.

The visualizations of the flow in Figures 44 and 46 show that in the near field the fuselage wake effect draws the particles upward and inward. This upward draft lasts only a short distance downstream while the particles are near the aircraft and this causes the initial increase in the fraction aloft.

While in the near field the fuselage wake effect causes an increase in the fraction aloft this does not result in particles staying aloft longer downstream. There are two key differences between the flow fields predicted by AGDISP and the CFD model which may explain this:

1. The complex interaction of the vortical wake of the C-130A. Not only is there a flap vortex and wingtip vortex pair present, but there is an effect from the tail of the C-130A, which generates its own tip vortices rotating in the opposite direction to those created by the main wing and flap (as shown in Figure 45). The three vortices generated on each side of the aircraft process around each other and may force some particles down earlier than predicted in AGDISP, which only models the main wingtip vortices.

2. The likely cause of the earlier settling is the fuselage wake itself as it draws the particles both upwards and inwards, as shown in Figure 46. As the wake draws the spray droplets inward, this has the effect of pulling the spray away from the stronger wingtip vortex pair. As the influence of the fuselage wake decays the particles are not entrained in vortices which would otherwise keep them aloft further downstream.

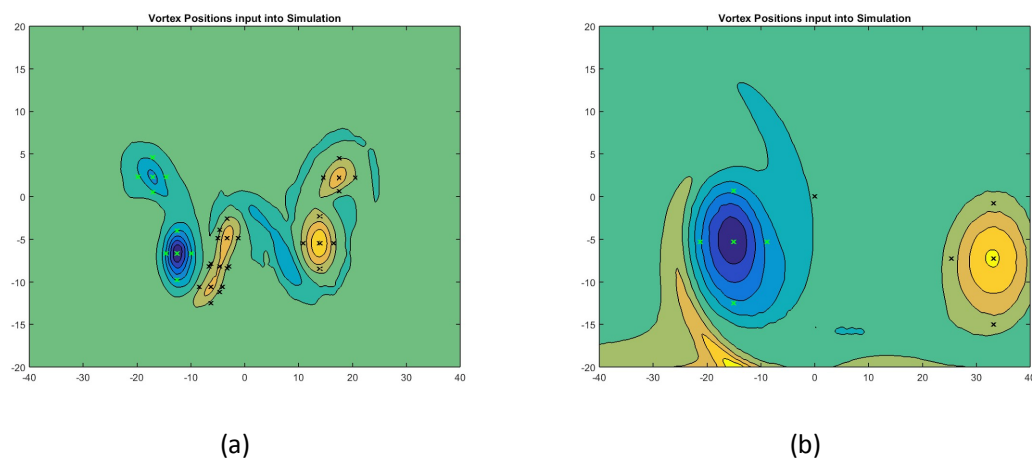(a)   (b)

Figure 45 : Wake vortices extracted from the C-130A CFD model at (a) 650 ft and (b) 5,000 ft
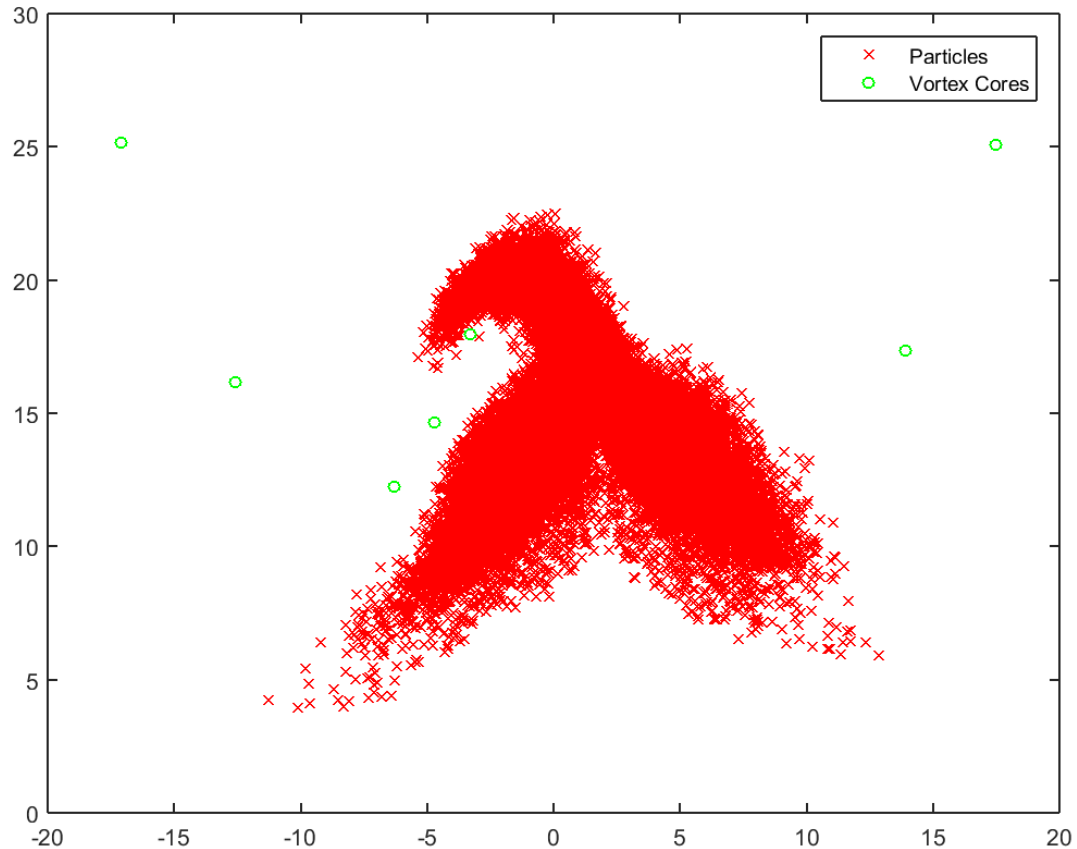
Figure 46 : Visualization of particles in the near-field fuselage wake effect at 650 ft behind the C-130A.

5.2.2   Summary Of C-130A Evaluation

Given the presence of the fuselage wake effect and the generally poor far field correlation between the AGDISP and CFD results as shown in Figure 43, it was concluded that AGDISP cannot be used directly to predict the maximum extent of spray drift for the C-130A. However, the results of the various CFD simulations conducted may be compared. The cases which resulted in the greatest drift were:

- Headwind regulatory maximum case with 35 kn headwind – the CFD predicted that 90 % of mass would touch down at 1,200 ft behind the aircraft.

- The maximum altitude crosswind case - the CFD predicted that 90 % of mass would touch down at 1,037 ft perpendicular to the track of the aircraft.

- Headwind base case with 20 kn headwind – the CFD predicted that 90 % of mass would touch down at 765 ft behind the aircraft.

As with the AT-802A, the distribution of deposited mass was comparable for similar headwind and crosswind conditions. These results show that 90 % of mass would touch down at 765 ft behind the aircraft in a 20 kn headwind and 730 ft perpendicular to the aircraft track in a 20 kn crosswind.

Document Number - t2015.j520.009
Issued as Revision 0, September 30th 2016
Doc Ref: Atlas:\...\t2015.j520.009.0.odt
amogconsulting.com
EIN 20-4906471
TX PE Firm F-11821

AI-E253-09v20130508

In the near field, the CFD and AGDISP both indicate a similar particle deposition gradient behind the aircraft, although the CFD indicates that this occurs further behind the aircraft, as shown in Figure 43. This indicates that AGDISP is at least predicting the same dry deposition process, and is only not accounting for the temporary lift provided by the fuselage wake effect.

Beyond 650 ft, the two solutions reverse and AGDISP appears to delay the deposition of the remaining particles in the wake, leading to a more conservative estimate in the far field. As such, there is a reasonable expectation that AGDISP provides a conservative prediction of the far-field extent of drift. Given the simplifications made in the CFD model and its limited applicability in modeling the far field spray drift, it was considered appropriate to use the most conservative features of the spray drift behavior predicted by both models.

Based on the results presented in Figures 43 and 44 and Tables 20 and 21 the following conclusions are drawn about the prediction of spray drift from a Lockheed C-130A using AGDISP:

Table 22: Conclusions For The C-130A AGDISP-CFD Comparison

No.	Question	Answer
1	In general, is there good correlation between the CFD and AGDISP results in the near field region?	No
2	For crosswind cases which model is more conservative?	Inconclusive
3	For intermediate wind direction cases which model is more conservative?	Inconclusive
4	For headwind cases which model is more conservative?	Inconclusive
5	Does altitude change which model is more conservative?	Inconclusive
6	Does aircraft speed change which model is more conservative?	Inconclusive
7	Does dispersant particle size distribution change which model is more conservative?	Not assessed

5.3 DOUGLAS DC-3

The extent of aerial spray from the Douglas DC-3 airframe was predicted using both AGDISP and the CFD model. Initial results for the DC-3 showed a large difference between the predicted spray extent obtained from AGDISP and the CFD model. Given the large difference in predicted spray behavior the full case list was not run. For the abbreviated case list, Figure 24 shows the predicted distance perpendicular to the aircraft track for 50 %, 75 %, 90 % and 95 % of the mass to touch down. Figure 47 illustrates the significant difference between the predicted particle transport behavior using AGDISP and CFD. The CFD predicts the particles to remain aloft much further downstream in both the near and far field regions.

The flow field behind the DC-3 was analyzed to determine the cause of the observed difference. Figure 48 shows the flow field immediately behind the DC-3. The gray iso-contour indicates the presence of vortices while the streamlines show the trajectory of the particles. This image clearly shows that the spray boom extends into the wing tip vortex region which causes a large number of

Document Number - t2015.j520.009
Issued as Revision 0, September 30th 2016
Doc Ref: Atlas:\...\t2015.j520.009.0.odt
amogconsulting.com
EIN 20-4906471
TX PE Firm F-11821

AI-E253-09v20130508

particles to be entrained in the wing-tip vortex. It is noted that extending the boom beyond 65 % to 70 % of the wing semi-span is not recommended practice for agricultural spraying operations (Barbosa, 2010; Teske, Thistle, Barry, & Eav, 1998).
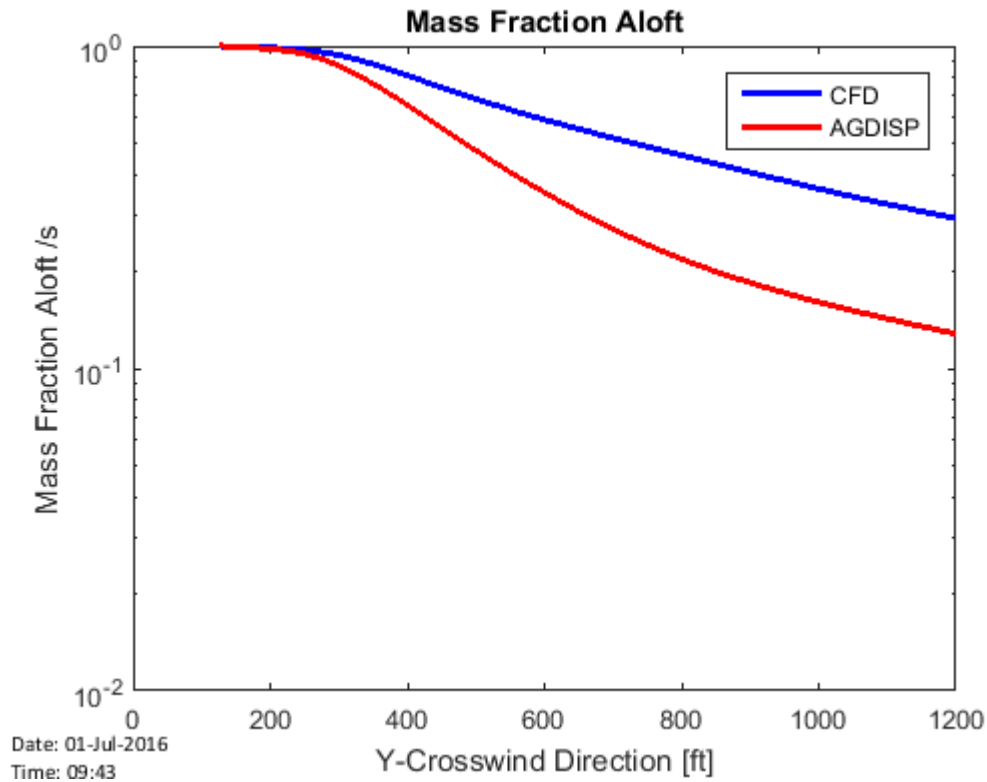
Figure 47 : DC-3 Comparison of CFD and AGDISP results for crosswind base case
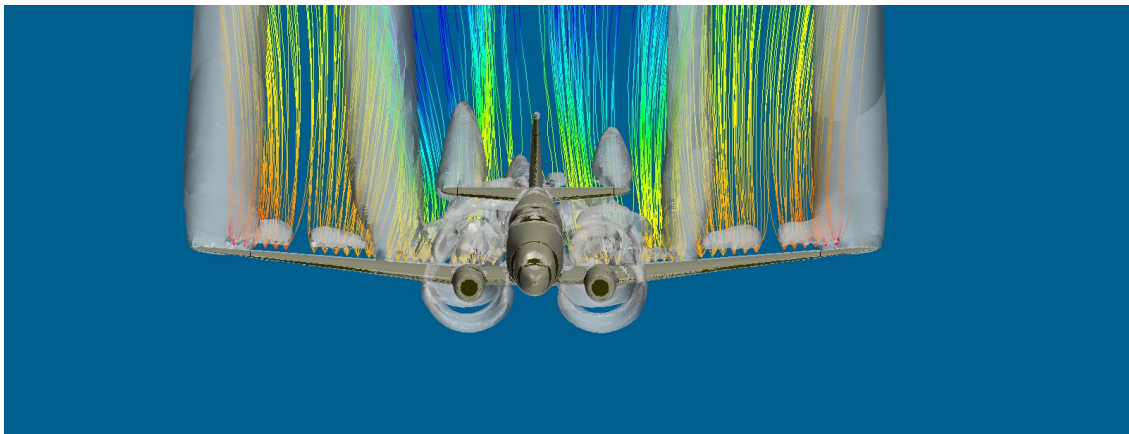

Figure 48 : DC-3 visualization of particles released in wing tip and flap vortices
The gray iso-contours indicate the presence of vortex cores. Streamlines show particle tracks

Document Number - t2015.j520.009
Issued as Revision 0, September 30th 2016
Doc Ref: Atlas:\...\t2015.j520.009.0.odt
amogconsulting.com
EIN 20-4906471
TX PE Firm F-11821

AI-E253-09v20130508

In addition to the wing-tip vortex Figure 48 shows a strong vortex being shed off the edge of the deployed flap. Given the limited information provided by the Oil Spill Response Organizations (OSROs) with regard to spray operating conditions, the exact amount of flap deployment during dispersant spraying operations was not directly known, although analysis accounting for the regulatory speeds for spray dispersal from the DC-3 indicate that flap deployment is required to maintain sufficient lift. The presence of the flap vortex affects the spray trajectory in both the near and far field. Figure 49 shows that in the far field the wing-tip and flap vortices interact in a co-rotating vortex pair. The two vortices process around each other such that the inner flap vortex travels down beneath the wing tip vortex before being pulled upward, lifting the particles entrained in the flap vortex further off the ground and keeping them aloft longer.

As AGDISP is based on lifting line theory it does not account for multiple vortex interactions and, as such, is not capable of capturing this behavior.

Figure 49 : DC-3 visualization of particles in flap-wingtip vortex interaction
The grey iso-contours indicate the presence of vortices. Streamlines show particle tracks

Table 23: DC-3 Comparison Of Results Perpendicular To The Aircraft Track

Case	Altitude (ft)	Ground Speed (kn)	Wind Speed (kn)	Wind Angle (°)	PSD[1]	CFD (ft)				AGDISP (ft)				Ratio CFD/AGDISP				Comment
						50%[3]	75%	90%	95%	50%	75%	90%	95%	50%	75%	90%	95%	
Base Case (Crosswind)	75	130	20	90	Standard	729	1400	-	-	495	752	1543	2189	1.47	1.86	-	-	CFD Conservative
Intermediate Wind angle[2]	75	130	20	30	Standard	364	-	-	-	-	-	-	-	-	-	-	-	AGDISP cannot assess
Maximum Altitude	100	130	20	90	Standard	1002	-	-	-	688	1057	2089	3170	1.46	-	-	-	CFD Conservative

Notes:
1. Particle Size Distribution: Fine, Standard and Coarse refer to ASAE Fine to Medium, Medium to Coarse and Coarse to Very Coarse respectively.
2. Headwind, no wind and intermediate wind cases with wind angles less than 60° could not be simulated in AGDISP.
3. Position at which 50% of the released mass has touched down.

Document Number - t2015.j520.009
Issued as Revision 0, September 30th 2016

Doc Ref: Atlas:\...\t2015.j520.009.0.odt
amogconsulting.com
EIN 20-4906471
TX PE Firm F-11821

AI-E253-09v20130508

Given the presence of the flap vortex pair and the generally poor correlation between the AGDISP and CFD results described in Figure 47, AGDISP cannot be used to predict the maximum extent of spray drift for the DC-3. In any case, analysis of the CFD results showed that the worst case was the maximum altitude, maximum crosswind case, where the CFD predicted that 50 % of mass would touch down at 1000 ft perpendicular to the track of the aircraft.

Based on the results presented in Figures 47 and 48 the following conclusions are drawn about the prediction of spray drift from a Douglas DC-3 using AGDISP:

Table 24: Conclusions For The Douglas DC-3 AGDISP-CFD Comparison

No.	Question	Answer
1	In general, is there good correlation between the CFD and AGDISP results in the near field region?	No
2	For Crosswind cases which model is more conservative?	AGDISP Not suitable
3	For intermediate wind direction cases which model is more conservative?	AGDISP Not suitable
4	For headwind cases which model is more conservative?	AGDISP Not suitable
5	Does altitude change which model is more conservative?	AGDISP Not suitable
6	Does aircraft speed change which model is more conservative?	Not assessed
7	Does dispersant particle size distribution change which model is more conservative?	Not assessed

5.4   DOUGLAS DC-4

For the Douglas DC-4, comparison of the aerial spray dispersion patterns predicted by AGDISP and the CFD model was not possible. The DC-4 configuration modeled includes a unique spray boom position located above the trailing edge of the wing. AGDISP restricts spray configurations to those with an under wing spray arrangement. Therefore, it was not possible to model the Douglas DC-4 configured as identified for use in spray operations in AGDISP.

Despite the limitations of AGDISP, the aerial spray pattern behind the DC-4 was modeled using CFD. Figure 50 shows the interaction of flow particles (streamlines) with the vortices shed from the wing tips, wing flaps and tail. Similarly to the Douglas DC-3 the flow behind the DC-4 is affected by the presence of the flap vortex. In this case, the flap vortex and wing tip vortex merge to form a single vortex structure downstream of the aircraft. The interaction of these complex flow structures affects the dispersion of particles in the near field; care must be taken to consider this interaction when modeling the far field drift of aerial dispersant.

Document Number - t2015.j520.009
Issued as Revision 0, September 30th 2016
Doc Ref: Atlas:\...\t2015.j520.009.0.odt
amogconsulting.com
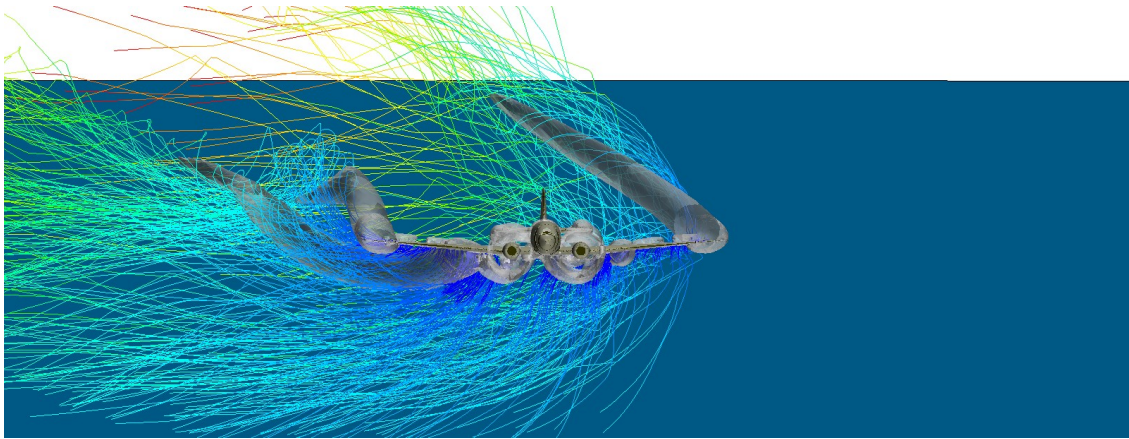EIN 20-4906471
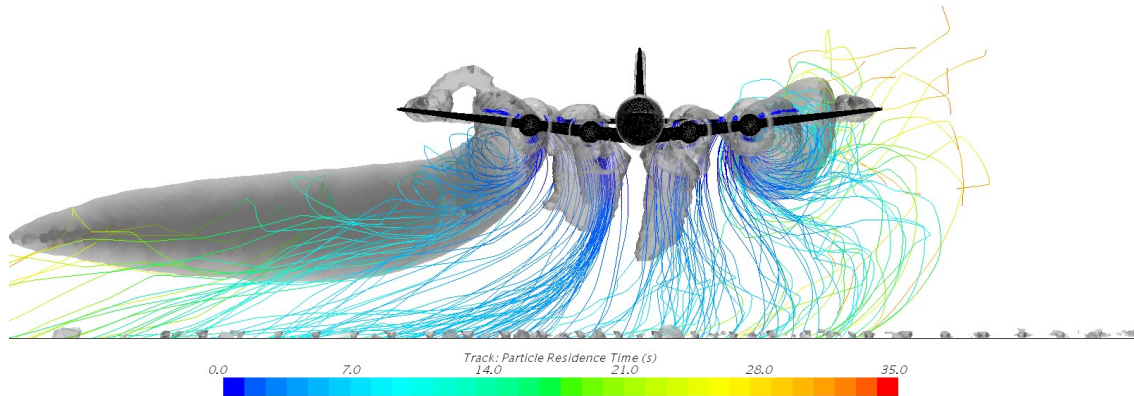TX PE Firm F-11821

AI-E253-09v20130508

Figure 50 : DC-4 visualization of particles in flap-wingtip vortex interaction
The gray iso-contours indicate the presence of vortices. Streamlines show particle tracks

5.5   SUMMARY OF STUDY

The key outcomes of the exploratory CFD evaluation of the AGDISP modeling system for use in offshore spill response are summarized as follows:

●   Air Tractor AT-802A: For the purposes of offshore spill response, the AT-802A is the only aircraft well represented by AGDISP in that no significant modifications to the results are required.

●   Lockheed C-130A: It has been identified that, due to the wake generated by the shape of the fuselage in the vicinity of the rear cargo door, the results from AGDISP are not representative in the near field, in that the fuselage wake delays the deposition of the spray. However, in the far field, AGDISP predicts a lower deposition rate compared to the CFD model, and as such AGDISP results may be modified in order to conservatively estimate the extent of spray drift.

●   Douglas DC-3: Due to the presence of significant flap vortices, the spray boom extending sufficiently along the wing semi-span to inject particles into the wingtip vortices, and the subsequent downstream interaction of the flap and wingtip vortices, the DC-3 is poorly represented by AGDISP, and an alternative approach is required to determine the drift impacted area.

●   Douglas DC-4: Due to the unique arrangement of the spray boom on the DC-4 above the trailing edge of the wing, AGDISP cannot model the influence of the wake on the spray, and an alternative approach is required to determine the drift impacted area. While the presence of flap vortices also appears to influence the DC-4 spray, the closer proximity of the flaps to the wing tips causes the two vortices to merge earlier than those generated by the DC-3, reducing the influence of the flap vortices.

Document Number - t2015.j520.009
Issued as Revision 0, September 30th 2016
Doc Ref: Atlas:\...\t2015.j520.009.0.odt
amogconsulting.com
EIN 20-4906471
TX PE Firm F-11821

AI-E253-09v20130508

6 EXTENSION OF CFD RESULTS FOR DC-3 AND DC-4

A key finding of the exploratory CFD study was that the existing regulatory models were not suitable for predicting the maximum drift extent for the Douglas DC-3 and DC-4 airframes. A methodology was developed by which the CFD results were extended in order to allow the prediction of spray drift extent. The methodology used to model the DC-3 and DC-4 is described by the following algorithm:

1. Using CFD results identify a distance behind the aircraft where the vortical structures have largely stabilized and formed clear, distinct vortices.

2. At this distance, extract from the CFD the following data on a plane perpendicular to the aircraft's direction of travel, through the aircraft wake:

    2.i. The position, strength and size of the wake vortices; and

    2.ii. The sizes and positions of the dispersant spray particles remaining aloft at the extraction plane.

3. Use an inviscid vortex transport and a Lagrangian particle modeling approach to calculate the distance at which 99 % of the particle mass has touched down.

Inviscid vortex transport modeling is a well established methodology in the literature, and forms the foundation of AGDISP. Employing this technique, the CFD modeling results were extended beyond the initial model domain by characterizing the aircraft wake vortices for the DC-3 and DC-4 to allow their input into the vortex model. An example of the extracted vortices is included for the C-130A model in Figure 51. This data, combined with the extracted locations of the particles which remain aloft was used to model how the vortices and wind transport the particles by using a Lagrangian particle modeling approach.

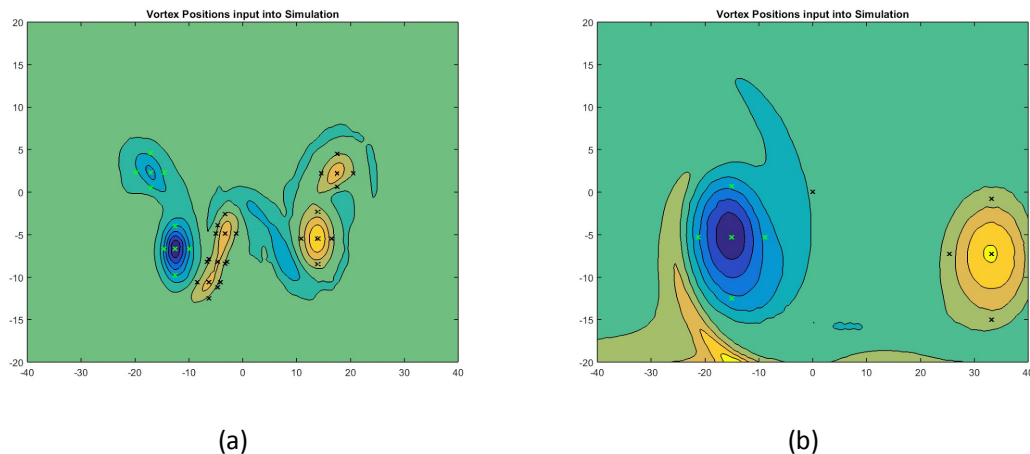(a)   (b)

Figure 51 : Wake vortices extracted from the C-130A CFD model at (a) 650 ft and (b) 5,000 ft

6.1   DEMONSTRATION OF ACCURACY

The CFD modeling explicitly provides calculated values for the vortex strength and position in the wake of the aircraft. As stated previously in Section 4.1.1.2, this explicit modeling is considered accurate in the first 4,000 ft behind the aircraft. The primary source of AGDISP's inability to accurately model the drift of dispersant sprayed by the DC-3 is its limited characterization of the vortices generated by the aircraft, particularly the flap vortices. While the DC-4 configuration cannot be modeled by AGDISP, it would be expected to be similarly affected by flap vortices.

As shown in Figure 52, it was identified that the Lagrangian particle modeling calculation can produce results consistent with both CFD model and AGDISP for the AT-802A, which was found to be well represented by AGDISP. Furthermore, for the C-130A, it was identified that an inviscid vortex transport extension model allowed a better representation of the influence of the wake vortices and agreed better with the CFD results.

As shown in Figure 53, applying the vortex transport extension methodology to the DC-3 has identified that the vortex transport approach provides a more consistent representation of the particle deposition than the Gaussian extension model. This approach is also able to capture the influence of the flap vortices on the particle deposition identified by the CFD results, thereby better representing the behavior of the particles.

(a) Air Tractor AT-802A   (b) Lockheed C-130A
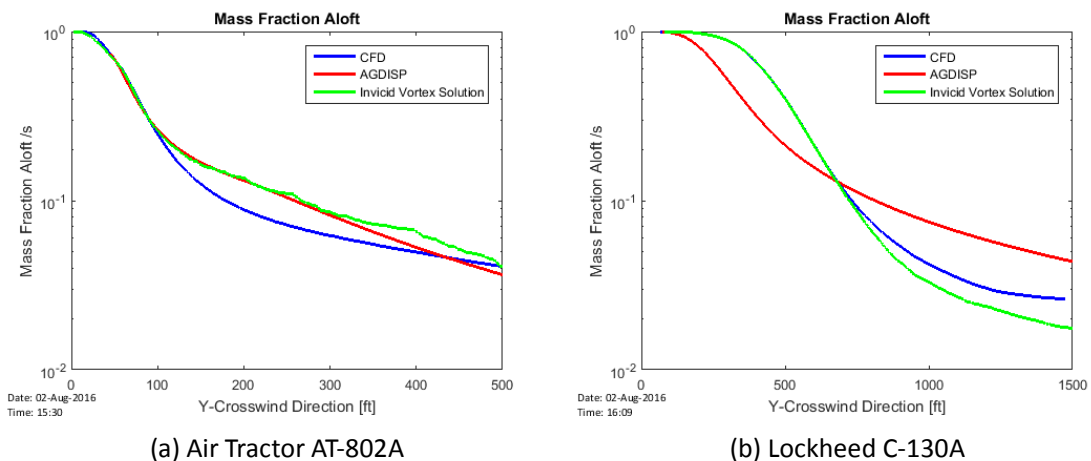
Figure 52 : Comparison of the use of Lagrangian particle calculation with CFD and AGDISP results

Document Number - t2015.j520.009
Issued as Revision 0, September 30th 2016
Doc Ref: Atlas:\...\t2015.j520.009.0.odt
amogconsulting.com
EIN 20-4906471
TX PE Firm F-11821

AI-E253-09v20130508
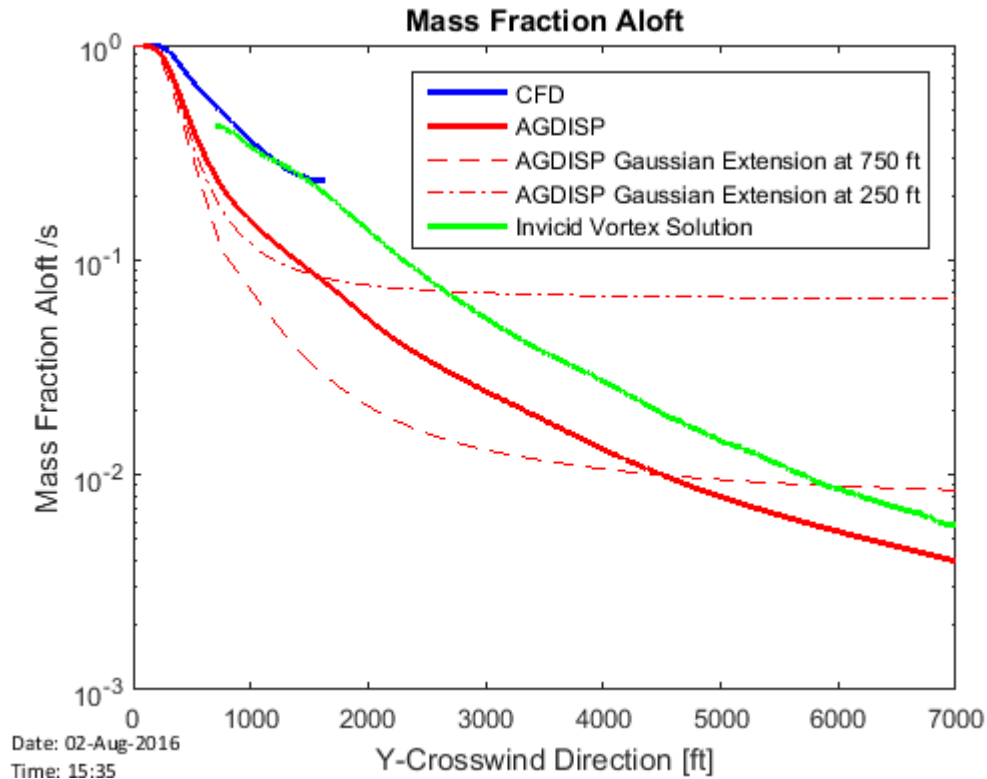
Figure 53 : Comparison of the Gaussian and Lagrangian particle calculation CFD result extension approaches for the DC-3

6.2 DC-3 RESULTS - NEAR FIELD CHARACTERIZATION

The vortex characteristics and particle positions were extracted at a number of locations behind the aircraft. Figure 54 shows the particle positions extracted 4900 ft behind the DC-3, at this distance the flow has developed into a two vortex system with a significant proportion of the particle mass entrained in the vortices.

Document Number - t2015.j520.009
Issued as Revision 0, September 30th 2016
Doc Ref: Atlas:\...\t2015.j520.009.0.odt
amogconsulting.com
EIN 20-4906471
TX PE Firm F-11821

AI-E253-09v20130508

Figure 54 : DC-3 visualization of particles entrained in wake vortices

Table 25 shows the vortex characteristic data extracted from a selection of the CFD simulations. The vortex characteristics were calculated in the following way:

1. Vortex position – Was determined by finding the local peak in vorticity.

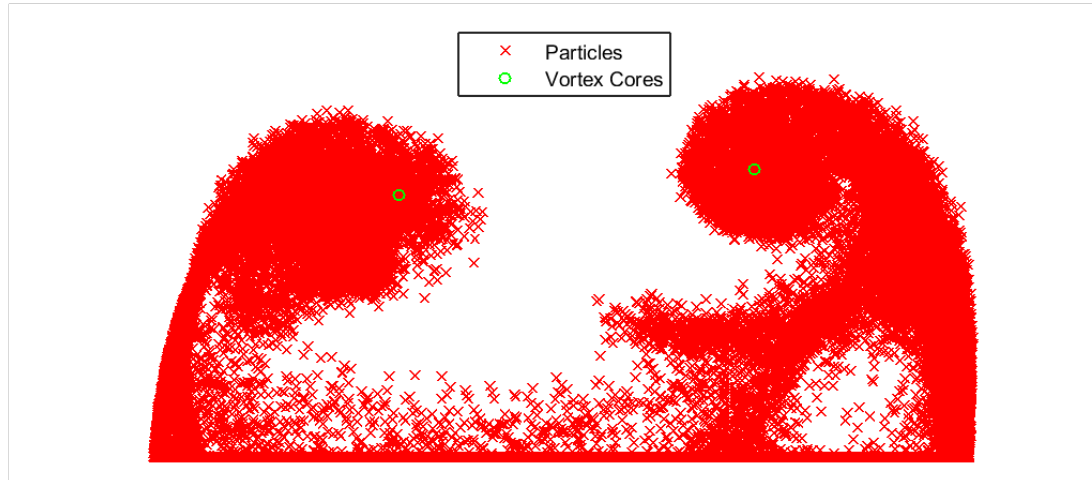2. Vortex characteristic radius – Was calculated by assuming that the vortices could be approximated as a theoretical Batchelor vortex core (del Pino, Parras, Felli, & Fernandez-Feria, 2011). The vortex characteristic radius was found by finding the distance from the vortex centre such that the average vorticity was reduced by a factor of 1/e (where e is the base of the natural logarithm).

3. Vortex Strength (Γ) – Was calculated by assuming that the vortices could be approximated as a theoretical Batchelor vortex core and calculating the vortex strength by substitution of the vortex characteristic radius into Equation 12.

$$\omega = \frac{\Gamma}{(\pi \, r_c^2)} e^{(\frac{-r^2}{r_c^2})}$$

Equation 12

Where ω is the axial vorticity, Γ is the circulation strength, r_c is the characteristic radius, and r is the radial distance.

Given the large amount of data associated with the particle mass distribution (due to the large number of parcels simulated) a full summary of the results for each CFD case has not been reported.

Although strictly beyond the typical maximum wind speeds for spray operations, wind speeds of up to 40 knots were considered in the CFD modeling to explore spray drift behavior at the upper operational limit and in support of data generation for the Decision Support Tool (DST). Generation of extent data beyond the 35 knot wind speeds ensured that no extrapolation was required for extent prediction. Restriction on allowable input parameters is considered as part of the DST design.

Table 25: DC-3 Vortex Results For The Near Field Characterization Study At 4900 Ft

Case	Wind Speed (kn)	Wind Angle (°)	Vortex 1				Vortex 2			
			Y (ft)	Z (ft)	Γ (ft^2/s)	Radius (ft)	Y (ft)	Z (ft)	Γ (ft^2/s)	Radius (ft)
1	0	0	-31	66	-1750	0	39	72	2004	12
2	10	0	-32	65	-1811	13	39	71	1820	12
3	10	30	-27	67	-1646	12	42	70	1826	12
4	10	60	-23	69	-1476	12	46	70	1799	12
5	10	90	-21	72	-1303	12	47	71	1760	13
6	35	0	-19	86	-1098	13	57	71	1926	15
7	40	30	-18	78	-1486	14	53	70	2062	15
8	23	60	-34	64	-2064	14	38	69	2186	14
9	20	90	-23	70	-1976	15	49	69	2418	15

6.3 DC-4 RESULTS - NEAR FIELD CHARACTERIZATION

Table 26 shows the vortex characteristic data extracted from a selection of the CFD simulations for the DC-4. The same methodology was applied to extract the vortex characteristics as described in Section 6.2.

Table 26: DC-4 Vortex Results For The Near Field Characterization Study At 4900 Ft

Case	Wind Speed (kn)	Wind Angle (°)	Vortex 1				Vortex 2			
			Y (ft)	Z (ft)	Γ (ft^2/s)	Radius (ft)	Y (ft)	Z (ft)	Γ (ft^2/s)	Radius (ft)
10	0	0	-44	51	-4456	14	45	51	4449	14
11	10	0	-41	57	-3700	14	43	56	3638	14
12	10	30	-35	57	-3665	14	48	53	3797	14
13	10	60	-34	61	-3659	14	54	51	3893	14
14	10	90	-33	63	-3726	14	59	49	3997	15
15	35	0	-26	70	-3628	15	73	51	4472	17
16	40	30	-27	69	-3397	14	65	53	4055	16
17	23	60	-37	61	-3320	14	37	60	3401	14
18	20	90	-28	69	-3126	14	53	58	3572	15

Document Number - t2015.j520.009
Issued as Revision 0, September 30th 2016
Doc Ref: Atlas:\...\t2015.j520.009.0.odt
amogconsulting.com
EIN 20-4906471
TX PE Firm F-11821

AI-E253-09v20130508

7 AGDISP RESULTS

AGDISP and CFD predictions of the maximum extent of spray drift have been compared in Section 5. Based on this comparison it was shown that AGDISP provides a comparable or conservative solution compared to that of the higher fidelity CFD model for most cases for two of the four modeled aircraft. In light of this finding, it was advantageous to use results from AGDISP in the DST.

When comparing the results from AGDISP and the CFD models, care was taken to match the inputs across the two models. When using AGDISP to develop data for the DST the model was configured to give both reasonable and conservative predictions of the maximum extent. With this in mind, the following sensitivity studies were undertaken:

- Sensitivity to different input parameters.

- Non crosswind cases.

Representative results for each of these studies are presented below.

7.1 AGDISP INPUT PARAMETER SENSITIVITY STUDY

A series of parameters were tested within AGDISP to determine the sensitivity of the program to aircraft weight, speed, propeller specifications, drag coefficients, vortex decay rates and environmental parameters (temperature and humidity).

To test the sensitivity of AGDISP to input parameters the default spraying parameters for the AT-802A flying at 16 ft with a crosswind of 20 kn were used. Sensitivity cases were created by altering variables to reflect those tested in the CFD simulations. Table 27 summarizes the results of the sensitivity study in terms of the distance perpendicular to the aircraft track to 99 % of the mass being deposited.

Document Number - t2015.j520.009
Issued as Revision 0, September 30th 2016
Doc Ref: Atlas:\...\t2015.j520.009.0.odt
amogconsulting.com
EIN 20-4906471
TX PE Firm F-11821

AI-E253-09v20130508

Table 27: AGDISP Sensitivity Study Summary – Maximum Perpendicular Extent

Variable Tested	Base Value	Sensitivity Value	Distance (ft)	Difference (%)
Base Case	-	-	950	-
Vortex Decay Rate	OGE[1] = 0.49 f/s and IGE[2] = 1.84 ft/s	OGE[1] = 0.98 ft/s and IGE[2] = 3.67 ft/s	814	-14
Aircraft Weight	11,160 lb	17,926 lb	906	-5
Aircraft speed	126 kn	151 kn	932	-2
Drag Coefficient	0.1	0.05	925	-3
Aircraft Weight and Speed	11,160 lb	17,926 lb	920	-3
	126 kn	151 kn		
Propeller Specifications	RPM = 1500	RPM = 1700	950	0
	Radius = 4.79 ft	Radius = 4.95 ft		
	Efficiency = 80%	Efficiency = 72%		
Humidity	50.00%	5.00%	950	0
		10.00%		
Temperature	65 °F	59 °F	950	0

Notes:
1. Vortex decay rate Out of Ground Effect (i.e. at altitude).
2. Vortex decay rate In Ground Effect (i.e. close to the ground).

These results indicate that vortex decay rate has the greatest impact on predicted maximum extent. Figure 55 shows the sensitivity cases involving the aircraft weight and vortex decay rates. It can be seen in Figure 55 that the increased vortex decay rate results in a decrease of the maximum extent for the 99% of the particles by mass threshold.

Document Number - t2015.j520.009
Issued as Revision 0, September 30th 2016
Doc Ref: Atlas:\...\t2015.j520.009.0.odt
amogconsulting.com
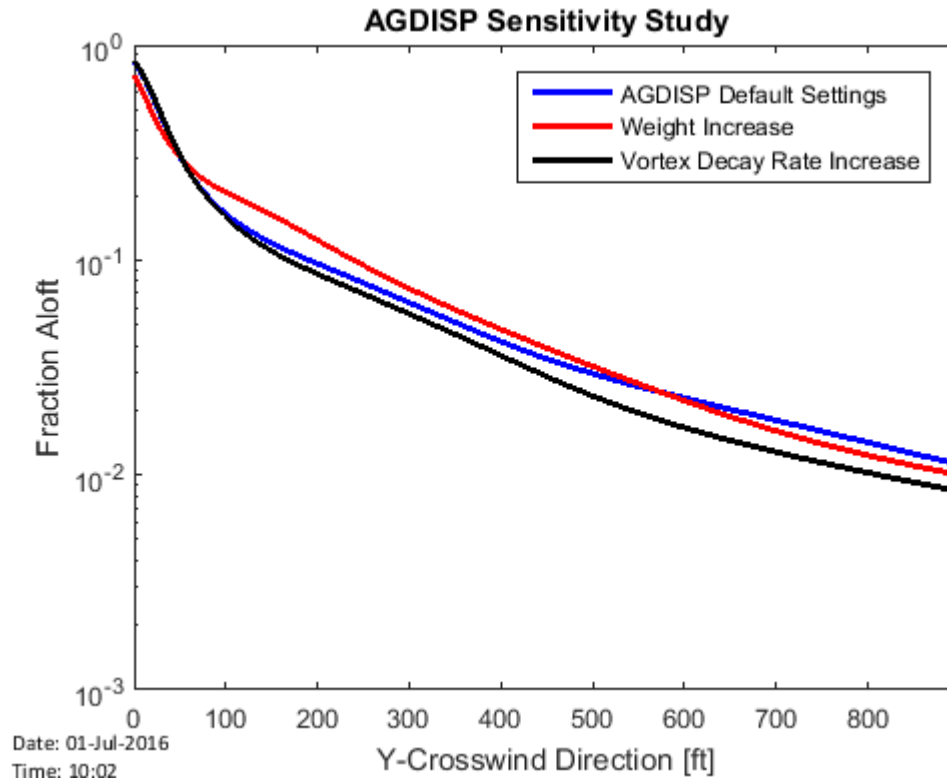EIN 20-4906471
TX PE Firm F-11821

AI-E253-09v20130508

Figure 55 : AGDISP results for propeller, drag coefficient and vortex decay sensitivity

The effects of the environmental parameters (temperature and humidity) appear to have no impact on the results. It is noted that these parameters relate more to the evaporation model not used in this assessment.

Similar studies were conducted for the remaining airframes. The maximum extent of the particle deposition was found to be affected inconsistently by the inputs of weight, velocity and thrust (via drag coefficient and propeller representation). The primary effect of changing these inputs is their impact on the strength of the modeled wingtip vortices. The inconsistency across the airframes is likely due to differences in spray boom and injector location with respect to the vortices generated by the wings.

In summary, to configure AGDISP to produce the most appropriately conservative solution for the DST the following settings were used:

- Vortex Decay Rate – Set to minimum values,

- Aircraft Weight – Set to representative weight,

- Drag Coefficient – Default value used,

- Propeller details – Default value used,

- Temperature and Humidity – Default values used.

Document Number - t2015.j520.009
Issued as Revision 0, September 30th 2016
Doc Ref: Atlas:\...\t2015.j520.009.0.odt
amogconsulting.com
EIN 20-4906471
TX PE Firm F-11821

AI-E253-09v20130508

7.2 NON CROSSWIND CASES IN AGDISP

AGDISP was developed to predict the downwind drift of aerially dispersed spray. As a result of this, the user is limited to modeling wind angles relative to the direction of travel (θ_{wind}) between 60 ° and 120 ° degrees as described in Figure 56. When developing data for the DST, a larger range of wind angles must be considered. As such, a study was undertaken to investigate the impact of wind angle on the AGDISP prediction to understand the relationship between wind angle and maximum extent.
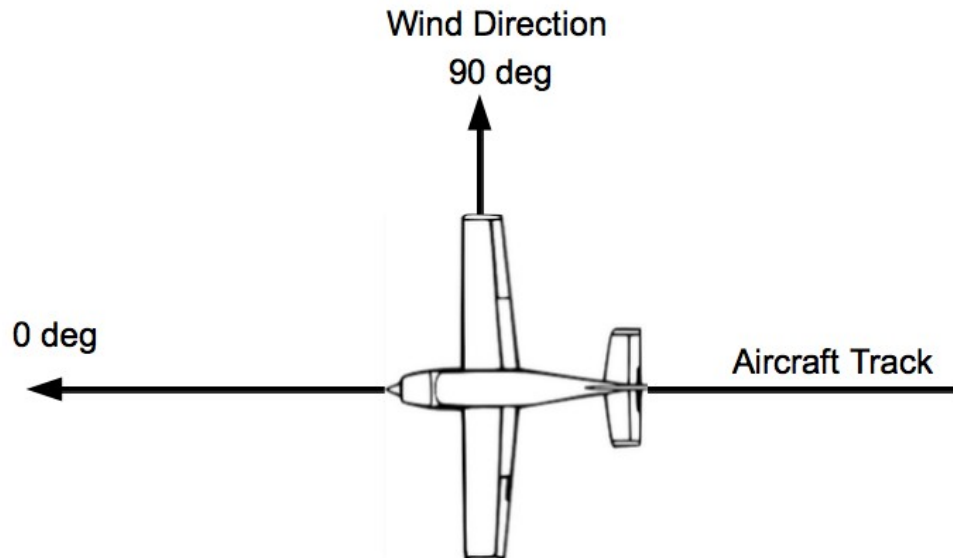

Figure 56 : Downwind axis definition

To assess the effect of wind angle a study was conducted using the AT-802A. It should be noted that the boom location and size of the AT-802A make it least likely to be affected by wing-tip vortex interactions and consequently the results of this study should only be applied to airframes without a significant degree of interaction between the dispersant and the tip vortices.

A study was conducted in which the trajectories of 1000 μm particles were analyzed and deposition distance extracted for five wind angles (60°, 75°, 90°, 105° and 120°).

Document Number - t2015.j520.009
Issued as Revision 0, September 30th 2016
Doc Ref: Atlas:\...\t2015.j520.009.0.odt
amogconsulting.com
EIN 20-4906471
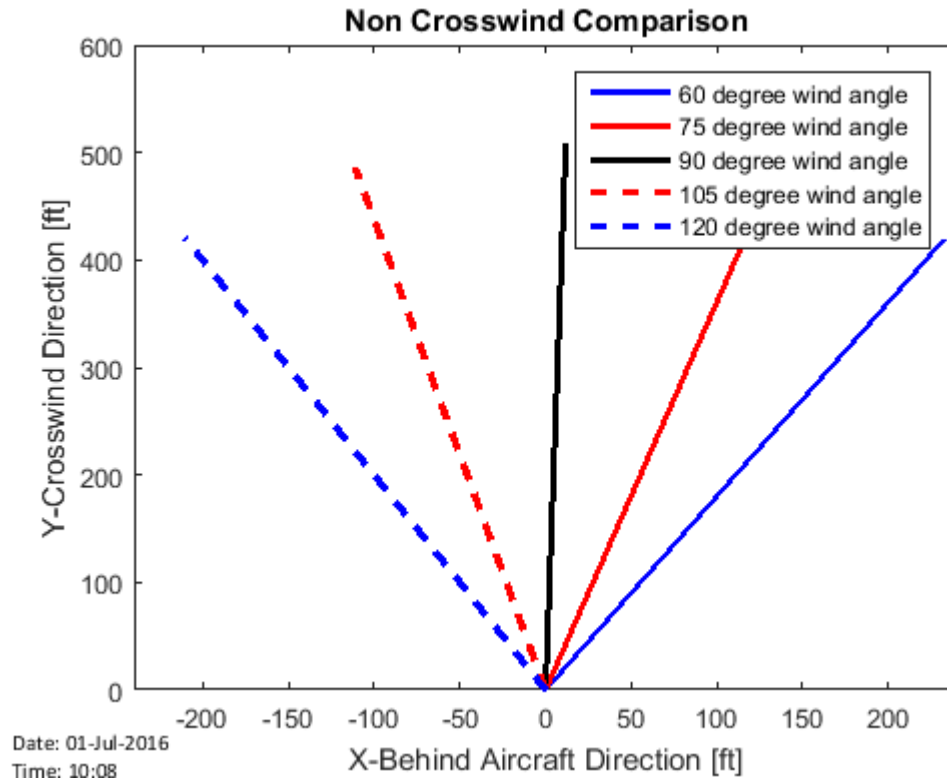TX PE Firm F-11821

AI-E253-09v20130508

Figure 57 : Particle trajectories for various wind angles.

Figure 57 Shows that the trajectory length is symmetric about the 90° crosswind case, with similar angles relative to 90° (e.g 75° and 105°) producing a total trajectory of the same length. The overall (or resultant) length of each trajectory is given in Table 28. Since not all particles reach the ground in this analysis only the heavier particles are included in the resultant length.

Table 28: Resultant Length Of Each Trajectory (Heavier Particles Only)

Θ_{wind} (Relative to Aircraft Track)	Resultant Drift Extent (ft)
60°	480.6
75°	502.3
90°	510.2
105°	496.4
120°	470.1

Document Number - t2015.j520.009
Issued as Revision 0, September 30th 2016
Doc Ref: Atlas:\...\t2015.j520.009.0.odt
amogconsulting.com
EIN 20-4906471
TX PE Firm F-11821

AI-E253-09v20130508

The values in Table 28 show that the resulting lengths from the varying wind directions are very similar in magnitude for symmetric angles. The discrepancy between symmetric angles (such as 502.3 ft for 75° and 496.4 ft for 105°) is likely due to the relative velocity between the released spray and the wind causing a change in the drag force experienced by the particle.

The fraction of particles aloft in AGDISP is output in the "downwind direction" which acts perpendicular to the aircraft track. The fraction aloft in this direction is plotted for three wind angles and an ASAE medium to coarse particle size distribution in Figure 58. Extracting the distance to a specific level of fraction aloft (see Table 29), it can be seen that the fraction aloft at a non 90° crosswind angle can be related to the crosswind case using a simple cosine relationship for the 0.8 fraction aloft case. For smaller fractions aloft the cosine relationship is not as strong, this is likely due to the lighter particles being deposited at these distances, as lighter particles are more likely to be affected by the wingtip vortices. At the maximum extent (99 % deposited or 1 % fraction aloft) the difference between the AGDISP result and that obtained using a cosine relationship is only 8 %.

The results presented in Figure 57, Figure 58 and Table 29 indicate that for the AT-802A with a large proportion of coarse particles, the wind angle does not significantly affect the total distance travelled by spray drift. To determine the maximum drift extents resolved in the spanwise and trackwise directions for wind angles not equal to 90° (crosswind cases) the maximum extent predicted in the crosswind (90°) case is extracted and applied at an angle inline with the wind with an appropriate safety factor applied.
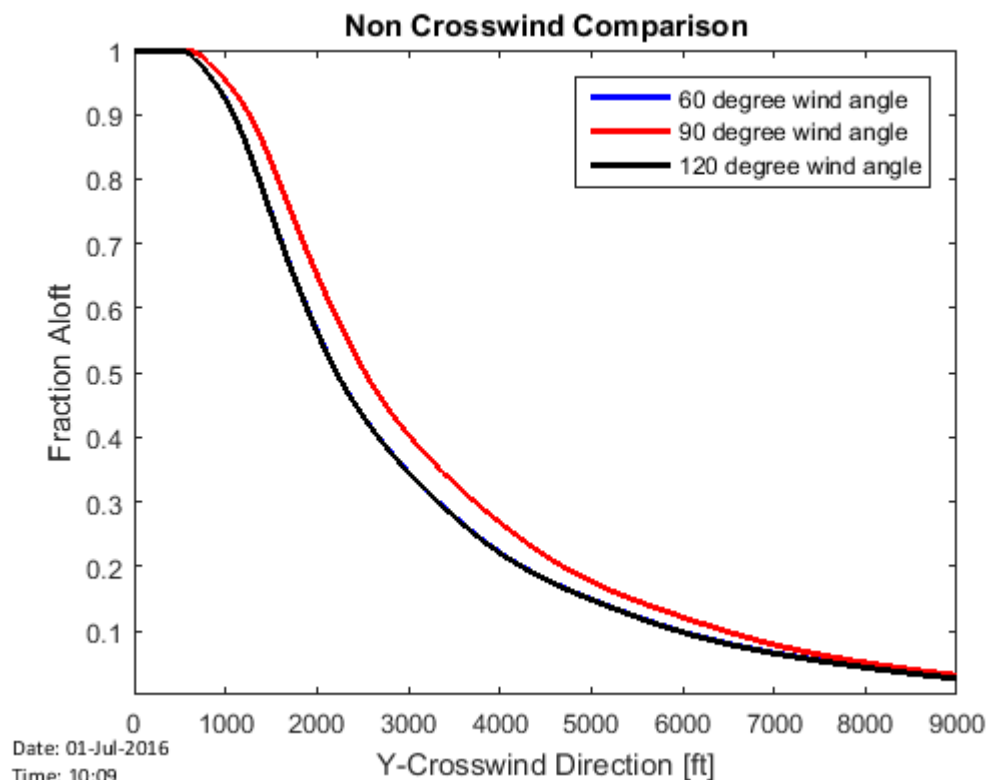

Figure 58 : Fraction aloft as a function of wind angle

Table 29: Distance To Fraction Aloft Threshold For Different Wind Angles

	Fraction Aloft	$\Theta_{wind} = 60°$ (intermediate headwind) (ft)	$\Theta_{wind} = 90°$ (extreme crosswind) (ft)	$\Theta_{wind} = 120°$ (intermediate tailwind) (ft)
Raw Output	80%	1,368	1,578	1,368
	50%	2,215	2,526	2,215
	20%	4,242	4,688	4,229
	1%	11,289	12,034	11,201
Distance / $\cos(\theta_{wind})$	80%	1,581	1,578	1,581
	50%	2,556	2,530	2,556
	20%	4,898	4,688	4,882
	1%	13,035	12,034	12,933

8   SUMMARY

The findings from the CFD modeling activities are summarized as follows:

1.   The CFD models have been constructed so as to accurately model the dispersant spray drift in the near field region close to the aircraft.

2.   Qualitative validation of the results shows that the CFD models are capturing the significant flow structures affecting the dispersant trajectories.

3.   The flap vortices and fuselage wake were found to have a significant effect on the dispersant spray drift for the C-130A, DC-3 and DC-4. These effects are widely acknowledged features of the wake generated by aircraft, but have not previously been studied with regard to their effect on dispersant spray drift.

4.   Appropriate methodologies for predicting the extent of spray drift were identified for each of the four aircraft under consideration, as follows:

    4.i.   Air Tractor AT-802A: This aircraft is well represented by AGDISP and no significant modifications to the AGDISP results are required.

    4.ii.   Lockheed C-130A: AGDISP results may be modified in order to conservatively estimate the extent of spray drift.

    4.iii.   Douglas DC-3: A Lagrangian particle calculation was used to extend the CFD results and predict the far field spray drift extent.

    4.iv.   Douglas DC-4: A Lagrangian particle calculation was used to extend the CFD results and predict the far field spray drift extent.

5.   The Lagrangian particle calculation used to extend the CFD results for the DC-3 and DC-4 provides a representation of the spray drift in the far field which is consistent with the results obtained by the CFD models and AGDISP.

6.   The Lagrangian particle calculation models the spray drift much more accurately than a Gaussian extension model, by capturing the influence of the flap vortices on the spray behavior.

7.   In terms of the maximum extent of particle drift (which is predominantly in the crosswind direction), the amount of propeller thrust does not affect the solution within the 50 ft accuracy with which results will be reported.

8.   The wind angle does not significantly affect the total distance travelled by spray drift. As such, wind directions other than crosswinds can be modeled using the results obtained by AGDISP.

9.   A set of AGDISP input parameters was developed which provides appropriately conservative estimates of spray drift for the C-130A and the AT-802A.

9   REFERENCES

Airborne Support Inc. (2016). Airborne Support Inc. DC-3. Retrieved April 7, 2016, from http://airbornesupport.com/dc31.html

Airfoils, Webpage. (2016). Retrieved April 7, 2016, from http://www.aerofiles.com/airfoils.html

Air Tractor Inc. (2016). AT-802A dimensional drawings. Retrieved from http://www.airtractor.com/sites/default/files/dimensional-drawings/AT_802A_dimensional_drawings.pdf

Air Tractor Inc. (n.d.). Air Tractor Aircraft Brochure. Retrieved from http://airtractor.com/sites/default/files/brochures/Air-Tractor-Choices-Brochure.pdf

AMOG Consulting Inc. (2016, January 22). DST Specification and Requirements Development Note.

Anderson, J. (2001). *Fundamentals of Aerodynamics*. McGraw-Hill.

Australian Maritime Safety Authority. (2000). The response to the Port Stanvac oil spill.

Barbosa, R. (2010, July). Equipment Setup for Aerial Application of Liquid Pesticides. Louisiana State University Agricultural Center. Retrieved from http://www.lsuagcenter.com/NR/rdonlyres/9AFA5406-4522-407B-8E3D-934A1F1DDAE4/72021/pub3160liquidpesticidesHIGHRES.pdf

BETE. (n.d.). NF Standard Fan Nozzle. Retrieved from http://www.bete.com/pdfs/BETE_NF.pdf

Brodersen, O. P., Rakowitz, M., Amant, S., Larrieu, P., Destarac, D., & Suttcliffe, M. (2005). Airbus, ONERA, and DLR Results from the Second AIAA Drag Prediction Workshop. *Journal of Aircraft*, *42*(4), 932–940. http://doi.org/10.2514/1.8662

C Smith Plans. (2016). CMSmithPlans, Products. Retrieved April 7, 2016, from http://www.csmithplans.com/products.html

DC3Training.com. (2012, April 26). DC-3 Pilot's Handbook, Section 8: Flight Controls.

del Pino, C., Parras, L., Felli, M., & Fernandez-Feria, R. (2011). Structure of trailing vortices: Comparison between particle image velocimetry measurements and theoretical models. *Physics of Fluids*, *23*(1), 013602. http://doi.org/10.1063/1.3537791

Delta Flight Museum. (2016). Delta Flight Museum, DC-3. Retrieved April 8, 2016, from https://www.deltamuseum.org/exhibits/delta-history/aircraft-by-type/propeller/douglas-dc-3

Douglas DC-4 | Airliners.net. (2016). Retrieved April 7, 2016, from http://www.airliners.net/aircraft-data/stats.main?id=189

Douglas DC-4 (C-54) - Specifications - Technical Data / Description. (2016). Retrieved April 7, 2016, from http://www.flugzeuginfo.net/acdata_php/acdata_dc4_en.php

Douglas DC-4 commercial aircraft. Pictures, specifications, reviews. (2016). Retrieved April 7, 2016, from http://www.airlines-inform.com/commercial-aircraft/Douglas-DC-4.html

Ebert, T. A., Downer, R., Clark, J., & Huber, C. A. (2008). Summary of Studies of Corexit Dispersant Droplet Impact Behavior into Oil Slicks and Dispersant Droplet Evaporation. In *International Oil Spill Conference* (Vol. 2008, pp. 797–800). American Petroleum Institute. Retrieved from http://ioscproceedings.org/doi/abs/10.7901/2169-3358-2008-1-797

Florida Air Transport. (2016). Florida Air Transport - DC-4. Retrieved April 8, 2016, from http://www.floridaairtransport.com/

Genwest Systems. (2008). Dispersant Mission Planner (Version 2). National Atmospheric and Oceanographic Administration. Retrieved from http://response.restoration.noaa.gov/oil-and-chemical-spills/oil-spills/response-tools/dispersant-mission-planner-dmp2.html

Hamilton Sundstrand. (2011, October). Propeller Modernization Update. Retrieved April 8, 2016, from http://www.lockheedmartin.com.au/content/dam/lockheed/data/aero/documents/global-sustainment/product-support/2011HOC-Presentations/Mon_1340-Ham_Sundstrand.pdf

Hartzell Propeller Inc. (2014a). Hartzell Map Interpolator, using B5MA-11691 propeller performance maps (Version v1.5.1).

Hartzell Propeller Inc. (2014b). Propeller Overhaul Periods and Service Life Limits for Hartzell Propeller Inc. Aviation Components.

Hoerner, S. (1952). *Aerodynamic shape of the wing tips*. DTIC Document. Retrieved from http://oai.dtic.mil/oai/oai?verb=getRecord&metadataPrefix=html&identifier=ADA800374

Hoffmann, C. (2010, February 25). Corexit 9500 and Gel Dispersant Spray Deposition Study. USDA-ARS-Areawide Pest Management Research Unit.

International Air Response. (2015a, December 11). Untitled. Retrieved from https://www.facebook.com/105293866192596/photos/pb.105293866192596.-2207520000.1454314139./904125312976110/?type=3&theater

International Air Response. (2015b, December 11). Untitled. Retrieved from https://www.facebook.com/105293866192596/photos/pb.105293866192596.-2207520000.1454314139./904125312976110/?type=3&theater

Lawrence, J. (n.d.). N117TG (CN: 182-3018) International Air Response Lockheed C-130A Hercules by Justin Lawrence. Retrieved August 19, 2016, from http://www.jetphotos.net/photo/8094647

Lockheed Aircraft Corporation. (1953). *Aerodynamic Data for Structural Loads*. Lockheed Aircraft Corporation.

Maircraft. (2016). Douglas DC-3. Retrieved from http://www.douglasdc3.com/tecnew/tecnew.htm

Melling, A., Noppenberger, S., Still, M., & Venzke, H. (1997). Interpolation correlations for fluid properties of humid air in the temperature range 100 C to 200 C. *Journal of Physical and Chemical Reference Data*, *26*(4), 1111–1123.

Menter, F. R., Kuntz, M., & Langtry, R. (2003). Ten years of industrial experience with the SST turbulence model. *Turbulence, Heat and Mass Transfer*, *4*(1). Retrieved from http://citeseerx.ist.psu.edu/viewdoc/download?doi=10.1.1.460.2814&rep=rep1&type=pdf

MSRC. (2016). Oil Spill Response. Retrieved January 29, 2016, from https://www.msrc.org/services/oil-spill-response/

National Aeronautics and Space Administration. (1976). US Standard Atmosphere.

Norris, S. E., & Richards, P. J. (2010). Appropriate boundary conditions for computational wind engineering models revisited. Presented at the The Fifth International Symposium on Computational Wind Engineering, Chapel Hill, North Carolina, USA.

PNR Nozzles. (n.d.). Spray Engineering Handbook. Retrieved from http://www.pnr.eu/catalogo_sfoglia/spray-engineering-handbook/spray-engineering-handbook.pdf

Quebecair Inc. Regulations. (1957a). DC-3 General Arrangement, Part1. Retrieved from http://pcmuseum.tripod.com/dc3/dc3generalarrangementpart1.pdf

Quebecair Inc. Regulations. (1957b). DC-3 Operating Limitations. Retrieved from http://pcmuseum.tripod.com/dc3/dc3generalarrangementpart1.pdf

Raymer, D. P. (2003). *Simplified aircraft design for homebuilders* (1. ed). Los Angeles, CA: Design Dimension Press.

Raymer, D. P. (2006). *Aircraft Design: A Conceptual Approach* (4th ed.). AIAA Education Series.

Ryan, S. D., Gerber, A. G., & Holloway, A. G. L. (2013). A Computational Study on Spray Dispersal in the Wake of an Aircraft. *Transactions of the ASABE*, *56*(3), 847–868.

Sommerfeld, M. (2000). Theoretical and Experimental Modelling of Particulate Flows. von Karman Institute for Fluid Dynamics.

Sverdrup, H. U. (1946). Humidity Gradient Over the Sea Surface. *Journal of Meteorology*, *3*.

Take Flight Video Productions - The Makers of the Real Life Aviator Video Series! (2016). Retrieved April 7, 2016, from http://www.takeflightvideo.com/dc4.htm

Teske, M. E., Thistle, H. W., Barry, J. W., & Eav, B. (1998). A simulation of boom length effects for drift minimization. *Transactions of the ASAE*, *41*(3), 545.

The Douglas DC-4, DC-6, & DC-7. (2016). Retrieved April 7, 2016, from http://www.airvectors.net/avdc4.html

The Vietnam Center and Archive: Virtual Vietnam Archive. (n.d.). Retrieved April 13, 2016, from http://www.virtualarchive.vietnam.ttu.edu/starweb/virtual/vva/servlet.starweb

Torenbeek, E. (1982). *Synthesis of subsonic airplane design*. Retrieved from http://dx.doi.org/10.1007/978-94-017-3202-4

TurboSquid. (2012). max realistic c 130 hercules. Retrieved from http://www.turbosquid.com/3d-models/max-realistic-c-130-hercules/646668

US Air Force. (2003, September 1). C130 Hercules. Retrieved November 26, 2015, from http://www.af.mil/AboutUs/FactSheets/Display/tabid/224/Article/104517/c-130-hercules.aspx

Document Number - t2015.j520.009
Issued as Revision 0, September 30th 2016
Doc Ref: Atlas:\...\t2015.j520.009.0.odt
amogconsulting.com
EIN 20-4906471
TX PE Firm F-11821

AMOG®

AI-E253-09v20130508

Wieringa, J. (1992). Updating the Davenport roughness classification. *Journal of Wind Engineering and Industrial Aerodynamics*, *41*(1-3), 357–368.

Document Number - t2015.j520.009
Issued as Revision 0, September 30th 2016
Doc Ref: Atlas:\...\t2015.j520.009.0.odt
amogconsulting.com
EIN 20-4906471

TX PE Firm F-11821

AI-E253-09v20130508

APPENDIX C DST SOFTWARE REQUIREMENTS SPECIFICATION

Appendix Contents List

Document Name/Number	No Of Pages
t2015.j520.001.1	17
Notes: 1. All documents in this appendix maintain their original numbering.	

Document Number - r2015.j520.001
Issued as Revision 1, October 14th 2016
Doc Ref: Atlas:\...\r2015.j520.001.1.odt
amogconsulting.com
EIN 20-4906471
TX PE Firm F-11821

AI-E253-10v20130508

DST Specification and Requirements Development Note

Developing An Innovative Dispersant Spray Drift Model

Bureau of Safety and Environmental Enforcement (BSEE)

Engineering solutions

02/17/16

DST Specification and Requirements Development Note

Developing An Innovative Dispersant Spray Drift Model

Bureau of Safety and Environmental Enforcement (BSEE)

AMOG
770 South Post Oak Lane
Suite 310
Houston Texas 77056
United States
T   +1 713 255 0020

amogconsulting.com

Document Number - t2015.j520.001, Issued as Revision 1   Reference # t2015.j520.001rev1

DOCUMENT ISSUE AND DISTRIBUTION

Document Number	Document Title
t2015.j520.001	DST Specification and Requirements Development Note

Job Number	Job Title
2015.j520	Developing an Innovative Dispersant Spray Drift Model

Client	Recipient
Bureau of Safety and Environmental Enforcement (BSEE)	Kimberly Bittler

Client Address	Position
Oil Spill Preparedness Division 45600 Woodland Road, Mail Stop VAE-OSPD Sterling, VA 20166	Research Specialist

Issue	Date Issued	Author	Checked	Authorised
Revision 1	02/17/16	C Dillon-Gibbons	A Kilner	D. Washington
Revision 0	01/22/16	C Dillon-Gibbons	A Kilner	D. Washington

DISTRIBUTION OF COPIES

Copy Number	Location
1	AMOG Consulting
2	Bureau of Safety and Environmental Enforcement (BSEE)

REVISION REGISTER

Page	Revision	Date	Comment
9	1	02/17/16	Removal of tail wind from operational limits

Document Number - t2015.j520.001
Issued as Revision 1, 02/17/16
Doc Ref: Atlas:\...\t2015.j520.001.1.odt
amogconsulting.com
EIN 20-4906471
TX PE Firm F-11821

AI-E253-09v20130508

TABLE OF CONTENTS

Document Number - t2015.j520.001

Issued as Revision 1, 02/17/16

Doc Ref: Atlas:\...\t2015.j520.001.1.odt

amogconsulting.com

EIN 20-4906471

TX PE Firm F-11821

AI-E253-09v20130508

1   INTRODUCTION

1.1   OVERALL PROJECT BACKGROUND

Aerial application of dispersants is an important tool used to respond to oil spills both in coastal waters, and in the deeper waters of the Outer Continental Shelf.

A number of tools currently exist for aerial dispersant planning, such as the pesticide spray tool AgDRIFT. These tools have previously been used in Oil Spill Response Operations, however they were not developed for such use in scenarios.

There is a need to improve upon the existing tools (such as AgDRIFT) and apply them to the equipment and missions used for oil spill dispersant spraying missions; rather than the agricultural equipment and missions that AgDRIFT was developed for. The key differences between application include height, scale and aircraft used.

AMOG has been contracted by the Bureau of Safety and Environmental Enforcement (BSEE) under Contract Number E15PC00015 to develop a decision support software tool, to assist planners to identify operability windows and exclusion zones based on forecast meteorological conditions, spray pattern, aircraft types and release rates.

As part of the development of the rapid response tool AMOG will develop numerical Computational Fluid Dynamic (CFD) models of representative oil spill response aircraft. The CFD models will facilitate examination of the effects of the combination of environmental conditions likely to be experienced by the aircraft coupled with the specific configuration of the aircraft/dispersal system geometry (such as nozzle configurations). This will then be used to evaluate the existing inventory of dispersion models in order to determine their suitability for use in a decision support tool.

Parameters that the tool will seek to incorporate include:

- An inventory of aircraft likely to be used in the response.

- The dispersion characteristics of dispersants (i.e. droplet size distribution).

- The characteristics of spray equipment employed such as the current Rapid Installation and Deployment Spray Systems (RIDSS) for the C130.

- The forecast weather conditions to occur within the target area.

The objective of this package of work is the production of a decision support software tool which is capable of achieving the following function:

1.   Determining the maximum extent of dispersant drift based on environmental conditions at the site. As a minimum, to protect the safety of workers on response vessels in the field and sea animals in the area, the tool needs to be capable of providing input into the decision for establishing the minimum safe distance from the aerial dispersant operations an exclusion zone would need to enforced.

Document Number - t2015.j520.001
Issued as Revision 1, 02/17/16
Doc Ref: Atlas:\...\t2015.j520.001.1.odt
amogconsulting.com
EIN 20-4906471
TX PE Firm F-11821

1.2   DOCUMENT SCOPE

This specification document covers the aerial dispersant spray Decision Support Tool (DST) to be developed by AMOG for BSEE under Contract Number E15PC00015.

The requirements in this document fall broadly into two categories:

- For planning purposes: aircraft spray dispersant operability limits. These define the conditions in which it is either:

    ○   safe to conduct spraying missions; or

    ○   effective to conduct spraying missions.

- Response Management Team's requirements for a decision support tool. These define the requirements of personnel managing oil spill response, with particular regard to:

    ○   defining requirements such as expected solution time;

    ○   required input data formats; and

    ○   prioritizing requirements and/or features.

Document Number - t2015.j520.001
Issued as Revision 1, 02/17/16
Doc Ref: Atlas:\...\t2015.j520.001.1.odt
amogconsulting.com
EIN 20-4906471
TX PE Firm F-11821

AI-E253-09v20130508

2 USER PROFILES

The Decision Support Tool (DST) is envisaged to be employed by a set of users who will participate in the response to oil spill emergencies under the National Incident Management System (NIMS). In particular, two specific types of users have been identified as having the potential requirement for the DST during a Tier II or Tier III response. Furthermore, there is a potential for OSROs to use the tool to plan their initial Tier I response. These users are:

- Operations Section Personnel (under NIMS framework) such as Air Operations for establishing where spraying may or may not occur at the start of a day in order to protect on-water assets and personnel;

- Planning Section Personnel (under NIMS framework) to evaluate how forecast conditions will affect the ability to conduct spraying operations in the response area to provide advice to the Federal On-Scene Coordinator (OSC); and

- Oil Spill Response Organisations (OSROs) to assist with evaluating their initial Tier I response to a spill, prior to the response being escalated to a Tier II or Tier III incident. In these incidents, the OSRO may require both operational and planning support capabilities.

2.1 OPERATIONS SECTION PERSONNEL (TIER II AND III EVENTS)

The Operations Section under the NIMS framework provides the tactical command of available resources during the event. Falling within the Operations Section will typically be the Air Operations Group for the management of aviation resources including dispersant aircraft. Based on advice received during the engagement process, it was advised that the operations group needs a single, worst-case value to employ during the course of the day to establish setback distances for on-water or on-land resources.

As such, these personnel may be expected to run the DST with a single, worst-case wind speed and direction for a given airframe to determine the maximum likely distance impacted by drift. On the basis of this information, they may then decide on an appropriate exclusion zone for vessels, or setback distance for spray operations.

2.2 PLANNING SECTION PERSONNEL (TIER II AND TIER III EVENTS)

The Planning Section under the NIMS framework is responsible for the collection, evaluation and dissemination of tactical information about the incident, including the current and forecasted situation. As such, the planning section may be interested in understanding whether the forecast conditions for the next 24 or 48 hours will be conducive to dispersant spray operations, and for what period.

As such, these personnel may be expected to run the DST with forecast meteorological data to identify operability windows. The tool would incorporate operability limits based on advice received from OSROs or other relevant organisations in order to identify these windows. This may assist with understanding the number of aircraft capable of operating effectively in the forecast conditions, and assist with planning activities for the following day and provide advice to the OSC and Operations Section.

Document Number - t2015.j520.001
Issued as Revision 1, 02/17/16
Doc Ref: Atlas:\...\t2015.j520.001.1.odt
amogconsulting.com
EIN 20-4906471
TX PE Firm F-11821

AI-E253-09v20130508

2.3   OIL SPILL RESPONSE ORGANISATIONS

During a Tier I response, where the incident is still under local control, a Tier I certified OSRO will provide the initial response, including the planning and execution. In this instance, the Tier I responder conducts the Operations and Planning capability which a larger Tier II or Tier III response may require under NIMS.

As such, these OSROs may be expected to operate a DST in both contexts, both with a single worst-case meteorological condition to establish a setback distance for spraying operations, as well as operating with forecast meteorological data and either forecast or pre-prepared oil spill trajectories to allow the identification of windows of opportunity to conduct spray operations.

Document Number - t2015.j520.001
Issued as Revision 1, 02/17/16
Doc Ref: Atlas:\...\t2015.j520.001.1.odt
amogconsulting.com
EIN 20-4906471
TX PE Firm F-11821

AI-E253-09v20130508

3 FUNCTIONAL DESCRIPTION

3.1 COMPUTATIONAL MODES OF THE DST

Depending on the user of the DST program and intended data required there will be two modes which the DST program can be run in. These two modes are detailed in the subsections below.

3.1.1 Operational Mode

The operational mode of the DST will facilitate the decisions required to be made by the operational personnel in conducting Tier I to Tier III responses. The purpose of this mode will be to allow the input of a single, worst-case wind speed and direction likely to occur over the course of a day in order to provide input into establishing setback distances.

3.1.1.1 Intended Users For This Mode

The following users are envisaged as having a need for this mode:

- OSROs (Tier I); and

- Operations Section Personnel (Tier II and Tier III).

3.1.1.2 Intended Inputs For This Mode

- Selection of an aircraft that will conduct spray operations;

- A single, time-invariant wind speed; and

- A single time-invariant wind direction.

3.1.1.3 Intended Output For This Mode

- Advice on the likely maximum extent of drift transverse to the direction of spraying as a single number (no graphical output).

3.1.2 Planning Mode

The planning mode of the DST will facilitate the identification of suitable spraying windows for the purposes of assisting with making planning decisions on the basis of forecast data. The purpose of this mode will be to allow the input of forecast, time-varying data to facilitate the identification of windows conducive to spraying operations (operability windows).

3.1.2.1 Intended Users For This Mode

The following users are envisaged as having a need for this mode:

- OSROs (Tier I); and

Document Number - t2015.j520.001
Issued as Revision 1, 02/17/16
Doc Ref: Atlas:\...\t2015.j520.001.1.odt
amogconsulting.com
EIN 20-4906471
TX PE Firm F-11821

AI-E253-09v20130508

- Planning Section Personnel (Tier II and Tier III).

3.1.2.2   Intended Inputs For This Mode

- Selection of an aircraft that will conduct spray operations;

- Forecast meteorological data over the intended run period as either:

  ○   single-value time series of wind speed and direction; or

  ○   gridded, time series of wind speed and direction over the area.

- Forecast oil spill trajectory data or projections of location of oil over the intended run period.

- The definition of an area where spraying is acceptable.

3.1.2.3   Intended Output For This Mode

- A map layer indicating the intersection of the forecast oil spill impacted area, and the area predicted to be impacted by drift.

- A list of contiguous windows during daylight hours where meteorological conditions are conducive to spraying.

Document Number - t2015.j520.001
Issued as Revision 1, 02/17/16
Doc Ref: Atlas:\...\t2015.j520.001.1.odt
amogconsulting.com
EIN 20-4906471
TX PE Firm F-11821

AI-E253-09v20130508

4 REQUIREMENTS

4.1 GENERAL

This section defines the requirements design set for the DST.

4.2 PERFORMANCE

4.2.1 Functional Mode

The program will be capable of estimating the area impacted by drift caused by meteorological conditions using either:

I. Operational Mode: use of a single time-invariant, wind speed and direction to provide input into the establishment of setback distances; or

II. Planning Mode: use of gridded, time-varying meteorological data to assist with the identification of windows conducive to spraying operations.

4.2.2 Solution Time

The solution time for the DST shall be within 5 minutes per airframe configuration for the single wind speed and direction condition (operational mode).

The solution time for the DST should be within 15 minutes per airframe configuration (planning mode).

4.2.3 Prediction Of Extent Of Dispersant Drift

The prediction of extent of dispersant drift distance at the sea surface shall be set from the 99th percentile horizontal spread of the dispersant particulates from the aircraft flight path. This distance shall be rounded up to the nearest 50 ft.

The DST development should include the possibility of a concentration gradient output. *Note: This is a preference that was raised at the Working Group Meeting; whether is it included in the final program will depending on its feasibility with the CFD technique implemented.*

4.2.4 Number Of Airframes

The DST shall be able to predict dispersant drift from 4 airframes. The DST shall be able to predict dispersant drift from the following airframes:

- Air Tractor AT-802;

- Lockheed C-130 A Hercules;

- Douglas DC-4; and

Document Number - t2015.j520.001
Issued as Revision 1, 02/17/16
Doc Ref: Atlas:\...\t2015.j520.001.1.odt
amogconsulting.com
EIN 20-4906471
TX PE Firm F-11821

AMOG®

AI-E253-09v20130508

- Douglas DC-3.

The specific configuration of each airframe will be included as a data sheet accessible from within the tool.

4.2.5   Aircraft Fleet Composition

A breakdown for the fleet composition is provided below for the airframes chosen:

- Air Tractor AT-802.

    ○   Manufacturer: Air Tractor Inc.

    ○   Type: Single Engine Air Tanker.

    ○   Spray System: Underwing boom system.

    ○   Ownership type (private or public asset): private.

- Lockheed C-130 A Hercules.

    ○   Manufacturer: Lockheed Martin.

    ○   Type: Large Multi Engine Propeller Aircraft.

    ○   Spray System: Internal dispersant tank, RIDDS System.

    ○   Ownership type (private or public asset): International Air Response, Inc. / MSRC (Private).

- Douglas DC-4.

    ○   Manufacturer: Douglas Aircraft Company.

    ○   Type: Four-engine (piston) propeller-driven airliner.

    ○   Spray System: 4 spray tanks installed, equipped with spray pump.

    ○   Ownership type (private or public asset): Airborne Support Inc. (private).

- Douglas DC-3.

    ○   Manufacturer: Douglas Aircraft Company.

    ○   Type: Twin Engine fixed wing propeller - driven monoplane.

    ○   Spray System: 1 spray tank installed, equipped with spray pump.

    ○   Ownership type (private or public asset): Airborne Support Inc. (private).

4.2.6   Generic Airframe Performance Envelopes

The DST shall be able to make predictions for dispersant drift for the airframes listed in Section 4.2.4 and for the input parameter limits listed below. The specific configuration of each aircraft considered will be included in the model as a configuration sheet accessible from within the DST.

Document Number - t2015.j520.001
Issued as Revision 1, 02/17/16
Doc Ref: Atlas:\...\t2015.j520.001.1.odt
amogconsulting.com
EIN 20-4906471
TX PE Firm F-11821

AI-E253-09v20130508

Category 1: Operational Limits

- Maximum head wind speed - 35 knots.

- Maximum crosswind (up to 90° from direction of travel) speed - 20 knots.

- Seastate limit - 10ft.

- Visibility limit - 3nm.

- Ceiling limit - 1000ft.

Category 2: Airframe Limits

- Dispersant pump rate – 3 to 7 gal per acre.

- Spray nozzle configuration.

- Droplet size – 300 to 700 um.

- Application ground speed – 120 to 180 knots, 150 knots median.

- Dispersant release height – 50ft to 100ft, 75ft median.

Category 2 limits are airframe specific and may vary during operations, due to environmental influences, in order to optimize dispersant spray application.

Note: The CFD model will not capture turbulent droplet break up. In the absence of advice from the operators on the typical droplet size distribution, AMOG will employ a generic distribution. The droplet size distributions used will be the ASAE Medium to Coarse distribution, which includes droplets in the size range for 300 to 700 microns with a median droplet size of 400 microns. This will include finer fractions and coarser fractions as part of the distribution.

4.2.7 Simultaneous Operation Requirements

The DST shall be able to predict dispersant drift for one airframe per simulation.

4.2.8 Modeling Domain Size

The DST program shall be able to determine dispersant drift for at least the length of the maximum distance of a dispersant spray run for the airframes listed in Section 4.2.4.

4.2.9 Number Of Spray Units

The DST program shall predict dispersant drift for a single spray system configuration per airframe.

4.2.10 Number Of Dispersants

The DST program shall be able to model 1 dispersant type, as follows:

- Corexit EC9500A.

Document Number - t2015.j520.001
Issued as Revision 1, 02/17/16
Doc Ref: Atlas:\...\t2015.j520.001.1.odt
amogconsulting.com
EIN 20-4906471
TX PE Firm F-11821

AI-E253-09v20130508

4.3 INTERFACE, INTEROPERABILITY & COMPATIBILITY REQUIREMENTSINPUT DATA FORMAT REQUIREMENTS

The DST program shall be able to accept one of the following available sources of wind environmental information from the NOAA NWS (National Weather Service) website. Two different environmental data sources are available from the NOAA NWS, Aviation Weather Center and the NWS Marine Forecast. An example file image for each of the available data forms is shown below in Figures 1 and 2.

The choice of which data form to be used in the final version of the DST program is to be determined in a later development of this project.


```
Level:  ● Low  ○ High   [20Z-03Z ◇]  [North Central (Chicago) ◇]  [Print]

 (Extracted from FBUS31 KWNO 122000)
FD1US1
DATA BASED ON 121800Z
VALID 130000Z    FOR USE 2000-0300Z. TEMPS NEG ABV 24000

FT   3000    6000    9000    12000   18000   24000   30000   34000   39000
BRL  3118 3129-13 3041-13 3155-15 3175-24 3080-34 308448 308657 309065
DBQ  3218 3130-16 3037-17 3153-19 3180-26 3199-35 810649 811358 319964
DSM  3017 3134-11 3148-11 3156-14 3170-23 3065-34 306049 305957 306864
MCW  3018 3131-15 3145-14 3153-17 3169-25 3174-34 318149 318558 328566
JOT  3224 3133-17 3147-17 3159-22 3193-28 8113-36 812750 812658 800360
SPI  3122 3131-12 3041-13 3057-15 3077-23 3084-33 308948 309057 309364
EVV  3224 3135-10 3045-11 3062-13 3076-22 2985-33 299348 299457 299562
FWA  3031 3036-18 3048-21 3159-24 3183-33 8121-39 802550 801454 299855
IND  2927 3139-15 3056-15 3067-20 3196-26 8014-35 802749 802957 790260
```

Figure 1 : Aviation Weather Center Example Wind / Temperature Data Form

Document Number - t2015.j520.001
Issued as Revision 1, 02/17/16
Doc Ref: Atlas:\...\t2015.j520.001.1.odt
amogconsulting.com
EIN 20-4906471
TX PE Firm F-11821

AI-E253-09v20130508

```
SEAS GIVEN AS SIGNIFICANT WAVE HEIGHT...WHICH IS THE AVERAGE
HEIGHT OF THE HIGHEST 1/3 OF THE WAVES. INDIVIDUAL WAVES MAY BE
MORE THAN TWICE THE SIGNIFICANT WAVE HEIGHT.


GMZ001-130315-
SYNOPSIS FOR THE GULF OF MEXICO
1014 AM EST TUE JAN 12 2016


.SYNOPSIS...A STATIONARY TROUGH WILL PERSIST OVER THE SW AND W
CENTRAL GULF THROUGH LATE WED. LOW PRESSURE WILL DEVELOP OFF THE
MOUTH OF THE RIO GRANDE WED NIGHT...MOVE NE ACROSS THE N CENTRAL
WATERS ON THU...AND INTO THE LOWER MISSISSIPPI VALLEY THROUGH LATE
THU. THE FOLLOWING TROUGH WILL MOVE ACROSS THE EASTERN GULF
THROUGH SAT.

$$
```

```
SEAS GIVEN AS SIGNIFICANT WAVE HEIGHT...WHICH IS THE AVERAGE
HEIGHT OF THE HIGHEST 1/3 OF THE WAVES. INDIVIDUAL WAVES MAY BE
MORE THAN TWICE THE SIGNIFICANT WAVE HEIGHT.


GMZ019-130315-
CENTRAL GULF FROM 22N TO 26N BETWEEN 87W AND 94W-
1014 AM EST TUE JAN 12 2016


TODAY
NE TO E WINDS 15 TO 20 KT. SEAS 3 TO 5 FT. SCATTERED
SHOWERS AND ISOLATED TSTMS.

TONIGHT
NE TO E WINDS 15 TO 20 KT. SEAS 4 TO 6 FT. SCATTERED
SHOWERS AND ISOLATED TSTMS.

WED
E WINDS 15 TO 20 KT. SEAS 5 TO 7 FT. SCATTERED SHOWERS
AND ISOLATED TSTMS.
```

Figure 2 : NWS Marine Forecast Example Data Form

Document Number - t2015.j520.001
Issued as Revision 1, 02/17/16
Doc Ref: Atlas:\...\t2015.j520.001.1.odt
amogconsulting.com
EIN 20-4906471
TX PE Firm F-11821

AI-E253-09v20130508

4.3.1 Output Data Requirements

The following output data requirements for the DST shall be put in place:

- Operational Mode:

    - A single limit for all aircraft.

    - The output from the DST is a single setback distance which will be rounded to the nearest 50 ft based upon the 99th percentile horizontal spread of the dispersant from the aircraft flight path. (The DST development should include the possibility of a concentration gradient output. Implementation will depend on its feasibility.

    - The dispersant drift distance will be based on a flat sea surface.

- Planning Mode

    - A map layer indicating the intersection of the forecast oil spill impacted area, and the area predicted to be impacted by drift.

    - A list of contiguous windows during daylight hours where meteorological conditions are conducive to spraying.

Based on feedback form the Working Group meeting there will be no direct interface requirements for linking the outputs from the DST program to any other existing aerial dispersant management or logistics tools.

4.3.2 Operating System Requirements

The DST program shall be usable on the following operating systems:

- Windows 7 and Mac OSX – Mountain Lion and Yosemite.

4.4 MAINTAINABILITY

4.4.1 Suitability For Future Program Development

The program should be written in such a way that the following additional items can be added to or modified easily:

- Airframes.

- Rounding to nearest 50 ft.

- Dispersant Type.

Document Number - t2015.j520.001
Issued as Revision 1, 02/17/16
Doc Ref: Atlas:\...\t2015.j520.001.1.odt
amogconsulting.com
EIN 20-4906471
TX PE Firm F-11821

AI-E253-09v20130508

5   VERIFICATION

The verification of requirements for the DST program shall be undertaken through two separate stages. Validation activities will be reported as part of the report contract deliverables for the project.

5.1   CFD MODELING VALIDATION

The type of validation (quantitative vs qualitative) will be based on the availability of field-trial data. As a result, AMOG proposes that the validation process be conducted as follows:

1.   Where no field-trial data exists, due to the opaque nature of the dispersant upon initial release, a qualitative assessment of the spreading/dispersion behavior in the wake of the aircraft will be undertaken against operational photographs of the aircraft as a minimum;

2.   Where field-trial data exists, AMOG would seek to conduct a CFD model as close to the field-trial conditions as practicable to undertake a quantitative assessment of the model predictions.

The purpose of validating the CFD modeling will be to allow the evaluation of the other models such as AGDISP or AGDRIFT against an adequate representation of the physics of the dispersant.

5.2   DST RAPID RESPONSE TOOL

The DST rapid response tool will be internally verified and evaluated against results, generated in the course of the project or from external sources.

A verification activity of the DST against the requirements included in this specification will also be conducted to ensure that no functionality is missing. The program will be tested to minimise the chance of software bugs or other errors which will negatively impact performance.

Document Number - t2015.j520.001
Issued as Revision 1, 02/17/16
Doc Ref: Atlas:\...\t2015.j520.001.1.odt
amogconsulting.com
EIN 20-4906471
TX PE Firm F-11821

AI-E253-09v20130508

APPENDIX D   DST VERIFICATION

Document Number - r2015.j520.001
Issued as Revision 1, October 14th 2016
Doc Ref: Atlas:\...\r2015.j520.001.1.odt
amogconsulting.com
EIN 20-4906471
TX PE Firm F-11821

AI-E253-10v20130508

Table D1 : Verification Of DST Performance Against Requirements Specification

Reference[1]	Requirement	DST Performance	Notes
3.1.1.2	The inputs to the Operational Mode will be: • Selection of an aircraft that will conduct spray operations; • A single, time-invariant wind speed; and • A single time-invariant wind direction.	Full compliance	Additional inputs were identified as being required: • Aircraft heading • Altitude (optional) • Aircraft velocity (optional) • Safety Factor
3.1.1.3	The output from the Operational Mode will be: • Advice on the likely maximum extent of drift transverse to the direction of spraying as a single number (no graphical output).	Full compliance	Additional outputs were implemented: • Whether the selected aircraft is operable for spraying in the input conditions. • The maximum drift extent in line with the direction of spraying. • The distance and direction the point of maximum spray drift extent.

AMOG®

Table D1 : Verification Of DST Performance Against Requirements Specification

Reference[1]	Requirement	DST Performance	Notes
3.1.2.2	The inputs to the Planning Mode will be: • Selection of an aircraft that will conduct spray operations; • Forecast meteorological data over the intended run period as either: ○ single-value time series of wind speed and direction; or ○ gridded, time series of wind speed and direction over the area. • Forecast oil spill trajectory data or projections of location of oil over the intended run period. • The definition of an area where spraying is acceptable.	Full compliance	Additional inputs were identified as being required: • Aircraft heading • Altitude (optional) • Aircraft velocity (optional) • Safety Factor Forecast data including: • Sea state • Visibility • Wind speed and wind direction • Time Advice from OSROs indicated gridded meteorological data was not readily available during oil spill response operations.
3.1.2.3	The outputs from the Planning Mode will be: • A map layer indicating the intersection of the forecast oil spill impacted area, and the area predicted to be impacted by drift. • A list of contiguous windows during daylight hours where meteorological conditions are conducive to spraying.	Full compliance	A single map layer is generated as the output of the planning mode. The area impacted by spray drift includes all areas from the forecast period provided as input.

AMOG®

Table D1 : Verification Of DST Performance Against Requirements Specification

Reference[1]	Requirement	DST Performance	Notes
4.2.2	The solution time for the DST shall be within 5 minutes per airframe configuration for the single wind speed and direction condition (operational mode). The solution time for the DST should be within 15 minutes per airframe configuration (planning mode).	Full compliance	Testing indicates that the DST when run on a 3.1 GHz Intel Core i7 achieves the following runtimes: • Less than 1 s in operational mode. • Less than 10 s in planning mode for a test forecast file with 100 forecast data points.
4.2.3	The prediction of extent of dispersant drift distance at the sea surface shall be set from the 99th percentile horizontal spread of the dispersant particulates from the aircraft flight path. This distance shall be rounded up to the nearest 50 ft. The DST development should include the possibility of a concentration gradient output. *Note: This is a preference that was raised at the Working Group Meeting; whether is it included in the final program will depending on its feasibility with the CFD technique implemented.*	Partial Compliance	The extent of spray drift was determined by the point at which 99 % of the mass of released spray behind the aircraft has been deposited. An extent perpendicular to the aircraft track and parallel to the aircraft track have been rounded up to the nearest 50 ft. The architecture of the DST has been developed such that only minor alterations to the database structure would be required to provide a concentration gradient output. However, Concentration gradient was not developed in this scope of work.

Document Number - r2015.j520.001
Issued as Revision 1, October 14th 2016

Doc Ref: Atlas:\...\r2015.j520.001.1.odt
amogconsulting.com
EIN 20-4906471
TX PE Firm F-11821

AI-E253-10v20130508

Table D1 : Verification Of DST Performance Against Requirements Specification

Reference[1]	Requirement	DST Performance	Notes
4.2.4	The DST shall be able to predict dispersant drift from the following airframes: • Air Tractor AT-802; • Lockheed C-130 A Hercules; • Douglas DC-4; and • Douglas DC-3. • The specific configuration of each airframe will be included as a data sheet accessible from within the tool.	Full compliance	
4.2.6	Operational Limits: • Maximum head wind speed - 35 knots. • Maximum crosswind (up to 90° from direction of travel) speed - 20 knots. • Seastate limit - 10ft. • Visibility limit - 3nm. • Ceiling limit - 1000ft.	Full compliance	Additional operational limits were included following advice from OSROs: • No spray operations in tail wind conditions • Operations only within the regulatory guidance airspeeds and altitudes.

Document Number - r2015.j520.001
Issued as Revision 1, October 14th 2016

Doc Ref: Atlas:\...\r2015.j520.001.1.odt
amogconsulting.com
EIN 20-4906471
TX PE Firm F-11821

AI-E253-10v20130508

Table D1 : Verification Of DST Performance Against Requirements Specification

Reference[1]	Requirement	DST Performance	Notes
4.2.6	Airframe Limits: • Dispersant pump rate – 3 to 7 gal per acre. • Spray nozzle configuration. • Droplet size – 300 to 700 um. • Application ground speed – 120 to 180 knots, 150 knots median. • Dispersant release height – 50ft to 100ft, 75ft median. Category 2 limits are airframe specific and may vary during operations, due to environmental influences, in order to optimize dispersant spray application. *Note: The CFD model will not capture turbulent droplet break up. In the absence of advice from the operators on the typical droplet size distribution, AMOG will employ a generic distribution. The droplet size distributions used will be the ASAE Medium to Coarse distribution, which includes droplets in the size range for 300 to 700 microns with a median droplet size of 400 microns. This will include finer fractions and coarser fractions as part of the distribution.*	Full Compliance	The operational limits are specific to each airframe, in terms of application ground speed and dispersant release height.
4.2.7	The DST shall be able to predict dispersant drift for one airframe per simulation.	Full compliance	
4.2.8	The DST program shall be able to determine dispersant drift for at least the length of the maximum distance of a dispersant spray run for the airframes listed in Section 4.2.4.	Full compliance	Due to the architecture of the DST, there is no limit on the length of spray runs for which drift can be predicted.
4.2.9	The DST program shall predict dispersant drift for a single spray system configuration per airframe.	Full compliance	

Table D1 : Verification Of DST Performance Against Requirements Specification

Reference[1]	Requirement	DST Performance	Notes
4.2.10	The DST program shall be able to model 1 dispersant type, as follows: ● 　Corexit EC9500A.	Full compliance	
4.3	The DST program shall be able to accept one of the following available sources of wind environmental information from the NOAA NWS (National Weather Service) website. Two different environmental data sources are available from the NOAA NWS, Aviation Weather Center and the NWS Marine Forecast. An example file image for each of the available data forms is shown below in Figures 1 and 2. The choice of which data form to be used in the final version of the DST program is to be determined in a later development of this project.	Full compliance	Forecast data input into the DST is in a .csv format. The required variables match the NWS Marine Forecast data type from NOAA NWS but require the user to amalgamate the data. The NOAA NWS Aviation Weather Centre data does not include the full data set required to define the operational limits of offshore spraying.
4.3.2	The DST program shall be usable on the following operating systems: ● 　Windows 7 ● 　Mac OS X – Mountain Lion and Yosemite.	Full compliance	
4.4.1	The program should be written in such a way that the following additional items can be added to or modified easily: ● 　Airframes. ● 　Rounding to nearest 50 ft. ● 　Dispersant Type.	Full compliance	The architecture of the DST allows for additional data sets to be input with minimal rewriting of the code.

Notes:
1.　Each requirement is referenced against the relevant section of the Requirements Specification, as included in Appendix C.

AI-E253-10v20130508